## Synthetic Manifestation of Polynitro Functionalized Azoles (Pyrazole/Imidazole/1,2,4-Oxadiazole) as Potential Energetic Materials

# A Thesis Submitted for the Degree of DOCTOR OF PHILOSOPHY in CHEMISTRY

By

#### Srinivas Vangara



School of Chemistry University of Hyderabad Hyderabad 500 046 Telangana India

December, 2021



### My Family Members

(Vangara Pentayya, V. Kanakamma, V. Polamma, V. Appa Rao, V. Rama, V. Usha, V. Trinadha, and other family members)

#### **DECLARATION**

I hereby declare that the matter embodied in the thesis entitled "Synthetic Manifestation of Polynitro Functionalized Azoles (Pyrazole/Imidazole/1,2,4-Oxadiazole) as Potential Energetic Materials" is the result of investigation carried out by me in the School of Chemistry, University of Hyderabad, Hyderabad, India, under the supervision of Prof. Akhila Kumar Sahoo.

In keeping with the general practice of reporting scientific observations, due acknowledgements have been made on the basis of the findings of other investigators. Any omission, which might have occurred by oversight or error, is regretted. This research work is free from Plagiarism. I hereby agree that my thesis can be deposited in Shodhganga/INFLIBNET. A report on plagiarism statistics from the University Librarian is enclosed.

Srinivas Vangara (15CHPH10)

Prof. Akhila Kumar Sahoo

(Supervisor)

Prof. A.K. Sahoo School of Chemistry, University of Hyderabad Hyderabad-500046. T.S., India.

University of Hyderabad

December, 2021



This is to certify that the thesis entitled "Synthetic Manifestation of Polynitro Functionalized Azoles (Pyrazole/Imidazole/1,2,4-Oxadiazole) as Potential Energetic Materials" submitted by Srinivas Vangara holding registration number 15CHPH10 in partial fulfilment of the requirements for award of Doctor of Philosophy in the School of Chemistry is a bonafide work carried out by him under my supervision and guidance.

This thesis is free from plagiarism and has not been submitted previously in part or in full to this or any other University or Institution for award of any degree or diploma.

Further the student has passed the following courses towards fulfilment of course work requirement for Ph.D.

Course code	Name	Credits	Pass/Fail
CY-801	Research Proposal	3	Pass
CY-802	Chemistry Pedagogy	3	Pass
CY-805	Instrumental Methods-A	3	Pass
CY-502	Advanced Organic Synthesis	3	Pass

Kumaia Swampul Dean

School of Chemistry

Dean School of Chemistry University of Hyderabad Hyderabad - 500 046 Akhila K. Sahoo
(Thesis Supervisor)

Prof. A.K. Sahoo School of Chemistry, University of Hyderabad Hyderabad-500046. T.S., India.

#### **Acknowledgements**

I express my hearty gratitude and profound thanks to my supervisor **Prof. Akhila Kumar Sahoo** for his excellent guidance, encouragement, support, and the freedom that he gave to me in carrying out various research projects. His optimistic approach and patience towards every aspect was admirable and inspiring. Throughout my Ph.D tenure, he was always been approachable, helpful, and friendly. I am fortunate to be a part of his research group. He considered me as one of his family members.

It's my pleasure to thank Dr. V. Kameswara Rao, Director, Advanced Center of Research in High Energy Materials (ACRHEM), University of Hyderabad and Dr. K. Venkateswara Rao, (former Director of ACRHEM) for their support, encouragement and helpful discussions throughout my research work. I take this opportunity to thank Prof. K. C. Kumara Swamy, Dean, School of Chemistry (SoC) and Prof. T. P. Radhakrishnan, Prof. M. Durga Prasad (former Directors of SoC) for providing the facilities needed for our research. I sincerely thank my doctoral committee members Prof. P. K. Panda and Prof. K. Muralidharan for their guidance and encouragement. I extend my sincere thanks to the former Deans, Directors and all the faculty members of ACRHEM and School of Chemistry for their cooperation and encouragement on various aspects. I also want to thank the CMSD, University of Hyderabad, for providing computational facilities.

I sincerely thank all the non-teaching staffs in ACRHEM and School of Chemistry for their assistance on various occasions. I am thankful to all my colleagues in ACRHEM and School of Chemistry for helping me in various aspects. I would like to acknowledge DRDO, HEMRL and ACRHEM for the financial support.

From the bottom of my heart, I thank Dr. K. Nagarjuna for being such generous co-worker, guide, and friend. Without his support encouragement and

kind help my Ph.D work is unsuccessful. In addition, he only taught me all the computational calculations. His help in my Ph.D life is greatly pleased.

A special thanks to Dr. Raveendra, M. Balaraju, R. Prasad, Dr. Tirumaleswararao, and Dr. Vikranth for their help & support. I value my association with my friends and labmates Dr. Koushik Ghosh, Dr. Shankar, Dr. Prabagar, Dr. Rajendra, Dr. Ramesh, Dr. Kallol, Dr. Suresh, Dr. Arjith, Shubham, Manash, Arghadip, Somratan, Dr. Sudhakar, Aravind, Durga, and Shivanand for their encouragement, helpful discussion, pleasant company, and cooperation during my Ph.D. tenure.

My hearty thanks to Prof. A. K. Sahoo's family, Madam (Rashmita Sahoo) and Sonu (Amlesh) for the support and hosting group dinner at their home.

I record my special thanks to my juniors Shubham and Manash for their time to time discussion and making my life enjoyable and memorable in the University of Hyderabad.

I am very much thankful to instruement operators from School of Chemistry (Ramana Sir, Durgesh, Mahesh, Mahendra, Rajesh, and others) and ACRHEM (Srikanth, Shivanand, Ashok, Sathish, and Siva) for their encouragement and support given to me for writing this book.

Without my parents (Vangara AppaRao and Vangara Rama), sister (Sirisha/Usha) and brother (Trinadha) relentless support and love, I would have not reached at this position. I owe everything to them. I would like to express my sincere thanks to all my family members; Pentayya, Kanakamma, K. P. Raju, Sushma, Bharath, Girish, Ramana, Padma, and Roopa for their close association with me.

It's my pleasure to thank my teachers (Narayana rao sir, Trinadha rao sir, Murali sir, Nookaraju sir, Telugu master, Anil sir, Botany-Zoology sir, Samuel sir, Ramakranthi madam, Usha madam, Prasanthi madam, CVK sir, MSN sir, Nageswara rao sir), where I learned the importance of my life.

I am lucky to have friends like Arun, John, Ramesh, Surendra, Prasad, Sashi, Ravi,

Srinu, Kurumurthy, Srikanth, Khaja, Ramu, Jagadheesh, Javeed, in HCU.

I express my gratitude and profound thanks to my best friends Gowri Shankar

(Pandu), Keerthi, Santhosh, Mallik, Mahesh, Sudheer, Siva, Uma, Srilatha,

Hemalatha, Niranjani, Siva.au, Suresh, Basheer, Amesh, Gopal, Vamsi, Govindh,

Mahesh, Srinu, all childhood friends, and 1st class to M.Sc class friends for their

love, encouragement and support.

Lastly this acknowledgement would be incomplete without express my gratitude

to my family members, teachers, lab mates, and friends who have been a constant

source of inspiration and support throughout my Ph.D tenure.

Srinivas Vangara

University of Hyderabad

Dec, 2021

V

#### **TABLE OF CONTENTS**

Statement	i
Certificate	ii
Acknowledgements	iii-v
List Abbreviations	xi-xiii
Chapter 1: Thermally Stable and Insensitive Energetic Materials: An	
Update on Recent Advances 2009-2021	
1.1. History & Background of High Energy Materials (HEMs)	3
1.2. Definition and Introduction	5
1.3. Explosophores	5
1.4. Classification of High Energy Materials	5
1.4.1. Explosives	6
1.4.1.1. Classification of Explosives	6
1.4.1.1.1 Thermally Stable Explosives	7
1.4.1.1.2. High Performance Explosives	7
1.4.1.1.3. Melt Cast Explosives	8
1.4.1.1.4. Insensitive Explosives	8

1.4.2. Propellants	9
1.4.2.1. Gun Propellants	10
1.4.2.1. Gun Fropenants	10
1.4.2.2. Rocket Propellants	10
1.4.3. Pyrotechnics	10
<b>,</b>	
	11
<b>1.5.</b> Parameters Responsible for Explosive and Energetic Materials	11
1.6 Thermally Stable and Insensitive Energetic Materials (TSI-EMs)	13
1.6.1. Pyrazole based TSI-EMs	13-15
1.0.1. I yluzole bused 151 Elvis	13 13
1.6.2. Imidazole based TSI-EMs	16
1.6.3. Triazole based TSI-EMs	
1.6.3.1. 1,2,3-Triazole based TSI-EMs	17-18
1.0.3.1. 1,2,3-111azoic based 131-Livis	17-10
1.6.3.2. 1,2,4-Triazole based TSI-EMs	19-21
1.6.4. Oxadiazole based TSI-EMs	21
1.6.4.1. 1,2,4-oxadiazole based TSI-EMs	21-23
1.0.4.1. 1,2,4-0xadiazole based 151-Elvis	21-23
1.6.4.2. 1,2,5-oxadiazole based TSI-EMs	23-27
1.6.4.3. 1,3,4-oxadiazole based TSI-EMs	27-29
1.0 2,0, . 0.1.4.4.2.0.2 04.004 1.0.2 22.1.4.0	
1.65 m. 1.1 1.007 77.5	20.21
1.6.5. Tetrazole based TSI-EMs	29-31

<b>1.7.</b> Objective of the thesis	32
1.8. References	33-39
Chapter 2: Thermally Stable and Insensitive Energetic Materials: Synthesis	
of Polynitro-N-aryl-C-nitro Pyrazole/Imidazole Derivatives	
2.1. Introduction	42
2.1.1. Background of polynitro azole/aryl-azole derivatives towards	
	12 10
energetic material applications	43-48
2.2 Mativation and Design plan	49
<b>2.2.</b> Motivation and Design plan	49
2.3. Results and Discussion	50-52
Zio. Results and Discussion	30 32
<b>2.4.</b> <sup>15</sup> N NMR Spectroscopy	53
2.5. X-ray Crystallography	54-58
2.6. Energetic Properties	59-61
2.7. Hirshfeld Surface Analysis	61-63
2.8. Conclusions	63
2.0 Europinontal	64.76
<b>2.9.</b> Experimental	64-76
2.10. References	77-79
2.11. Spectra	80-96

Chapter 3: Polynitro-azido Functionalized N-aryl-C-nitro	
Pyrazole/Imidazole Derivatives as Energetic Materials	
3.1. Introduction	99
3.1.1. Background of azido-substituted derivatives towards	
energetic material applications	99-104
3.2. Motivation and Design plan	105
3.3. Results and Discussion	106-109
<b>3.4.</b> X-ray Crystallography	109-113
3.5. Energetic Properties	113-115
3.6. Hirshfeld Surface Analysis	115-117
3.7. Conclusions	117
3.8. Experimental	118-129
3.9. References	130-132
<b>3.10.</b> Spectra	133-149
Chapter 4: Combination of 1,2,4-oxadiazole and Nitro/nitroamino Substituted Azoles as Energetic Derivatives	
4.1. Introduction	152
4.1.1. Background of applications of 1,2,4-oxadiazole derivatives	153.156

as energetic materials	
<b>4.2.</b> Motivation and Design plan	157
4.3. Results and Discussion	158-160
<b>4.4.</b> <sup>15</sup> N NMR Spectroscopy	160-161
4.5. X-ray Crystallography	161-164
<b>4.6.</b> Energetic Properties	164-166
4.7. Hirshfeld Surface Analysis	166-167
4.8. Conclusions	167
4.9. Experimental	168-176
4.10. References	177-179
4.11. Spectra	180-192
List of Publications	193
Conference Attended	194
Plagiarism Report	195-197

#### **List of Abbreviations**

NMR - Nuclear Magnetic Resonance

FTIR - Fourier Transform Infrared

GC-MS - Gas Chromatography-Mass Spectrometry

LC-MS - Liquid Chromatography-Mass Spectrometry

HPLC - High Pressure Liquid Chormatography

GPC - Gas Phase Chromatography

TLC - Thin-layer chromatography

El - Electron Ionization

ESI - Electronic Spray Ionization

XRD - X-Ray Diffraction

s - singlet

d - doublet

m - multiplet

q - quartet

bs - broad singlet

bd - broad doublet

dd - double doublet

mp - Melting Point

aq - aqueous

AcOH - acetic acid

Ac - acetyl

Ar - aryl

 $\alpha$  - alpha

 $\beta$  - beta

aq. - Aqueous

°C - degree Celsius

Cat. - catalyst

Calcd - calculated

<sup>1</sup>H NMR - Proton-nuclear magnetic spectroscopy

<sup>13</sup>C NMR - Carbon-13 nuclear magnetic spectroscopy

 $\delta$  - delta

equiv - equivalent

e.g. - exempli gratia

g - gram h - hour

ppm - parts per million

mg - milligram

m.p - melting point

mmol - millimole mL - millileter

cm - centimeter

v - nu (greek word)

J - coupling constant in hertz

N<sub>2</sub> - Nitrogen

ND - Not determined
TMS - Trimethylsilyl

DMSO - Dimethylsulfoxide

CH<sub>3</sub>CN - acetonitrile

MeOH - Methanol

DMF - Dimethylformamide

THF - TetrahydrofuranTEA - Triethylamine

HCl - Hydrochloric acid

H<sub>2</sub>SO<sub>4</sub> - Sulphuric acid

HNO<sub>3</sub> - Nitric acid

H<sub>2</sub>O<sub>2</sub> - Hydrogen peroxide

Ac2O - Acetic anhydride

NaN<sub>3</sub> - Sodium azide

NH<sub>2</sub>OH - Hydroxylamine hydrochloride

Sc(OTf)<sub>3</sub> - Scandium triflate

HC(OMe)<sub>3</sub> - Trimethyl orthoformate

N<sub>2</sub>H<sub>5</sub>.H<sub>2</sub>O - Hydrazine hydrate

KHSO<sub>5</sub> - Potassium peroxymonosulfate or Oxone

MVK - Methyl vinyl ketone

rt - Room Temperature

K<sub>3</sub>PO<sub>4</sub> - Tripotassium phosphate

CuI - Copper (I) iodide

NCS - *N*-chlorosuccinimide

TNT - Trinitrotoluene

NC - Nitrocelluose

NG - Nitroglycerine

TATB - Triaminotrinitrobenzene

PETN - Pentaerythritoltetranitrate

RDX - 1,3,5-trinitro-1,3,5-triazinane

HMX - 1,3,5,7-tetranitro-1,3,5,7-tetrazocane

TNAZ - 1,3,3-Trinitroazetidine

CL-20 - 2,4,6,8,10,12-Hexanitro-2,4,6,8,10,12-hexaazaisowurtzitane

ONC - Octanitrocubane

OAC - Octaazidocubane

TEX - 4,10-Dinitro-4,10-diaza-2,6,8,12-tetraoxaisowurtzitane

CBTNE - Cyclobutane tetranitrate ester

MTNI - 1-Methyl-2,4,5-trinitroimidazole

DNAN - 2,4-Dinitroanisole

BINF - Bis(nitroxymethyl isoxazolyl)furoxan

FOX-7 - 1,1-Diamino-3,5-dinitro-pyrazine-1-oxide

NTO - 3-Nitro-1,2,4-triazol-5-one

LLM-105 - 2,6-Diamino-3,5-dinitro-pyrazine-1-oxide

DFT - Density Functional Theory

ESP - Electrostatic Potential

AM1 - Austin Model 1

DSC - Differential Scanning Calorimetry

TGA - Thermogravimetic Analysis

DTA - Differential Temperature Analysis

HOF - Heat of Formation

VOD or <sub>v</sub>D - Velocity of Detonation

DP - Detonation Pressure

IS - Impact Sensitivity

FS - Friction Sensitivity

**Chapter-1** 

## Thermally Stable and Insensitive Energetic Materials: An Update on Recent Advances 2009–2021

Chapter 1

#### **Abstract**

This chapter narrates brief history of high energy materials origination and categorization of explosives, propellants and pyrotechnics. It is also discussed how high energy materials are applied to military, space, and civil purposes. Additionally, the role of azoles (N-heterocycles with five and six members) as energetic materials (EMs) is discussed. This thesis aims to develop thermally stable and insensitive EMs.

#### 1.1. An Overview of High Energy Materials (HEMs)

The history of energetic materials dates back to the 11<sup>th</sup> century when black powder or gunpowder was made by Chinese alchemists from coal, saltpeter, and sulphur. In the 19<sup>th</sup> century, Ascanio Sobrero developed nitroglycerine (NG) as the first practical explosive, stronger than black powder. Due to its high instability, nitroglycerin was replaced by nitrocellulose, trinitrotoluene (TNT) in 1863 and smokeless powder, dynamite, and gelignite in 1867. However, severe explosions occurred during the manufacture of nitroglycerine. With the growing demand of the explosives in coal mining, replacement of the existing explosives was essential. This allowed in discovery of picric acid or trinitrotoluene (TNT) as explosive materials. During the 1<sup>st</sup> World War, TNT has been used as the standard explosive because it is less sensitive, picric acid formed complexes with heavy metals and was highly sensitive; Research into high-performance explosives for military applications was commenced by the end of the 2<sup>nd</sup> World War; thus, pentaerythritoltetranitrate (PETN) and cyclotrimethylene trinitramine (RDX) energy materials were developed. In various applications, RDX has proved more powerful but less sensitive than PETN. Some of the known explosives are listed in **Figure 1.1.1.** 

Figure 1.1.1. Structures of popular explosives

The 20<sup>th</sup> century saw the development of other major explosives for special purposes such as high performance and high insensitivity, but none gained as much use as RDX.<sup>3,4</sup> A brief historical overview of explosives is arranged in **Table 1.1.1**.

 Table 1.1.1. History of explosives

Anonymous Roger Bacon	China or India	~ 1000 AD
Roger Bacon		
	United Kingdom	13 <sup>th</sup> Century
Earl of Warwick	United Kingdom	14 <sup>th</sup> Century
Henri Braconnot	France	19 <sup>th</sup> Century
Theophile J Pelouze	France	19 <sup>th</sup> Century
Christian Schoenbein	Germany	19 <sup>th</sup> Century
Major E Schultze	Germany	19 <sup>th</sup> Century
Alfred Nobel	Sweden	19 <sup>th</sup> Century
Hermann Sprengel	Germany	19 <sup>th</sup> Century
Paul Vieille	France	19 <sup>th</sup> Century
Julius Wilbrand	Germany	19 <sup>th</sup> Century
		19 <sup>th</sup> Century
EI DuPont de Nemours	USA	20th Century
	United Kingdom	20 <sup>th</sup> Century
	United Kingdom	20 <sup>th</sup> Century
Robert Schmitt and Jeffrey C Bottars	United Kingdom	20 <sup>th</sup> Century
Kurt Bann and Tom Archibald	USA	20 <sup>th</sup> Century
Arnold Nielsen	United Kingdom	20th Century
	USA	20 <sup>th</sup> Century
	Henri Braconnot Theophile J Pelouze Christian Schoenbein Major E Schultze Alfred Nobel Hermann Sprengel Paul Vieille Julius Wilbrand I DuPont de Nemours  Robert Schmitt and Jeffrey C Bottars Kurt Bann and Tom Archibald	Henri Braconnot Theophile J Pelouze Theophile J Pelouze Christian Schoenbein Major E Schultze Alfred Nobel Hermann Sprengel Germany Paul Vieille France Julius Wilbrand Germany  I DuPont de Nemours USA United Kingdom United Kingdom Jeffrey C Bottars Kurt Bann and Tom Archibald Arnold Nielsen United Kingdom United Kingdom United Kingdom

#### 1.2. Definition & Introduction

The energetic material is a class of compounds with a great amount of available stored chemical energy that can be released mainly by reactivity/sensitivity. Upon external stimulation, the energetic materials release high levels of energy that result in heat, light, and sound, as well as large volume of gases.

The typical energetic materials are the organic compounds containing carbon, hydrogen, nitrogen, and oxygen elements. During detonation, nitrogen atoms transform into nitrogen ( $N_2$ ) gas, carbon and hydrogen atoms bind with oxygen to form gaseous products. While,  $-NO_2$  and  $-ONO_2$  groups are the major source of oxygen, which helps for the detonation or combustion processes. Thus, explosive materials are designed based on density, positive heats of formation, high oxygen content.

#### 1.3. Explosophores

Explosophore is named as "phospophore" and was first originated by Russian scientist "V. Pletz" in 1935. By reacting with oxygen, the chemical groups in the energetic molecules form stable products; this could enhance heat of formation by producing gaseous products. The chemical groups are called 'explosophores' and are segregated in eight categories:<sup>5</sup>

- i)  $-NO_2$ , -ONO,  $-ONO_2$
- ii)  $-N=N-, -N=N^+=N-$
- iii) -NX<sub>2</sub> group like NCl<sub>3</sub> and RNCl<sub>2</sub>
- iv) –C=N–O– group
- v) –OClO<sub>2</sub> and –OClO<sub>3</sub>
- vi) -O-O and -O-O-O-
- vii) –C≡C<sup>-</sup> M<sup>+</sup> group
- viii) A metal atom connects with unstable bonded to carbon of organic radicals

Particularly nitrogen containing groups, shown in i, ii, and iii are explosophoric. The oxygen source in these molecules produce heat when react with other groups and the overall process is exothermic.

#### 1.4. The classification of High-Energy Materials (HEMs)

Explosives, propellants, and pyrotechnic materials are under energetic materials. **Figure 1.4.1** presents a schematic representation of EMs classification based on the rate of reactions and products created during the reactions.<sup>6</sup>

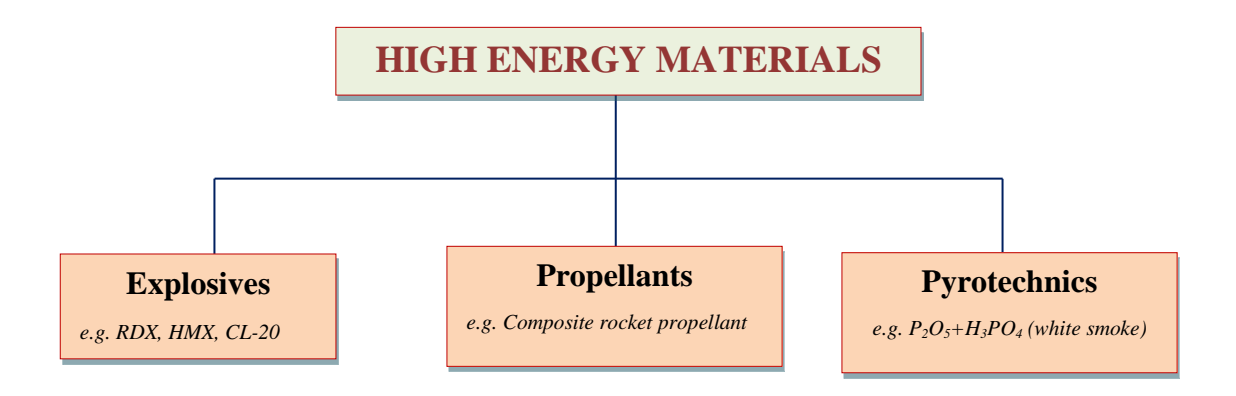


Figure 1.4.1. Category of high energy materials

#### 1.4.1. Explosives:

An explosive is a material, either a pure single substance or a mixture of substances, which is capable of producing an explosion by its own energy.

In this process, sudden transformations occur in the molecules that produce heat and gas.<sup>7</sup> The production of heat alone by the inherent energy of the substance also makes the compound explosive.



**Figure 1.4.1.1.** An overview representation of explosives

#### **1.4.1.1.** Classification of Explosives:

- ➤ Depending upon chemical composition, properties, and applications, HEMs are classified into:
  - a) Nitro explosives: These compounds contain nitro (-NO<sub>2</sub>) groups in the carbon skeleton. i.e. C-NO<sub>2</sub>

Eg: Trinitrobenzene, Trinitrotoluene, Picric acid, etc.

b) Nitrate esters: These compounds contain nitric ester (-ONO<sub>2</sub>) groups in the carbon skeleton. i.e C-ONO<sub>2</sub>

Eg: Nitroglycerine, Diethylene glycol dinitrate (DEGDN), Pentaerythritol tetranitrate (PETN), Nitrocellulose (NC), Polyvinylnitrate (PVN), etc.

c) Nitramines: These compounds contain nitramine (N–NO<sub>2</sub>) groups in the carbon skeleton.

Eg: Tetryl, Cyclonite (RDX), Octogen (HMX), etc.

d) Heavy metal azides

Eg:  $AgN_3$ ,  $Pb(N_3)_2$ ,  $TlN_3$ , etc.

- e) Others: Peroxides, Ozonides, Acetylides, etc.
- > The explosives have been classified as follows.
  - 1.4.1.1.1 Thermally stable or heat resistant explosives
  - 1.4.1.1.2. High-performance explosives
  - 1.4.1.1.3. Melt-cast explosives
  - 1.4.1.1.4. Insensitive explosives

#### 1.4.1.1.1. Thermally stable explosives:

Explosives that are thermally stable at high temperatures are commonly referred to as 'Thermally stable explosives'. Thermostability is a key characteristic of energetic materials (safe working temperature >180 °C). Production of these explosives or explosive compositions are safe, as they are stable at high temperature. These materials used in the development of space programs, drilling of oil-wells etc.

The following synthetic techniques help making molecules by better thermal stability.

- Condensation with a five-membered triazole
- Introducing amino groups
- Introducing conjugation
- Formation of salt

#### 1.4.1.1.2. High Performance Explosives:

High density and high velocity of detonation (VOD) makes the molecule a high performance energetic material. Thus, significant workforce always gone to develop a high performing explosive for warhead applications. Detonation performance primarily depends on density of the molecule because detonation velocity and pressure of the explosives increase proportionally with the density and square of the densities, respectively. On the other hand, an increase in oxygen balance (O.B.) and heat of formation generally increases its performance. Few notable familiar high-performance explosives are presented in **Figure 1.4.1.1.2.1.** For example: 1,3,3-Trinitroazetidine (TNAZ), Hexahydro-1,3,5-trinitro-1,3,5-triazine (RDX), 1,3,5,7-Tetranitro-1,3,5,7-tetrazoctane (HMX), 4,10-Dinitro-4,10-diaza-2,6,8,12-tetraoxaisowurtzitane (TEX),

2,4,6,8,10,12-Hexanitro-2,4,6,8,10,12-hexaazaisowurtzitane (CL-20), Octanitrocubane (ONC), and Octaazidocubane (OAC)

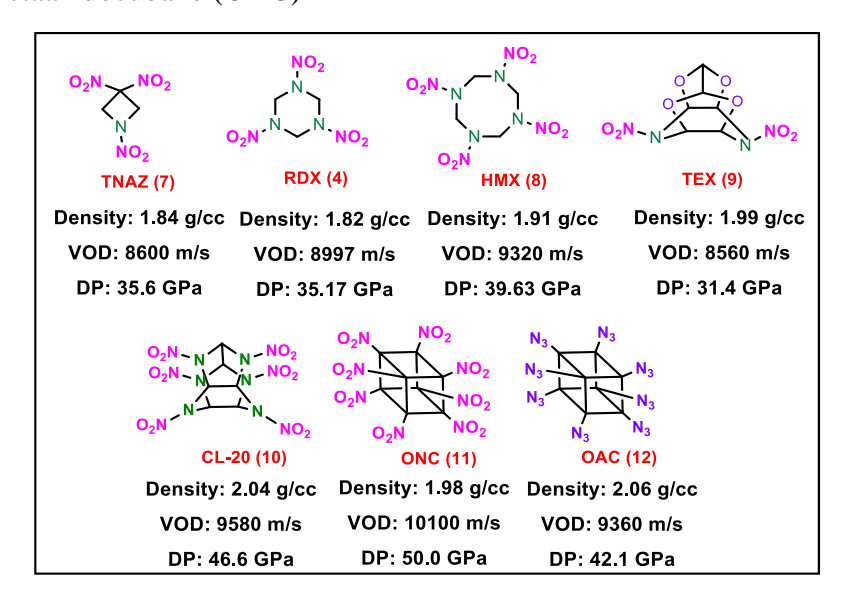


**Figure 1.4.1.1.2.1.** The known high-performance explosives

#### 1.4.1.1.3. Melt-Cast explosives:

Melt-cast explosives are usually molecules with large variations in melting and decomposition temperatures (Td > 240 °C). Melt-cast explosives are loaded in the ammunition of a melt state. In general, to avoid compression by inertia, the charge density must be at least equal to the inertial pressure (impact). Few examples of prominent melt-castable explosives are highlighted in **Figure 1.4.1.1.3.1.** For example: 2,4,6-Trinitrotoluene (TNT), Cyclobutane tetranitrate ester (CBTNE), 1-Methyl-2,4,5-trinitroimidazole (MTNI), 2,4-Dinitroanisole (DNAN), and Bis(nitroxymethylisoxazolyl) furoxan (BINF)

**Figure 1.4.1.1.3.1.** The known melt-cast explosives

#### 1.4.1.1.4. Insensitive Explosives:

The insensitive explosives have been largely used for various applications. Mainly the insensitive energetic materials can be transported in large quantities with less vulnerability of armored vehicles. In general, introduction of a) nitrogen-rich heterocycles or their *N*- oxides, b) nitro and amino groups in the ring *ortho* to each other, and c) picryl moiety that could enhance material insensitivity. The formation of hydrogen bonds between nitro and amino

groups increases molecule stability.<sup>11</sup> Some of the most prominent insensitive explosives are shown in **Figure 1.4.1.1.4.1.** For example: Triaminotrinitrobenzene (TATB), 1,1-Diamino-3,5-dinitro-pyrazine-1-oxide (FOX-7), 3-Nitro-1,2,4-triazol-5-one(NTO), 2,6-Diamino-3,5-dinitro-pyrazine-1-oxide (LLM-105), and Tetra-oxadinitramino-isowurtzitane (TEX)

**Figure 1.4.1.1.4.1.** The known insensitive explosives

#### 1.4.2. Propellants:

A propellant is a kind of substance that can cause something to move forwards by applying motive force. Which is burned with an oxidizer resulting large volume of hot gas. <sup>12</sup> The charge of explosive can propel a projectile from something, *i.e.* gun and rocket. Propellants have been used to disperse aerosol, powders, and products as cleaners, waxes and aerosol spray cans etc. It may be gas, liquid or solid.

The classification of propellants is illustrated in **Figure 1.4.2.1**, which categorizes as gun propellants and rocket propellants.

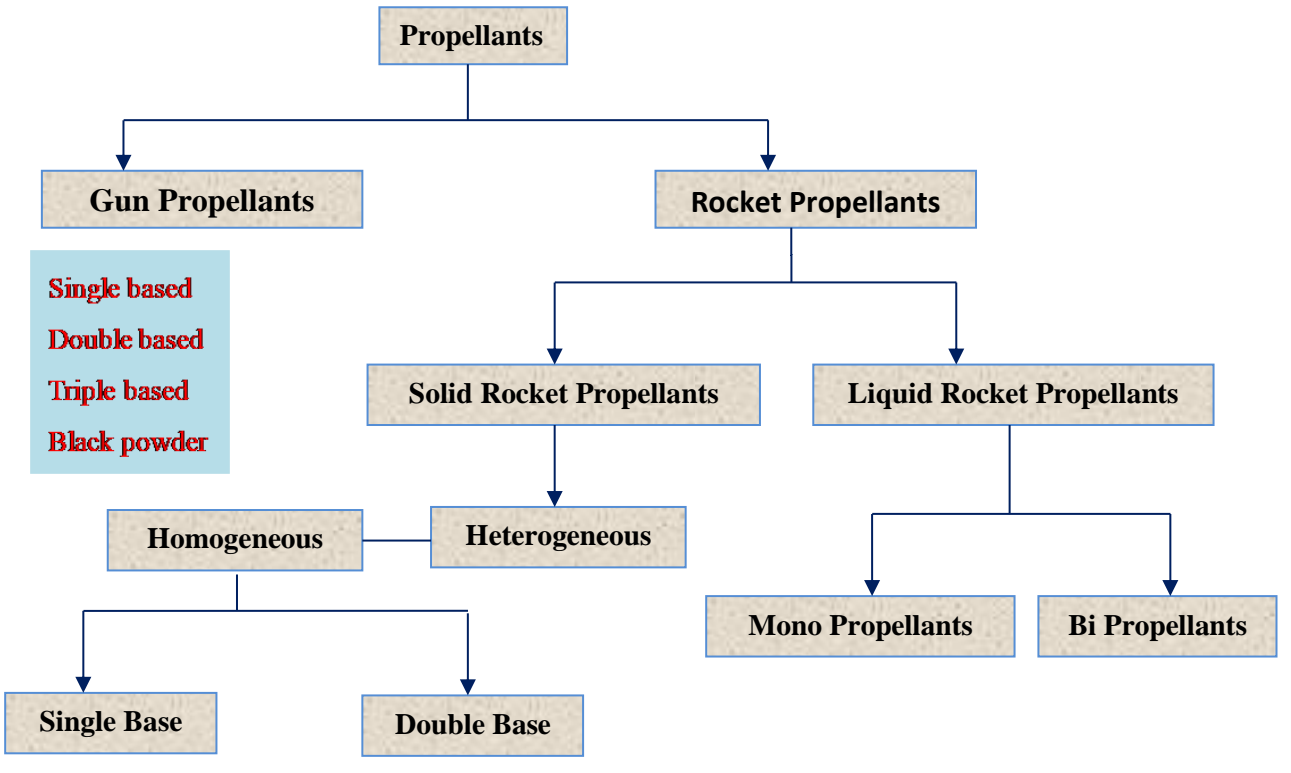
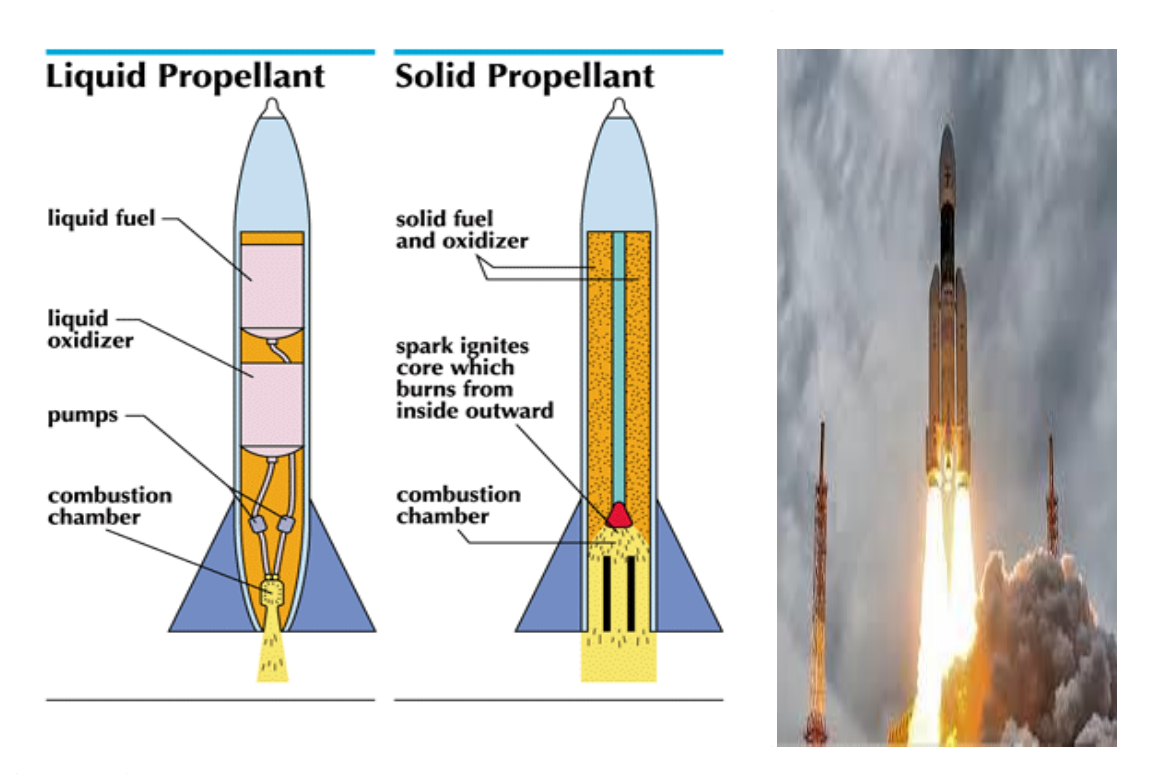


Figure 1.4.2.1. Classification of propellants.

**1.4.2.1. Gun Propellants:** Gun propellant generates large amount of gases and propel projectiles at high kinetic energy. Nitrocellulose (NC) materials are generally used for making gun-propellants. Likewise nitroglycerine (NG), nitroguanidine, and nitramines have also been used for building gun-propellants. In addition, size and shape of the propellant grain plays important.

**1.4.2.2. Rocket Propellants:** Rocket propellant produces hot gas that can be expanded and accelerated through a nozzle, thereby producing a reaction force or thrust in the opposite direction. The solid, liquid, and hybrid (combination of solid and liquid) propellants have been used.



**Figure 1.4.2.2.1.** Diagrammatic representation of solid and liquid propellants

#### 1.4.3. Pyrotechnics:

Pyrotekhnikos is a Greek word for art and pyr (fire). Thus, the effect observed by burning materials composition is called 'pyrotechnic'. Pyrotechnics can firmly produce smoke or fire and light when ignited. The heat generating pyrotechnics have been used for priming charges, detonators, incendiary compositions, or matches. While smoke generating pyrotechnics have been used for camouflage and signalling purposes. The light emitting pyrotechnics are used for illumination (visible and infrared), fireworks or decoy flares.<sup>13</sup>



Figure 1.4.3.1. Diagrammatic representation of pyrotechnics.

#### 1.5. Parameters Responsible for Explosive and Energetic Materials:

#### **1.5.1. Density** (ρ)

Density (also known as 'specific mass') is indicated in terms of specific gravity. Density is an important factor for both propellants and explosives. <sup>14-16</sup> It is directly proportional to both VOD and brisance that the mass of EM per unit volume is determined. It is also defined as ratio between explosive weight and explosion volume, referred to "theoretical maximum density" (TMD), and can be measured by using gas pycnometer.

#### 1.5.2. Detonation Performance

Performance is the ability of the explosive to deliver energy and is determined by Kamlet and Jacobs as density, detonation velocity (vD), detonation pressure (P), and heat of detonation. <sup>16,17</sup> Kamlet-Jacobs equations were used to evaluate **D** and **P** values of an EMs of CHNO explosives:

$$\begin{split} D &= A(\text{NM}^{1/2}Q^{1/2})^{1/2}(1+B\rho) &\qquad (A=1.01,B=1.30) \\ P &= K\rho^2\text{NM}^{1/2}Q^{1/2} &\qquad (K=15.58) \end{split}$$

Where, **D** is the detonation velocity (expressed in units of kms<sup>-1</sup>), **P** is the detonation pressure (expressed in units of **GPa**), **N** is moles of gaseous detonation products per gram of explosives, **M** is the average weight of gaseous products, **Q** is the chemical energy of the detonation (kJ mol<sup>-1</sup>) and  $\rho$  is the initial density of explosive (g/cm<sup>3</sup>). Commonly, used EMs has VODs ranging from 1500 m/s to over 9000 m/s.

#### 1.5.3. Heat of Formation ( $\Delta H_f$ )

A thermo chemical property of EM is the heat of formation (also called 'enthalpy of formation'), which plays a significant role in the heat of detonation, as well as in prediction of other associated parameters. Heat of formation (HOF) is defined as the amount of heat released or

absorbed from its elements during the formation of substances at normal physical state (gas, liquid, or solid) and is expressed in kJ mol<sup>-1</sup>. The value could be positive or negative. <sup>14,18,19</sup>

#### 1.5.4. Heat of Explosion (Q)

The 'Heat of detonation' or 'Heat of explosion' (also denoted by  $Q_{\rm expl}$ ) is used to measure the energy content of organic energetic compounds that can be liberated during the detonation and reported in kJ mol<sup>-1</sup> or kJ kg<sup>-1</sup>. Heat of explosion plays vital for measuring detonation pressure or velocity of EM.

#### 1.5.5. Oxygen Balance (OB)

Oxygen balance determines oxidizer or explosive property of EM. The oxygen content is represented by OB. Basically the amount of oxygen remains upon carbon, hydrogen, and metal oxidation to produce carbon dioxide, water, and metal oxide, etc.  $^{14,20,21}$  By using the formula  $C_xH_yN_aO_z$  and the mass M of the molecule, the OB is calculated by applying the following formula: The unit of OB is %.

OB% = 
$$\frac{-1600}{\text{Mol. wt. of explosive}} (2X + Y/2 + M - Z)$$

Where

X = number of carbon atoms, Y = number hydrogen atoms, Z = number of oxygen atoms, and M = number of metal atoms (metallic oxide produced).

#### 1.5.6. Sensitivity

The sensitivity of high energy materials (HEMs) is affected by external stimuli such as impact, friction, shock, and electrostatic discharge. Extreme care is therefore required for the synthesis as well characterization of HEMs (e.g., formulation, processing, storage, and transportation). Thus, sensitivity studies must be tested before handling/transporting the HEMs. 13,16,22

#### 1.5.7. Sensitivity to Impact

An EM's impact sensitivity is the ability to tolerate the impact caused by a weight dropping from a certain height. The standard BAM Fall Hammer instrument is used for its measurement. Impact energy is expressed in joules (J).<sup>6,16,22</sup>

#### 1.5.8. Sensitivity to Friction

The friction sensitivity of a HEM measures the sensitivity of two objects in contact while they move relative to each other. The standard BAM-friction tester determines the friction energy and is described in Newton (N).<sup>6,16,22</sup>

#### 1.6. Thermally Stable and Insensitive Energetic Materials (TSI-EMs):

Explosive with better performance in combination of safety to handle, thermal stability, and insensitivity are essential. Thus, continuous studies have been directed for the synthesis of thermally stable and insensitive energetic materials. In this context, synthesis of N and Orich five-membered azole-substituted compounds have been made and used as energetic materials. A brief account to the synthetic strategies developed for the azole based energetic molecules is herein discussed.

1.6.1. Pyrazole based TSI-EMs

1.6.2. Imidazole based TSI-EMs

1.6.3. Triazole based TSI-Ems

1.6.3.1. 1,2,3-triazole based EMs

1.6.3.2. 1,2,4-triazole based EMs

1.6.4. Oxadiazole based TSI-EMs

1.6.4.1. 1,2,4-oxadiazole based Ems

1.6.4.2. 1,2,5- oxadiazole based Ems

1.6.4.3. 1,3,4- oxadiazole based EMs

1.6.5. Tetrazole based TSI-EMs

#### 1.6.1. Pyrazole based energetic materials:

Pyrazole belongs to the family of five-membered rings with three carbon atoms and two adjacent nitrogen atoms. Pyrazole exist in three tautomers, i.e. 1*H*-pyrazole, 3*H*-pyrazole, and 4*H*-pyrazole (**Figure 1.6.1.1**).

Figure 1.6.1.1. Three tautomeric forms of pyrazole

In 1883, the pyrazole motif was at first synthesized from 3-oxoburtanoate and phenyl hydrazide.<sup>23</sup> The structure of 3-methyl-1-phenyl-1*H*-pyrazol-5-ol was found in 1887. The decarboxylation of 1*H*-pyrazole-3,4,5-tricarboxylic acid has led to 1*H*-pyrazole.<sup>24</sup>

In recent years, pyrazole-based compounds have been widely used as energetic materials due to its large enthalpy of formation and high density. Nitrated-pyrazole-based energetic compounds showed good applications in explosives, propellants, and pyrotechnics, because of high thermal stability, low sensitivity, and high detonation performance. Moreover, these compounds are environment eco-friendly.

Figure 1.6.1.2. Pyrazole fused thermally stable and insensitive energetic molecules (20–36)

Some of the representative pyrazole based thermally stable energetic molecules are shown in **Figure 1.6.1.2.** In addition, the pyrazole-linked-*N*-heterocycles have also served potential energetic materials; some of the compounds in this arena have been depicted in **Figure 1.6.1.3.** Thus, design and synthesis of pyrazole based energetic molecules always draw continuous attention.<sup>25-29</sup>

Figure 1.6.1.3. Pyrazole bridged thermally stable and insensitive energetic materials (37–58)

#### 1.6.2. Imidazole based energetic materials:

Imidazole motif contains three carbon atoms and two non-adjacent nitrogen atoms. In recent years, nitrated-imidazole-based molecules have been largely used as energetic applications.

Figure 1.6.2.1. The nitrated-imidazole derivatives (59–63)

The nitroimidazole derivatives such as 2,4-dinitroimidazole, 4,5-diniroimidazole, 1,4-dinitroimidazole, and 2,4,5-trinitroimidazole (TNI) have been synthesized and used as high energy materials. The TNI-species is unstable at room temperature, while the N-methyl-TNI is thermally stable (310 °C). Some of the representative imidazole bearing thermal stable and low sensitive energetic compounds are listed in **Figure 1.6.2.2.**<sup>30-32</sup>

Figure 1.6.2.2. Imidazole bearing thermal stable insensitive energetic molecules (64–80)

#### **1.6.3.** Triazole based energetic materials:

Triazole is a five-membered aromatic heterocycle possessing two carbons and three nitrogen atoms. Triazoles exhibit as 1,2,3-triazole and 1,2,4-triazole.

Figure 1.6.3.1. Basic skeleton of 1,2,3-triazole and 1,2,4-triazole

The nitrogen-rich triazole heterocycles are useful energetic compounds showing broad applications in military and civilian domains. Recently, triazole compounds received considerable interest for the construction of new energetic materials.

#### 1.6.3.1. 1,2,3-Triazole based energetic materials:

1,2,3-Triazole five-membered aromatic heterocycle has two carbon atoms and three nitrogen atoms; the nitrogen atoms are attached adjacent to each other. Moreover, 1,2,3-triazoles exist in two tautomers: 1*H*-1,2,3-triazoles and 2*H*-1,2,3-triazole. Substituted 1,2,3-triazole has been readily prepared by "azide-alkyne Huisgen 1,3,-dipolar cycloaddition.<sup>33</sup>

1,2,3-Triazole is a potential energetic backbone exhibiting heat of formation 240 kJmol<sup>-1</sup>. Incorporation of nitro, nitramino, dinitromethyl, and trinitromethyl moieties into triazole backbone improves density as well energetic performance of the compound. In this context, pyrazole, tetrazole, and oxadiazole linked 1,2,3-triazole compounds showed better performance and useful as primary and secondary explosives. Some of the representative molecules are listed in **Figure 1.6.3.1.1**.<sup>34-38</sup>

**Figure 1.6.3.1.1.** Thermally stable and insensitive coupled and azo-linked 1,2,3-triazole derivatives (81–88).

**Figure 1.6.3.1.2.** Heteroaryl fused 1,2,3-triazole derivatives as thermally stable and insensitive energetic materials (**89–97**)

#### 1.6.3.2. 1,2,4-Triazole based energetic materials:

In case of 1,2,4-triazole, two nitrogen atoms are attached adjacent to each other. The 1,2,4-triazoles exist in two tautomers: 1*H*-1,2,4-triazoles and 4*H*-1,2,3-triazole. Moreover, 1,2,4-triazole possess heat of formation 182 kJ mol<sup>-1</sup>. The 1,2,4-triazole motif has been present in the energetic molecules of high-performance, propellants, and pyro-techniques. In addition, 1,2,4-triazole offers wide opportunity for further substitution. Thus, various *N*-heterocycles e.g., pyrazole, triazoles, tetrazole, and furazan can be readily incorporated on 1,2,4-triazole skeleton.

Furthermore, introduction of energy-rich functional groups: such as  $-NO_2$ ,  $-ONO_2$ ,  $-NNO_2$ , -N=N-, and  $-N_3$  on 1,2,4-triazole could enhance density, enthalpy of formation, stability, as well insensitivity of the compounds. While the polyazido substituted derivatives are relatively more sensitive. Further functionalization of 1,2,4-triazole framework by N-amination, C-amination, N-hydroxylation, and N-alkylation has led to new molecular entities (**Figure 1.6.3.2.1**, **Figure 1.6.3.2.2**, and **Figure 1.6.3.2.3**).

Figure 1.6.3.2.1. Poly N-rich fused 1,2,4-triazole derivatives (98–107)

**Figure 1.6.3.2.2.** Coupled and bridged 1,2,4-triazole derivatives as thermally stable and insensitive materials (**108–120**)

Figure 1.6.3.2.3. Heteroaryl fused 1,2,4-triazole derivatives (121–128)

#### 1.6.4. Oxadiazole based energetic materials:

The five-membered oxadiazole heterocycles contain two-carbon atoms, two-nitrogen atoms, and one-oxygen atom. Oxadiazole scaffolds exist in four isomers: 1,2,3-oxadiazole, 1,2,4-oxadiazole, 1,2,5-oxadiazole, and 1,3,4-oxadiazole as shown in **Figure 1.6.4.1.** 

Figure 1.6.4.1. Four isomers of oxadiazole

1,2,4-Oxadiazole, 1,2,5-oxadiazole, and 1,3,4-oxadiazole are widely used in drugs with better pharmaceutical properties; moreover, these motifs have been used in the energetic materials due to its high positive heat of formation. Among all the isomers, 1,2,3-oxadiazole is unstable; the ring opens readily to produce diazoketone tautomer. Importantly, 1,2,4-oxadiazole possesses high positive heat of formation and slightly low energy than 1,3,4-oxadiazole. Thus, significant research has been directed for the development of stable and insensitive energetic materials on 1,2,4-oxadiazole and 1,3,4-oxadiazole.

#### 1.6.4.1. 1,2,4-Oxadiazole based energetic materials:

The five membered 1,2,4-oxadiazoles are aromatic heterocycles contain two nitrogen and one oxygen heteroatoms. The common synthetic methods for 1,2,4-oxadiazole and its derivatives

are shown in **Figure 1.6.4.1.1.** The basic skeleton can be made by condensation of nitriles with hydroxylamine followed by cyclization cascade (**Figure 1.6.4.1.1**).

The 1,2,4-oxadiazoles are largely found in bioactive compounds as bioisosters. N, O-rich 1,2,4-oxadiazole derivatives have been found in great abundance in energetic materials due to their good balance of energy and stability. Moreover, 1,2,4-oxadiazole ring possesses high positive heat of formation than 1,3,4-oxadiazole ring. Thus, a large variety of thermally stable and insensitive 1,2,4-oxadiazole-based EMs have been synthesized (**Figure 1.6.4.1.2** and **Figure 1.6.4.1.3**). 45-48

$$RCN - \begin{bmatrix} N^{+}OCOR' & A & N^{+}OCOR' \\ NH_{2} & R' & NH_{2} & A \\ NH_{2} & R' & NH_{2} & A \\ R' & NH_$$

Figure 1.6.4.1.1. Synthetic methods for 1, 2, 4-oxadiazole

**Figure 1.6.4.1.2.** 1,2,4-Oxadiazole bearing thermally stable insensitive EMs (129–137)

**Figure 1.6.4.1.3.** 1,2,4-Oxadiazole bearing thermally stable insensitive energetic materials (138–153)

#### 1.6.4.2. 1,2,5-Oxadiazole (furazan) based energetic materials:

1,2,5-Oxadiazole, a member of oxadiazole family, also known as furazan. Furazan is a five-membered aromatic heterocycle consisting of two carbon atoms, one oxygen and two nitrogen heteroatoms. The furazan derivatives are mostly synthesized from oximes of 1,2-diketones.

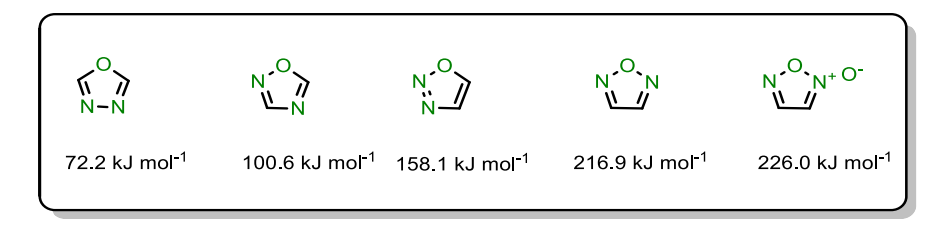


Figure 1.6.4.2.1. Positive enthalpy of formation for oxadiazole isomers

Among oxadiazole isomers, 1,2,5-oxadiazole constitutes high heat of formation. Importantly, 1,2,5-oxadiazole-2-oxide (furoxan) received significant attention in the development of energetic materials. The furazan or furoxan ring possess high detonation performance and good oxygen balance. The furoxan ring exhibits highest positive heat of formation among the oxadiazole family (**Figure 1.6.4.2.1**). Thus, furazan motif has been widely employed for the synthesis the new HEDMs. Installation of energetic functional groups, such as –NO<sub>2</sub>, –NHNO<sub>2</sub>, and –N=N– on furazan backbone enhances detonation performance and stability of the molecule. The thermally stable and insensitive 1,2,5-oxadiazole and furoxan-based energetic materials are shown in **Figure 1.6.4.2.2**, **Figure 1.6.4.2.3**, **Figure 1.6.4.2.4**, **Figure 1.6.4.2.5**, and **Figure 1.6.4.2.6**.

**Figure 1.6.4.2.2.** 1,2,5-Oxadiazole bridged thermally stable insensitive energetic materials (154–160)

**Figure 1.6.4.2.3.** 1,2,5-Oxadiazole based thermally stable insensitive energetic materials (161–182)

Figure 1.6.4.2.4. Furoxan based thermally stable insensitive energetic materials (183–190)

**Figure 1.6.4.2.5.** Imine bridged furoxan based thermally stable insensitive energetic materials (191–195)

**Figure 1.6.4.2.6.** *N*,*N'*-Azo bridged 1,2,5-oxadiazole based thermally stable insensitive energetic materials (**196–206**)

#### 1.6.4.3. 1,3,4-Oxadiazole based energetic materials:

The heterocycle 1,3,4-oxadiazole contains one oxygen and two nitrogen heteroatoms. The common synthetic pathways for 1,3,4-oxadiazole and its derivatives are shown in **Figure 1.6.4.3.1.** 

$$R' \stackrel{N}{\longrightarrow} N^{H_2}$$

$$R' \stackrel{N}$$

Figure 1.6.4.3.1. Synthetic pathway for 1,3,4-oxadiazole scaffolds

In recent decades, 1,3,4-oxadiazole has attracted attention in the design of novel HEDMs due to its high density, high positive heat of formation, good oxygen balance, and thermal stability. In comparison to 1,2,5-oxadiazole ring, 1,3,4-oxadiazole ring is symmetric; as a result, 1,3,4-oxadiazole ring is relatively more stable. In corporation of explosophore groups, such as nitramino, dinitromethyl, trinitromethyl, dinitroethyl and trinitroethyl on 1,3,4-oxadiazole backbone enhances energetic performance of the molecule. Thus, a wide range of N,O-rich 1,3,4-oxadiazole-based molecules have been synthesized; these molecules exhibit good energetic properties and are thermally stable and insensitive (**Figure 1.6.4.3.2** and **Figure 1.6.4.3.3**). <sup>56-59</sup>

**Figure 1.6.4.3.2.** 1,3,4-Oxadiazole bearing thermally stable and insensitive energetic molecules (207–212)

**Figure 1.6.4.3.3.** 1,3,4-Oxadiazole bridged thermally stable and insensitive energetic molecules (213–226)

#### 1.6.5. Tetrazole based energetic materials:

The aromatic tetrazole heterocycles is five-membered four nitrogen and one carbon bearing species. Tetrazole exist in three isomers: 1*H*-tetrazole, 2*H*-tetrazole, and 5*H*-tetrazole, wherein the double bond positions are different (**Figure 1.6.5.1**). The 1*H*-tetrazole and 2*H*-tetrazole isomers are tautomers and are aromatic, while 5*H*-tetrazole is non-aromatic.

**Figure 1.6.5.1.** Three isomers of tetrazole

1*H*-Tetrazole was at first synthesized from the reaction of anhydrous hydrazoic acid and hydrogen cyanide under pressure. Wherein 5-aminotetrazole was readily accessed from

aminoguanidine through diazotization and base mediated intramolecular cyclization and is commercially available (**Scheme 1.6.5.1**)..<sup>60</sup>

**Scheme 1.6.5.1:** Synthesis of 5-aminotetrazole and 1*H*-tetrazole

Owing to the high nitrogen contents, tetrazole motifs have been largely used for the synthesis of new energetic nitrogen-rich compounds with high heats of formation (+237 kJ mol<sup>-1</sup>; 5*H*-tetrazole).

**Figure 1.6.5.2.** Tetrazole derivatives as thermally stable and insensitive energetic materials (227–242)

Among nitrogen-containing heterocycles, tetrazole possess second-highest nitrogen content (above 80%). For example, the nitrogen-content of 5*H*-tetrazole, 5-azido tetrazole, and anion of this compound is 80%, 88.28%, and 89.09%, respectively. However, tetrazole derivatives are energetically powerful but are sensitive to heat and friction. To address these inherent drawbacks, alkyl and aryl substitutes on tetrazole moiety have been introduced; effort has therefore been devoted to develop new molecular regime of tetrazole bearing energetic molecules with low sensitivity to impact and friction along with enhanced thermal stability (**Figure 1.6.5.2** and **Figure 1.6.5.3**). 61-68

Figure 1.6.5.3. Tetrazole coupled thermally stable and insensitive energetic molecules (243–256)

## 1.7. Objective of the thesis

This chapter enumerates highlighting the importance of energetic materials with better performance and stability. The synthesis of high energy materials (HEDMs) based on high density; good detonation velocity and pressure, high heat of formation and thermal stability along with insensitivity to impact and friction are highlighted. As compounds insensitivity and thermal stability are highly important, thus, new molecular regime of energetic materials has been accordingly designed and new pathways have been envisaged. The research area connected to the synthesis of energetic molecules with better performance, therefore, attracts attention. This chapter summarizes addressing the importance of five-membered N- and O-bearing heterocycle scaffolds in connection to the development of eco-friendly energetic material application.

From the above discussion, design and development of five-membered N- and O-rich heterocycle energetic molecules with low sensitivity and high thermal stability has been envisaged and the efforts have been detailed in the subsequent chapters. The design and synthesis of new energetic materials have been attempted by seriously considering the following factors:

- ✓ Theoretical calculations to predict the HOF
- ✓ Aboriginal availability of starting materials
- ✓ Simple and ease of its preparation
- ✓ Cost effectiveness process
- ✓ Compounds insensitivity and thermal stability

#### 1.8. References

- 1. Urbanski and Tadeusz, Chemistry and Technology of Explosives, Vols.1-4 pergamon press, 1964, 1965, 1967, 1984.
- 2. S. Venugopalan, *Demystifying Explosives: Concenpts in high energy materials*, 1st edn. Elsevier, **2015**.
- 3. J. P. Agarwal, *High Energy Materials: Propellants, Explosives and Pyrotechnics*, Wiley-VCH, Verlag GmbH, Weinheim, **2010**.
- 4. M. Gobel, Dissertation, MUNCHEN, Ludwing Maximilians University, 2009, 25.
- 5. (a) Handrick, G.R., Lothrop, W.C. *Chem. Rev.*, **1949**, *44* (3) p 419–445; (b) Warey, Philip. B. ed. *New Research on Hazardous Materials*, Nova Science Publishers, **2007**.
- 6. M. Gobel, *Dissertation*, MUNCHEN, Ludwing Maximilians University, **2009**, p. 49–50;
- 7. A. Bailey, S. G. Murrey, *Explosives propellants and pyrotechnics*, Brassey's, London, **2000**.
- 8. (a) G. B. Mannelis, G. M. Nazin, Y. I. Rubtsov and V. A. Stunnin, *Thermal decomposition and combustion of explosives and propellants*, Taylor & Francis, **2003**; (b) G. I. Brown, *Explosives*, the history press ltd, **2010**.
- 9. M. J. Kamlet, S. J. Jacobs, J. Chem. Phys. 1968, 48, 23.
- (a) R. M. Matyas and J. Pachman, *Primary Explosives*, Springer-Verlag Berlin and Heidelberg GmbH & Co. K, 2013;
   (b) J. I. Gransden, M. J. Taylor, *Propellants Explos. Pyrotech.*, 2007, 32, 435.
- 11. (a) J. P. Agrawal, Central European journal of energetic materials. 2012, 9(3), 273; (b)C. D. Kalb, Manual of explosives, Biblio Bazaar, LLC, 2009.
- 12. W. R. Quinan, *High explosives*, Biblio Bazaar, LLC, **2009**.
- 13. (a) J. A. Conkling, *Chemistry of Pyrotechnics: Basic Principles and Theory*, Marcel Dekker, Inc., New York, USA, **1985**; (b) J. H. McLain, *Pyrotechnics*. The Franklin Institute Press, Philadelphia, Pennsylvania, USA, **1980**.
- 14. J. Akhavan, The chemistry of explosives, RSC Paperbacks, Cambridge, 1998.
- 15. N. Kubota, *Propellants and explosives*, John Wiley & Sons, 2007.
- 16. T. M. Klapötke, Chemistry of High Energy Materials, 2011.
- 17. J. P. Agarwal, Propellants Explos. Pyrotech. 2005, 30, 316.
- 18. J. Stierstorfer, K. R. Tarantik, Thomas M. Klapötke, Chem. Eur. J., 2009, 15, 5775.
- 19. N. Fischer, T. M. Klapötke, M. Reymann, J. Stierstorfer, Eur. J. Inorg. Chem., 2013, 2167.

- 20. R. Meyer, J. Kohler, A. Homburg, *Explosives*.5th edn. Wiley-VCH, Verlag GmbH, Weinheim, **2002**.
- 21. S. Nauckhoff, O. Bergstrom, Nitroglycerine and dynamite, Nitroglycerin, Sweden, 1959.
- 22. G. I. Brown, *Explosives*, the history press ltd, **2010**.
- 23. Knorr, L. (1883). "Action of ethyl acetoacetate on phenylhydrazine. I". *Chemische Berichte*. 16: 2597–2599.
- 24. Von Pechmann, Hans (**1898**). "Pyrazol aus Acetylen und Diazomethan". *Berichte der deutschen chemischen Gesellschaft* (in German). *31* (3): 2950–2951.
- 25. (a) Y. Tang, C. He, H. Gao and J. M. Shreeve, *J. Mater. Chem. A*, **2015**, *3*, 15576–15582;
  (b) J. Zhang, C. He, D. A. Parrish, and J. M. Shreeve, *Chem. Eur. J.*, **2013**, *19*, 8929–8936;
  (c) P. Yin, J. Zhang, D. A. Parrish, and J. M. Shreeve, *Chem. Eur. J.*, **2014**, *20*, 16529–16536;
  (d) D. Kumar, G. H. Imler, D. A. Parrish and J. M. Shreeve, *Chem. Eur. J.*, **2017**, *23*,7876–7881;
  (e) H. Li, L. Zhang, N. Petrutik, K. Wang, Q. Ma, D. Shem-Tov, F. Zhao, and M. Gozin, *ACS Cent. Sci.*, **2020**, *6*, 1, 54–75;
  (f) N. P. Burlutskiy and A. S. Potapov, *Molecules*, **2021**, *26*, 413.
- 26. (a) P. Yin, J. Zhang, C. He, D. A. Parrish and J. M. Shreeve, *J. Mater. Chem. A*, **2014**, 2, 3200–3208; (b) P. Yin, D. A. Parrish, and J. M. Shreeve, *J. Am. Chem. Soc.*, **2015**, *137*, 4778–4786; (c) C. Lei, H. Yang and G. Cheng, *Dalton Trans.*, **2020**, *49*, 1660–1667.
- 27. (a) J. Zhang, D. A. Parrish, and J. M. Shreeve, *Chem. Asian J.*, 2014, 9, 2953–2960; (b) J. Zhang, P. Yin, L. A. Mitchell, D. A. Parrish and J. M. Shreeve, *J. Mater. Chem. A*, 2016, 4, 7430–7436; (c) P. Yin, J. Zhang, G. H. Imler, D. A. Parrish, and J. M. Shreeve, *Angew. Chem. Int. Ed.*, 2017, 56, 8834–8838; (d) W. Zhang, H. Xia, R. Yu, J. Zhang, K. Wang, and Q. Zhang, *Propellants Explos. Pyrotech.*, 2020, 45, 546–553; (e) C. Lei, G. Cheng, Z. Yi, Q. Zhang, H. Yang, *Chemical Engineering Journal*, 2021, 416, 129190.
- (a) C. Li, M. Zhang, Q. Chen, Y. Li, H. Gao, W. Fua and Z. Zhou, *Dalton Trans.*, 2016, 45, 17956–17965; (b) Y. Tang, C. He, G. H. Imler, D. A. Parrish and J. M. Shreeve, *J. Mater. Chem. A*, 2018, 6, 5136–5142; (c) D. Kumar, Y. Tang, C. He, G. H. Imler, D. A. Parrish, and J. M. Shreeve, *Chem. Eur. J.*, 2018, 24, 17220–17224; (d) K. V. Domasevitch, I. Gospodinov, H. Krautscheid, T. M. Klapötke and J. Stierstorfer, *New J. Chem.*, 2019, 43, 1305–1312.
- 29. (a) M. Xu, G. Cheng, H. Xiong, B. Wang, X. Ju and H. Yang, *New J. Chem.*, **2019**, *43*, 11157–11163; (b) D. Chen, H. Xiong, H.Yang, J.Tang, G. Cheng, *FirePhysChem.*, **2021**, *1*, 71–75.

- (a) T. M. Klapötke, A. Preimesser, and J. Stierstorfer, Z. Anorg. Allg. Chem., 2012, 638, (9), 1278–1286; (b) M. M. Breiner, D. E. Chavez, D. A. Parrish, SYNLETT, 2013, 24, 0519–0521. (c) P. Yin and J. M. Shreeve, Angew. Chem. Int. Ed., 2015, 54, 14513–14517; (d) A. J. Paraskos, E. D. Cooke, and K. C. Caflin, Propellants Explos. Pyrotech., 2015, 40, 46–49; (e) P. Yin, C. He, and J. M. Shreeve, Chem. Eur. J., 2016, 22, 2108–2113; (f) R. Lewczuk, M. Szala, J. Rećko, T. M. Klapötke, S. Cudziło, Chemistry of Heterocyclic Compounds, 2017, 53(6/7), 697–701; (e) Y. Tang, C. He, P. Yin, G. H. Imler, D. A. Parrish, and J. M. Shreeve, Eur. J. Org. Chem., 2018, 2273–2276.
- (a) P. Yin, Q. Zhang, J. Zhang, D. A. Parrish and J. M. Shreeve, *J. Mater. Chem. A*, 2013, 1, 7500–7510;
   (b) Y. Xu, C. Shen, Q. Lin, P. Wang, C. Jiang and M. Lu, *J. Mater. Chem. A*, 2016, 4, 17791–17800.
- 32. (a) Y. Tang, G. H. Imler, D. A. Parrish, and J. M. Shreeve, *ACS Appl. Energy Mater.* **2019**, 2, 8871–8877; (b) Y. Liu, X. Qi, W. Zhang, P.Yin, Z. Cai, and Q. Zhang, *Org. Lett.*, **2021**, 23, 734–738.
- 33. Huisgen, R. (1961). "Centenary Lecture 1,3-Dipolar Cycloadditions". *Proceedings of the Chemical Society of London*: 357.
- 34. S. Feng, F. Li, X. Zhao, Y. Qian, T. Fei, P. Yin, S. Pang, *Energetic Materials Frontiers*, **2021**, 2, 125–130.
- 35. (a) T. M. Klapötke, B. Krumm, and C. Pflüger, *J. Org. Chem.*, 2016, 81, 14, 6123–6127;
  (b) J. Qin, T. Li, J. G. Zhang and Z. B. Zhang, *RSC Adv.*, 2016, 6, 101430–101436;
  (c) Y. Liu, C. He, Y. Tang, G. H. Imler, D. A. Parrish and J. M. Shreeve, *Dalton Trans.*, 2019, 48, 3237–3242;
  (d) C. He and J. M. Shreeve, *Angew. Chem.*, 2015, 127, 6358–6362.
- 36. (a) A. A. Dippold, D. Izsák, T. M. Klapötke, and C. Pflüger, *Chem. Eur. J.*, **2016**, 22, 1768–1778; (b) H. Gu, G. Cheng and H. Yang, *New J. Chem.*, **2021**, *45*, 7758–7765.
- 37. Y. V. Filippova, A. G. Sukhanova, S. V. Voitekhovich, V. E. Matulis, G. T. Sukhanov, Y. V. Grigoriev, and O. A. Ivashkevich, *J. Heterocyclic Chem.*, **2012**, *49*, 965.
- 38. Y. Tang, K. Li, A. K. Chinnam, R. J. Staples and J. M. Shreeve, *Dalton Trans.*, **2021**, *50*, 2143–2148.
- (a) R. Wang, H. Xu, Y. Guo, R. Sa, and J. M. Shreeve, *J. Am. Chem. Soc.*, 2010, 132, 11904–11905; (b) A. A. Dippold, D. Izsák, and T. M. Klapötke, *Chem. Eur. J.*, 2013, 19, 12042–12051; (c) J. Zhang and J. M. Shreeve, *J. Am. Chem. Soc.*, 2014, 136, 4437–4445; (d) T. M. Klapötke, P. C. Schmid, S. Schnell and J. Stierstorfer, *J. Mater. Chem. A*, 2015, 3, 2658–2668; (d) A. A. Dippold and T. M. Klapötke, *J. Am. Chem. Soc.*, 2013, 135, 9931–9938; (e) T. M. Klapçtke, M. Leroux, P. C. Schmid, and J. Stierstorfer, *Chem. Asian*

- J., **2016**, 11, 844–851; (f) W. Yao, Y. Xue, L. Qian, H. Yang, G. Cheng, *Energetic Materials Frontiers*, **2021**, 2, 131–138.
- 40. W. Cao, W. Dong, Z. Lu, Y. Bi, Y. Hu, T. Wang, C. Zhang, Z. Li, Q. Yu, and J. Zhang, *Chem. Eur. J.*, **2021**, *27*, 1–13.
- 41. (a) M. Joas, S. Kießling, T. M. Klapötke, P. C. Schmid, and J. Stierstorfer, *Zeitschrift für anorganische Chemie*, **2014**, *14*, 640; (b) C. Bian, M. Zhang, C. Lia and Z. Zhou, *J. Mater. Chem. A*, **2015**, *3*, 163–169.
- 42. (a) T. M. Klapötke, P. C. Schmid, S. Schnell, and J. Stierstorfer, *Chem. Eur. J.*, **2015**, *21*, 9219–9228; (b) S. Liao, Z. Zhou, K. Wang, Y. Jin, J. Luo, T. Liu, *Energetic Materials Frontiers*, **2020**, *1*, 172–177; (c) X. Nie, C. Lei, H. Xiong, G. Cheng, H. Yang, *Energetic Materials Frontiers*, **2020**, *1*, 165–171.
- 43. (a) J. Zhu, S. Jin, Li Wan, C. Zhang, L. Li, S. Chen and Q Shu, *Dalton Trans.*, **2016**, *45*, 3590–3598; (b) Y. Li, B. Wang, P. Chang, J. Hu, T. Chen, Y. Wang and B. Wang, *RSC Adv.*, **2018**, *8*, 13755–13763.
- 44. Q. Ma, Y. chen, L. Liao, H. Lu, G. Fan and J. Huang, *Dalton Trans.*, **2017**, *46*, 7467–7479.
- (a) T. M. Klapötke, N. Mayr, J. Stierstorfer, and M. Weyrauther, *Chem. Eur. J.*, 2014, 20, 1410–1417; (b) Q. Yu, G. Cheng, X. Ju, C. Lu, Q. Linab and H. Yang, *New J. Chem.*, 2017, 41, 1202–1211; (c) Y. Cao, H. Huang, X. Lin, J. Yang and X. Gong, *New J. Chem.*, 2018, 42, 11390–11395; (d) L. Bauer, M. Benz, T. M. Klapötke, T. Lenz, and J. Stierstorfer, *J. Org. Chem.*, 2021, 86, 6371–6380; (e) W. Cao, W. Dong, Z. Lu, Y. Bi, Y. Hu, T. Wang, C. Zhang, Z. Li, Q. Yu, and J. Zhang, *Chem. Eur. J.* 2021, 27, 1–13; (f) I. Y. Gudkova, I. N. Zyuzin, and D. B. Lempert, *Russian Journal of Physical Chemistry B*, 2020, 14, 2, 302–313.
- 46. (a) Y. Tang, H. Gao, L. A. Mitchell, D. A. Parrish, and J. M. Shreeve, *Angew. Chem. Int. Ed.*, 2016, 55, 1147–1150; (b) Q. Yu, G. Cheng, X. Ju, C. Lu and H. Yang, *New J. Chem.*, 2017, 41, 4797–4801; (c) T. Lu, Y. He, J. Song, Z. Hou, H. Yin, G. Fan and F. Chen, *New J. Chem.*, 2021, 45, 526–529.
- 47. (a) F. Pang, G. Wang, T. Lu, G. Fan and F. Chen, *New J. Chem.*, **2018**, *42*, 4036–4044;
  (b) B. Wang, H. Xiong, G. Cheng, Z. Zhang and H. Yang, *New J. Chem.*, **2018**, *42*, 19671–19677;
  (c) H. Xiong, H. Yang, C. Lei, P. Yang, W. Hu and G. Cheng, *Dalton Trans.*, **2019**, *48*, 14705–14711.
- 48. (a) Y. Cao, X. Lin, J. Yang, X. Gong, G. Fan and H. Huang, *New J. Chem.*, **2019**, *43*, 5441–5447; (b) L. L. Fershtat, I. V. Ananyev and N. N. Makhova, *RSC Adv.*, **2015**, *5*, 47248–47260; (c) T. Yan, G. Cheng, and H. Yang, *ChemPlusChem.*, **2019**, *84*, 1567–1577.

- 49. (a) Z. Xu, H. Yang and G. Cheng, *Journal of Energetic Materials*, 2018, 36, 1, 29–37; (b)
  Z. Xu, H. Yang and G. Cheng, *New J. Chem.*, 2016, 40, 9936–9944; (c) Y. Du, Z. Qu, H. Wang, H. Cui, and X. Wang, *Propellants Explos. Pyrotech.*, 2021, 46, 860–874; (d) Y. Tang, J. Zhang, L. A. Mitchell, D. A. Parrish, and J. M. Shreeve, *J. Am. Chem. Soc.*, 2015, 137, 15984–15987.
- (a) Y. Liu, C. He, Y. Tang, G. H. Imler, D. A. Parrish and J. M. Shreeve, *Dalton Trans.*,
   2018, 47, 16558–16566; (b) J. Zhang, L. A. Mitchell, D. A. Parrish, and J. M. Shreeve, *J. Am. Chem. Soc.*, 2015, 137, 10532–10535.
- 51. (a) Z. Xu, G. Cheng, H. Yang, J. Zhang, and J. M. Shreeve, *Chem. Eur. J.*, **2018**, *24*, 10488–10497; (b) Y. Liu, Y. Xu, F. Yang, Z. Dong, Q. Sun, L. Ding, and M. Lu, *Cryst. Growth Des.*, **2020**, *20*, 6084–6092; (c) L. Qian, H. Yang, H. Xiong, H. Gu, J. Tang, Y. Xue, G. Cheng, *Energetic Materials Frontiers*, **2020**, *1*, 74–82; (d) W. Yao, Y. Xue, L. Qian, H. Yang, G. Cheng, *Energetic Materials Frontiers*, **2021**, *2*, 131–138; (e) A. O. Finogenov, A. S. Kulikov, M. A. Epishina, I. V. Ovchinnikov, Yu. V. Nelyubina, and N. N. Makhova, *J. Heterocyclic Chem.*, **2013**, *50*, 135.
- 52. (a) B. Wang, H. Xiong, G. Cheng, and H. Yang, *Chempluschem.*, 2018, 83(5), 439–447;
  (b) J. Ma, A. K. Chinnam, G. Cheng, H. Yang, J. Zhang, and J. M. Shreeve, *Angew. Chem. Int. Ed.*, 2021, 60, 5497–5504;
  (c) J. Tang, H. Yang, Y. Cui and G. Cheng, *Mater. Chem. Front.*, 2021, Advance Article;
  (d) L. Zhai, F. Bi, Y. Luo, N. Wang, J. Zhang and B. Wang, *Scientific Reports*, 2019, 9, 4321;
  (e) Y. Tang, C. He, L. A. Mitchell, D. A. Parrish, and J. M. Shreeve, *Chem. Eur. J.*, 2016, 22, 11846–11853.
- 53. (a) H. Li, F. Zhao, B. Wang, L. Zhai, W. Lai and N. Liu, *RSC Adv.*, **2015**, *5*, 21422–21429;
  (b) D. Herweyer, J. L. Brusso, and M. Murugesu, *New J. Chem.*, **2021**, *45*, 10150–10159;
  (c) Z. Xu, G. Cheng, H. Yang, X. Ju, P. Yin, J. Zhang, and J. M. Shreeve, *Angew. Chem. Int. Ed.*, **2017**, *56*, 5877–5881.
- 54. (a) S. Feng, F. Li, X. Zhao, Y. Qian, T. Fei, P. Yin, S. Pang, Energetic Materials Frontiers,
  2021, 2, 125–130; (b) J. Zhang and J. M. Shreeve, J. Am. Chem. Soc. 2014, 136,
  4437–4445; (c) D. Fischer, T. M. Klapötke, M. Reymann, and J. Stierstorfer, Chem. Eur. J., 2014, 20, 6401–6411; (d) H. Wei, J. Zhang, C. He, and J. M. Shreeve, Chem. Eur. J.
  2015, 21, 8607–8612; (e) Y. Qu, Q. Zeng, J. Wang, Q. Ma, H. Li, Haibo Li, and G. Yang, Chem. Eur. J., 2016, 22, 12527–12532; (f) B. Wang, H. Xiong, G. Cheng, Z. Zhang and H. Yang, New J. Chem., 2018, 42, 19671–19677.
- 55. J. Tang, H. Yang, H. Xiong, W. Hu, C. Lei and G. Cheng, *New J. Chem.*, **2020**, *44*, 5895–5902.

- (a) J. Tian, H. Xiong, Q. Lin, G. Cheng and H. Yang, New J. Chem., 2017, 41, 1918–1924;
   (b) Y. Tang, C. He, L. A. Mitchell, D. A. Parrish and J. M. Shreeve, J. Mater. Chem. A, 2015, 3, 23143–23148;
   (c) J. Tian, H. Xiong, Q. Lin, G. Cheng and H. Yang, New J. Chem., 2017, 41, 1918–1924.
- 57. (a) Q. Yu, P. Yin, J. Zhang, C. He, G. H. Imler, D. A. Parrish, and J. M. Shreeve, *J. Am. Chem. Soc.*, 2017, 139, 8816–8819; (b) J. Ma, J. Zhang, G. H. Imler, D. A. Parrish, and J. M. Shreeve, *Org. Lett.*, 2020, 22, 4771–4775; (c) T. Liu, S. Liao, S. Song, K. Wang, Y. Jin and Q. Zhang, *Chem. Commun.*, 2020, 56, 209–212; (d) Y. Du, Z. Qu, H. Wang, H. Cui, and X. Wang, *Propellants Explos. Pyrotech.*, 2021, 46, 860–874.
- 58. Q. Wang, Y. Shao, and M. Lu, Cryst. Growth Des. 2019, 19, 839–844.
- 59. J. Ma, A. K. Chinnam, G. Cheng, H. Yang, J. Zhang and J. M. Shreeve, *Angew. Chem.*, **2021**, *133*, 5557–5564.
- 60. (a) Henry, Ronald A.; Finnegan, William G. (**1954**-01-01). "An Improved Procedure for the Deamination of 5-Aminotetrazole". *Journal of the American Chemical Society*. 76 (1): 290–291; (b) Kurzer, F.; Godfrey, L. E. A. (**1963**). "Syntheses of Heterocyclic Compounds from Aminoguanidine". *Angewandte Chemie International Edition* in English. 2 (8): 459–476.
- (a) T. Abe, G. Tao, Y. Joo, R.W. Winter, G. L. Gard, and J. M. Shreeve, *Chem. Eur. J.*,
   2009, 15, 9897–9904; (b) T. M. Klapötke, D. G. Piercey, F. Rohrbacher, and J. Stierstorfer,
   Z. Anorg. Allg. Chem., 2012, 638, 2235–2242; (c) G. Zhang, Z. Wang, X. Yin, and J. Zhang, Z. Anorg. Allg. Chem., 2018, 644, 598–601; (d) Y. Zheng, X. Zhao, X. Qi, K. Wang, T. Liu, Energetic Materials Frontiers, 2020, 1, 83–89.
- 62. (a) Y. Joo and J. M. Shreeve, *Angew. Chem. Int. Ed.*, **2009**, *48*, 564–567; (b) Y. H. Joo and J. M. Shreeve, *J. Am. Chem. Soc.*, **2010**, *132*, 15081–15090.
- (a) K. Karaghiosoff, T. M. Klapötke, and C. M. Sabaté, Eur. J. Inorg. Chem., 2009, 238–250; (b) D. Fischer, T. M. Klapötke, D. G. Piercey, and J. Stierstorfer, Chem. Eur. J., 2013, 19, 4602–4613; (c) D. R. Wozniak, D. G. Piercey, Engineering, 2020, 6, 981–991; (d) P. Yin, D. A. Parrish, and J. M. Shreeve, Chem. Eur. J., 2014, 20, 6707–6712.
- 64. (a) J. Stierstorfer, K. R. Tarantik, and T. M. Klapötke, *Chem. Eur. J.*, 2009, 15, 5775–5792; (b) T. M. Klapötke, J. Stierstorfer, B. Weber, *Inorganica Chimica Acta*, 2009, 362, 2311–2320; (c) M. Göbel, K. Karaghiosoff, T. M. Klapötke, D. G. Piercey, and J. Stierstorfer, *J. Am. Chem. Soc.*, 2010, 132, 17216–17226; (d) N. Fischer, K. Karaghiosoff, T. M. Klapötke, and J. Stierstorfer, *Z. Anorg. Allg. Chem.*, 2010, 636, 735–749.

- (a) N. Fischer, T. M. Klapötke, J. Stierstorfer, C. Wiedemann, *Polyhedron*, 2011, 30, 2374–2386; (b) T. M. Klapötke, F. A. Martin, and J. Stierstorfer, *Chem. Eur. J.*, 2012, 18, 1487–1501; (c) Q. Lin, Y. Li, Cai Qi, W. Liu, Y. Wang and S. Pang, *J. Mater. Chem. A*, 2013, 1, 6776–6785; (d) Z. Yin, Y. Dong, Z. Zeng, W. Huang, and Y. Tang, *New J. Chem.*, 2021, 45, 11752–11757; (e) Z. Yin, Wei Huang, and Y. Tang, *Propellants Explos. Pyrotech.*, 2021, 46, 1150–1154.
- (a) D. Fischer, T. M. Klapötke, and J. Stierstorfer, *Propellants Explos. Pyrotech.*, 2012, 37, 156–166; (b) J. Yang, X. Yin, Le Wu, J. Wu, J. Zhang, and M. Gozin, *Inorg. Chem.*, 2018, 57, 15105–15111.
- 67. P. He, J. Zhang, K. Wang, X. Yin, and T. Zhang, J. Org. Chem., 2015, 80, 5643–5651.
- 68. (a) T. M. Klapötke, D. G. Piercey and J. Stierstorfer, *Dalton Trans.*, 2012, 41, 9451–9459;
  (b) N. Fischer, T. M. Klapötke, M. Reymann, and J. Stierstorfer, *Eur. J. Inorg. Chem.*2013, 2167–2180; (c) A. A. Larin, L. L. Fershtat, *Energetic Materials Frontiers*, 2021, 2, 3–13; (d) D. Fischer, T. M. Klapötke, and J. Stierstorfer, *Angew. Chem. Int. Ed.*, 2014, 53, 1–5.

# **Chapter-2**

# Thermally Stable and Insensitive Energetic Materials: Synthesis of Polynitro-*N*-aryl-C-nitro-Pyrazole/Imidazole Derivatives

**Chapter 2** 

#### **Abstract**

A wide array of methoxy-substituted-polynitro-aryl-pyrazole/imidazole with readily oxidizable – NH<sub>2</sub>/NO<sub>2</sub>/NHNO<sub>2</sub>/diazo functional groups is synthesized. Single crystal X-ray diffraction (XRD) analysis confirms molecular structure of the compounds. Energetic properties of the synthesized compounds are determined by theoretical and experimental studies. In most cases, these compounds are thermally stable and resistant to friction and impact. Some of the molecules possess better detonation velocity and detonation pressure over TNT.

## 2.1. Introduction

Trinitrotoluene (TNT)<sup>1</sup> finds wide utility in industrial, mining, and military environments. Likewise, 2,4,6-triamino-1,3,5-trinitrobenzene (TATB)<sup>2</sup> is a powerful explosive insensitive to shock, friction, and impact. In this line, RDX (1,3,5-trinitro-1,3,5-triazine)<sup>3</sup> and HMX (1,3,5,7-tetranitro-1,3,5,7tetrazoctene)<sup>4</sup> are also powerful high density energetic materials (HEDMs) and are broadly useful in military applications. In a broad sense, thermally stable and insensitive explosives (for example: TNT and TATB) exhibit low detonation performance, while high performance energetic compounds (for example: RDX) show less thermal stability. Hence, high performance energetic materials are highly sensitive to heat and impact. Thus, the design and synthesis of new HEDMs with high density, high detonation velocity, detonation pressure, and high thermal stability is always desirable although exceedingly challenging. In this context, polynitro-functionalized azole derivatives exhibit balanced energetic properties. Among azole derivatives, pyrazole and imidazole species are advantageous over triazole and tetrazole skeletons (Figure 2.1.1). Thus, C-nitrated pyrazole/imidazole based energetic compounds have gained attention in the field of energetic materials due to their heat of formation, high thermal stability, high density, and detonation performance.<sup>5</sup> In addition; the low-cost synthetic strategies involved for the synthesis of pyrazoles and imidazoles make the process sustainable.



Figure 2.1.1.Important properties of pyrazole and imidazole rings

# 2.1.1. Background of polynitro azole/aryl-azole derivatives towards energetic material application

Figure 2.1.2. Well-known pyrazole/imidazole based energetic materials

Intramolecular hydrogen-bond interactions between nitramino and nitro groups in the molecules could largely influence energetic properties and stability of the compounds. The Shreeve group demonstrated the synthesis of nitro-rich pyrazole nitramine derivatives 1–3 from the corresponding amino-substituted pyrazoles 11–13 (Scheme 2.1.1).<sup>6</sup> The precursor's amino-dintropyrazoles 11–13 were readily accessed from commercially available pyrazole-derivatives.<sup>7</sup> Subjecting 11 with 70% HNO<sub>3</sub> and concentrated H<sub>2</sub>SO<sub>4</sub> led to the nitramine derivative 1. Likewise, nitramine product 2 (94%) was synthesized from 12 by nitrating with fuming nitric acid at 0–5 °C. The reaction of 13

**Scheme 2.1.1:** Synthesis of N-(3,5-1H-pyrazol-4-yl)nitramide (1), N-(4,5-dinitro-1H-pyrazol-5-yl)nitramide (2), and N-(3,5-dinitro-1H-pyrazol-1-yl)nitramide (3)

-with a mixture of concentrated  $H_2SO_4$  and fuming  $HNO_3$  at -10 °C provided nitramine product **3** (**Scheme 2.1.1**). Among **1–3**, compound **2** is only stable at room temperature and showed high density (1.97 g/cm<sup>3</sup>) and excellent detonation properties (P = 41.6 GPa, VD = 9430 m/s). Interestingly, energetic properties of **2** is comparable with high explosive HMX (P = 39.5 GPa, VD = 9320 m/s). Disappointingly, compound **2** is thermally less-stable ( $T_d = 135$  °C); moreover, the compound is impact sensitive 4 J and friction sensitive 40 N.

The Zhang group in 2019, reported the synthesis of 4-diazo-3,5-bis(4-amino-3,5-dinitropyrazol-1-yl)pyrazole (**4**); the compound exhibits high thermal stability (T<sub>d</sub> = 278 °C) and density (1.83 g/cm<sup>3</sup>) (**Scheme 2.1.2**).<sup>8</sup> In addition, product **4** is insensitive to impact and friction. The hydrogen bond between –NH<sub>2</sub> and –NO<sub>2</sub> groups and intermolecular interaction between diazo and nitro groups make the product **4** stable. The acid mediated nitration of 4-amino-3,5-dinitropyrazole **11** successfully occurred when exposed to the combination of aqueous H<sub>2</sub>SO<sub>4</sub> and HNO<sub>2</sub> at 0–5 °C and provided 4-diazo-3,5-dinitropyrazole **14**. Next, nucleophilic substitution of nitro-group of **14** with **11** makes **4** in 51% yield (**Scheme 2.1.2**).

Scheme 2.1.2: Synthesis of 4-diazo 3,5-bis(4-amino-3,5-dinitropyrazol-1-yl)pyrazole (4)

A route to the synthesis of new class of N,N'-ethylene bridged bis-nitropyrazole derivatives **5**, **6** and **7** from diaminotetranitro-ethylene-bis-pyrazole **16** was developed by Yin and co-workers (**Scheme 2.1.3**). Thus, 4-amino-3,5-dinitropyrazolate **15** was reacted with dibromoethane in the presence of phase transfer catalyst tetraethylammonium bromide (TEAB) produced diaminotetranitro-ethylene-bis-pyrazole **16**. Next, oxidation of amino group in **16** was readily performed in the presence of 50%  $H_2O_2/H_2SO_4$  to afford bis-trinitropyrazole derivative **5**. Next, nitration of **16** with 100% nitric acid at 0 °C resulted dinitramino derivative **6**. Furthermore, amino group of **16** was converted into diazonium salt **7** by using sodium nitrite/sulfuric acid mixture. Notably, compound **5** showed high thermal stability ( $T_d = 250$  °C), high density (1.84 g/cm<sup>3</sup>), and good detonation performance (P = 34.1 GPa,  $V_d = 8759$  m/s); these properties are similar to RDX (P = 35.0 GPa,  $V_d = 8762$  m/s). The high detonation performance could make **5** as secondary explosive. While the nitramine derivative **6** and the diazonium salt **7** can be considered as potential primary explosives (**6**, IS = 7 J; FS = 80 N and **7**, IS = 20 J; FS = 80 N).

**Scheme 2.1.3:** Synthesis of 1,2-bis(3,4,5-trinitro-1*H*-pyrazol-1-yl)ethane (**5**), *N*,*N*′-(1,1′-(ethane-1,2-diyl)bis-(3,5-dinitro-1*H*-pyrazole-4,1-diyl)dinitramide (**6**), and 1,1′-(ethane-1,2-diyl)bis(3-nitro-4-diazo-1*H*-pyrazol-5-olate (**7**)

Shreeve and co-workers in 2015 revealed the synthesis of a high-density N-nitramino functionalized bis-imidazole derivative **8** (Scheme 2.1.4). To start with, nitration of bis-imidazole 17 with acidic mixture (NaNO<sub>3</sub>/H<sub>2</sub>SO<sub>4</sub>) under reflux at 90 °C delivered tetranitro-bisimidazole 18. Next, N-amination of 18 with O-tosylhydroxylamine provided 19. Finally, nitration of amino group of 19 in the presence of H<sub>2</sub>SO<sub>4</sub>/HNO<sub>3</sub> mixture at -15 to -10 °C yielded the final dinitramino product 8 in 81% yield. The compound 19 and 8 exhibited good detonation performance: (for 19, P = 36.6 GPa, vD = 9012 m/s; for 8, P = 40.1 GPa, vD = 9350 m/s). Performance of these compounds is comparable to RDX and HMX. The compound 8 show low decomposition temperature (T<sub>d</sub> = 116 °C) and is more sensitive to impact (3 J) and friction (40 N).

**Scheme 2.1.4:** Synthesis of N,N'-(4,4',5,5'-tetranitro-1H,1'H-[2,2'-biimidazole]-1,1'-diyl)dinitramide (8)

In 2016, Fischer *et al.* showcased the synthesis of *N*,*N'*-methylene bridged bis-nitropyrazole-based energetic materials (**Scheme 2.1.5**).<sup>11</sup> The coupling of dinitro-aminopyrazole **15** with dibromomethane at first makes bis-pyrazole **20**. Next, oxidation of **20** by 50% H<sub>2</sub>O<sub>2</sub>/H<sub>2</sub>SO<sub>4</sub> mixture gives the hexanitro-bis-pyrazole **9** in 73% yield. Next, ammonia mediated replacement of –NO<sub>2</sub> groups followed by acidification with HCl delivers **21**. Later, *N*-amination of **21** with *O*-

tosylhydroxylamine provides **22**. Finally, exposing **22** with HNO<sub>3</sub>/NH<sub>4</sub>NO<sub>3</sub> mixture delivers the desired nitramine product **10** in 92% yield. Importantly, compound **10** showed excellent density 1.94 g/cm<sup>3</sup> and high detonation performance (vD = 9226 m/s, P = 38.8 GPa); these energetic parameters are comparable with HMX. The nitramine compound **10** showed  $T_d = 117$  °C; while the other compounds exhibit favorable thermal stability (207 to 307 °C). Interestingly, compound **9** exhibited detonation velocity 9304 m/s, which is comparable to CL-20 (9673 m/s).

**Scheme 2.1.5:** Synthesis of bis(3,4,5-trinitro-1H-pyrazol-1-yl)methane (9) and N-(2,3,5,6-tetranitrodipyrazolo[1,5-a:5',1'-d][1,3,5]triazin-4(9H)-yl)nitramide (10)

The O- and S-bridged nitro-rich biaryls bis(2,4-dinitrophenyl)ether (24), bis(2,4,6-trinitrophenyl)ether (25), and bis(2,4,6-trinitrophenyl)thioether (27) were readily synthesized by Shreeve and coworkers (Scheme 2.1.6) and the structures are established by single crystal XRD analysis. The Hirshfeld surface and finger print plot analysis of 24, 25, and 27 offer in-sights in understanding the sensitivity of the compounds (24 being most in-sensitive while 25 is sensitive and 27 is moderate). The detonation velocities of 25 (7634 m/s) and 27 (6912 m/s) are higher than TNT (6881 m/s); whereas 24 exhibits detonation velocity 6582 m/s due to less number of nitro groups.

**Scheme 2.1.6:** Synthesis of 4,4'-oxybis(1,3-dinitrobenzene) (**24**), 2,2'-oxybis(1,3,5-trinitrobenzene) (**25**), and bis(2,4,6-trinitrophenyl)sulfane (**27**)

A tetranitroaryl-pyrazole product **29** was synthesized by coupling of picryl chloride **26** with 3-nitro pyrazole **28** (**Scheme 2.1.7**). <sup>13a</sup> The presence of strong withdrawing –NO<sub>2</sub> groups on the benzene ring of picryl chloride makes the nucleophilic substitution reactions facile. By contrast, nucleophilic substitution of pyrazole, nitropyrazole, and nitrotriazole independently with picryl chloride were ineffective because of the low nucleophilicity of the respective coupling partners. <sup>13</sup> To make this coupling viable, Klapötke *et al.* employed potassium salt of pyrazole **30** as nucleophilic partner for the coupling with picryl chloride to make **31** (**Scheme 2.1.7**). <sup>13b</sup> Similarly, compound **32** was synthesized by subjecting pyrazole **12** with **26** in the presence of LiOMe base at room temperature; Dalinger group demonstrated this reaction (**Scheme 2.1.7**). <sup>13c</sup> Energetic properties of **29**, **31**, and **32** are comparable to the commonly used explosive RDX.

**Scheme 2.1.7:** Synthesis of 3-nitro-1-(2,4,6-trinitrophenyl)-1*H*-pyrazole (**29**), 3,5-dinitro-1-(2,4,6-trinitrophenyl)-1*H*-pyrazol-4-amine (**31**), and 3,4-dinitro-1-(2,4,6-trinitrophenyl)-1*H*-pyrazol-5-amine (**32**)

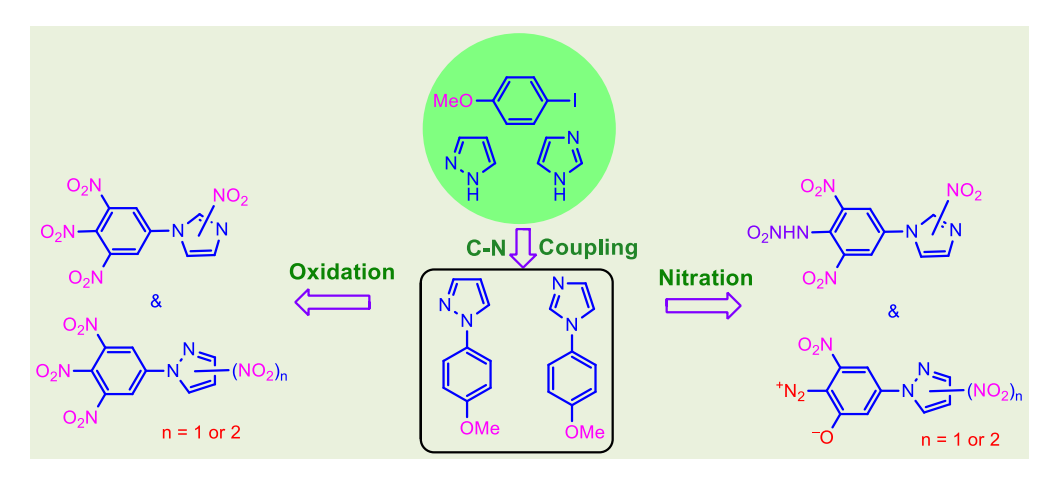
Dinitroimidazoles-picryl chloride derivatives **34**, **36**, **38**, and **39** as energetic materials were constructed by Z. Lui and co-workers (**Scheme 2.1.8**). <sup>14</sup> The inter- and intramolecular hydrogen bonding of amino and nitro groups contribute to the stability and crystal density of the compounds. An independent coupling of 2,4-dinitroimidazoles (**33**) or 4,5-dinitroimidazoles (**35**) with picryl chloride **26** and their amino derivatives (**37**), respectively delivered the corresponding polynitro-aryl based energetic materials **34**, **36**, **38**, and/or **39**. The synthesized compounds exhibited high decomposition temperature (250 to 350 °C), positive heat of formation, density (in the range

between 1.75 to 1.84 g/cm<sup>3</sup>), and detonation velocity (8280 to 8480 m/s). Most of the compounds show better explosive performance than TNT and comparable with RDX.

**Scheme 2.1.8:** Synthesis of 2,4-dinitro-1-(2,4,6-trinitrophenyl)-1*H*-imidazole (**34**), 4,5-dinitro-1-(2,4,6-trinitrophenyl)-1*H*-imidazole (**36**), 5-(2,4-diniro-1*H*-imidazol-1-yl)-2,4,6-trinitrobenzene-1,3-diamine (**38**), and 5-(4,5-diniro-1*H*-imidazol-1-yl)-2,4,6-trinitrobenzene-1,3-diamine (**39**)

## 2.2. Motivation and Design Plan

The polynitro-azole compounds are energetic materials with high density, thermal stability, and are less sensitive comparable to well-known energetic materials. Thus, design, synthesis, and examination of energetic properties of such compounds are always attractive. These compounds could exhibit enhanced physico-chemical properties in comparison to that of the individual polynitroarenes and C-nitro azoles. In general, aromatic polynitroarenes are more stable possessing resistance to high temperature, insensitive to impact, and friction, and is also less hygroscopic. However, most of these compounds exhibit poor performance. In contrast, C-nitro-azoles display high performance but are thermally less stable and are highly sensitive. Therefore, envisaging polynitroarene-coupled-nitroazole moieties could offer solution balancing performance, thermal stability, and sensitivity of the materials. In this regard, five membered nitrogen containing pyrazole and imidazole show various advantages, as nitro groups could be easily introduced in the molecular scaffold through nitration.<sup>15</sup> This chapter aims the synthesis of nitro-rich *N*-aryl-pyrazole/imidazole derivatives by Cu-mediated cross coupling of 4-iodoanisole with pyrazole/imidazole followed by nitration/amination/oxidation sequence (**Scheme 2.2.1**).



Scheme 2.2.1: Synthesis of polynitro-aryl-pyrazole/imidazole derivatives

#### 2.3. Results and Discussion

The readily accessible methoxy substituted aryl-azoles are being broadly used for the synthesis of N-and O-rich molecular skeletons for various energetic applications. Intrigued with the electron-rich nature of *p*-methoxy-aryl-pyrazole (42) and *p*-methoxy-aryl-imidazole (44) motifs, we considered introducing highly oxidizable (N- and O- bearing) and explosophoric (NO<sub>2</sub>, ONO<sub>2</sub>, N<sub>3</sub>, NHNO<sub>2</sub> etc) groups on its molecular periphery. Classically, base mediated Cu(I)-catalyzed C–N coupling of pyrazole (41), imidazole (43) independently with *p*-iodoanisole (40) could make 42 (80%) and 44 (84%), respectively (Scheme 2.3.1).

MeO 
$$\stackrel{N}{\longrightarrow}$$
  $\stackrel{N}{\longrightarrow}$   $\stackrel{N}{\longrightarrow}$ 

**Scheme 2.3.1:** Synthesis of *p*-methoxy-aryl-pyrazole/imidazole

Next, nitration of 42 in presence of 98%  $H_2SO_4$  and 95%  $HNO_3$  at 0 °C for 2 h afforded tri-nitro substituted p-methoxy aryl-pyrazole 45 in 70% yield (Scheme 2.3.2). Further nitration of 45 under the nitrating mixture at 90 °C produced tetra-nitro substituted p-methoxy aryl-pyrazole 46 in 32% yield (Scheme 2.3.2). The structure 46 was elucidated by X-ray analysis (Figure 2.5.1). The synthesis of tetranitro-N-aryl pyrazole skeleton 46 from easily accessible p-OMe-N-aryl pyrazole (42) is noteworthy.

**Scheme 2.3.2:** Nitration of *p*-methoxy-aryl-pyrazole (42)

To enhance density and performance of **45** and **46**, we next embarked converting the modifiable – OMe to –NH<sub>2</sub>/–NO<sub>2</sub> groups. Thus, independently treating **45** and **46** with aqeous ammonia in CH<sub>3</sub>CN yielded amino-substituted tri/tetra-nitro-N-arylpyrazoles **47** (**Scheme 2.3.3**) and **50** (**Scheme 2.3.4**), respectively. Next, acid mediated oxidation of amine group of **47** and **50** in presence of H<sub>2</sub>SO<sub>4</sub>/H<sub>2</sub>O<sub>2</sub>, respectively, produced tetra/penta-nitro-N-aryl-pyrazoles **48** (55%) and **51** (74%) (**Scheme 2.3.3** and **2.3.4**). While nitration of **47** and **50** with fuming HNO<sub>3</sub> at 0 °C led to diazo-nitro-N-aryl-pyrazoles **49** and **52**, respectively, in moderate yield (**Scheme 2.3.3** and **2.3.4**). Once again, X-ray analysis validates the molecular topology of **47–51** (**Figure 2.5.1**).

45 
$$\xrightarrow{\text{aq.NH}_3}$$
  $\xrightarrow{\text{H}_2\text{N}}$   $\xrightarrow{\text{H}_2\text{N}}$   $\xrightarrow{\text{NO}_2}$   $\xrightarrow{\text{NO}_2}$   $\xrightarrow{\text{98\% H}_2\text{SO}_4}$   $\xrightarrow{\text{O}_2\text{N}}$   $\xrightarrow{\text{NO}_2}$   $\xrightarrow{\text{$ 

Scheme 2.3.3: Functionalization of trinitro-N-aryl-pyrazole 45

46 
$$\xrightarrow{\text{aq.NH}_3}$$
  $\xrightarrow{\text{H}_2\text{N}}$   $\xrightarrow{\text{NO}_2}$   $\xrightarrow{\text{NO}$ 

Scheme 2.3.4: Functionalization of tetranitro-N-aryl-pyrazole 46

Likewise, nitration of p-methoxy-aryl-imidazole **44** was examined. Exposing **44** with nitrating mixture (98%  $H_2SO_4$  and 95%  $HNO_3$ ) could produce a regioisomeric mixture of tri-nitro substituted p-methoxy aryl-imidazole derivatives **53** (17%) and **54** (13%), when conducted at 90 °C for 3–5 h (**Scheme 2.3.5**).

44 
$$\xrightarrow{98\% \text{ H}_2\text{SO}_4}$$
  $\xrightarrow{95\% \text{ HNO}_3}$   $\xrightarrow{\text{MeO}}$   $\xrightarrow{\text{NO}_2}$   $\xrightarrow{\text{NO}_2}$ 

**Scheme 2.3.5:** Nitration of *p*-methoxy-aryl-imidazole (44)

It appears that pyrazole moiety is amenable to poly-nitrations over imidazole ring (**Scheme 2.3.2** and **2.3.5**). This is possibly due to better electron-density of p-methoxy aryl-pyrazole motif **42**. The molecular electrostatic potential graphs of compound **42** and **44** [The density functional theory (DFT) was applied at the B3PW91/+6-31G (d,p) level, with electronegative and electropositive regions] justifies this observation (**Figure 2.3.1**). A contour of electron density at 0.001 au (electrons/Bohr<sup>3</sup>) was proposed by Bader *et al.*<sup>18</sup>

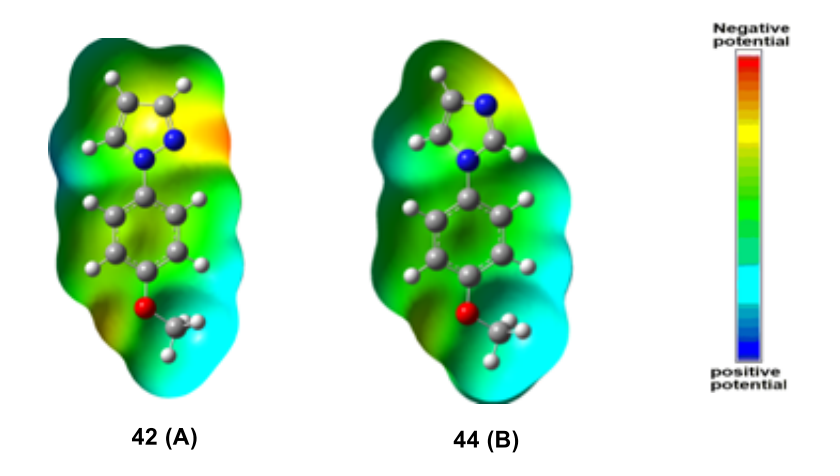


**Figure 2.3.1.** (A) Electrostatic potential surface of 4-methoxy-aryl-pyrazole (**42**), (B) Electrostatic potential surface of 4-methoxy-aryl-pyrazole (**44**)

Next, methoxy-substituted trinitro-arylimidazoles **53** and **54** were converted to amino-substituted trinitro-arylimidazoles **55** (95%) and **58** (92%), respectively, when exposed to aqueous ammonia in CH<sub>3</sub>CN (**Scheme 2.3.6**). Next, acid mediated oxidation of **55** and **58** in presence of H<sub>2</sub>SO<sub>4</sub>/H<sub>2</sub>O<sub>2</sub> led to tetranitro-aryl-imidazoles **56** (95%) and **59** (75%), respectively (**Scheme 2.3.6**). While nitramino substituted arylimidazole derivatives **57** (90%) and **60** (62%) were accessed from the nitration of **55** and **58** in presence of fuming HNO<sub>3</sub> at 0 °C, respectively (**Scheme 2.3.6**). The nitramine arylimidazole derivatives **57** and **60** are stable; whereas respective species of arylpyrazoles rapidly converted to diazo-nitro-aryl-pyrazoles (**49** and **52**; **Scheme 2.3.3** and **2.3.4**).

Scheme 2.3.6: Synthesis of -NH<sub>2</sub>/-NO<sub>2</sub>/-NHNO<sub>2</sub> substituted aryl-imidazole derivatives 55-60

# 2.4. <sup>15</sup>N NMR Spectroscopy

To distinguish different classes and connectivity of nitrogen in the molecule, <sup>15</sup>N NMR spectrum of few representative compounds **47**, **48**, **50**, **51**, **56**, and **57** were recorded in DMSO–d<sub>6</sub> (**Figure 2.4.1**). Gaussian 09 suite program was used to assign the peaks based on GIAO NMR calculations. <sup>20</sup> Taking CH<sub>3</sub>NO<sub>2</sub> as external standard, chemical shifts of <sup>15</sup>N NMR spectra were given. The <sup>15</sup>N signals resonated downfield in the range of –30 to –10 ppm corresponds to C–NO<sub>2</sub> functional groups, indicating N1/N2/N3 for compound **47**, N1/N2/N3/N4/N5 for compound **51** and N1/N2/N3/N4 for compounds **48**, **50**, **56**, and **57** (**Figure 2.4.1**). Whereas <sup>15</sup>N signal of C–NH<sub>2</sub> group are found at  $\delta = -300$  ppm (N6; for compound **47**), –298 ppm (N7; for compound **50**). Compound **57** displays nitrogen signals of the –NHNO2 group at  $\delta = -27$  (N4) and –196 (N7) ppm. The respective <sup>15</sup>N signals of pyrazole ring (N4/N5 for compound **47**, N5/N6 for compounds **48** and **50**, N6/N7 for compound **51**) resonate downfield in comparison to the imidazole rings (N5/N6 for compounds **56** and **57**) as shown in **Figure 2.4.1**.

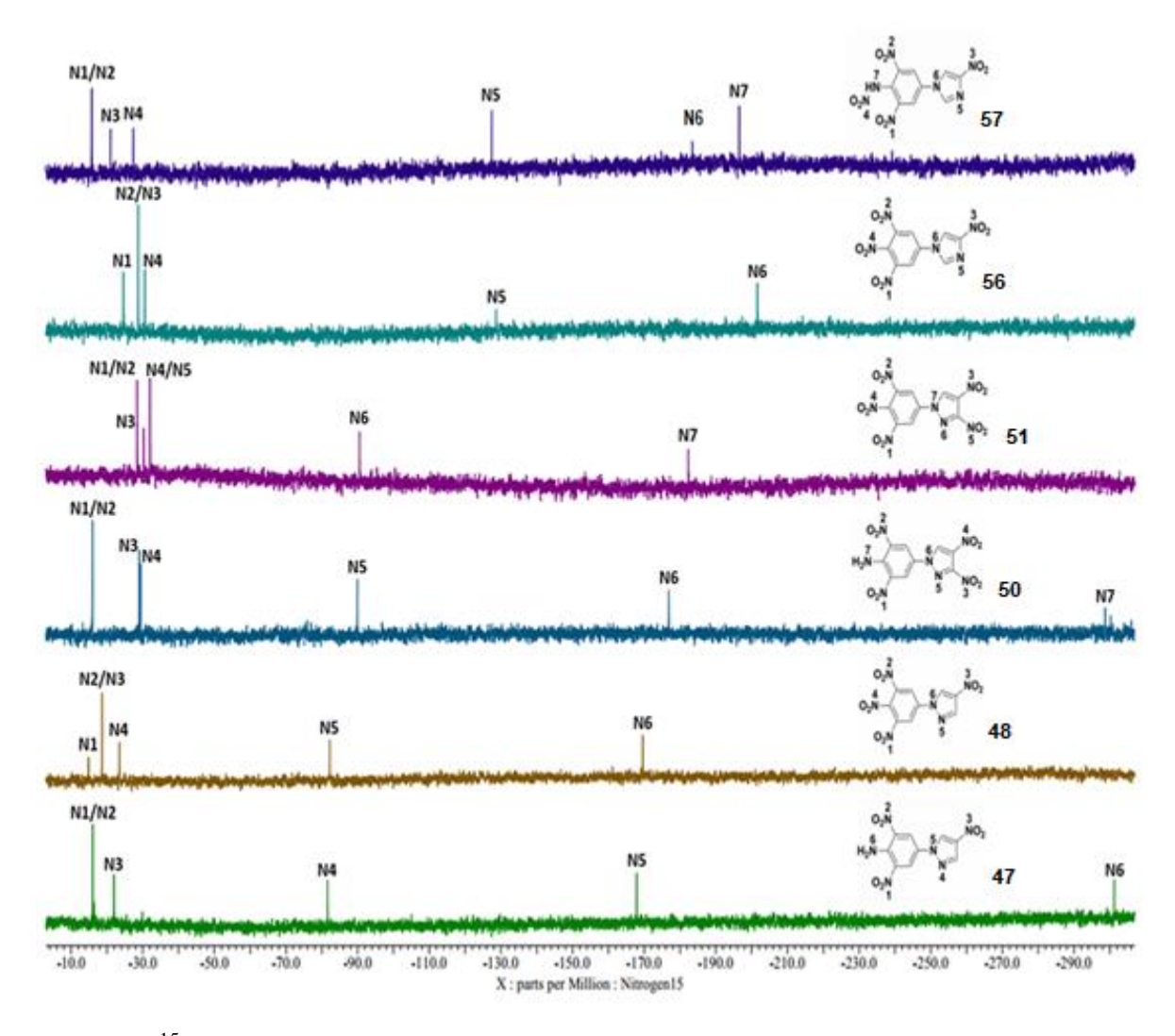
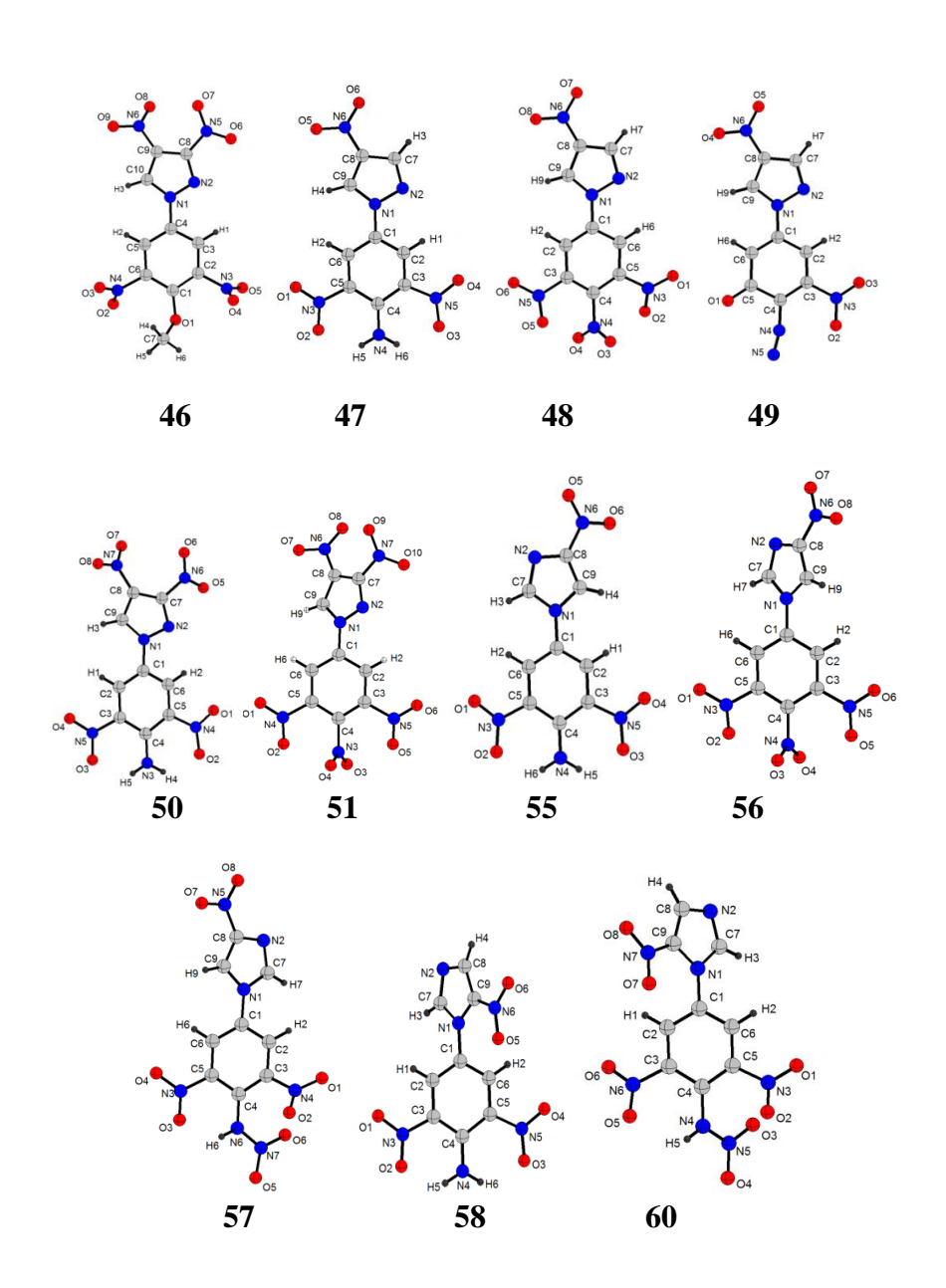


Figure 2.4.1. 15N NMR spectrums of compounds 47, 48, 50, 51, 56 and 57

# 2.5. X-ray crystallography

Single crystals were grown by slowly evaporating solutions of **46**, **47**, **48**, **49**, **50**, **51**, **55**, **56**, **57**, **58**, and **60** in EtOAc at room temperature and atmospheric pressure. X-ray diffraction analysis of single-crystal **46**, **47**, **48**, **49**, **50**, **51**, **55**, **56**, **57**, **58**, and **60** unambiguously revealed their structures. Compounds **46**, **47**, **49**, **50**, and **60** were crystallized in orthorhombic space groups with a cell volume 2696.5(2), 2251.3(3), 4320.30(19), 1297.43(6), and 1276.13(12) Å, respectively.



**Figure 2.5.1.** Molecular structures of compound **46**, **47**, **48**, **49**, **50**, **51**, **55**, **56**, **57**, **58**, and **60**; thermal ellipsoids are set at 30% probability and hydrogen atoms are labelled for clarity.

Whereas compounds **48**, **51**, **55**, **56**, and **57** were crystallized in monoclinic space groups with a cell volume 3707.2(5), 687.9(7), 1131.05(8), 2471.4(2), and 339.20 Å, respectively. Density plays vital in deciding strength of the energetic material. Based on data, density of the respective compounds

are measured at 293 K: **46** (1.75 g/cm<sup>3</sup>), **49** (1.70 g/cm<sup>3</sup>), **50** (1.74 g/cm<sup>3</sup>), **55** (1.73 g/cm<sup>3</sup>), and also measured at 294 K: **58** (1.71 g/cm<sup>3</sup>); **47** (1.74 g/cm<sup>3</sup>), **48** (1.74 g/cm<sup>3</sup>), **56** (1.74 g/cm<sup>3</sup>), **57** (1.78 g/cm<sup>3</sup>), and **60** (1.77 g/cm<sup>3</sup>). While compounds **48**, **51**, **56**, and **60** exhibit high density when measured at low temperature (**Table 2.5.1–2.5.4**).

Table 2.5.1. Crystallographic Data for Compound 46, 47, and 48

Compound	46	47	48
CCDC	2101474	2101414	2104519
Formula	$C_{10}H_6N_6O_9$	$C_9H_6N_6O_6$	$C_9H_4N_6O_8$
$ m M_{ m w}$	354.21	294.20	324.18
Crystal system	orthorhombic	orthorhombic	monoclinic
Space group	Pbca	$Pna2_1$	$P2_1/c$
T[K]	293 K	300 K	100 K
a [Å]	13.7126(6)	12.7676(12)	20.6354(16)
$b~[ ext{Å}]$	13.3853(7)	4.6897(4	11.9690(10)
$c~[ ext{Å}]$	14.6908(7)	37.599(3)	15.6184(12)
α [°]	90	90	90
eta [°]	90	90	106.049(3)
γ [°]	90	90	90
Z	8	8	12
V [Å]	2696.5(2)	2251.3(4)	3707.2(5)
$D_{calc} \; [g \; cm^{-3}]$	1.745	1.736	1.742
$\mu \ [mm^{-1}]$	0.157	0.149	0.157
Total reflns	2774	5188	9288
Unique reflns	2723	5171	9208
Observed reflns	2133	3438	7031
$R_1[I > 2\sigma(I)]$	0.0588	0.0497	0.0723
$wR_2$ [all]	0.1407	0.0952	0.2204
GOF	1.112	1.046	1.053
Diffractometer	Bruker D8 Quest CCD	Bruker D8 Quest CCD	Bruker D8 VENTURE Photon III detector

Table 2.5.2. Crystallographic Data for Compound 49, 50, and  $51^{[a]}$ 

	_		
Compound	49	50	51 <sup>[a]</sup>
CCDC	2104518	2101412	2101477
Formula	$C_9H_4N_6O_5$	$C_9H_5N_7O_8$	$C_9H_3N_7O_{10}$
$ m M_w$	276.18	339.20	369.18
Crystal system	orthorhombic	orthorhombic	monoclinic
Space group	Pbca	P2 <sub>1</sub> 2 <sub>1</sub> 2 <sub>1</sub>	P2 <sub>1</sub>
T[K]	293 K	293 K	297 K
a [Å]	9.8603(2)	7.6666(2)	7.575(5)
<i>b</i> [Å]	16.3464(5)	9.6255(3)	8.742(5)
c [Å]	26.8041(7)	17.5816(5)	10.390(6)
α[°]	90	90	90
eta [°]	90	90	90.98(2)
γ [°]	90	90	90
Z	16	4	2
V [Å]	4320.30(19)	1297.43(6)	687.9(7)
$D_{calc}$ [g/cm <sup>3</sup> ]	1.699	1.737	1.782
$\mu \ [mm^{-1}]$	0.143	0.155	0.165
Total reflns	4713	2876	3205
Unique reflns	4496	2632	3182
Observed reflns	3313	2467	1479
$R_1[I > 2\sigma(I)]$	0.0433	0.0337	0.0658
$wR_2$ [all]	0.1204	0.0904	0.1589
GOF	1.074	1.048	1.007
Diffractometer	Bruker D8 Quest CCD	Bruker D8 Quest CCD	Bruker D8 Quest CCD

<sup>[</sup>a] Data collected at room temperature (297K)

Table 2.5.3. Crystallographic Data for Compound  $51^{[b]}$ ,55, and 56

Compound	51 <sup>[b]</sup>	55	56
CCDC	2101478	2101413	2101476
Formula	$C_9H_3N_7O_{10}$	$C_9H_6N_6O_6$	$C_9H_4N_6O_8$
$M_{ m w}$	369.18	294.20	324.18
Crystal system	Triclinic	monoclinic	monoclinic
Space group	P 1	$P2_{1}/c$	C2/c
T[K]	100 K	293 K	100 K
a [Å]	7.5785(5)	8.0897(3)	25.2940(15)
$b~[ ext{Å}]$	8.6722(6)	19.9732(5)	7.5294(4)
c [Å]	10.2425(7)	7.6798(3)	13.1614(8)
<i>α</i> [°]	88.095(3)	90	90
eta [°]	88.446(3)	114.288(5)	99.609(2)
γ [°]	88.476(3)	90	90
Z	2	4	8
V [Å]	672.32(2)	1131.05(7)	2471.4(2)
$D_{calc}$ [g/cm <sup>3</sup> ]	1.824	1.728	1.743
$\mu \ [mm^{-1}]$	1.506	0.148	1.386
Total reflns	3880	2474	2050
Unique reflns	3749	2376	862
Observed reflns	3720	1632	733
$R_1[I > 2\sigma(I)]$	0.0226	0.0499	0.0356
$wR_2$ [all]	0.0582	0.1369	0.0971
GOF	1.042	1.039	1.071
Diffractometer	Bruker D8 VENTURE Photon III detector	Bruker D8 Quest CCD	Bruker D8 VENTURE Photon III detector

<sup>[</sup>b] Data collected at low temperature (100K)

Table 2.5.4. Crystallographic Data for Compound 57, 58, and 60

Compound	57	58	60	
CCDC	2101475	2104520	2101415	
Formula	$C_9H_5N_7O_8$	$C_9H_6N_6O_6$	$C_9H_5N_7O_8$	
$ m M_w$	339.20	294.20	339.20	
Crystal system	monoclinic	Triclinic	Orthorhombic	
Space group	$P2_{1}/c$	P -1	P2 <sub>1</sub> 2 <sub>1</sub> 2 <sub>1</sub>	
$T\left[ \mathbf{K} ight]$	298 K	294 K	110 K	
a [Å]	7.8948(3)	7.5582(15)	6.9295(4)	
$b~[ ext{Å}]$	22.0545(7)	7.7146(16)	10.1008(6)	
c [Å]	7.3318(3)	10.414(2)	18.2321(9)	
<i>α</i> [°]	90	88.077(8)	90	
eta [°]	97.904(2)	70.378(7)	90	
γ [°]	90	86.697(7)	90	
Z	4	2	4	
V [Å]	339.20	571.0(2)	1276.13(12)	
$D_{calc}$ [g/cm $^3$ ]	1.782	1.711	1.765	
$\mu \ [mm^{-1}]$	0.159	0.147	1.397	
Total reflns	2907	2970	1835	
Unique reflns	2900	2948	1776	
Observed reflns	2308	2213	1735	
$R_1[I > 2\sigma(I)]$	0.0548	0.0461	0.0262	
$wR_2$ [all]	0.1486	0.0951	0.0626	
GOF	1.084	0.742	1.159	
Diffractometer	Bruker D8 Quest CCD	Bruker D8 VENTURE Photon III detector	Bruker D8 VENTURE Photon III detector	

# 2.6. Energetic Properties

The energetic properties of tri/tetra/penta-nitro substituted aryl-pyrazoles (46, 47, 48, 49, 50, and 51) and tri/tetra-nitro substituted aryl-imidazoles (55, 56, 57, 58, 59, and 60) are detailed in **Table 2.6.1** and **Table 2.6.2**. All the calculations are computed using Gaussian 09 program suite.<sup>22</sup> B3LYP functional with 6-31G (+d,p) basis set is used for geometric optimization of structures and frequency analysis. Isodesmic reactions are used for the determination of HOFs of the compounds.

Among the synthesized compounds, pentanitro substituted aryl-pyrazole **51** exhibits density (1.82 g/cm<sup>3</sup> at 100K; 1.78 g/cm<sup>3</sup> at 297 K). The strong hydrogen bond interaction of the nitramino-trinitro substituted aryl-imidazole **57** reflects its density 1.78 g/cm<sup>3</sup>. The tri/tetranitro substituted aryl-pyrazole/imidazole derivatives (**46**, **47**, **48**, **50**, **55**, **56**, **58**, and **59**) displayed densities 1.70–1.76 g/cm<sup>3</sup>. Most of the compounds showed positive heat of formation.

Table 2.6.1. Energetic properties of 46, 47, 48, 49, 50, and 51 compared with TNT and TATB.

	46	47	48	49	50	51	TNT <sup>1</sup>	TATB <sup>2</sup>
ρ <sup>[a]</sup> (g cm <sup>-3</sup> )	1.75	1.74	1.73 <sup>[b]</sup>	1.70	1.74	1.78 (1.82) <sup>[b]</sup>	1.65	1.93
OB <sup>[d]</sup> (%)	-63.2	-81.6	-59.2	-86.9	-59.0	-41.1	-74.4	-55.8
$\begin{array}{c} \Delta H_{f}^{[e]} \\ \text{(kJ mol}^{\text{-}1}) \end{array}$	268.0	285.5	391.1	420.0 <sup>[f]</sup>	336.9	448.8	-67.0	-137
$T_m^{[g]}(^{\circ}C)$	149	198	197	_	180	234	80	_
T <sub>d</sub> [h] (° C)	276	301	281	180	313	287	295	360
$IS^{[i]}(J)$	>40	>40	>40	25	>40	35	15	50
FS <sup>[j]</sup> (N)	>360	>360	>360	320	>360	320	353	>360
vD <sup>[k]</sup> (ms <sup>-1</sup> )	7526	7152	7506	6817	7586	8203	6881	8114
P <sup>[l]</sup> (GPa)	24.0	20.4	23.5	18.2	24.0	29.5	19.5	31.2

Table 2.6.2. Energetic properties of 55, 56, 57, 58, 59, and 60 compared with TNT and TATB.

	55	56	57	58	59	60	TNT <sup>1</sup>	TATB <sup>2</sup>
ρ <sup>[a]</sup> (g cm <sup>-3</sup> )	1.73	1.74 <sup>[b]</sup>	1.78	1.71	1.77 <sup>[c]</sup>	1.77 <sup>[b]</sup>	1.65	1.93
OB <sup>[d]</sup> (%)	-81.6	-59.2	-59.0	-81.6	-59.2	-59.0	-74.4	-55.8
$\Delta H_{f}^{[e]}$	245.8	355.9	441.6	258.0	369.0	453.1	-67.0	-137
(kJ mol <sup>-1</sup> )								
$T_m^{[g]}({}^{\circ}C)$	237	238	_	221	_	_	80	_
T <sub>d</sub> [h] (° C)	321	279	98	275	158	109	295	360
$\mathbf{IS^{[i]}}(\mathbf{J})$	>40	>40	25	>40	>40	20	15	50
FS <sup>[j]</sup> (N)	>360	>360	240	>360	>360	240	353	>360
vD <sup>[k]</sup> (ms <sup>-1</sup> )	7075	7446	7843	6888	7738	7834	6881	8114
P <sup>[l]</sup> (GPa)	19.7	23.2	26.3	18.7	25.6	26.2	19.5	31.2

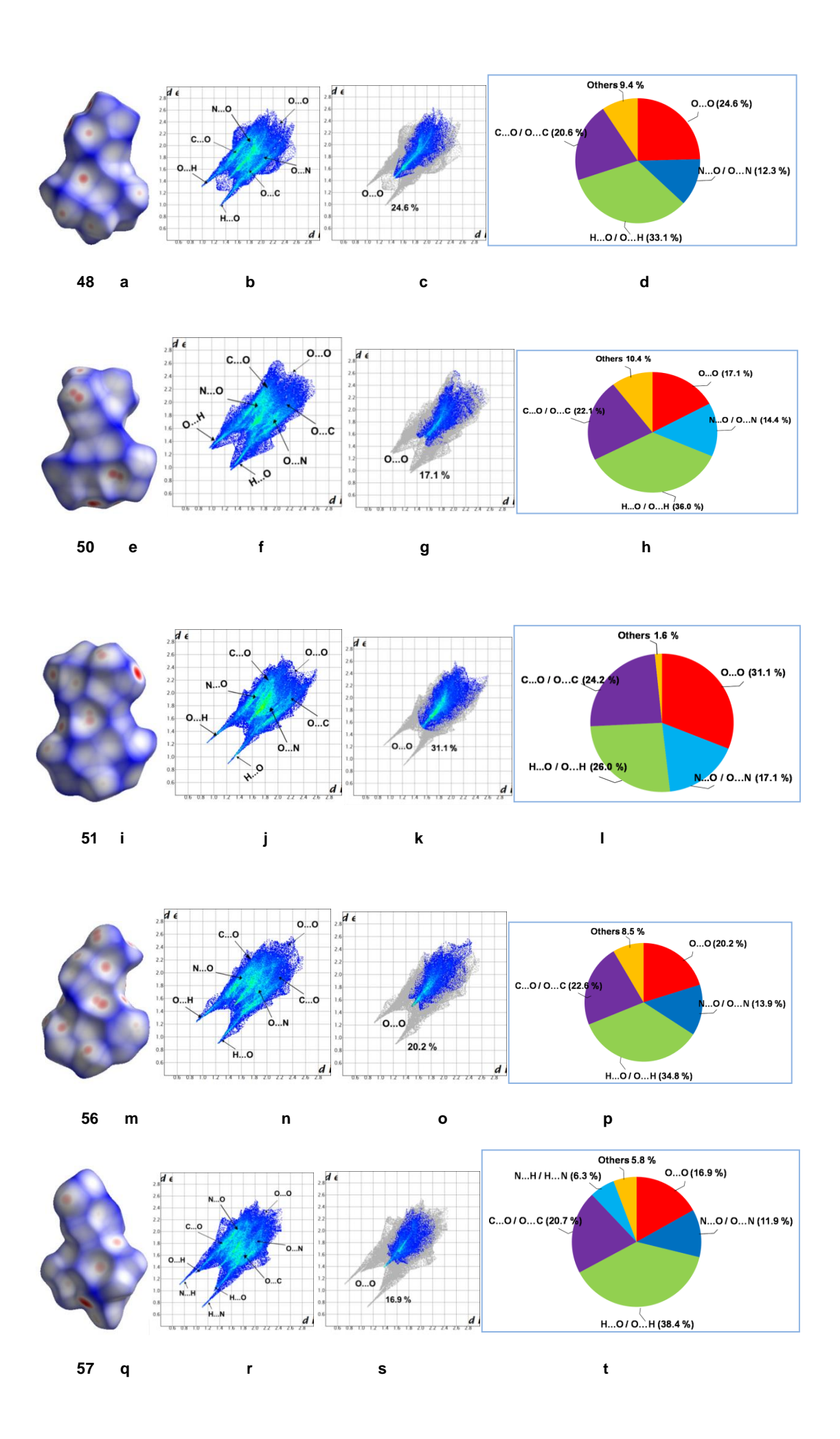
<sup>a</sup> Crystal density (298K); <sup>b</sup> Crystal density (100K); <sup>c</sup> Theoretical density by Material studio. <sup>d</sup> OB = oxygen balance (%); for C<sub>a</sub>H<sub>b</sub>O<sub>c</sub>N<sub>d</sub>: 1600(c-2a-b/2)/MW; MW = molecular weight of the compound; <sup>e</sup> Heat of formation using isodesmic reaction; <sup>f</sup> Heat of formation using MOPAC software; <sup>g</sup> Melting point (onset); <sup>h</sup> Temperature of decomposition (onset) under nitrogen gas (DSC−TGA, 10 °C min<sup>-1</sup>); <sup>i</sup> Impact sensitivity (BAM draphammer, method 1 of 6); <sup>j</sup> Friction sensitivity (BAM friction tester, method 1 of 6); <sup>k</sup> Calculated detonation velocity (EXPLO5 v6.03); <sup>l</sup> Calculated detonation pressure (EXPLO5 v6.03).

Table 2.6.1 and Table 2.6.2). In case of imidazole series, the nitramino substituted compounds 57 (441.6 kJ/mol) and 60 (453.1 kJ/mol) display high positive heat formations (a consequence of extra N–NO<sub>2</sub> functional group). Next, the detonation properties of compounds 46, 47, 48, 49, 50, 51, 55, 56, 57, 58, 59, and 60 are calculated from Explo5 version 6.03 software by using HOFs and crystal densities.<sup>23</sup> Interestingly, a majority of the synthesized compounds exhibited better detonation characteristics than TNT and were comparable to TATB (see: Table 2.6.1 and Table 2.6.2). The pentanitro-aryl-pyrazole 51 displayed high detonation velocity (8203 m/s) and detonation pressure

(29.5 GPa) (Table 2.6.1 and Table 2.6.2). While the tetranitro aryl-pyrazole derivatives 48 and 50 and the respective aryl-imidazoles 56 and 59 showed similar detonation properties. In case of -NHNO<sub>2</sub> substituted trinitro-aryl-imidazoles, **57** and **60** exhibited high detonation properties over tetranitro derivatives of aryl-pyrazole/imidazoles. The number of nitro groups in the amine-nitro contained aryl-pyrazole/imidazoles 47, 50, 55, and 58 affected detonation properties. Thus, compound 50 showed reasonable detonation properties (vD = 7586 m/s, P = 24.0 GPa), as it has more nitro groups over 47, 55, and 58. Likewsie, dinitro/diazo-oxo functionalized aryl-pyrazole 49 exhibits good detonation properties (vD =6817 m/s, P = 18.2 GPa) comparable to that of TNT. Thermal stabilities of polynitro-aryl-pyrazole/imidazole derivatives were measured using DSC-TGA analysis. To note, the -NH2 incorporated compounds 47, 50, 55, and 58 decomposed above 270 °C (**Table 2.6.1** and **Table 2.6.2**); this might be due to intra and inter hydrogen bonding between –NH<sub>2</sub> and -NO<sub>2</sub> groups. By contrast, -NHNO<sub>2</sub> substituted polynitro-aryl-imidazoles 57 and 60 are decomposed at 98 °C and 109 °C with sharp exothermic effect. Most of the polynitro bearing compounds 48, 51, and 56 are stable above 270 °C (Except 60; T<sub>d</sub> = 158 °C). The diazo-oxosubstituted derivatives 49 decomposed at 180 °C. The compounds impact sensitivity (IS) is determined using a BAM Fall-hammer apparatus with 5 kg drop weight on 15-20 mg samples. Among the molecules synthesized, the amino (-NH<sub>2</sub>) substituted derivatives 47, 50, 55, and 58 are insensitive to impact and friction (IS: >40 J; FS: >360 N). Whereas the nitramino (-NHNO2) derivatives 57 (IS: 25 J; FS: 240 N) and 60 (IS: 20 J; FS: 240 N) are relatively sensitive. The compound 49 (IS: 25 J; FS: 320 N) is less sensitive.

# 2.7. Hirshfeld Surface Analysis

To understand structure and property relationship, the Hirshfeld surfaces and two-dimensional finger print plots of **48**, **50**, **51**, **56**, **57**, and **60** are calculated by using Crystal explorer17.5<sup>24</sup> (**Figure 2.7.1**). The compounds generally possess H···O/O···H, O···O, C···O/O···C, and N···O/O···N interactions (**Figure 2.7.1**). The –NH<sub>2</sub>/–NHNO<sub>2</sub> group in **50**, **57**, and **60** contributes showing strong H···O/O···H interactions. In addition, **57** and **60** also exhibits H···N/N···H interactions (**Figure 2.7.1**, **57-n** and **60-v**). The O···O interaction percentages of the compounds **48**, **51**, **57**, and **59** showed 24.6%, 31.1%, 20.2%, and 20.3%, respectively. In general, the molecules sensitive to impact show 20.9–80.3% O···O contacts percentage.<sup>25</sup> Irrespective of high O···O interaction percentage, **48**, **51**, **56**, and **60** are largely insensitive.



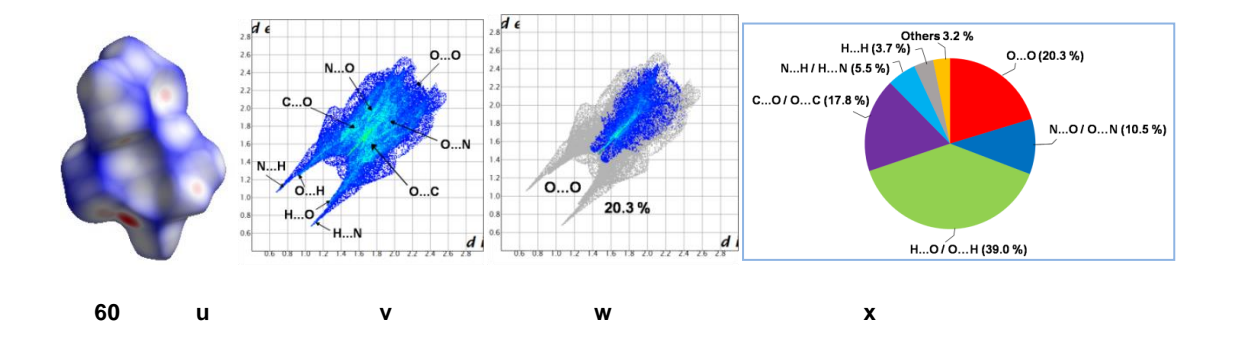


Figure 2.7.1. Hirshfeld surface calculations of 48, 50, 51, 56, 57, and 60 as well as two-dimensional fingerprint plots in the crystal structures. Images (a), (e), (i), (m), (q) and (u) are the Hirshfeld surface graphs with proximity of close contacts around 48, 50, 51, 56, 57, and 60 molecules (white, d = van der Waals (vdW) distance; blue, d >vdW distance; red, d <vdW distance). The fingerprint plots in crystal stacking are found in 48 (b), 50 (f), 51 (j), 56 (n), 57 (r), 60 (v). Images of (c), (g), (k), (o), (s) and (w) reveal the O···O atomic contact percentage contribution to the Hirshfeld surface for 48, 50, 51, 56, 57, and 60. The pie graphs (d), (h), (l), (p), (t) and (x) for 48, 50, 51, 56, 57, and 60 show percentage contributions of the individual atomic contacts to the Hirshfeld surface.

# 2.8. Conclusions

In summary, a series of N- and O-rich ploynitro/nitroamino/diazo-*N*-aryl-C-nitro pyrazole/imidazole derivatives are synthesized from readily accessible inexpensive *p*-methoxy-aryl-pyrazole/imidazole precursors. Single-crystal X-ray diffraction analysis unambiguously confirms the structure of representative compounds. The synthesized compounds are useful energetic materials (supported from theoretical and experimental studies); moreover, the compounds are thermally stable and insensitive towards impact and friction sensitivity. Importantly, pentanitro-aryl-pyrazole **51** is thermally stable insensitive high energy material as it exhibits density [1.82 g/cm<sup>3</sup> (100 K)], decomposition temperature (287 °C), impact sensitivity (IS: 35 J), and friction sensitivity (FS: 320 N) with detonation velocity (8203 m/s). The C···O/O···C, N···O/O···N, O···H/H···O, and O···O intermolecular interactions support crystal lattice stabilization of the compounds; Hirshfeld surface graphs and fingerprint plot analysis support this observation.

# 2.9. Experimental

### 2.9.1. General Information

All the reactions were performed in an oven-dried round bottomed flask. Commercial grade solvents were distilled prior to use. Column chromatography was performed using silica gel (100–200 Mesh) with hexanes and ethyl acetate mixture. Thin layer chromatography (TLC) was performed on silica gel GF254 plates. Visualization of spots on TLC plate was accomplished with UV light (254 nm) and staining over I<sub>2</sub> chamber.

Proton and carbon nuclear magnetic resonance spectra ( $^{1}$ H NMR,  $^{13}$ C NMR) were recorded on a 400 MHz ( $^{1}$ H NMR, 400 MHz;  $^{13}$ C NMR, 101 MHz) spectrometer, 500 MHz ( $^{1}$ H NMR, 500 MHz;  $^{13}$ C NMR, 126 MHz) spectrometer and 600 MHz ( $^{1}$ H NMR, 600 MHz;  $^{13}$ C NMR, 151 MHz;  $^{15}$ N NMR, 61 MHz; spectra were recorded with a JEOL JNM-ECZ-600R/M1) spectrometer, respectively. The chemical shift values (ppm) are expressed relative to the chemical shift of [D] solvent or to the external standard Liq. NH<sub>3</sub> without correction ( $^{15}$ N NMR). Data for  $^{1}$ H NMR are reported as follows: chemical shift (ppm), multiplicity (s = singlet; bs = broad singlet; d = doublet; bd = broad doublet; dd = doublet of doublet; dt = doublet of triplet; tt = triplet of triplet; t = triplet; bt= broad triplet; q= quartet; pent = pentet, m = multiplet), coupling constants *J* in (Hz), and integration.  $^{13}$ C NMR was reported in terms of chemical shift (ppm). Melting points and decomposition temperatures (DTA) were determined by DSC-TGA measurements. IR spectra were recorded on FT/IR spectrometer and are reported in cm<sup>-1</sup>. High resolution mass spectra (HRMS) were obtained in ESI mode. X-ray data was collected on a 'Bruker D8 Quest CCD' and 'Bruker D8 VENTURE Photon III detector' diffractometer using Mo-K $\alpha$  radiation (0.71073 Å) and Cu-K $\alpha$  radiation (1.54 Å).

- **2.9.2.** Caution! All the nitro substituted aryl-azole (pyrazole/imidazole) derivatives are energetic materials and it tends to explode under certain conditions unpredictably. However, none of the compounds described herein has exploded or detonated in the course of this research. Caution should be exercised at all times during the synthesis, characterization, and handling of any of these materials, and mechanical actions involving scratching or scraping must be avoided. Ignoring safety precautions can lead to serious injuries.
- **2.9.3. Materials:** Unless otherwise noted, all the reagents and intermediates were obtained commercially and used without purification. 4-Iodoanisole, pyrazole, imidazole, 30% H<sub>2</sub>O<sub>2</sub>, sodium bicarbonate (NaHCO<sub>3</sub>), aqueous ammonia, acetonitrile (CH<sub>3</sub>CN), *N*,*N*-dimethylformamide (DMF), tripotassium phosphate, and copper (I) iodide (CuI, 98%) were commercially available and used as received. Commercially available H<sub>2</sub>SO<sub>4</sub>/HNO<sub>3</sub> was used for nitration.

# 2.9.4. Theoretical study:

Density functional theory (DFT) has been broadly applied to study energetic material properties for synthesis related systems. Electronic-structure calculations were assigning with the Gaussian 09 suite. The geometries of the molecules were calculated at the B3LYP level in conjugation with 6–31G\*\* basis set. <sup>26</sup> By using CVFF force field, optimized geometries were submitted to the polymorph module of the Material studio suite for density calculations. <sup>27</sup> By using Austin Model 1 (AM1), Parameterization Method 3 (PM3), and Parameterization Method 6 (PM6), heats of formation of the pyrazole/imidazole derivatives were obtained. <sup>28</sup> The detonation properties (*D* and *P*) of the compounds were evaluated by using Kamlet–Jacobs (K-J) equations are given as follows. <sup>29</sup>

$$D=1.01 (NM^{0.5}Q^{0.5})^{0.5} (1+1.30\rho_0)$$
 [Eq. (1)]

$$P = 1.55 \ \rho_0^2 N M^{0.5} \ Q^{0.5}$$
 [Eq. (2)]

Where, D is detonation velocity (km s<sup>-1</sup>), P is detonation pressure (GPa), N is the number of moles of detonation gaseous products per gram of explosive, M is average molecular weight of the gases, Q is the heat of detonation (cal g<sup>-1</sup>), which is defined as the difference between the HOFs of the products and the reactants, and  $\rho$  is the density of the explosive (g/cm<sup>3</sup>).

## 2.9.5. X-ray Crystallography<sup>21</sup>

**X-ray crystallography of compound:** Single crystal X-ray data of the compounds **46**, **47**, **49**, **50**, **51**<sup>[a]</sup>, **55**, and **57** were collected using 'Bruker D8 Quest CMOS detector' system  $[\lambda(\text{Mo-K}\alpha) = 0.71073 \text{ Å}]$  at 293 K, 300 K, 293 K, 293 K, 297 K, 293 K, and 298 K graphite monochromator with a  $\omega$  scan width of 0.30, crystal-detector distance 60 mm, collimator 0.5 mm. The SMART software was used for the intensity data acquisition and the SAINTPLUS Software was used for the data extraction. In each case, absorption correction was performed with the help of SADABS program, an empirical absorption correction using equivalent reflections was performed with the program. The structure was solved using SHELXS-97, and full-matrix least-squares refinement against F2 was carried out using SHELXL-97. All non-hydrogen atoms were refined anisotropically. Aromatic and methyl hydrogens were introduced on calculated positions and included in the refinement riding on their respective parentatoms.

Single crystal X-ray data for the compounds **48**, **51**<sup>[b]</sup>, **56**, **58**, and **60** were collected using 'Bruker D8 VENTURE Photon III detector' system [Mo-K $\alpha$  fine focus sealed tube  $\lambda$ = 0.71073 Å] at 100 K, 100 K, 294 K, and 110 K graphite monochromator with a  $\omega$  scan. Data reduction was

performed using Bruker SAINT<sup>2</sup> software. Intensities for absorption were corrected using SADABS 2014/5. Structure solution and refinement were carried out using Bruker SHELX-TL.

# 2.9.6. Hirshfeld Surface Analysis/Fingerprint plot Analysis<sup>24</sup>

The Hirshfeld surface image (**Figure 2.7.1**) in which the red spots signify the high contact populations, while blue and white spots are for low contact populations. This suggests that the negative (red) or positive value (blue and white) of  $d_{norm}$  depends on the intermolecular contacts being shorter (red) or longer (blue and white) than the vander Waals separations. For each point on the Hirshfeld surface, the normalized contact distance ( $d_{norm}$ ) was determined by the equation shown below.

$$[d_{norm} = (\ d_i - {d_i}^{vdW})/{r_i}^{vdW} + (d_e - {d_e}^{vdW}/{r_e}^{vdW}]$$

In which,  $d_i$  is measured from the surface to the nearest atom interior to the surface interior, while  $d_e$  is measured from the surface to the nearest atom exterior to the surface interior, where  $r_i^{vdW}$  and  $r_e^{vdW}$  are the van der Waals radii of the atoms. Hirshfeld surface graphs and two-dimensional fingerprint plots of **48**, **50**, **51**, **56**, **57**, and **60** were analyzed using Crystal explorer17.5 software.

### 2.9.7. Isodesmic reactions for the prediction of heat of formation:

### 2.9.8. General N-arylation procedure for the preparation of 42 and 44 (GP-1):

A mixture of aryliodide (**40**, 1.0 mmol), azole (1.2 mmol), K<sub>3</sub>PO<sub>4</sub> (2.0 mmol), and copper (I) iodide (20 mol%) was taken in an oven-dried pressure tube under an argon atmosphère and DMF (60.0 mL) was added. The resulting reaction mixture was heated at 60 °C or 100 °C for 24 h. The reaction was cooled to room temperature, diluted with EtOAc, and washed with brine. The organic layer was dried over Na<sub>2</sub>SO<sub>4</sub>, concentrated in vacuo, and purified by flash chromatography on silica gel.

Physical characterization data are exactly matching with the reported values for the respective compound 42 and 44.

# 1-(4-Methoxyphenyl)-1*H*-pyrazole (42):

Following the general procedure (GP-1), mixture of *p*-methoxy aryliodide (**40**; 10 g, 42.73 mmol), pyrazole (**41**; 3.49 g, 51.27 mmol), K<sub>3</sub>PO<sub>4</sub> (18.11 g, 85.46 mmol), CuI (1.62 g, 8.54 mmol) in DMF (60.0 mL) was heated to 100 °C for 24 h. The crude product was purified by silica gel column chromatography eluting with hexane: ethyl acetate (9:1) to afford **42** (6.6g) in 80% as white solid.

114.6, 107.5, 55.5 ppm; HRMS (ESI) for C<sub>10</sub>H<sub>11</sub>N<sub>2</sub>O<sup>+</sup> (M+H)<sup>+</sup>: calcd 175.0871, found 175.0871.

# 1-(4-Methoxyphenyl)-1*H*-imidazole (44):

Following the general procedure (GP-1), mixture of p-methoxy aryliodide (**40**; 10 g, 42.73 mmol), imidazole (**43**; 3.48 g, 51.27 mmol), K<sub>3</sub>PO<sub>4</sub> (18.11 g, 85.46 mmol), CuI (1.62 g, 8.54 mmol) in DMF (60.0mL) was heated at 60 °C for 24 h. The crude product was purified by silica gel column chromatography eluting with hexane: ethyl acetate (6:4) to afford **44** (6.24 g) in 84% yield as white solid.

<sup>1</sup>H NMR (600 MHz, DMSO–
$$d_6$$
):  $\delta$  = 8.11 (s, 1H), 7.62 (s, 1H), 7.53 (d,  $J$  = 9.0 Hz, 2H), 7.07 (s, 1H), 7.04 (d,  $J$  = 9.0 Hz, 2H), 3.77 (s, 3H); <sup>13</sup>C NMR (151 MHz, DMSO– $d_6$ ):  $\delta$  = 158.2, 135.6, 130.4, 129.6, 122.1, 118.5, 115.0, 55.5 ppm; HRMS (ESI) for C<sub>10</sub>H<sub>11</sub>N<sub>2</sub>O<sup>+</sup> (M+H) +: calcd 175.0871, found 175.0870.

### 2.9.9. General procedure for the preparation of 45 and 46 (GP-2):

A mixture of 98% sulphuric acid and 95% nitric acid (2:1) were added to compound (42 or 45) at 0 °C. The reaction was carried out at 0 °C (for compound 42) and 90 °C (for compound 45). Upon completion, the reaction mixture was cooled by the addition of ice and neutralized with saturated aqueous solution of NaHCO<sub>3</sub>. The organic layer was extracted with ethyl acetate (4×50 mL). The combined organic extracts were washed with water (3×30 mL), brine (30 mL), and dried over Na<sub>2</sub>SO<sub>4</sub>. Solvent was filtered and evaporated under the reduced pressure. The crude residue was purified using column chromatography on silica gel to afford the desired nitration products (45 or 46) in moderate yield.

### 1-(4-Methoxy-3, 5-dinitrophenyl)-4-nitro-1*H*-pyrazole (45):

Following the general procedure (GP-2), mixture of 98% sulphuric acid (10.0 mL) and 95% nitric acid (5.0 mL) were added to **42** (1.0 g, 5.74 mmol) at 0 °C. After 2 h, the reaction mixture was cooled by the addition of ice and neutralized with saturated aqueous solution of NaHCO<sub>3</sub>. The organic layer was extracted with ethyl acetate and compound **45** (1.25 g) in 70% yield as yellow color solid upon purification through column chromatography on silica gel.

DSC–TGA (10 °C min<sup>-1</sup>, °C): 148 °C ( $T_m$ ) and 235 °C ( $T_d$ ); <sup>1</sup>H NMR (600 MHz, DMSO– $d_6$ ):  $\delta = 9.84$  (s, 1H), 8.89 (s, 2H), 8.65 (s, 1H), 4.00 (s, 3H); <sup>13</sup>C NMR (151 MHz, DMSO– $d_6$ ):  $\delta = 145.3$ , 144.8, 137.8, 137.4, 133.5,

129.5, 120.1, 64.6 ppm; IR(Neat)  $\upsilon_{max}$  3689, 3674, 3014, 2969, 2163, 1747, 1541, 1506, 1488, 1418, 1230, 1056, 963, 888, 748, 694 cm<sup>-1</sup>; HRMS (ESI) for  $C_{10}H_6N_5O_7^-$  (M–H)<sup>-</sup>: calcd 308.0267, found 308.0271.

### 1-(4-Methoxy-3, 5-dinitrophenyl)-3,4-nitro-1*H*-pyrazole (46):

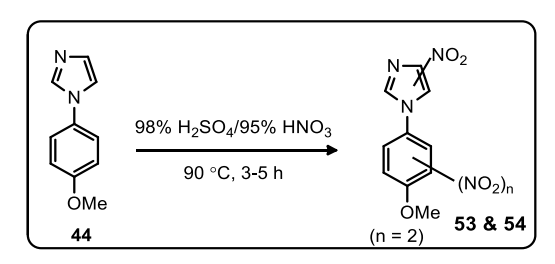
Following the general procedure (GP-2), mixture of 98% sulphuric acid (20 mL) and 95% nitric acid (10 mL) were added to 45 (2.0 g, 6.47 mmol) at 0 °C and heated to 90 °C for 7 h. The reaction was monitored by TLC. After completion of the reaction, the solution was poured into crushed ice, and neutralized with saturated aqueous solution of NaHCO<sub>3</sub>. Upon work-up, the crude mixture was purified by silica gel column chromatography eluting with hexane: ethyl acetate (9:1) to afford 46 (736 mg) in 32% yield as yellow solid.

DSC–TGA (10 °C min<sup>-1</sup>, °C): 149 °C ( $T_m$ ) and 276°C ( $T_d$ ); <sup>1</sup>H NMR (600 MHz, DMSO– $d_6$ ):  $\delta = 10.07$  (d, J = 4.2 Hz, 1H), 8.94 (s, 2H), 4.01 (s, 3H); <sup>13</sup>C NMR (151 MHz, DMSO– $d_6$ ):  $\delta = 148.3$ , 146.4, 144.7, 133.3, 132.4,

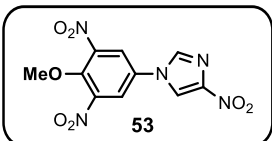
128.1, 121.2, 64.7 ppm; IR(Neat)  $\nu_{max}$  3142, 2920, 1543, 1520, 1458, 1411, 1355, 1329, 1255, 1115, 1080, 968, 875, 743 cm<sup>-1</sup>; HRMS (ESI) for  $C_{10}H_5N_6O_9^-$  (M–H)<sup>-</sup>: calcd 353.0118, found 353.0121.

## 2.9.10. General procedure for preparation of 53 and 54 (GP-3):

A mixture of 98% sulphuric acid (20.0 mL) and 95% nitric acid (10.0 mL) were added to 44 (2.0 g, 11.48 mmol) at 0 °C for 1 h and the reaction mixture was heated to 90 °C for 3–5 h. After completion of the reaction, the solution was poured into ice and neutralized with saturated aqueous solution of NaHCO<sub>3</sub>. Upon work-up, the crude mixture was purified by silicagel column chromatography eluting with hexane: ethyl acetate (7:3) to afford 53 (612 mg) and 54 (486 mg) in 17% and 13% yield, respectively, as yellow solids.



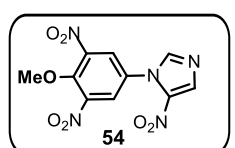
# 1-(4-Methoxy-3, 5-dinitrophenyl)-4-nitro-1*H*-imidazole (53):



Following the general procedure (GP-3) compound **53** (612 mg) was synthesized in 17% yield as yellow solid.

O<sub>2</sub>N 53 DSC-TGA (10 °C min<sup>-1</sup>, °C): 303 °C(T<sub>d</sub>); <sup>1</sup>H NMR (500 MHz, DMSO- $d_6$ ):  $\delta = 9.19-9.13$  (m, 1H), 8.88 (d, J = 1.5 Hz, 2H), 8.63–8.57(m, 1H), 3.99 (d, J = 1.5 Hz, 3H); <sup>13</sup>C NMR (126 MHz, DMSO- $d_6$ ):  $\delta = 148.1$ , 145.4, 144.6, 136.0, 130.9, 122.4, 120.1, 64.6 ppm; IR(Neat)  $\upsilon_{\text{max}}$  3142, 3074, 3020, 2922, 1636, 1598, 1554, 1514, 1369, 1317, 1211, 1146, 1060, 904, 831, 783, 717, 619 cm<sup>-1</sup>; HRMS (ESI) for C<sub>10</sub>H<sub>8</sub>N<sub>5</sub>O<sub>7</sub>+ (M+H) +: calcd 310.0423, found 310.0422.

### 1-(4-Methoxy-3,5-dinitrophenyl)-2-nitro-1*H*-imidazole (54):



Following the general procedure (GP-3), compound **54** (486 mg) was synthesized in 13% yield as yellow solid.

DSC-TGA (10 °C min<sup>-1</sup>, °C): 146 °C (T<sub>m</sub>) and 288 °C (T<sub>d</sub>); <sup>1</sup>H NMR (600 MHz, DMSO- $d_6$ ):  $\delta = 8.80$  (s, 2H), 8.29 (s, 2H), 4.03 (s, 3H); <sup>13</sup>C NMR (151 MHz, DMSO- $d_6$ ):  $\delta = 146.8$ , 143.9, 143.3, 139.1, 133.3, 130.1, 128.3, 64.7 ppm; IR(Neat)  $v_{max}$  3142, 3020, 2922, 2797,

1636, 1598, 1514, 1424, 1369, 1317, 1211, 1146, 1060, 904, 831, 717 cm<sup>-1</sup>; HRMS (ESI) for  $C_{10}H_8N_5O_7^+$  (M+H)<sup>+</sup>: calcd 310.0423, found 310.0423.

## 2.9.11. General procedure for the synthesis of compounds 47, 50, 55, and 58 (GP-4):

An aqueous solution of ammonia was added to an independent solution of compound (45, 46, 53, and 54) in acetonitrile. The resulting solution was stirred at room temperature or refluxed at 80 °C. Upon completion, the reaction mixture was cooled to room temperature. The reaction mixture was precipitated upon cooling. The solid was filtered and washed with DCM and dried in air to afford the desired products 47, 50, 55, and 58 in overall good to excellent yield.

$$(NO_2)_m$$

$$X'.N$$

$$(NO_2)_m$$

$$CH_3CN$$

$$r.t \text{ or } 80 \text{ °C}$$

$$45, 46, 53 \& 54$$

$$(NO_2)_n$$

$$RH_2$$

$$47, 50, 55 \& 58$$

$$(m = 1 \text{ or } 2$$

$$n = 2)$$

# 2,6-Dinitro-4-(4-nitro-1*H*-pyrazol-1-yl) aniline (47):

Following the general procedure (GP-4), an aqueous solution of ammonia (1.0 mL) was added to a solution of compound **45** (1.0 g, 3.23 mmol) in acetonitrile (35 mL). The resulting solution was refluxed at 80 °C for 24 h. The solvent was evaporated under reduced pressure and solid was filtered, washed with DCM, and dried in air to afford **47** (842 mg) in 88% yield as orange solid.

$$\begin{pmatrix}
O_2N & & & \\
H_2N & & & & \\
O_2N & & & & & \\
\end{pmatrix}$$

$$\begin{pmatrix}
O_2N & & & & \\
NO_2 & & & & \\
\end{pmatrix}$$

DSC-TGA (10°C min<sup>-1</sup>, °C): 198 °C (T<sub>m</sub>) and 301 °C (T<sub>d</sub>); <sup>1</sup>H NMR (600 MHz, DMSO- $d_6$ ):  $\delta = 9.81$  (s, 1H), 8.97 (s, 2H), 8.55 (s, 1H), 8.48 (s, 2H); <sup>13</sup>C NMR (151 MHz, DMSO- $d_6$ ):  $\delta = 139.9$ , 137.1, 136.8, 134.9, 128.7,

124.6, 124.5 ppm; <sup>15</sup>N NMR (61 MHz, DMSO– $d_6$ ): 362.8, 362.3, 356.9, 297.2, 210.9, 77.5 ppm; IR(Neat)  $\upsilon_{\text{max}}$  3471, 3445, 3335, 3158, 2920, 2104, 1650, 1571, 1537, 1408, 1350, 1320, 1062, 962, 896, 768, 650, 560 cm<sup>-1</sup>; HRMS (ESI) for C<sub>9</sub>H<sub>5</sub>N<sub>6</sub>O<sub>6</sub><sup>-</sup> (M–H)<sup>-</sup>: calcd 293.0271, found 293.0271.

### 4-(3,4-Nitro-1*H*-pyrazol-1-yl) 2, 6-dinitroaniline (50):

Following the general procedure (GP-4), an aqueous solution of ammonia (1.0 mL) was added to a solution of compound **46** (1.0 g, 2.82 mmol) in acetonitrile (35 mL). The resulting solution was stirred at room temperature for 3 h. The solvent was evaporated under reduced pressure and solid was filtered, washed with DCM, and dried in air to afford **50** (648 mg) in 67% yield as red solid.

$$\begin{pmatrix}
O_2N & N & NO_2 \\
H_2N & NO_2 & NO_2
\end{pmatrix}$$

DSC-TGA (10 °C min<sup>-1</sup>, °C): 180 °C (T<sub>m</sub>) and 313 °C (T<sub>d</sub>); <sup>1</sup>H NMR (600 MHz, DMSO- $d_6$ ):  $\delta = 10.03$  (s, 1H), 8.97 (d, J = 8.4 Hz, 2H), 8.59 (s, 2H); <sup>13</sup>C NMR (151 MHz, DMSO- $d_6$ ):  $\delta = 147.7$ , 140.6, 134.9, 132.7, 127.7,

125.5, 123.4 ppm; <sup>15</sup>N NMR (61 MHz, DMSO– $d_6$ ): 362.4, 349.3, 348.9, 288.4, 201.4, 79.5ppm; IR(Neat)  $\upsilon_{\text{max}}$  3465, 3353, 3085, 1648, 1540, 1518, 1456, 1418, 1326, 1360, 1232, 1120, 1090, 995, 852, 771 cm<sup>-1</sup>; HRMS (ESI) for C<sub>9</sub>H<sub>4</sub>N<sub>7</sub>O<sub>8</sub><sup>-</sup> (M–H)<sup>-</sup>: calcd 338.0122, found 338.0124.

## **2,6-Dinitro-4-(4-nitro-1***H***-imidazol-1-yl)** aniline (55):

Following the general procedure (GP-4), an aqueous solution of ammonia (1.0 mL) was added to a solution of compound **53** (1.0 g, 3.23 mmol) in acetonitrile (35 mL). The resulting solution was refluxed at 80 °C for 24 h. The solvent was evaporated under reduced pressure and solid was filtered, washed with DCM, and dried in air to afford **55** (908 mg) in 95% yield as orange color solid.

$$\begin{array}{c|c}
\hline
O_2N \\
H_2N \\
O_2N \\
\hline
55
\end{array}$$

$$\begin{array}{c|c}
N \\
NO_2
\end{array}$$

DSC–TGA (10 °C min<sup>-1</sup>, °C): 237 °C (T<sub>m</sub>) and 321 °C (T<sub>d</sub>); <sup>1</sup>H NMR (400 MHz, DMSO– $d_6$ ):  $\delta = 9.08$  (s, 1H), 8.89 (s, 2H), 8.48 (s, 3H); <sup>13</sup>C NMR (151 MHz, DMSO– $d_6$ ):  $\delta = 147.8$ , 140.1, 136.2, 134.8, 127.4, 121.6, 120.5 ppm;

IR(Neat)  $\nu_{\text{max}}$  3452, 3340, 3153, 2117, 1647, 1538, 1487, 1415, 1355, 1232, 1078, 981, 898, 771, 657, 545 cm<sup>-1</sup>; HRMS (ESI) for C<sub>9</sub>H<sub>7</sub>N<sub>6</sub>O<sub>6</sub><sup>+</sup> (M+H)<sup>+</sup>: calcd 295.0427, found 295.0426.

## 2,6-Dinitro-4-(2-nitro-1*H*-imidazol-1-yl) aniline (58):

Following the general procedure (GP-4), an aqueous solution of ammonia (1.0 mL) was added to a solution of compound **55** (1.0 g, 3.23 mmol) in acetonitrile (35 mL). The resulting solution was refluxed at 80 °C for 24 h. The solvent was evaporated under reduced pressure and the crude solid washed with DCM and dried in air to afford **58** (882 mg) in 92% yield as a red solid.

$$\begin{pmatrix}
O_2N \\
H_2N & N \\
O_2N & 58
\end{pmatrix}$$

DSC-TGA (10 °C min<sup>-1</sup>, °C): 221 °C (T<sub>m</sub>) and 275 °C (T<sub>d</sub>); <sup>1</sup>H NMR (600 MHz, DMSO- $d_6$ ):  $\delta = 8.83$  (s, 2H), 8.58 (s, 2H), 8.21 (d, J = 4.8 Hz, 2H); <sup>13</sup>C NMR (151 MHz, DMSO- $d_6$ ):  $\delta = 143.5$ , 141.0, 139.4, 134.3, 133.0, 132.4,

120.4ppm; IR(Neat)  $\nu_{max}$  3460, 3423, 3303, 3127, 2917, 2849, 1646, 1586, 1527, 1474, 1418, 1367, 1233, 1120, 1075, 900, 821, 736 cm<sup>-1</sup>; HRMS (ESI) for C<sub>9</sub>H<sub>7</sub>N<sub>6</sub>O<sub>6</sub><sup>+</sup> (M+H)<sup>+</sup>: calcd 295.0427, found 295.0420.

# 2.9.12. General procedure for the synthesis of compounds 48, 51, 56, and 59 (GP-5):

The compounds 47, 50, 55, and 58 were independently dissolved in sulphuric acid at 0 °C. Hydrogen peroxide (30%) was then added dropwise to the reaction mixture and the resulting mixture was stirred at room temperature for 24 h and then poured into ice cold water. The precipitate was filtered, washed with cold water, and recrystallized from ethyl acetate to afford desired products 48, 51, 56, and 59 in good yield as pale-yellow solid.

$$(NO_2)_m$$
X. N
$$(NO_2)_m$$
Y. N
$$(NO_2)_m$$
Y.

## 4-Nitro-1-(3, 4, 5-trinitrophenyl)-1*H*-pyrazole (48):

Following the general procedure (GP-5), compound **47** (300 mg, 1.02 mmol) was dissolved in sulphuric acid (20.0 mL) at 0 °C. Hydrogen peroxide (30%, 10.0 mL) was then added drop-wise to the reaction mixture and stirred at room temperature for 24 h and then poured into ice cold water. The precipitate was filtered and washed with cold water to provide **48** (184 mg) in 55% yield as pale-yellow solid.

$$\begin{array}{c|c}
O_2N & & \\
O_2N & & & \\
O_2N & & 48
\end{array}$$

$$NO_2$$

DSC–TGA (10 °C min<sup>-1</sup>, °C): 197 °C ( $T_m$ ) and 281 °C ( $T_d$ ); <sup>1</sup>H NMR (600 MHz, CD<sub>3</sub>CN):  $\delta = 9.32$  (s, 1H), 8.97 (s, 2H), 8.46 (s, 1H); <sup>13</sup>C NMR (151 MHz, DMSO– $d_6$ ):  $\delta = 145.6$ , 140.6, 137.6, 137.3, 129.2, 128.9, 120.7 ppm;

<sup>15</sup>N NMR (61 MHz, DMSO– $d_6$ ): 365.4, 361.6, 356.7, 298.0, 210.6 ppm; IR(Neat)  $v_{\text{max}}$  3348, 3137, 3098, 2349, 1623, 1541, 1513, 1429, 1407, 1335, 1319, 1190, 1046, 928, 889, 817, 725, 578 cm<sup>-1</sup>; HRMS (ESI) for C<sub>9</sub>H<sub>3</sub>N<sub>6</sub>O<sub>8</sub><sup>-</sup> (M–H)<sup>-</sup>: calcd 323.0013, found 323.0008.

# **3,4-Dinitro-1-(3, 4, 5-trinitrophenyl)-1***H***-pyrazole (51):**

Following the general procedure (GP-5), compound **50** (300 mg, 1.0 mmol) was dissolved in sulphuric acid (20 mL) at 0 °C. Hydrogen peroxide (30%, 10.0 mL) was then added drop-wise to the reaction mixture and stirred at room temperature for 24 h and then poured into ice cold water. The precipitate was filtered and washed with cold water to provide **51** (243 mg) in 74% yield as a pale-yellow solid.

$$\begin{pmatrix}
O_2N & NO_2 \\
O_2N & 51
\end{pmatrix}$$

DSC-TGA (10 °C min<sup>-1</sup>, °C): 234 °C ( $T_m$ ) and 287 °C ( $T_d$ ); <sup>1</sup>H NMR (500 MHz, DMSO- $d_6$ ):  $\delta = 9.93$  (s, 1H), 8.72 (s, 2H); <sup>13</sup>C NMR (126 MHz, DMSO- $d_6$ ):  $\delta = 148.2$ , 147.9, 140.8, 132.7, 127.7, 125.4, 121.8 ppm; <sup>15</sup>N

NMR (61 MHz, Acetone- $d_6$ ): 351.2, 349.3, 347.6, 289.0, 197.3 ppm; IR(Neat) $\upsilon_{\text{max}}$  3113, 2660, 2358,1721, 1657, 1545, 1455, 1325, 1206, 1115, 1025, 926, 840, 747, 587 cm<sup>-1</sup>; HRMS (ESI) for  $C_9H_2N_7O_{10}^-$  (M–H)<sup>-</sup>: calcd 367.9863, found 367.9867.

### **4-Nitro-1-(3, 4, 5-trinitrophenyl)-1***H***-imidazole (56):**

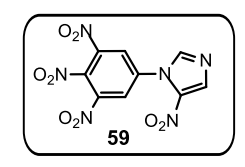
Following the general procedure (GP-5), compound **55** (300 mg, 1.02 mmol) was dissolved in sulphuric acid (20.0 mL) at 0 °C. Hydrogen peroxide (30%, 10.0 mL) was then added drop-wise to the reaction mixture and stirred at room temperature for 24 h and then poured into ice cold water. The precipitate was filtered and washed with cold water to provide **56** (314 mg) in 95% yield as a pale-yellow solid.

DSC-TGA (10 °C min<sup>-1</sup>, °C): 238 °C ( $T_m$ ) and 279 °C ( $T_d$ ); <sup>1</sup>H NMR (600 MHz, Acetone– $d_6$ ):  $\delta = 9.27$  (s, 2H), 9.09 (s, 1H), 8.64 (s, 1H); <sup>13</sup>C NMR (151 MHz, DMSO– $d_6$ ):  $\delta = 148.5$ , 141.6, 138.0, 136.5, 135.0, 123.7, 120.2

ppm; <sup>15</sup>N NMR (61 MHz, Acetone– $d_6$ ): 356.0, 351.8, 350.0, 251.9, 178.9 ppm; IR(Neat)  $\upsilon_{\text{max}}$  3146, 3119, 3087, 2355, 1574, 1549, 1510, 1494, 1343, 1303, 1271, 1063, 980, 819, 728, 597, 436 cm<sup>-1</sup>; HRMS (ESI) for C<sub>9</sub>H<sub>5</sub>N<sub>6</sub>O<sub>8</sub><sup>+</sup> (M+H)<sup>+</sup>: calcd 325.0169, found 325.0168.

# **2-Nitro-1-(3, 4, 5-trinitrophenyl)-1***H***-imidazole (60):**

Following the general procedure (GP-5), compound **58** (300 mg, 1.02 mmol) was dissolved in sulphuric acid (20 mL) at 0 °C. Hydrogen peroxide (30%, 10.0 mL) was then added drop-wise to the reaction mixture and stirred at room temperature for 24 h and then poured into ice cold water. The precipitate was filtered and washed with cold water to provide **59** (248 mg) in 75% yield as a pale-yellow solid.



DSC-TGA (10 °C min<sup>-1</sup>, °C): 158 °C (T<sub>d</sub>); <sup>1</sup>H NMR (600 MHz, CD<sub>3</sub>CN):  $\delta$  = 8.82 (s, 2H), 8.16 (s, 1H), 7.90 (s, 1H); <sup>13</sup>C NMR (151 MHz, CD<sub>3</sub>CN):  $\delta$  = 142.4, 141.1, 139.7, 137.6, 137.3, 133.4, 130.3 ppm; IR(Neat)  $\nu_{\text{max}}$  3131, 3088,

2920, 2187, 1704, 1633, 1538, 1486, 1433, 1338, 1241, 1112, 1068, 914, 821, 723, 641 cm $^{-1}$ ; HRMS (ESI) for C<sub>9</sub>H<sub>5</sub>N<sub>6</sub>O<sub>8</sub> $^+$  (M+H) $^+$ : calcd 325.0169, found 325.0166.

### 2.9.13. General procedure for the synthesis of compounds 49, 57 and 60 (GP-6):

To an ice-cold fuming nitric acid was independently added to compound 47, 55, and 58 in small portions and the reaction mixtures were stirred at 0–5 °C for 30 minutes. The resulting mixture was poured into crushed ice. The solid was collected by suction filtration and washed with cold water and dried in air to afford desired products 49, 57, and 60 in good yield.

# 4-Nitro-(3-nitro-4-diazo-phenyl-5-olate)-1*H*-pyrazole (49):

Following the general procedure (GP-6), to an ice-cold fuming nitric acid (4.0 mL) was added 47 (150 mg, 0.51 mmol) in small portions and the reaction mixture was stirred at 0–5 °C for 30 minutes. The resulting mixture was poured into crushed ice. The solid was collected by suction filtration and washed with cold water, and dried in air to afford 49 (88 mg) in 62% yield as a red solid.

DSC-TGA (10 °C min<sup>-1</sup>, °C): 180 °C (T<sub>d</sub>). <sup>1</sup>H NMR (600 MHz, DMSO- $d_6$ ):  $\delta = 9.87$  (s, 1H), 8.64 (s, 1H), 7.99 (d, J = 1.8 Hz, 1H), 7.57(d, J = 2.4 Hz, 1H); <sup>13</sup>C NMR (151 MHz, DMSO- $d_6$ ):  $\delta = 174.8$ , 143.8, 143.7, 138.4, 138.0, 130.2,

116.9, 107.2, 81.3 ppm; <sup>15</sup>N NMR (61 MHz, DMSO– $d_6$  + CD<sub>3</sub>CN): 357.0, 356.2, 354.8, 298.8, 245.2, 210.5 ppm; IR(Neat)  $v_{\rm max}$  3135, 3090, 2248, 2167, 1632, 1568, 1541, 1516, 1417, 1365, 1318, 1227, 1123, 1002, 948, 862, 711, 658, 584 cm<sup>-1</sup>; HRMS (ESI) for C<sub>9</sub>H<sub>5</sub>N<sub>6</sub>O<sub>5</sub>+ (M+H)+: calcd 277.0321, found 277.0320.

## N-(2, 6-Dinitro-4-(4-nitro-1H-imidazol-1-yl) phenyl)nitramide (57):

Following the general procedure (GP-6), to an ice-cold fuming nitric acid (4.0 mL), was added 55 (150 mg, 0.51 mmol) in small portions and the reaction mixture was stirred at 0–5 °C for 30 minutes. The resulting mixture was poured into crushed ice. The solid was collected by suction filtration and washed with cold water, and dried in air to afford 57 (156 mg) in 90% yield as a yellow solid.

$$\begin{array}{c|c}
 & O_2N \\
 & O_2N \\
 & HN \\
 & O_2N \\
 & 57
\end{array}$$

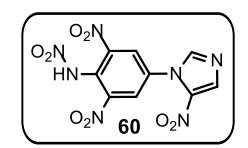
$$\begin{array}{c|c}
 & N \\
 & NO_2
\end{array}$$

DSC-TGA (10 °C min<sup>-1</sup>, °C): 98 °C (T<sub>d</sub>); <sup>1</sup>H NMR (600 MHz, DMSO- $d_6$ ):  $\delta = 9.17$  (s, 1H), 8.84 (s, 2H), 8.62 (s, 1H),7.38 (bs, 1H); <sup>13</sup>C NMR (151 MHz, DMSO- $d_6$  + one drop of Acetone- $d_6$ ):  $\delta = 148.2$ , 145.9, 136.3, 133.4,

126.5, 121.5, 120.3 ppm; <sup>15</sup>N NMR (61 MHz, DMSO– $d_6$ ): 362.4, 357.2, 350.8, 250.7, 194.7, 181.6 ppm; IR(Neat)  $v_{\text{max}}$  3132, 3080, 2350, 1613, 1581, 1539, 1514, 1497, 1447, 1398, 1341, 1268, 1077, 928, 867, 735, 686 cm<sup>-1</sup>; HRMS (ESI) for C<sub>9</sub>H<sub>6</sub>N<sub>7</sub>O<sub>8</sub><sup>+</sup> (M+H)<sup>+</sup>: calcd 340.0278, found 340.0274.

# N-(2, 6-Dinitro-4-(2-nitro-1*H*-imidazol-1-yl) phenyl)nitramide (60):

Following the general procedure (GP-6), ice-cold fuming nitric acid (4.0 mL) was added to **58** (150 mg, 0.51 mmol) in small portions and the reaction mixture was stirred at 0–5 °C for 30 minutes. The resulting mixture was poured into crushed ice. The solid was collected by suction filtration and washed with cold water and dried in air to afford **60** (108 mg) in 62% yield as a yellow solid.



DSC-TGA (10°C min<sup>-1</sup>, °C): 109 °C (T<sub>d</sub>); <sup>1</sup>H NMR (600 MHz, Acetone- $d_6$ ):  $\delta$  = 8.98 (s, 2H), 8.31 (s, 1H), 8.19 (s, 1H); <sup>13</sup>C NMR (151 MHz, Acetone- $d_6$ ):  $\delta$  = 147.3, 143.5, 137.7, 133.9, 131.2, 129.5, 123.6 ppm; IR(Neat)  $\nu_{\text{max}}$  3132,

3080, 2679, 1613, 1581, 1538, 1514, 1497, 1447, 1398, 1341, 1268, 1077, 928, 867, 735, 686 cm $^{-1}$ ; HRMS (ESI) for  $C_9H_6N_7O_8^+$  (M+H) $^+$ : calcd 340.0278, found 340.0279.

# 2.10. References

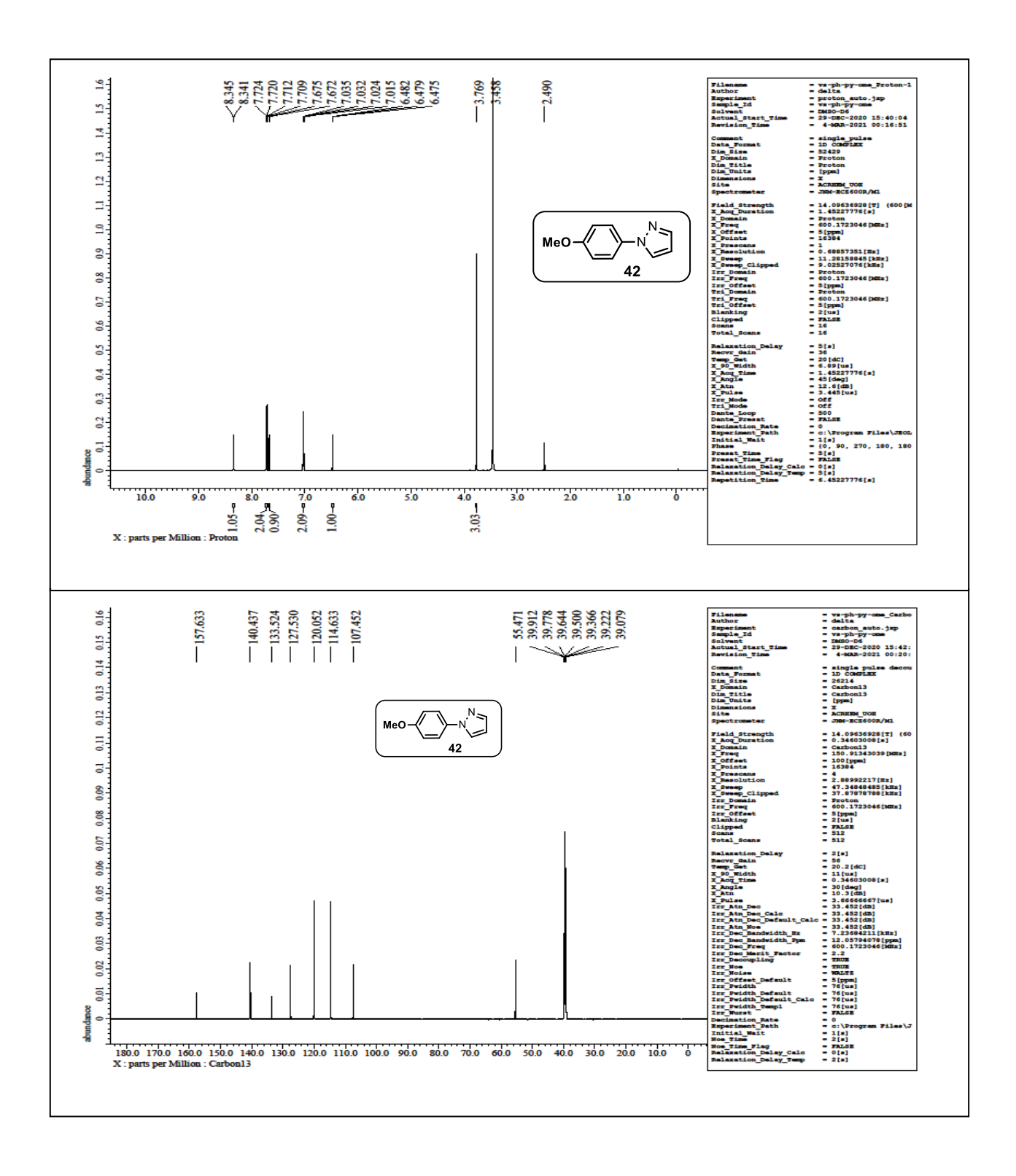
- 1. (a) C. E. Gregory, *Explosives for North American Engineers, Trans Tech Publications*, Clausthal-Zellerfeld, Germany, vol. 5, **1984**; (b) T. L. Davis, *The Chemistry of Powder and Explosives*, Wiley, New York, vol. 2, **1943**;
- 2. (a) V. M. Boddu, D. S. Viswanath, T. K. Ghosh and R. Damavarapu, *J. Hazard. Mater.*, **2010**, *181*, 1–8; (b) J. Sun, B. Kang, C. Xue, Y. Liu, Y. X. Xia, X. F. Liu and W. Zhang, *J. Energ. Mater.*, **2010**, *28*, 189–201; (c) C. M. Tarver, *J. Phys. Chem. A*, **2010**, *114*, 2727–2736.
- 3. (a) A. S. Kumar, V. B. Rao, R. K. Sinha and A. S. Rao, *Propellants, Explos., Pyrotech.*, **2010**, *35*, 359–364; (b) H. W. Qiu, V. Stepanov, A. R. Di Stasio, T. M. Chou and W. Y. Lee, *J. Hazard. Mater.*, **2011**, *185*, 489–493; (c) J. D. Zhang, X. L. Cheng and F. Zhao, *Propellants, Explos., Pyrotech.*, **2010**, *35*, 315–320.
- 4. (a) C. W. An, J. Y. Wang, W. Z. Xu and F. S. Li, *Propellants, Explos., Pyrotech.*, **2010**, *35*, 365–372; (b) Y. Bayat, M. Eghdamtalab and V. Zeynali, *J. Energ. Mater*, **2010**, *28*, 273–284; (c) Y. Q. Wu and F. L. Huang, *J. Hazard. Mater.*, **2010**, *183*, 324–333; (d) G. X. Zhang and B. L. Weeks, *Propellants, Explos., Pyrotech.*, **2010**, *35*, 440–445.
- 5. (a) P. Yin, Q. Zhang, J. Zhang, D. A. Parrish, and J. M. Shreeve, *J. Mater. Chem.A*, **2013**, *1*, 7500–7510; (b) Y. Zhang, D. A. Parrish, and J. M. Shreeve, *J. Mater. Chem.*, **2012**, 22, 12659–12665; (c) T. M. Klapötke, J. Stierstorfer, M. Weyrauther, and T. G. Witkowski, *Chem. Eur. J.*, **2016**, 22, 8619 –8626; (e) T. M. Klapotke, C. Pfluger, and M. W. Reintinger, *Eur. J. Inorg. Chem.*, **2016**, 138–147; (f) P. Yin, J. Zhang, C.He, D. A. Parrish and J. M. Shreeve, *J. Mater. Chem. A*, **2014**, 2, 3200–3208.
- 6. P.Yin, D. A. Parrish, and J. M. Shreeve, *J. Am. Chem. Soc.*, **2015**, *137*, 4778–4786.
- 7. (a) Dalinger, I. L.; Vatsadze, I. A.; Shkineva, T. K.; Popova, G. P.; Shevelev, S. A. *Synthesis*, **2012**, *44*, 2058–2064; (b) Dalinger, I. L.; Cherkasova, T. I.; Popova, G. P.; Shkineva, T. K.; Vatsadze, I. A.; Shevelev, S. A.; Kanishchev, M. I. *Russ. Chem. Bull. Int. Ed.*, **2009**, *58*, 410–413; (c) He, C.; Zhang, J.; Parrish, D. A.; Shreeve, J. M. *J. Mater. Chem. A*, **2013**, *1*, 2863–2868; (d)
- Yin, P.; Zhang, J.; He, C.; Parrish, D. A.; Shreeve, J. M. *J. Mater. Chem. A*, **2013**, *1*, 2863–2868; (d) Yin, P.; Zhang, J.; He, C.; Parrish, D. A.; Shreeve, J. M. *J. Mater. Chem. A*, **2014**, *2*, 3200–3208.
- 8. M. –X. Zhang, P. F. Pagoria, G. H. Imler, and D. Parrish, *J. Heterocyclic Chem.*, **2019**, *56*, 781–787.
- 9. P. Yin, J. Zhang, D. A. Parrish, J. M. Shreeve, *Chem. Eur. J.*, **2014**, *20*, 16529–16536.
- 10. P. Yin, C. He, and J. M. Shreeve, *Chem.Eur.J.*, **2016**,22,2108–2113.
- 11. P. Yin, J. Zhang, G. H. Imler, D. A. Parrish, and J. M. Shreeve, *Angew. Chem. Int. Ed.*, **2017**, 56, 8834–8838.

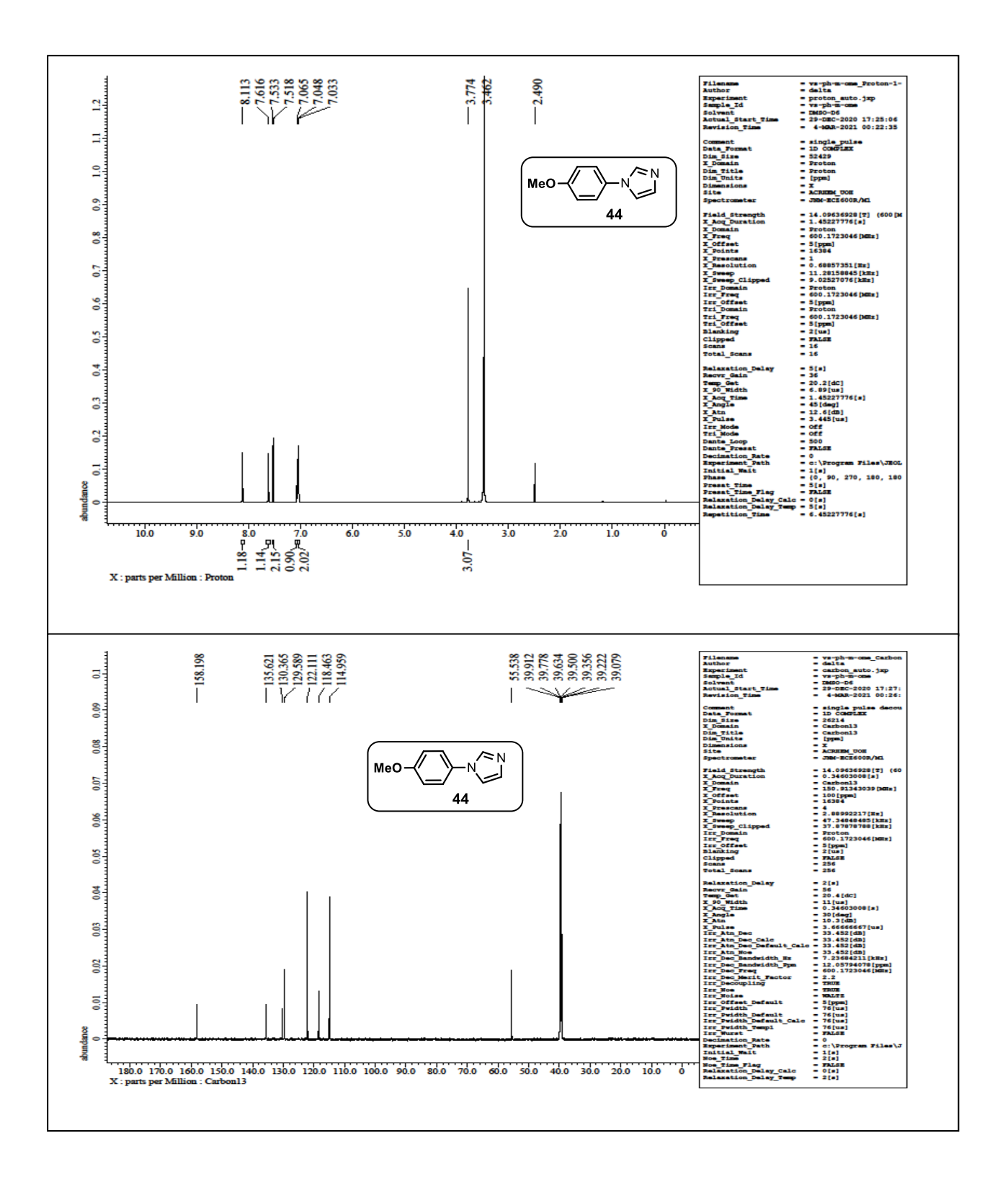
- 12. M. Reichel, D. Dosch, K. Karaghiosoff, and T. M. Klapötke, *J. Am. Chem. Soc.*, **2019**, *141*, 19911–19916.
- 13. (a) A. O. Yigiter, M. K. Atakol, M. L. Aksu, O. Atakol, *J. Therm. Anal. Calorim*, **2017**, *127*, 2199–2213; (b) D. Bauer, D. E. Dosch, V. Fuchs, K. Karaghiosoff, and T. M. Klapötke, *Eur. J. Org. Chem.*, **2021**, 1964–1970; (c) I. L. Dalinger, I. A. Vatsadse, T. K. Shkineva, G. P. Popova, B. I. Ugrak, and S. A. Shevelev, *Russian Chemical Bulletin, International Edition*, **2010**, *59*, 1631–1638.
- 14. K. Hou, C. Maz, and Z. Liu, New J. Chem., 2013, 37, 2837.
- 15. (a) P. Yin, J. Zhang, D. A. Parrish, J. M. Shreeve, *Chem. Eur. J.*, **2014**, *20*, 16529–16536; (b) D. Fischer, J. L. Gottfried, T. M. Klapötke, K. Karaghiosoff, J. Stierstorfer, T. G. Witkowski, *Angew. Chem. Int. Ed.*, **2016**, *55*, 16132–16135; (c) M. Zhang, H. Gao, C. Li, W. Fu, L. Tang, Z. Zhou, *J. Mater. Chem. A*, **2017**, *5*, 1769–1777.
- 16. (a) Po Man Liu, C. G. Frost, *Org. Lett.*, **2013**, *15*, 22, 5862–5865; (b) M. Taillefer, N. Xia, A. Ouali, *Angew. Chem. Int. Ed.*, **2007**, *46*, 934–936; (c) G. G. Pawar, W. Haibo, D. Subhadip, D. Maa, *Adv. Synth. Catal.*, **2017**, *359*, 1631–1636; (d) X. Wang, M. Wang, and J. Xie, *Syn. Commun.*, **2017**, *47*, 1797–1803; (e) S. Das, P. Natarajan, and B. König, *Chem. Eur. J.* **2017**, 23, 18161–18165.
- 17. N. Kommu, M. Balaraju, V. D. Ghule, A. K. Sahoo, J. Mater. Chem. A, 2017, 5, 7366–7371.
- 18. (a) R. F. W. Bader, M. T. Carroll, J. R. Cheeseman, C. Chang, *J. Am. Chem. Soc.*, **1987**, *109*, 7968–7979; (b) J. S. Murray, P. Politzer, *Croat. Chem. Acta*, **2009**, 82, 267–275; (c) P. Politzer, J. S. Murray, F. A. Bulat, *J. Mol. Model.*, **2010**, 16, 1731–1742; (d) V. D. Ghule, D. Srinivas, K. Muralidharan, *Asian J. Org. Chem.*, **2013**, 2, 662–668; (e) D. Srinivas, V. D. Ghule, K.
- Muralidharan, New J. Chem., 2014, 38, 3699-3707.
- 19. (a) P. Yin, D. A. Parrish, and J. M. Shreeve, *Chem. Eur. J.*, **2014**, *20*, 6707–6712; (b) J. Zhang, C. He, D. A. Parrish, and J. M. Shreeve, *Chem. Eur. J.*, **2013**, *19*, 8929–8936; (c) R. Wang, Y. Guo, R. Sa, and J. M. Shreeve, *Chem. Eur. J.*, **2010**, *16*, 8522–8529; (d) Y. Zhang, Y. Guo, Y. H. Joo, D. A. Parrish, and J. M. Shreeve, *Chem. Eur. J.*, **2010**, *16*, 10778–10784; (e) J. Zhang, D. A. Parrish and J. M. Shreeve, *Chem. Commun.*, **2015**, *51*, 7337–7340.
- 20. M. J. Frisch, et al., Gaussian 09, Revision C.01, Gaussian, Inc., Wallingford CT, 2010.
- 21. (a) O. V. Dolomanov, A. J. Blake, N. R. Champness, M. Schroder, *J. Appl. Cryst.* **2003**, 36,1283; (b) SAINT, version 6.45 /8/6/03 and version 8.34A, Bruker Apex-III, **2003**, **2014**.(c) G. M. Sheldrick, *SHELXS-97*, University of Gottingen, Germany, **1997** (d) Sheldrick, G. M.; SADABS and SADABS 2014/5, *Program for Empirical Absorption Correction of Area Detector Data*, University of Göttingen, Germany, **1997**, **2014**; (e) *SMART* (*version5.625*), *SHELX-TL* (*version6.12*), Bruker AXS Inc. Madison, WI, **2000**.

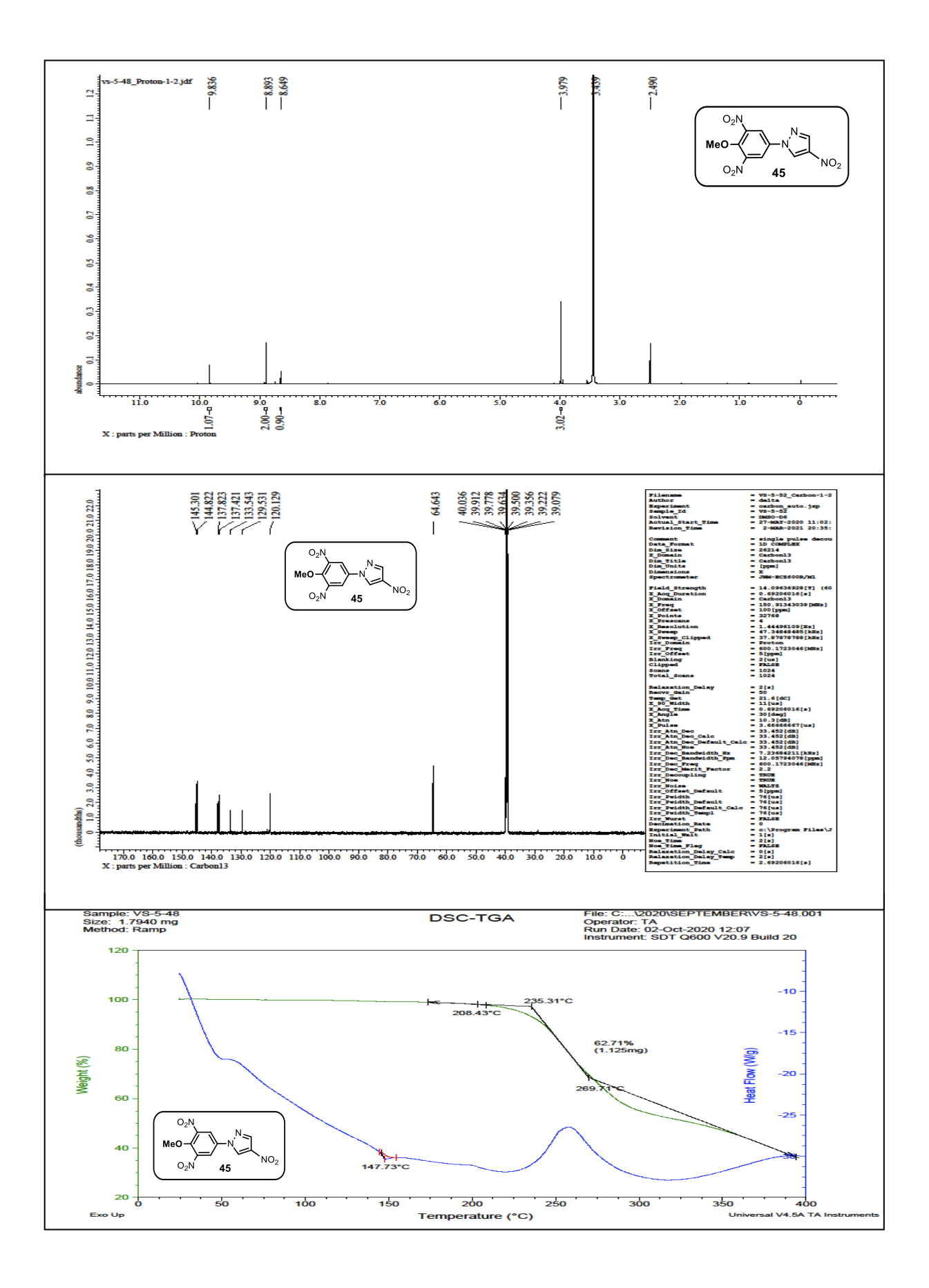
- 22. Gaussian 09, Revision C.01, M. J. Frisch, G. W. Trucks, H. B. Schlegel, G. E. Scuseria, M. A. Robb, J. R. Cheeseman, G. Scalmani, V. Barone, B. Mennucci, G. A. Petersson, H. Nakatsuji, M. Caricato, X. Li, H. P. Hratchian, A. F. Izmaylov, J. Bloino, G. Zheng, J. L. Sonnenberg, M. Hada, M. Ehara, K. Toyota, R. Fukuda, J. Hasegawa, M. Ishida, T. Nakajima, Y. Honda, O. Kitao, H. Nakai, T. Vreven, J. A. Montgomery, Jr., J. E. Peralta, F. Ogliaro, M. Bearpark, J. J. Heyd, E. Brothers, K. N. Kudin, V. N. Staroverov, R. Kobayashi, J. Normand, K. Raghavachari, A. Rendell, J. C. Burant, S. S. Iyengar, J. Tomasi, M. Cossi, N. Rega, J. M. Millam, M. Klene, J. E. Knox, J. B. Cross, V. Bakken, C. Adamo, J. Jaramillo, R. Gomperts, R. E. Stratmann, O. Yazyev, A. J. Austin, R. Cammi, C. Pomelli, J. W. Ochterski, R. L. Martin, K. Morokuma, V. G. Zakrzewski, G. A. Voth, P. Salvador, J. J. Dannenberg, S. Dapprich, A. D. Daniels, O. Farkas, J. B. Foresman, J. V. Ortiz, J. Cioslowski, D. J. Fox, Gaussian, Inc., Wallingford CT, 2009.
- 23. M. Suceska, EXPLO5 version6.03, 2014.
- 24. (a) Spackman, M. A.; McKinnon, J. J. Fingerprinting intermolecular interactions in molecular crystals. *CrystEngComm.*, **2002**, *4*, 378–392; (b) Spackman, M. A.; Jayatilake, D. Hirshfeld surface analysis. *CrystEngComm.*, **2009**, *11*, 19–32; c) Zhang, C.; Xue, X.; Cao, Y.; Zhou, Y.; Li, H.; Zhou, J.; Gao, T. Intermolecular friction symbol derived from crystal information. *CrystEngComm.*, **2013**, *15*, 6837–6844; (d) Turner, M.J.; McKinnon, J.J.; Wolff, S.K.; Grimwood, D.J.; Spackman, P.R.; Jayatilaka, D.; Spackman, M.A. Crystal Explorer 17; University of Western Australia: Pert, Australia, **2017**.
- 25. (a) C. J. Eckhardt and A. Gavezzotti, *J. Phys. Chem. B*, **2007**, *111*, 3430; (b) C. Zhang, X. Xue, Y. Cao, Y. Zhou, H. Li, J. Zhou and T. Gao, *CrystEngComm*, **2013**, *15*, 6837–6844; (c) J. Zhang, Q. Zhang, T. T. Vo, D. A. Parrish and J. M. Shreeve, *J. Am. Chem. Soc.*, **2015**, *137*, 1697–1704.

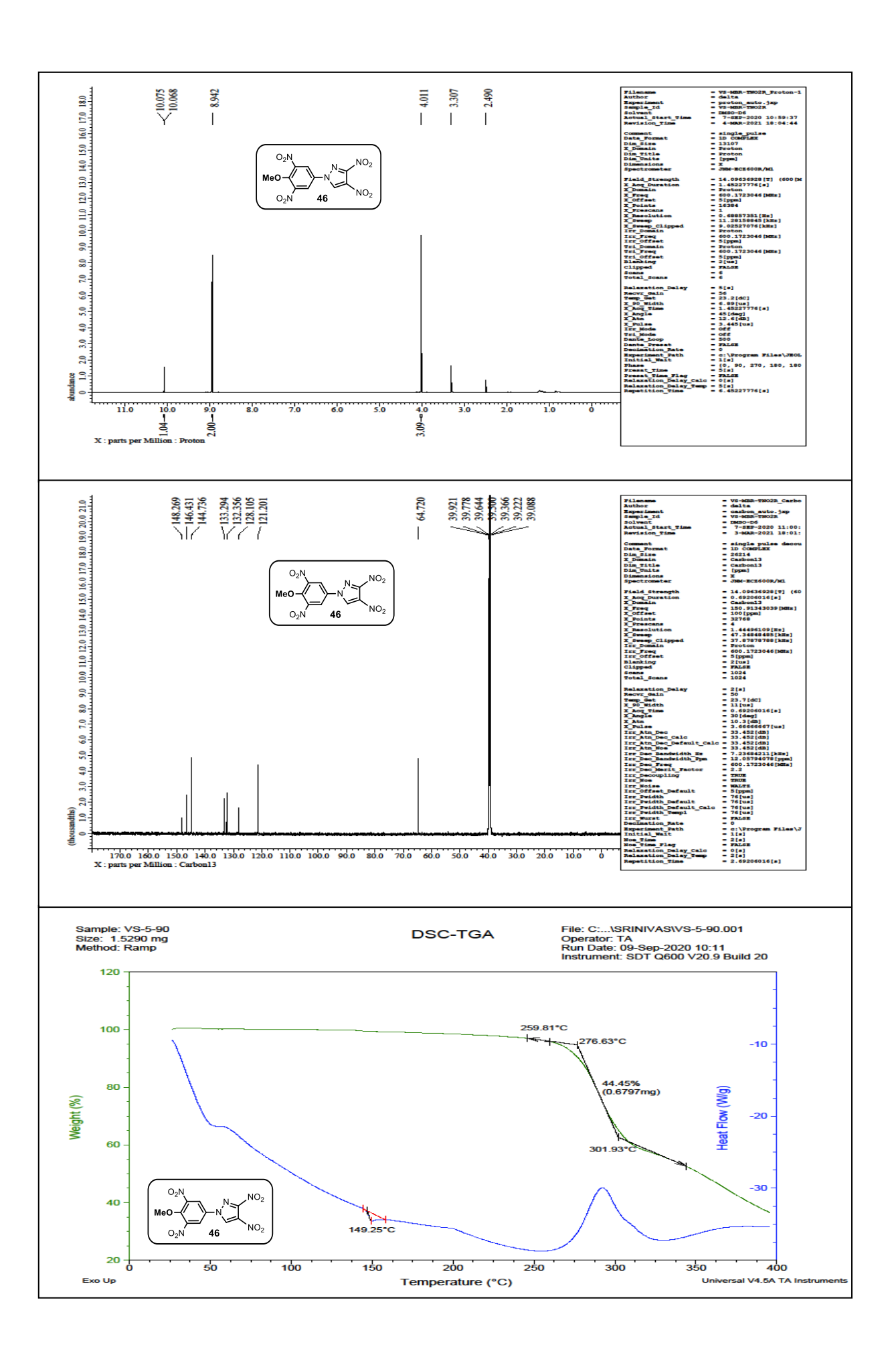
  26. (a) A. D. Becke, *J. Chem. Phys.*, **1993**, *98*, 5648–5652; (b) C. Lee, W. Yang, R. G. Parr, *Phys. Rev.*, **1988**, *B37*, 785–789.
- 27. Material Studio 5.5, Accerlys Inc. San Diego, 2010.
- 28. J. J. P. Stewart, J. Mol. Model., 2007, 13, 1173–1213.
- 29. (a) M. J. Kamlet, S. J. Jacobs, *J. Chem. Phys.*, **1968**, 48, 23; (b) M. J. Kamlet, J. E. Ablard, *J. Chem. Phys.*, **1968**, 48, 36.

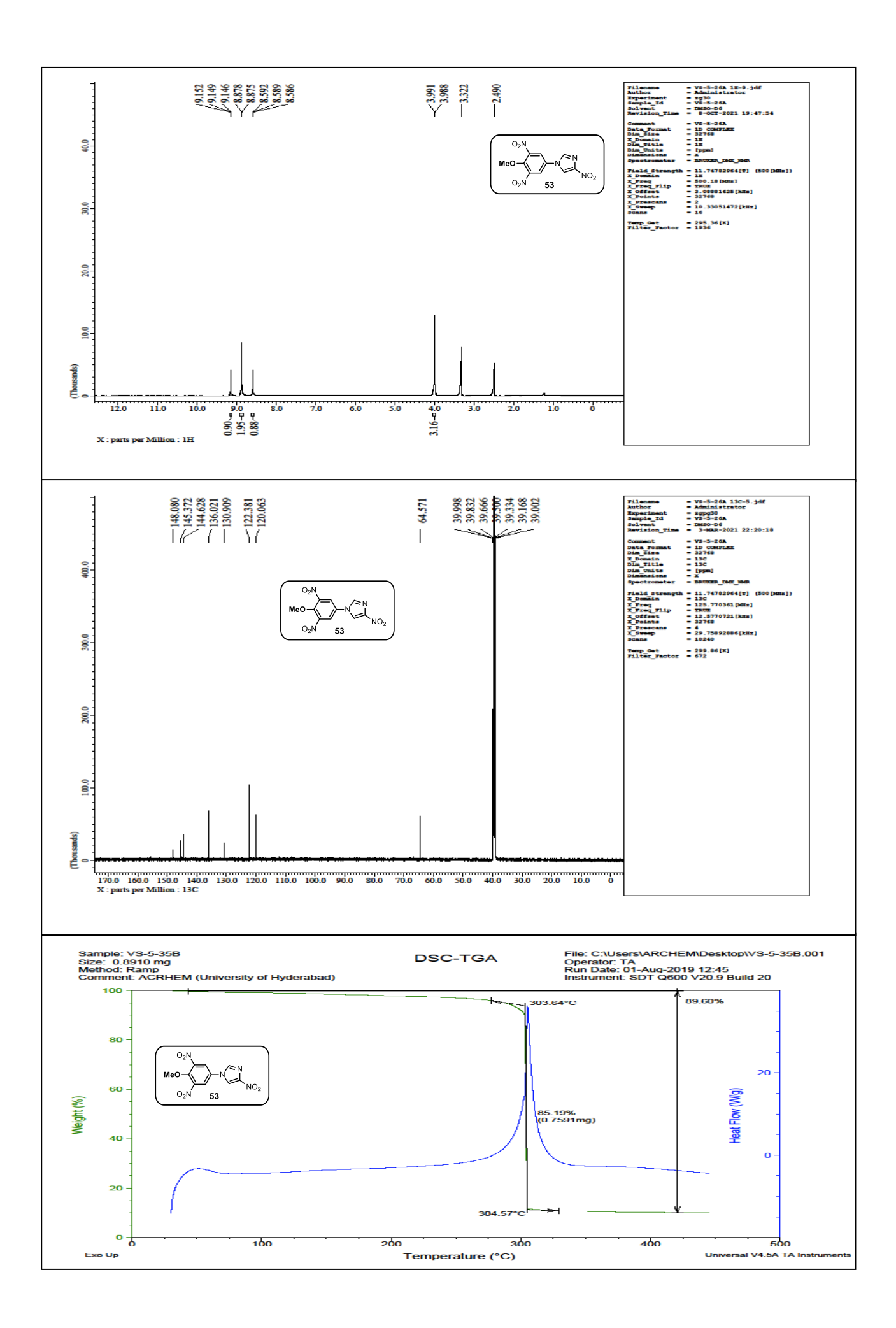
# 2.11. Spectral data

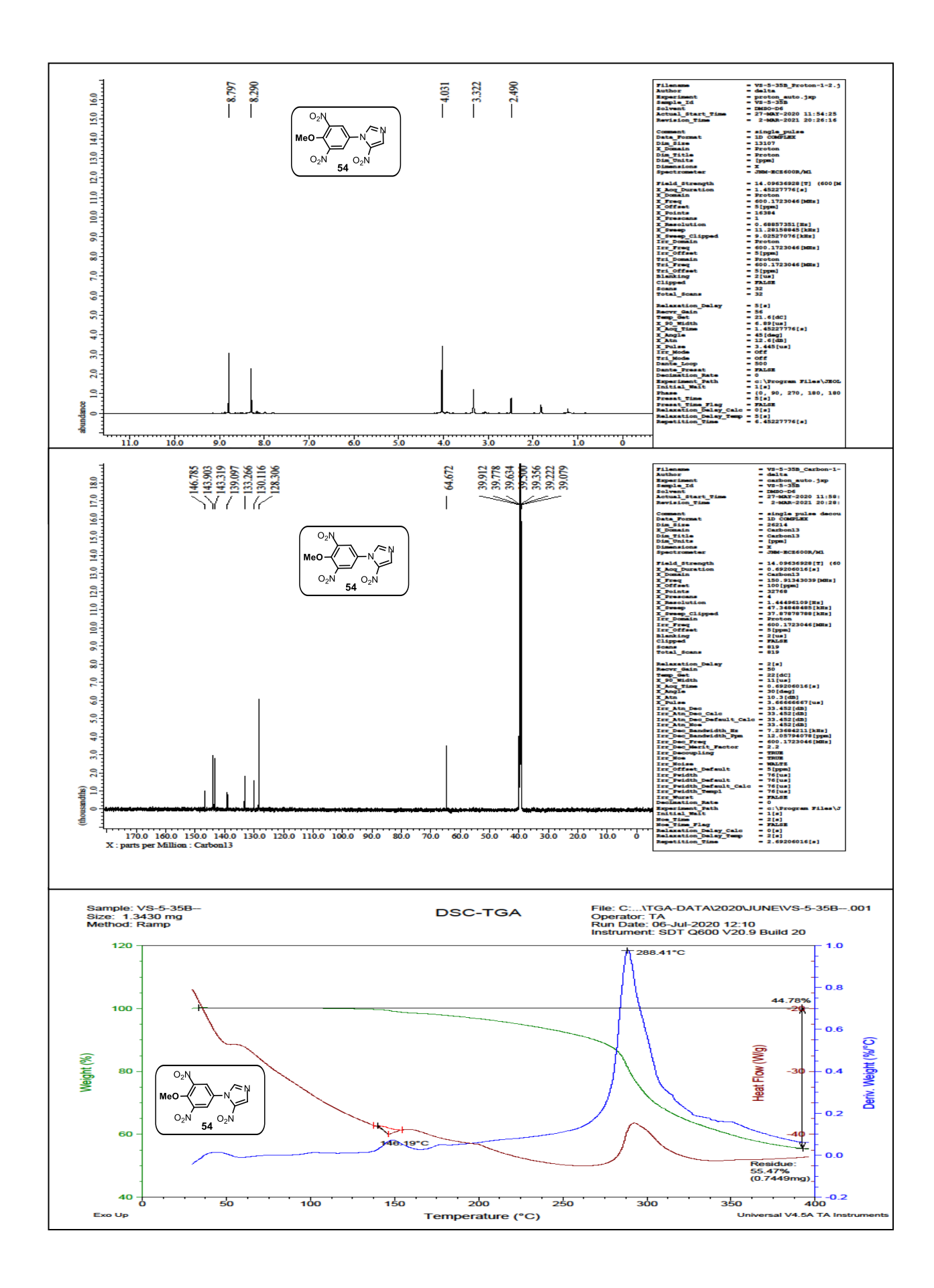


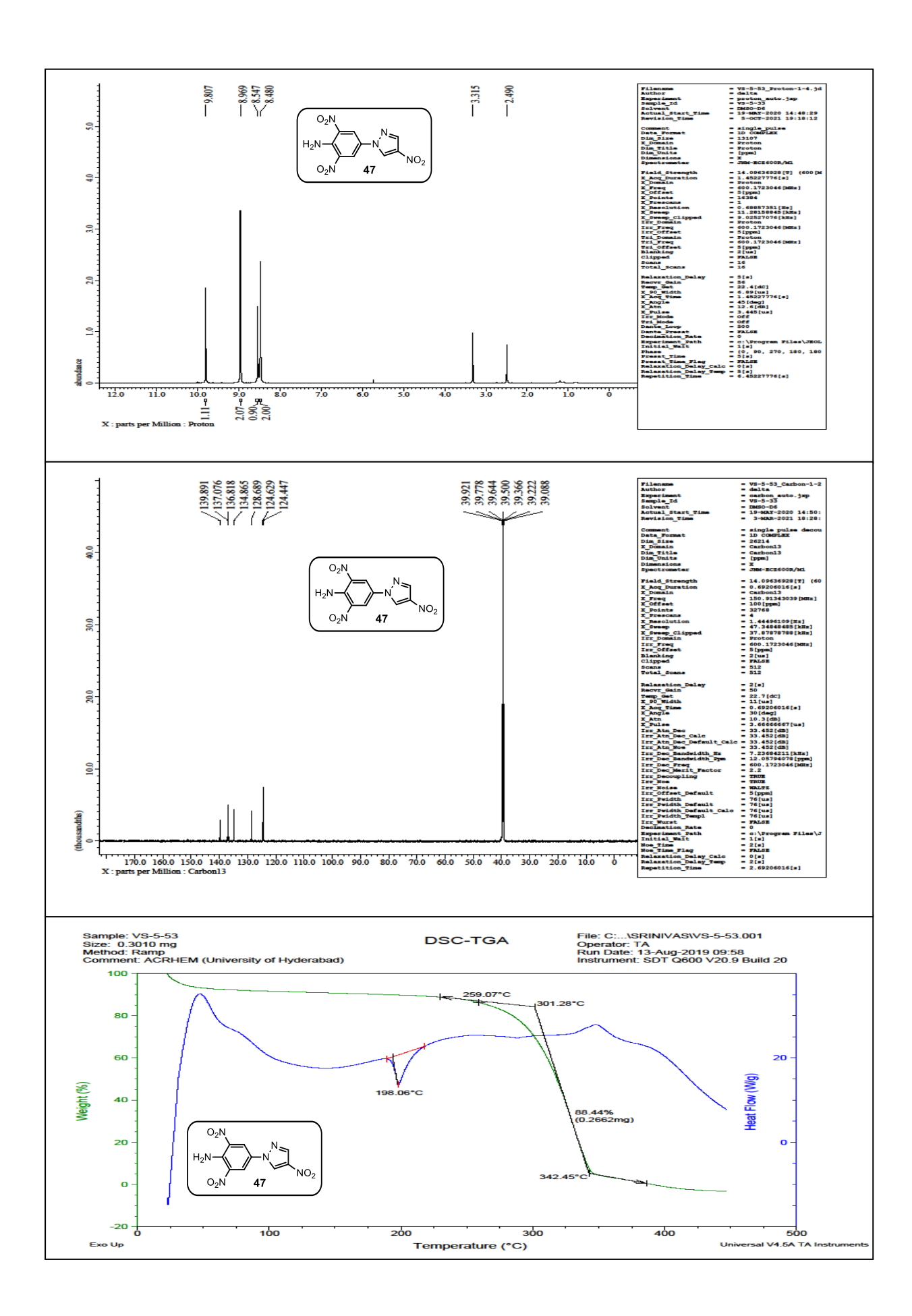


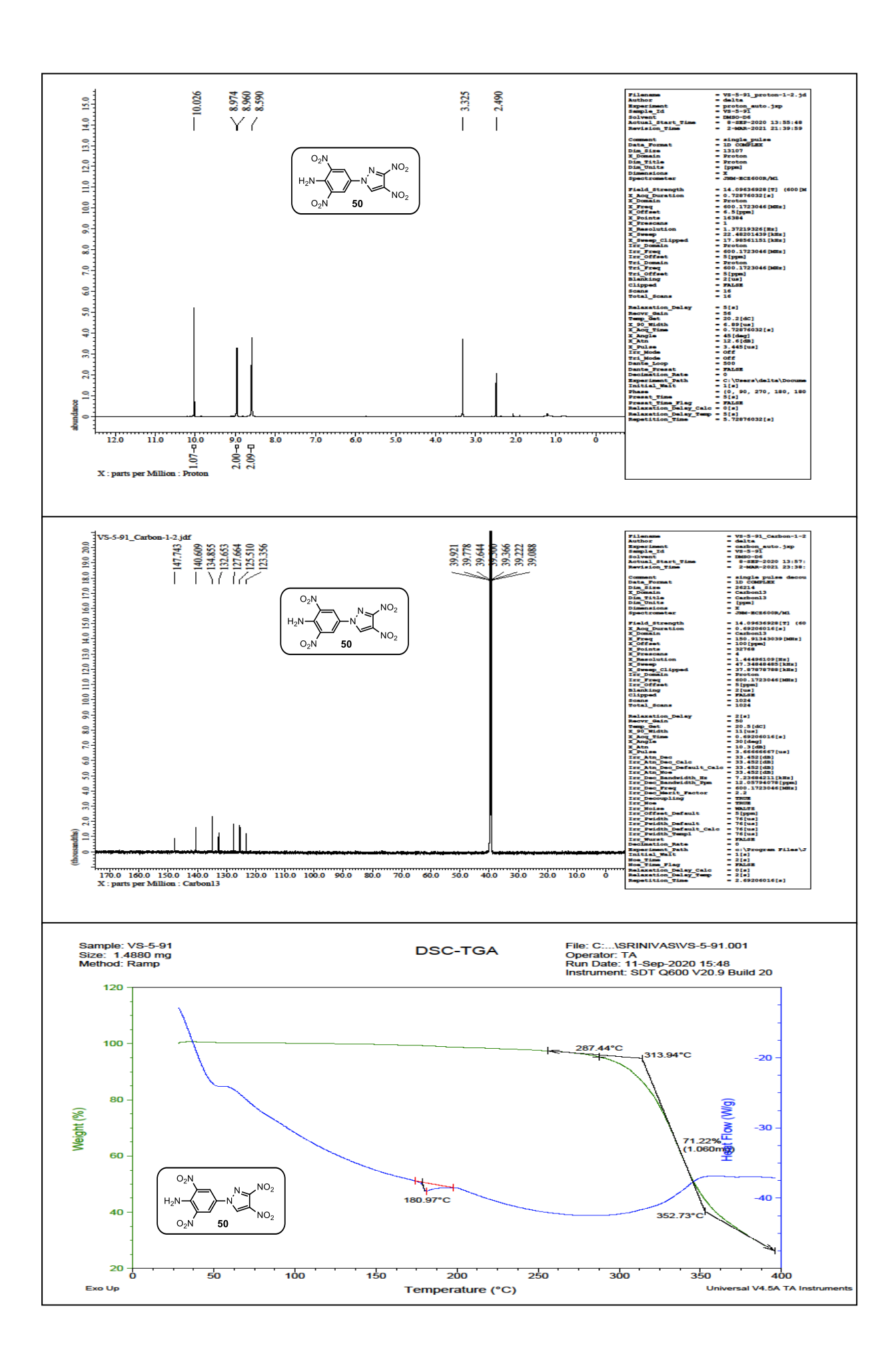


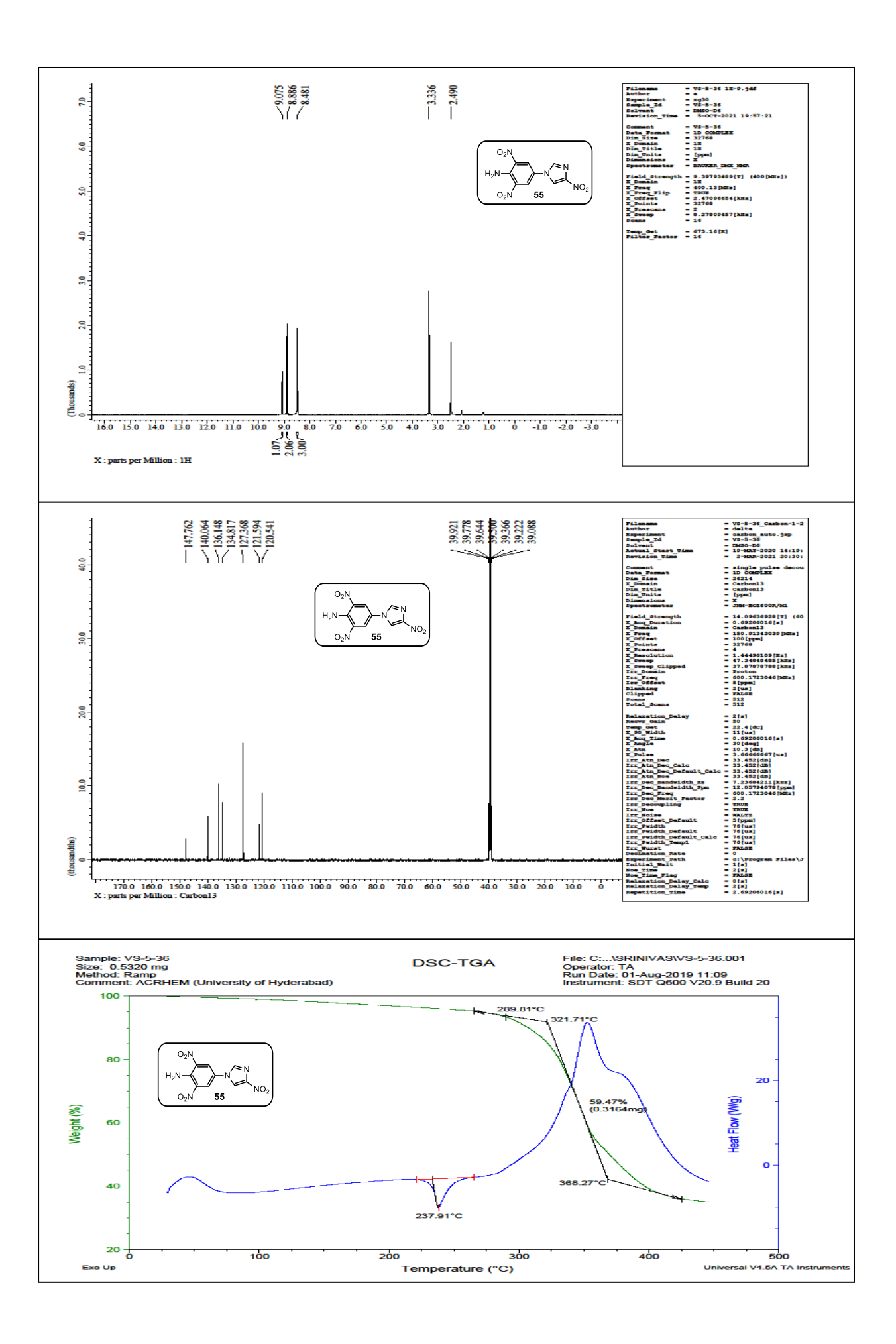


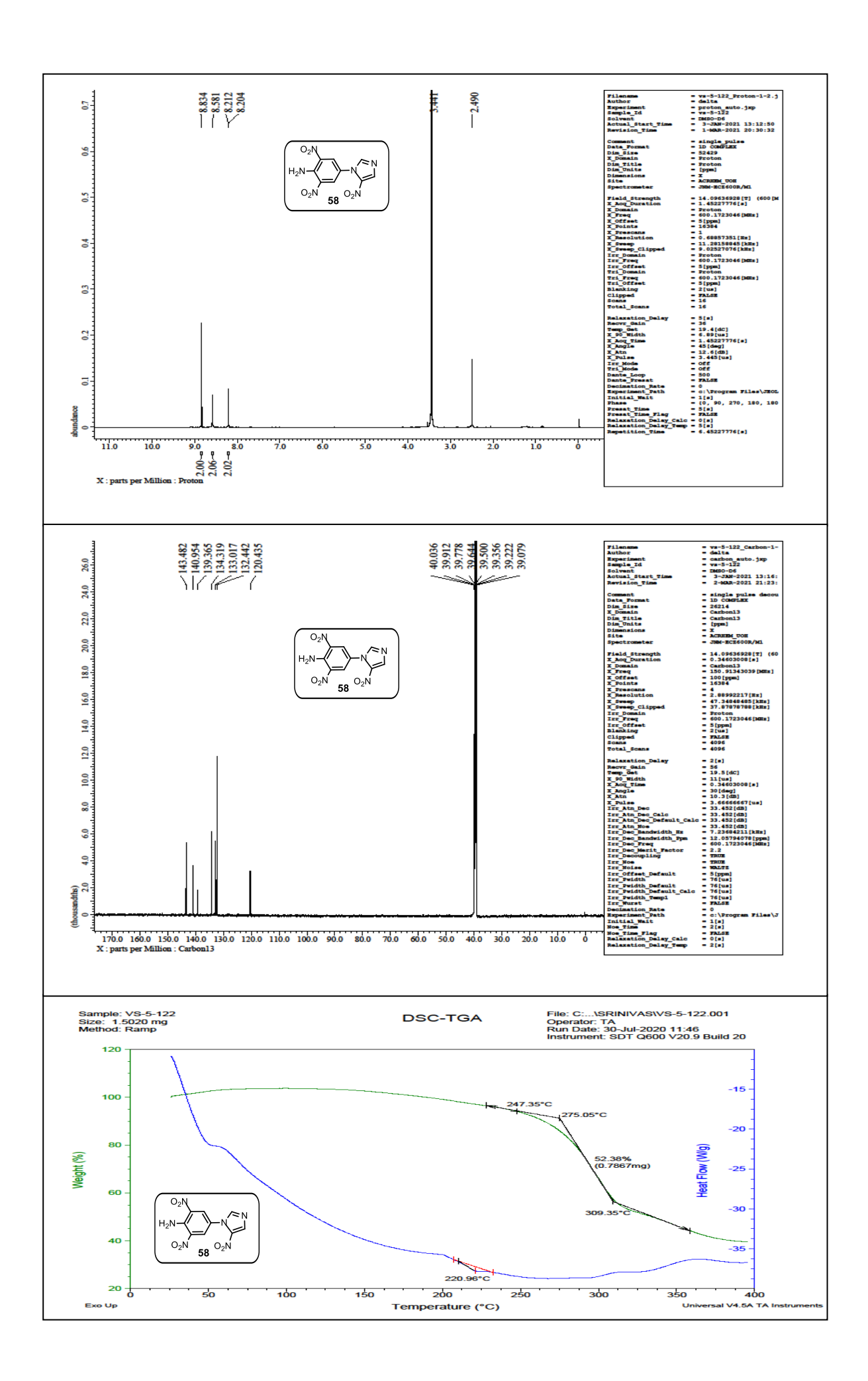


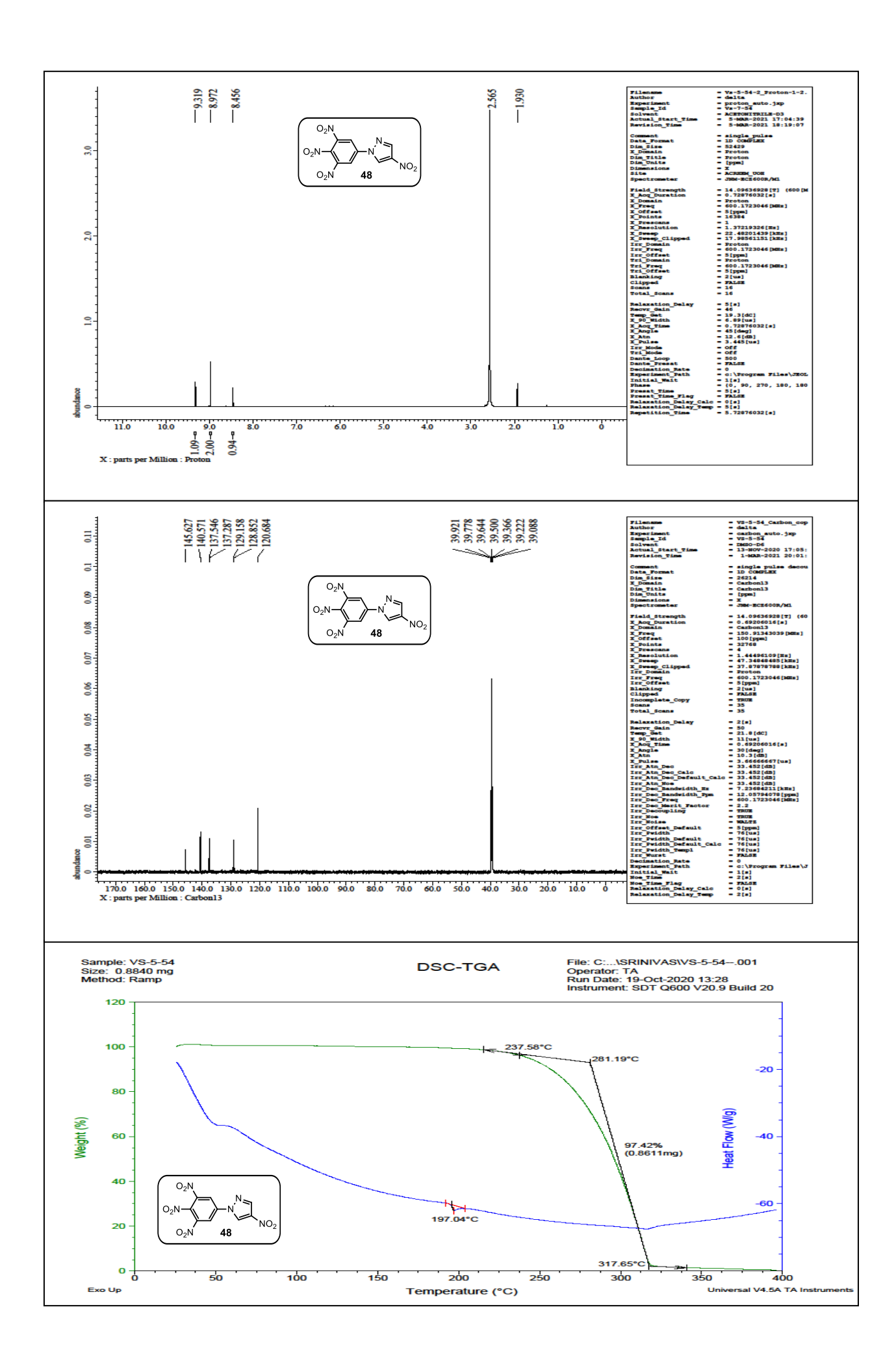


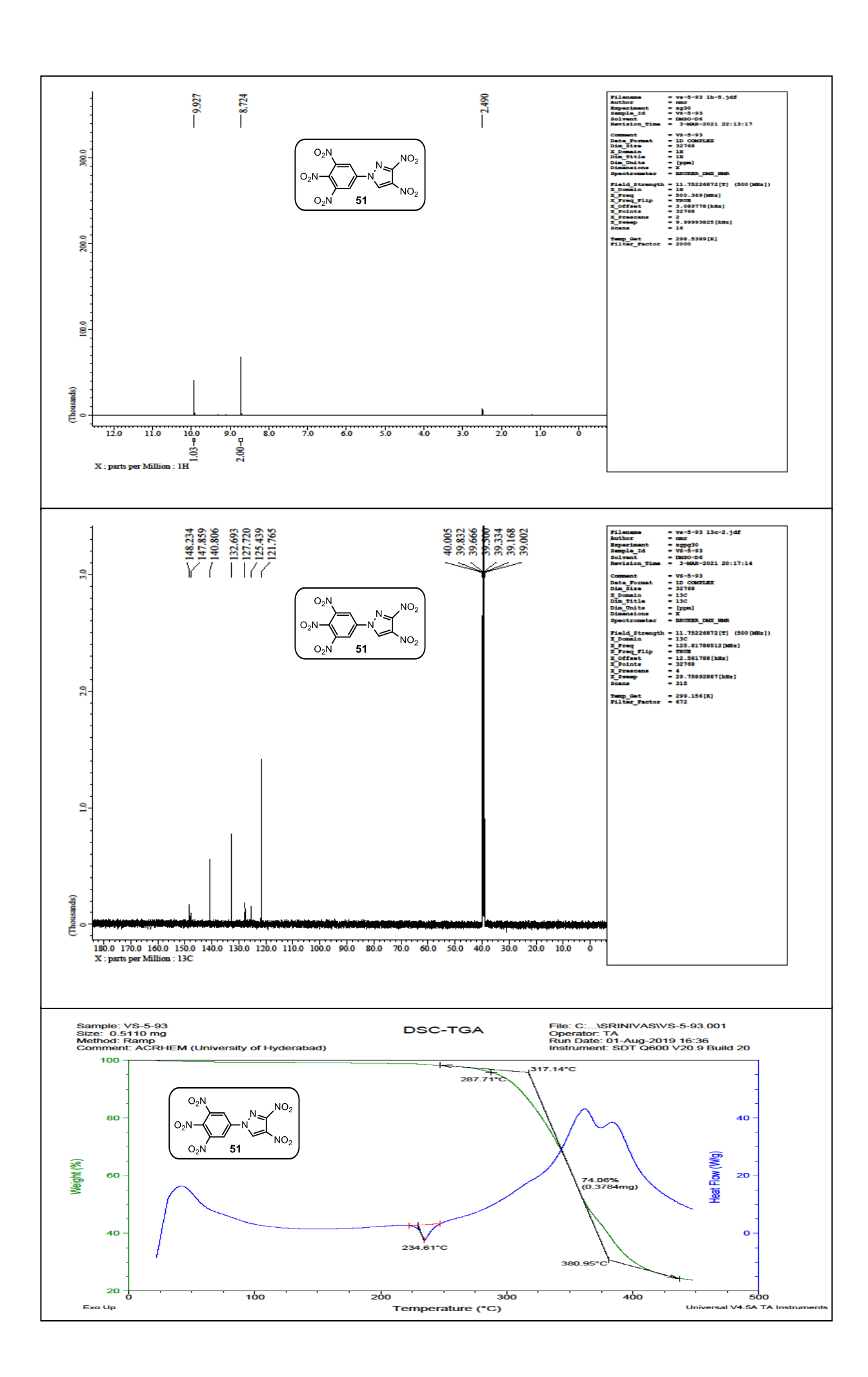


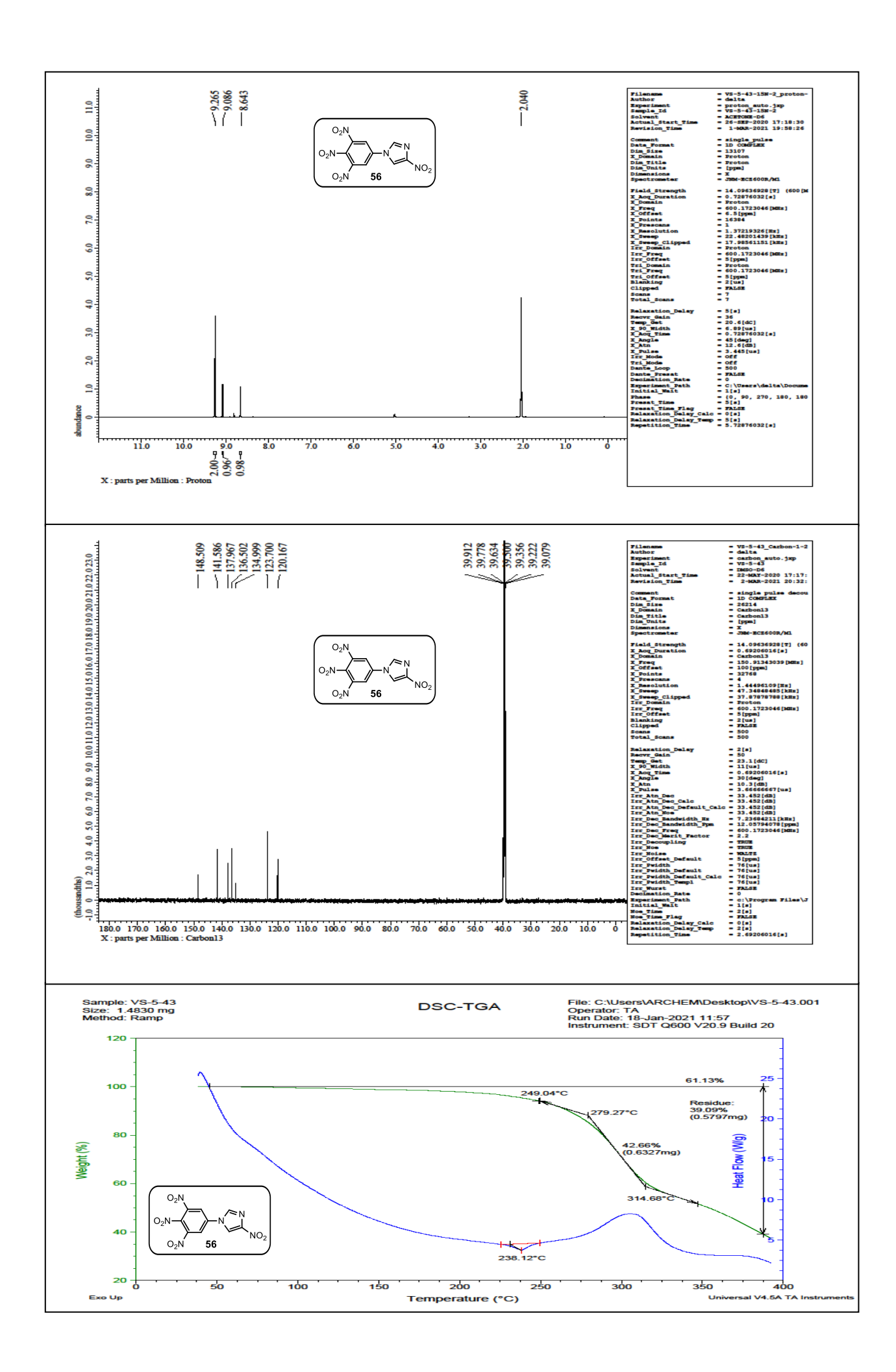


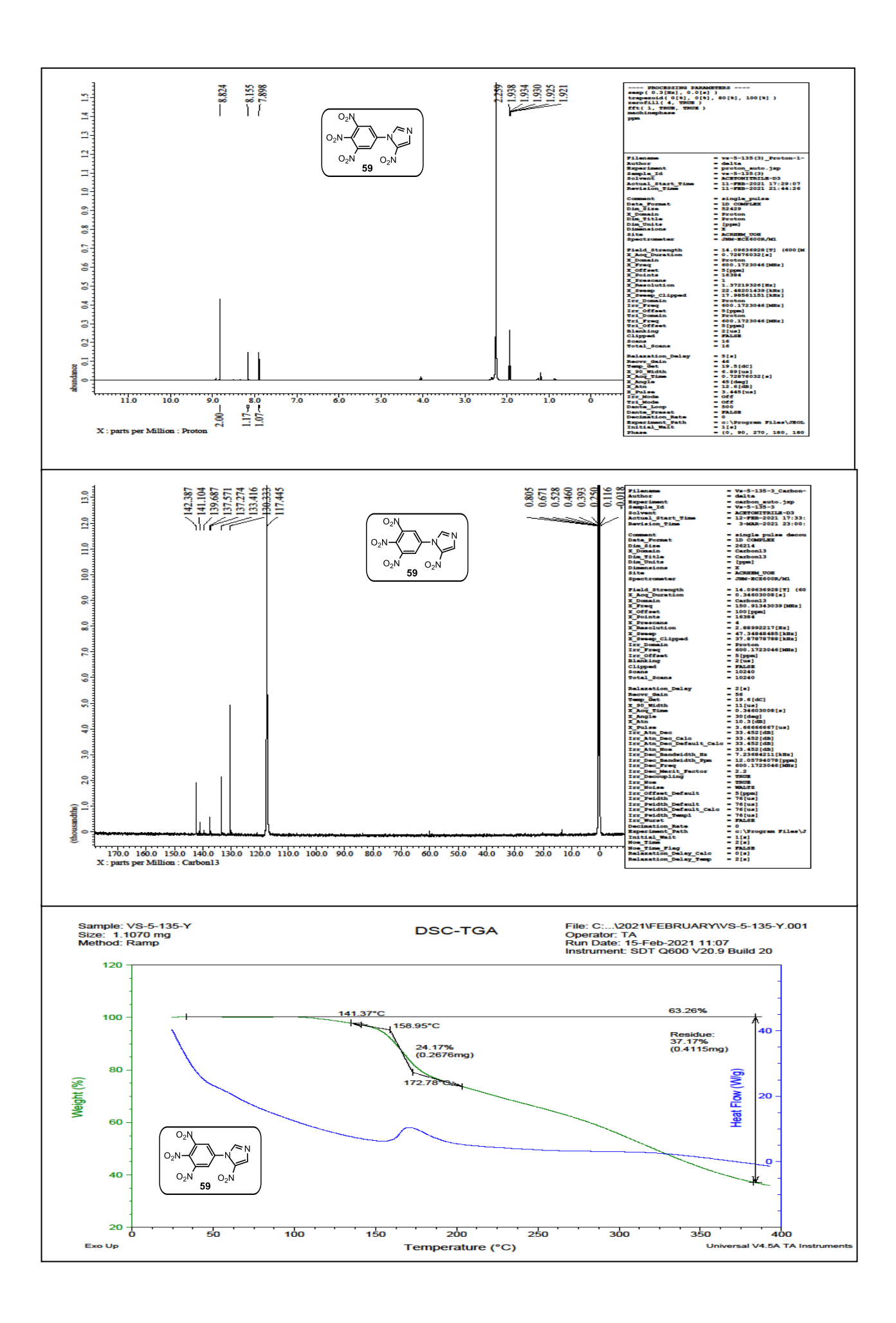


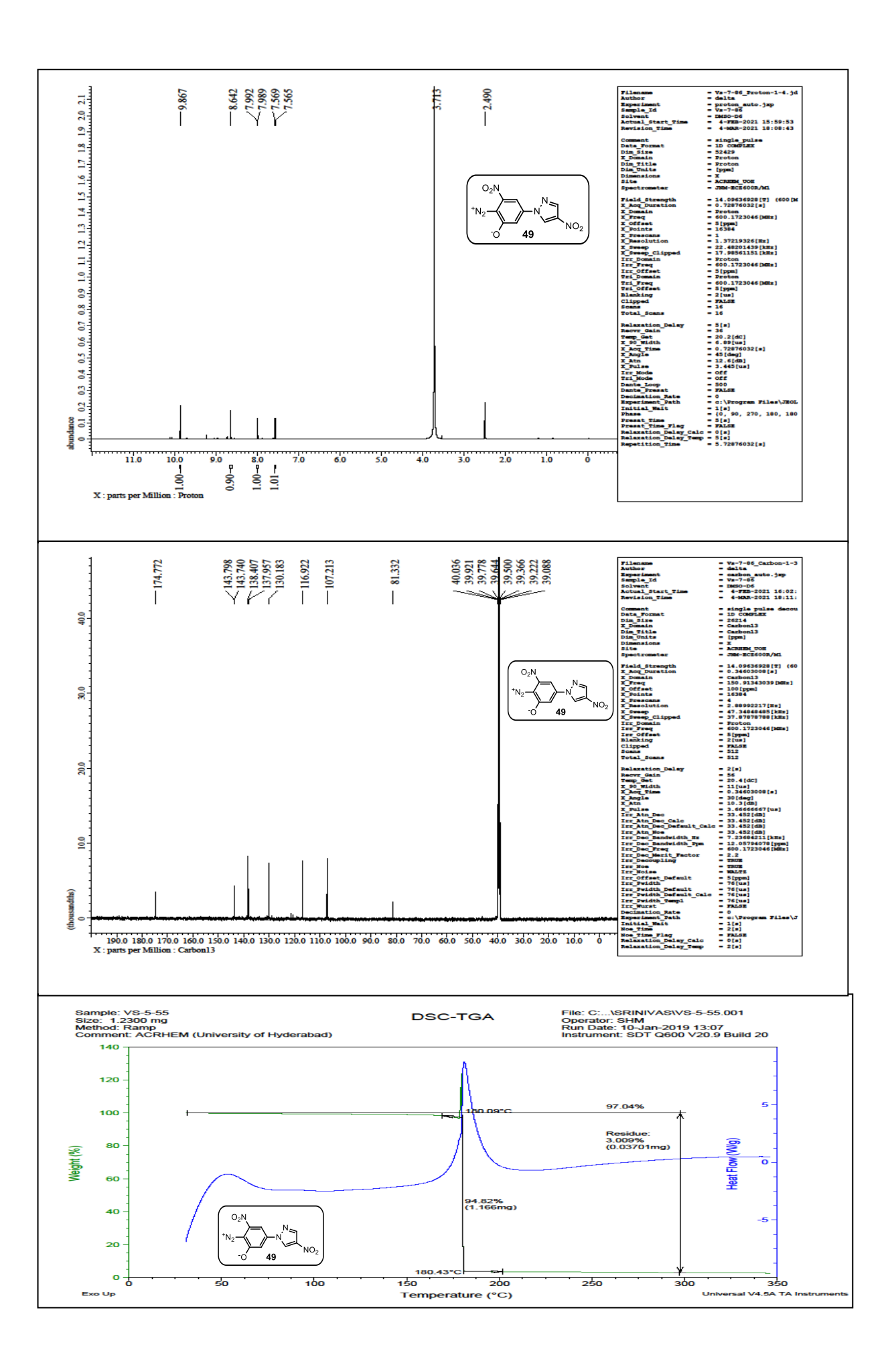


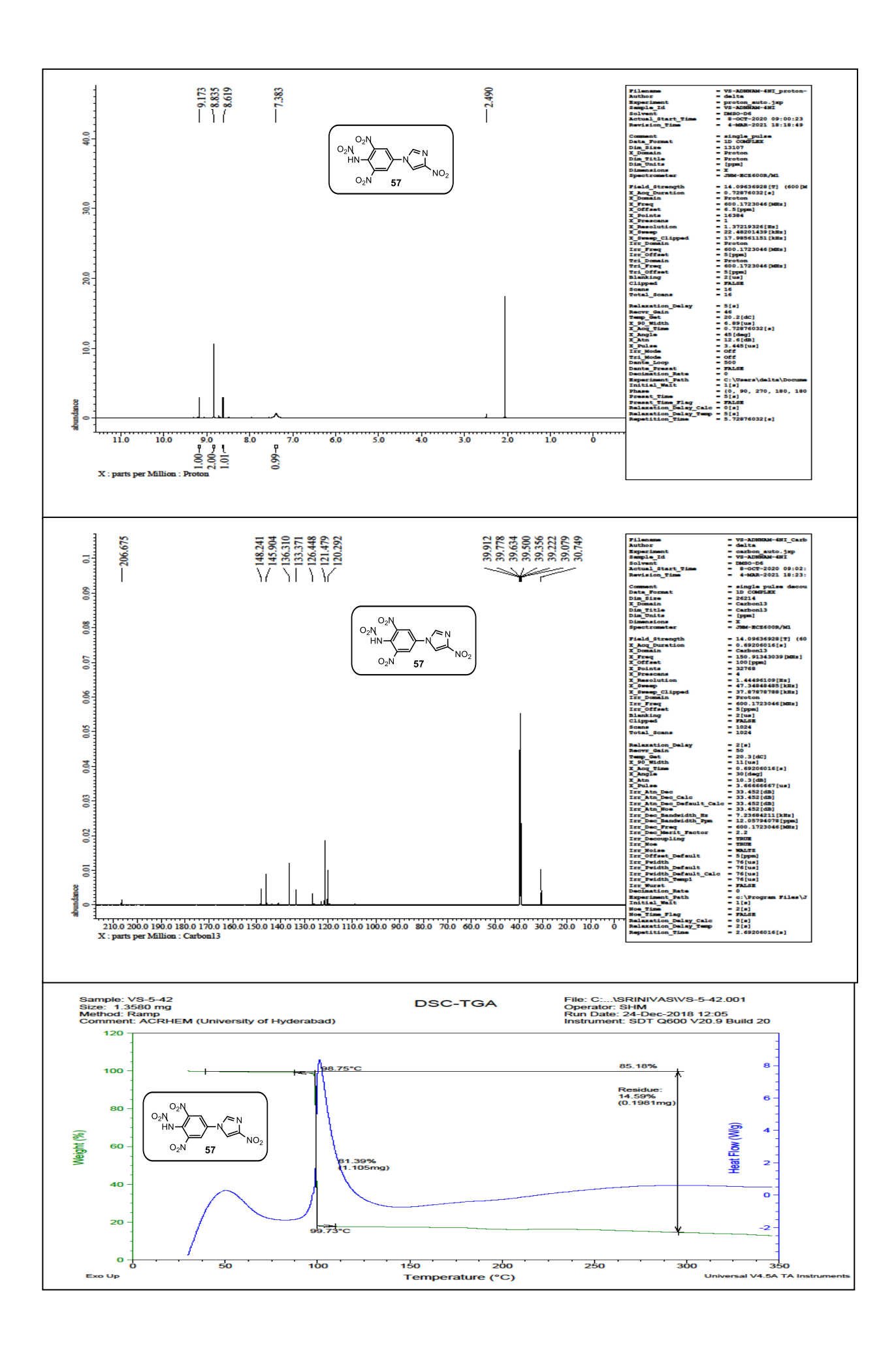


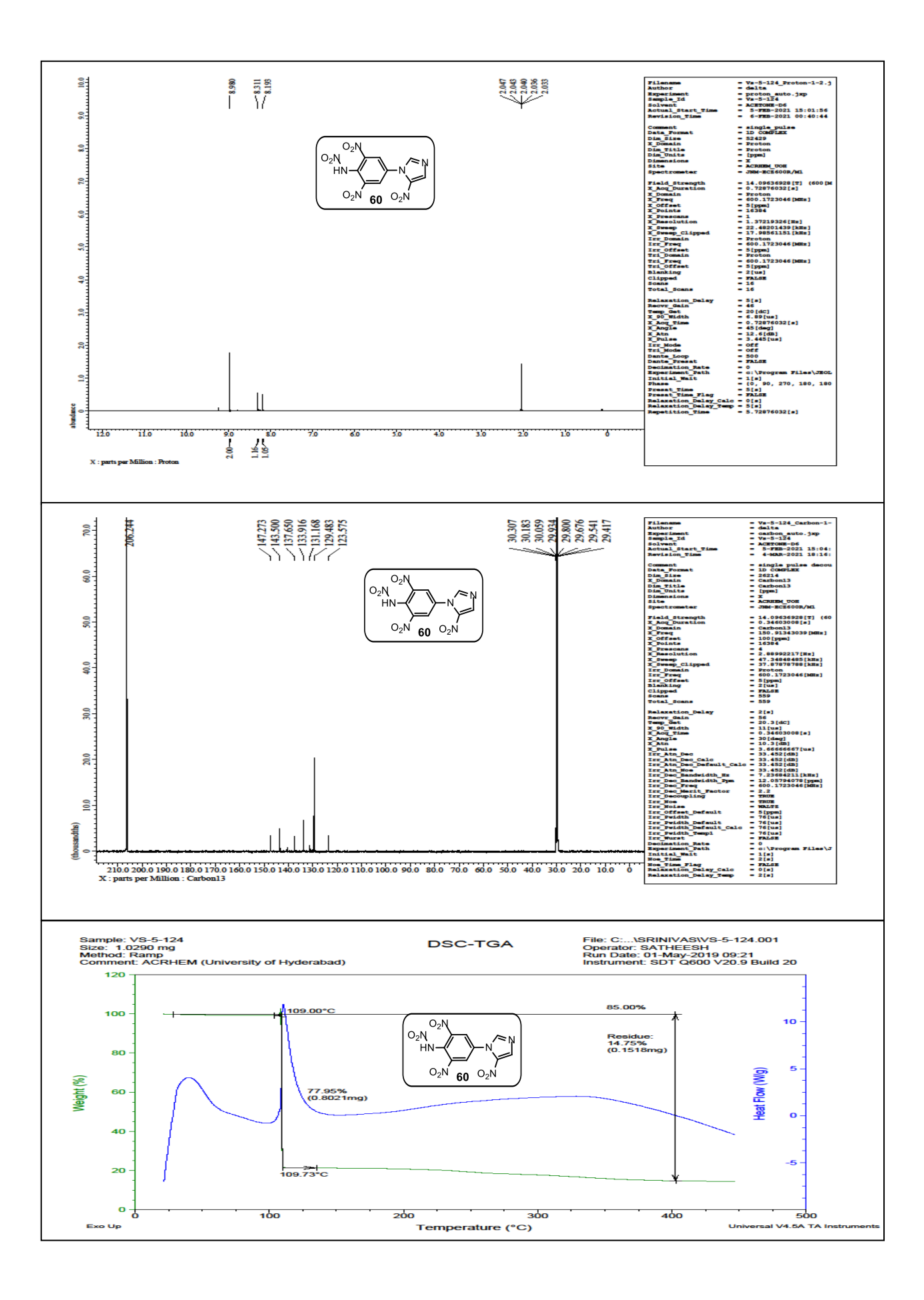












**Chapter-3** 

# Polynitro-azido Functionalized-N-aryl-C-nitro Pyrazole/Imidazole Derivatives as Energetic Materials

**Chapter 3** 

## **Abstract**

Nitration
$$O_2N$$
 $O_2N$ 
 $O_2N$ 
 $O_2N$ 
 $O_2N$ 
 $O_3NO_2$ 
 $O_2N$ 
 $O_3NO_2$ 
 $O_2N$ 
 $O_3NO_2$ 
 $O_3NO$ 

Triazido-dinitro-aryl-pyrazole/imidazole derivatives have been successfully synthesized from chloro-substituted-*N*-aryl-pyrazole/imidazole derivatives following nitration, amination, oxidation, and azidation reaction sequences. The synthesized compounds have been fully characterized by <sup>1</sup>H, <sup>13</sup>C NMR, IR, and HRMS. The molecular structures of the synthesized compounds are established by single crystal X-ray diffraction analysis. Most of the compounds exhibit high thermally stability (>180 °C) and high insensitivity (FS >360 N, IS >40 J). While the respective azido derivatives are relatively sensitive. Molecular sensitivity is likely a result of the lack of hydrogen bonds and the presence of large positive regions on nitrogen atoms of azido groups in the molecules (supported by ESP and Hirshfeld surface analysis). Importantly, triazidoaryl-pyrazole and triazido-aryl-imidazole show high positive heats of formation +1309.88 kJ/mol and +1230.31 kJ/mol, respectively, than polynitro-chloro-substituted-N-arylpyrazole/imidazole derivatives. All the compounds show better detonation velocity and detonation pressure than TNT.

# 3.1. Introduction

Polyazido organic compounds have gained enormous attention in the area of propellants, explosives, and pyrotechnics. In general, azido group in the molecule enhances positive heats of formation and energetic properties of the compound. Azido bearing molecules possess high HOFs due to the differences in the bond dissociation energies: for instance, single N-N bond exhibits 159 kJ/mol, while N=N double bond and N≡N triple bond display 419 kJ/mol, 946 kJ/mol, respectively. However, challenge remains for the efficient conversion of N-N and N=N bonds to N≡N triple bond, as the process is highly exergonic. In addition, polyazido group bearing compounds are generally sensitive to impact and friction and thermally less stable; thus synthesis of such compounds challenging. Interestingly, polyazido containing molecules are applicable as primary explosives. The compounds having nitro (-NO<sub>2</sub>), nitramino (-NHNO<sub>2</sub>), nitrate (-ONO<sub>2</sub>) groups show high density, close to positive oxygen balance and high detonation property. However, such compounds show low heat of formation. High density and acceptable positive HOFs play essential to enhance detonation performance of compound. In this regard, azide (-N<sub>3</sub>) moiety in the molecular backbone could improve heat of formation. On the other hand, incorporation of non-energetic fragments like methyl, methylene moieties in combination with azo link (N=N) decreases sensitivity of the azido-group containing molecules. In this chapter, effort has been directed for the synthesis of a series of azido-substituted polynitro compounds from readily available precursor. The energetic properties of the targeted molecules and their synthetic routes have been discussed.

#### 3.1.1. Background of azido-substituted derivatives towards energetic material applications

Figure 3.1.1. Well-known azido-group bearing energetic materials

Some of the representative azido-bearing heterocycles are shown in **Figure 3.1.1.** Thus, tremendous effort has been directed for the synthesis of polynitro-azole derived energetic material. In this regard, Shreeve's effort in the development of synthetic methods for the construction of such energetic compounds is noteworthy.

Synthesis of fully C-nitro/azide substituted polynitro-pyrazole derivatives have been showcased by Shreeve and coworkers (**Scheme 3.1.1**). Following the known method, dinitropyrazole **9** has been synthesized.<sup>1</sup> Exposing **9** to nitrating agent HNO<sub>3</sub>/(CF<sub>3</sub>CO)<sub>2</sub>O led to the corresponding *N*-nitrated pyrazole derivative **10**. Next, nucleophilic *cine*-substitution of azide group in 1,4-dinitropyrazoles when exposed to sodium azide delivered 5-azido-3,4-dinitropyrazole **11** in 95% yield. Later, *N*-amination of **11** in presence of *O*-tosylhydroxylamine followed by nucleophilic displacement to trinitroethanol delivered the desired product **1** in 52% yield.<sup>2</sup> The compound **1** exhibits high heat of formation (565 kJ/mol) and high detonation performance (P = 35.6GPa, vD = 8968 m/s). These properties are comparable with TATB (P = 31.7 GPa, vD = 8504 m/s) and RDX (P = 34.9 GPa, vD = 8795 m/s). Moreover, compound **1** is sensitive to impact (2.5 J) and friction (20 N).

Scheme 3.1.1: Synthesis of 5-azido-3,4-dinitro-*N*-(trinitromethyl)-1*H*-pyrazol-1-amine (1)

Shreeve and co-workers described the synthesis of polynitro-azido-imidazole derivatives (**Scheme 3.1.2**); the overall transformation involves *N*-amination, diazotization, and trinitroethylation. The C-amination of 4,5-dinitroimidazole **13** with aqueous ammonia followed by diazotization using  $H_2SO_4/NaNO_2$  mixture at first delivered **15**.<sup>3</sup> Next, *N*-amination of **15** with *O*-tosylhydroxylamine afforded *N*-aminated imidazole derivative **16** in 73% yield. Finally, trinitroethylation of **16** with trinitroethanol delivered the final product **2** in 53% yield.<sup>4</sup> The compound **2** exhibits high heat of formation (494 kJ/mol) and good detonation properties (P = 34.9 GPa, vD = 8795 m/s) and are comparable with TNT and TATB. However, it showed moderate thermal stability ( $T_d = 136$  °C) and is sensitive to impact (2 J).

Scheme 3.1.2: Synthesis of 5-azido-4-nitro-*N*-(trinitromethyl)-1*H*-imidazol-1-amine (2)

The same group in 2016, developed an electrophilic iodination of ethylene-bridged bis-pyrazole followed by nitration and azidation reactions to access 1,2-bis(5-azido-3-iodo-4-nitro-1H-pyrazol-1-yl) ethane **3** (Scheme 3.1.3).<sup>5</sup> The iodo groups can be readily replaced by nitro groups; this would enhance energetic performance of the compounds. Thus, iodination of 1,2-bis(1H-pyrazol-1-yl) ethane **17** gave **18** in good yield. Further nitration of **18** in the presence of 100% HNO<sub>3</sub> produced dinitro compound **19**. Next, reaction of **19** with sodium azide in DMSO delivered the final diazido/dinitro compound **3** in 60% yield. The compound **3** holds density 2.41 g/cm<sup>3</sup>, good oxygen balance (-16.4%), and moderate decomposition temperature ( $T_d = 171$  °C).

Scheme 3.1.3: Synthesis of 1,2-bis(5-azido-3-iodo-4-nitro-1*H*-pyrazol-1-yl)ethane (3)

A route to *N*-nitroethanamine substituted azido-dinitropyrazolate 4/4' starting from 1,3-dichoro-2-nitro-2-aza-propane (DCNP) **20** was reported (**Scheme 3.1.4**).<sup>6</sup> The reaction of DCNP and ammonium salt of 4-chloro-3,5-dinitropyrazole **21** gave di-pyrazolyl substituted product **22**. Likewise, DCNP when treated with ammonium salt of 3,4,5-trinitropyrazolate **23** delivered **24**. Compounds **22** and **24** were further treated with excess of sodium azide in DMSO to produce **4** and **4'** in 92% and 89% yield, respectively.<sup>7</sup> The product **4** and **4'** exhibited better detonation performance [P = 35.1 GPa, vD = 8717 m/s (for **4**) and P = 35.2 GPa, vD = 8724 m/s (for **4'**)], high heat of formation 1108 kJ/mol (for **4**) and 1118.7 kJ/mol (for **4'**), which are higher than that of TNT and comparable to RDX. These compounds showed low thermal stability ( $T_d = 166$  °C for **4** and  $T_d = 169$  °C for **4'**) and are sensitive to impact (2 J).

$$\begin{array}{c} \text{CI} & \text{NO}_2 \\ \\ \text{21} & \text{NH}_4^+ \\ \\ \text{O}_2\text{N} & \text{NO}_2 \\ \\ \text{65 °C, 16 h} & \text{CI} & \text{NO}_2 \\ \\ \text{20} & \text{O}_2\text{N} & \text{NO}_2 \\ \\ \text{21} & \text{NO}_2 & \text{O}_2\text{N} & \text{NO}_2 \\ \\ \text{22} & \text{NO}_2 & \text{NO}_2 \\ \\ \text{23} & \text{NH}_4^+ & \text{O}_2\text{N} & \text{NO}_2 \\ \\ \text{24} & \text{NO}_2 & \text{NO}_2 \\ \\ \text{25} & \text{NO}_2 & \text{NO}_2 \\ \\ \text{26} & \text{NO}_2 & \text{NO}_2 \\ \\ \text{26} & \text{NO}_2 & \text{NO}_2 \\ \\ \text{27} & \text{NO}_2 & \text{NO}_2 \\ \\ \text{28} & \text{NO}_2 & \text{NO}_2 \\ \\ \text{29} & \text{NO}_2 & \text{NO}_2 \\ \\ \text{29} & \text{NO}_2 & \text{NO}_2 \\ \\ \text{29} & \text{NO}_2 & \text{NO}_2 \\ \\ \text{20} & \text{NO}_2 & \text{NO}$$

**Scheme 3.1.4:** Synthesis of N,N-bis((4-azido-3,5-dinitro-1H-pyrazol-1-yl)methyl)nitramide(**4**) and N,N-bis((5-azido-3,4-dinitro-1H-pyrazol-1-yl)methyl)nitramide (**4'**)

Generally, fused-heterocyclic compounds exhibit better thermal stability, high detonation performance, and are insensitive when compared to compounds having single heterocyclic ring. The Shreeve and coworkers have synthesized a series of *N*-functionalized 3,6-dinitropyrazolo [4,3-c]pyrazole (DNPP) derivatives as high performance energetic material (**Scheme 3.1.5**). Following known procedure,<sup>8</sup> fused skeleton DNPP **25** was synthesized. The DNPP **25** at first undergoes Mannich reaction with formaldehyde to yield the diol product **26**. Later, subjecting **26** with thionyl chloride provided dichloro DNPP derivative **27**. Finally, reaction of **27** with sodium azide in DMSO delivered diazido-DNPP **5** in 77% yield.<sup>9</sup> The fused dinitro-diazide-pyrazole derivative **5** possess better thermal stability (T<sub>d</sub> = 196 °C) and high heat of formation (946.3 kJ/mol).

**Scheme 3.1.5:** Synthesis of 1,4-bis(azidomethyl)-3,6-dinitro-1,4-dihydropyrazolo[4,3-c]pyrazole (5)

The Shreeve and co-workers demonstrated the synthesis of azo-coupled fused tricyclic 1,2,3,4-tetrazine ring system with lucrative energetic properties (**Scheme 3.1.6**). The nitration of bisimidazole **28** with NaNO<sub>3</sub>/H<sub>2</sub>SO<sub>4</sub> mixture under reflux at 90 °C gave the corresponding tetra-nitro derivatives **29**. Next, *N*-amination of **29** with *O*-tosylhydroxylamine produced **30** in 63% yield (**Scheme 3.1.6**). Later, oxidation of **30** with *tert*-butyl hypochlorite (*t*-BuOCl) delivered the unexpected fused product **31** *via* an unusual halogenation reaction. Finally, the diazido product **6** was obtained in 90% yield from the reaction of **31** with sodium azide in MeCN/H<sub>2</sub>O mixture (**Scheme 3.1.6**). Interestingly, compound **6** exhibited high density and good detonation

performance (D =  $1.887 \text{ g/cm}^3$ , P = 36.7 GPa, vD = 9256 m/s), but the compound is sensitive to impact (2 J) and friction (20 N). Therefore, it could be useful as a promising primary explosive.

**Scheme 3.1.6:** Synthesis of 3,8-diazido-2,9-dinitrodiimidazo[1,2-d:2',1'-f][1,2,3,4]tetrazine (6)

In 2011, Shastin et al. developed a new method for the synthesis of 2,4-diazido-6-trinitromethyl-1,3,5-triazine (**Scheme 3.1.7**). At first, reaction of dihydrazide derivative **32** with sodium nitrite in acetic acid gave **33** (diazotization method). Then removal of Boc-group from **33** in the presence of trifluoroacetic acid (TFA) provided **34** in 96% yield. Subsequently, nitration of **34** with acidic mixture (H<sub>2</sub>SO<sub>4</sub>/HNO<sub>3</sub>) delivered the desired product **7** in 68% yield (**Scheme 3.1.7**). The compound **7** was thermally and hydrolytically stable with positive enthalpy of formation (191 kcal/mol).

Scheme 3.1.7: Synthesis of 2,4-diazido-6-(trinitromethyl)-1,3,5-triazine (7)

In another noteworthy discovery reported by Huynh *et al.* in 2004 is the synthesis of 1,2-bis(4,6-diazo-1,3,5-triazin-2-yl) diazene **8** with very high heat of formation (**Scheme 3.1.8**). Cyanuric azide **36**, which is extremely sensitive to friction and spark, was synthesized from cyanuric chloride **35**. The hydrazo-linkage product **38** was successfully accessed from the reaction of tetrachloro-hydrazo-1,3,5-triazine **37** with excess hydrazine monohydrate. Next, diazotization of **38** in presence of NaNO<sub>2</sub> in water and concentrated hydrochloric acid led to **39**. Finally, oxidation of **39** with chlorine gas in H<sub>2</sub>O:CHCl<sub>3</sub> afforded the azo-linkage product **8** (**Scheme 3.1.8**). These hydrazo-compound **39** and azo linked species **8** have led to high heats of formation (1753 kJ/mol and 2171 kJ/mol), better decomposition temperature (T<sub>d</sub> = 202 °C and 200 °C) and increased melting point. Importantly, compound **39** (IS = 18.3 cm, FS = 2.9 kg) and **8** (IS = 6.2 cm, FS = 2.4 kg) are relatively less sensitive than cyanuric azide **36** (IS = 6.2 cm, FS = < 0.5 kg).

Scheme 3.1.8: Synthesis of 1,2-bis(4,6-diazo-1,3,5-triazin-2-yl)diazene (8)

# 3.2. Motivation and Design Plan

As discussed, azido group  $(-N_3)$  in the organic compound enhances heat of formation of the molecule. However, due to low decomposition temperature and high sensitivity to impact and friction, synthesis of polyazido compounds is narrow. Moreover, presence of polar functional motifs could enhance stability of the molecule due probably to the viability of hydrogen bonding between the functional groups in the crystal structure. In this regard, introduction a nitro group adjacent to the azide moiety in the molecule could favor  $\pi$ - $\pi$  stacking and nitro- $\pi$  interactions. With this intention in mind, design and synthesis of new molecular scaffolds having two azido groups on adjacent carbons are planned. To my knowledge, synthesis of such molecules is so far remained unrealistic due probably to high sensitivity and instability of the compounds. Furthermore, introduction of two azido groups adjacent to each other in polynitroarenes could show better detonation performance, high positive heats of formation in comparison to TNT, PETN, and DDNP. Despite the challenges, this chapter focuses the design and synthesis of triazido-di/tri-nitro-aryl-pyrazole and triazido-dinitro-aryl-imidazole skeletons from chlorinated *N*-aryl-pyrazole/imidazole derivatives (**Scheme 3.2.1**).

$$\begin{array}{c} \text{MeO} & \begin{array}{c} \text{Nitration} \\ \text{CI Amination} \end{array} \\ \begin{array}{c} \text{N} \\ \text{O}_2 \text{N} \\ \text{O}_2 \text{N} \end{array} \\ \begin{array}{c} \text{Oxidation} \\ \text{O}_2 \text{N} \\ \text{O}_2 \text{N} \end{array} \\ \begin{array}{c} \text{Oxidation} \\ \text{O}_2 \text{N} \\ \text{O}_2 \text{N} \end{array} \\ \begin{array}{c} \text{Oxidation} \\ \text{O}_2 \text{N} \\ \text{O}_2 \text{N} \end{array} \\ \begin{array}{c} \text{Oxidation} \\ \text{N}_3 \\ \text{N}_3 \end{array} \\ \begin{array}{c} \text{N}_3 \\ \text{N}_3 \\ \text{N}_4 \end{array} \\ \begin{array}{c} \text{N}_3 \\ \text{N}_4 \end{array} \\ \begin{array}{c} \text{N}_3 \\ \text{N}_4 \end{array} \\ \begin{array}{c} \text{N}_4 \\ \text{N}_4 \end{array} \\ \begin{array}{c} \text{N}_4 \\ \text{N}_5 \\ \text{N}_5 \end{array} \\ \begin{array}{c} \text{N}_5 \\ \text{N}_5 \\ \text{N}_5 \\ \text{N}_5 \end{array} \\ \begin{array}{c} \text{N}_5 \\ \text{N}_5 \\ \text{N}_5 \\ \text{N}_5 \end{array} \\ \begin{array}{c} \text{N}_5 \\ \text{N}_5 \\ \text{N}_5 \\ \text{N}_5 \\ \text{N}_5 \\ \text{N}_5 \end{array} \\ \begin{array}{c} \text{N}_5 \\ \text{N}_$$

**Scheme 3.2.1:** Synthesis of polynitro/azido-aryl-pyrazole/imidazole derivatives

#### 3.3. Results and Discussion

To start with, a variety of precursors methoxy substituted aryl-azoles have been readily prepared following the known synthetic method. Thus, 4-chloro-p-methoxy-aryl-pyrazole **42** (85%) and 2-chloro-p-methoxy-aryl-imidazole **43** (23%) are synthesised from p-methoxy-aryl-pyrazole **40** and p-methoxy-aryl-imidazole **41**, respectively, when treated independently with N-chlorosuccinimide (**Scheme 3.3.1**). <sup>14</sup>

Scheme 3.3.1: Synthesis of precursor 42 and 43.

The nitration of **42** with 98% H<sub>2</sub>SO<sub>4</sub> and 95% HNO<sub>3</sub> at 0 °C for 2 h afforded tri-nitro substituted *p*-methoxy aryl-pyrazole regioisomers **44** (18% yield) and **45** (31% yield) (**Scheme 3.3.2**). While the identical nitration process of **42** at 70 °C provided tetra-nitro *p*-methoxy aryl-pyrazole **46** in 55% yield (**Scheme 3.3.2**). Likewise, nitration of **43** could deliver di-nitro **47** (81%) and tri-nitro **48** (50%), when conducted at 0 °C and 70 °C, respectively (**Scheme 3.3.3**). Attempts to introduce four nitro groups on **43** failed despite the reaction conducted even at elevated temperature at 120 °C (**Scheme 3.3.3**).

Scheme 3.3.2: Nitration of precursor 42

Scheme 3.3.3: Nitration of precursor 43

It appears that pyrazole skeleton is amenable to nitration over imidazole moiety. As a consequence, two nitro groups can be easily introduced in the pyrazole skeleton constructing 46. Whereas the respective tetra-nitro group bearing imidazole compound 49 was inaccessible. This result clearly indicates that pyrazole ring is electron-rich in comparison to imidazole ring. The molecular electrostatic potential graphs of 42 and 43 justifies this presumption (Figure 3.3.1).

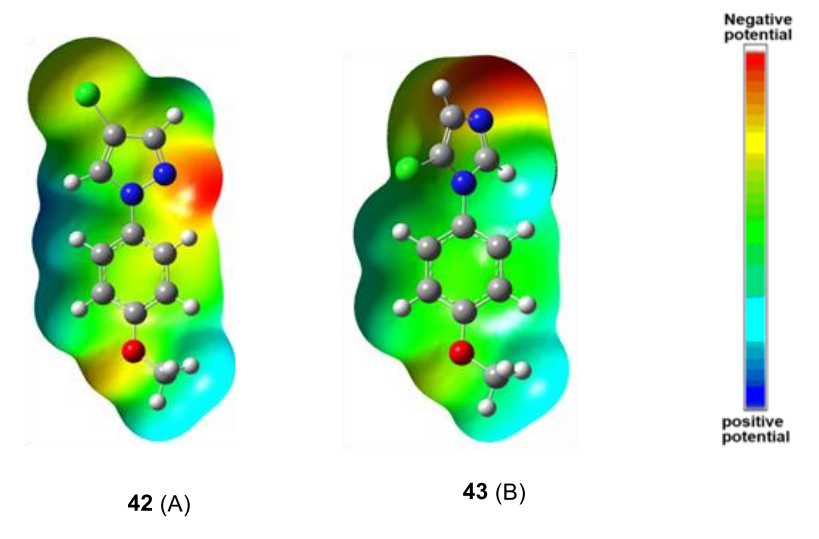


**Figure 3.3.1.** (A) Electrostatic potential surface of 4-methoxy-aryl-pyrazole **42** and (B) Electrostatic potential surface of 4-methoxy-aryl-imidazole **43**.

The molecular electrostatic potential graphs are generated by density functional theory (DFT) calculation applying at the B3PW91/6-31G (+d,p) level, with electronegative and electropositive regions in the molecule (**Figure 3.3.1**). A contour of electron density at 0.001 au (electrons/Bohr<sup>3</sup>) was proposed by Bader *et al.*<sup>15</sup>

To enhance the energetic property of the molecules (density and thermal stability), conversion of methoxy-moiety of the synthesized tri/tetranitroaryl-pyrazole **45**, **46** and/or di/tri-nitroaryl-imidazoles **47** and **48** to the –NH<sub>2</sub> group was attempted (**Scheme 3.3.4** and **3.3.5**). Exposing **45**, **46**, **47**, and **48** with aqeous ammonia in CH<sub>3</sub>CN could independently delivered amino-substituted di/tri/tetranitroaryl-pyrazole/imidazoles **50**, **52**, **54**, and **56**, respectively, in good yields (**Scheme 3.3.4** and **Scheme 3.3.5**). Later, oxidation of amine group of **50**, **52**, **54**, and **56** in the presence of H<sub>2</sub>SO<sub>4</sub>/H<sub>2</sub>O<sub>2</sub> produced the corresponding tri/tetra/penta nitro-aryl-pyrazole/imidazoles **51**, **53**, **55**, and **57**, respectively in good yields (**Scheme 3.3.4** & **Scheme 3.3.5**). <sup>16,17</sup>

45 
$$\xrightarrow{\text{aq.NH}_3}$$
  $\xrightarrow{\text{N}_2\text{N}}$   $\xrightarrow{\text{N}_2\text$ 

**Scheme 3.3.4:** Polynitroaryl-pyrazole derivatives.

47 
$$\xrightarrow{\text{aq.NH}_3}$$
  $\xrightarrow{\text{r.t, 3-5 h}}$   $\xrightarrow{\text{H}_2\text{N}}$   $\xrightarrow{\text{N}}$   $\xrightarrow{\text{N}}$ 

**Scheme 3.3.5:** Polynitroaryl-imidazole derivatives.

The  $-NO_2$  group flanked between electron-withdrawing groups in the aromatic skeleton can be easily substituted. In addition, the -Cl moiety in the electron-poor heteroaryl also can be reliably replaced. The synthesized molecules **51**, **53**, and **57** possess easily replaceable  $-NO_2$  and -Cl groups. Thus, reaction of **51**, **53**, and **57** with sodium azide (NaN<sub>3</sub>) was independently performed (**Scheme 3.3.6**). To our delight, an independent reaction of tetra-nitro-aryl-pyrazole/imidazoles **51**, **53**, and **57** with NaN<sub>3</sub> in DMSO successfully delivered triazido-dinitroaryl-pyrazole/imidazole compounds **58**, **59**, and **60**, respectively (**Scheme 3.3.6**). As expected, the chloro group as well two vicinal nitro groups in **51**, **53**, and **57** have been replaced by azide moiety. The anionic azido group is strongly nucleophilic and hence -Cl and  $-NO_2$  groups in the heteroaryl skeleton can be easily replaced by the azide moiety leading to unusual triazido derivatives **58**, **59**, and **60**. Disappointingly, triazido-trinitroaryl-pyrazole product **59** is unstable at room temperature and therefore decomposed rapidly during purification (**Scheme 3.3.6**).

**Scheme 3.3.6:** Polyazido/nitro aryl-pyrazole/imidazole derivatives

# 3.4. X-ray crystallography

Single crystals were grown by the slow evaporating solutions of **46**, **50**, **51**, **57**, and **58** in EtOAc at room temperature and atmospheric pressure. By single-crystal X-ray diffraction analysis, structures of **46**, **50**, **51**, **57**, and **58** were unambiguously revealed (**Figure 3.4.1**). Compounds **46** and **57** are crystallized in orthorhombic space group with a cell volume [15.6979(11), 8.0447(7), 23.8362(19) Å], [15.5810(16), 25.545(3), and 13.7141(10) Å], respectively. Whereas the compound **50** and **51** is crystallized in monoclinic space group with cell volume [8.4307(6), 6.0369(4), 24.8725(13) Å], [10.1383(9), 11.4586(13), and 11.6570(14) Å], respectively. Whereas compound **51** crystallized in triclinic space group with cell volume 7.5738(3), 8.1558(3) and 12.3306(4) Å. The crystal density of compounds **46** (1.71 g/cc), **50** (1.72 g/cc), **51** (1.83 g/cc), **57** (1.74 g/cc), and **58** (1.71 g/cc) are measured at 293 K, 296 K, 297 K, 298 K, and 294 K, respectively.

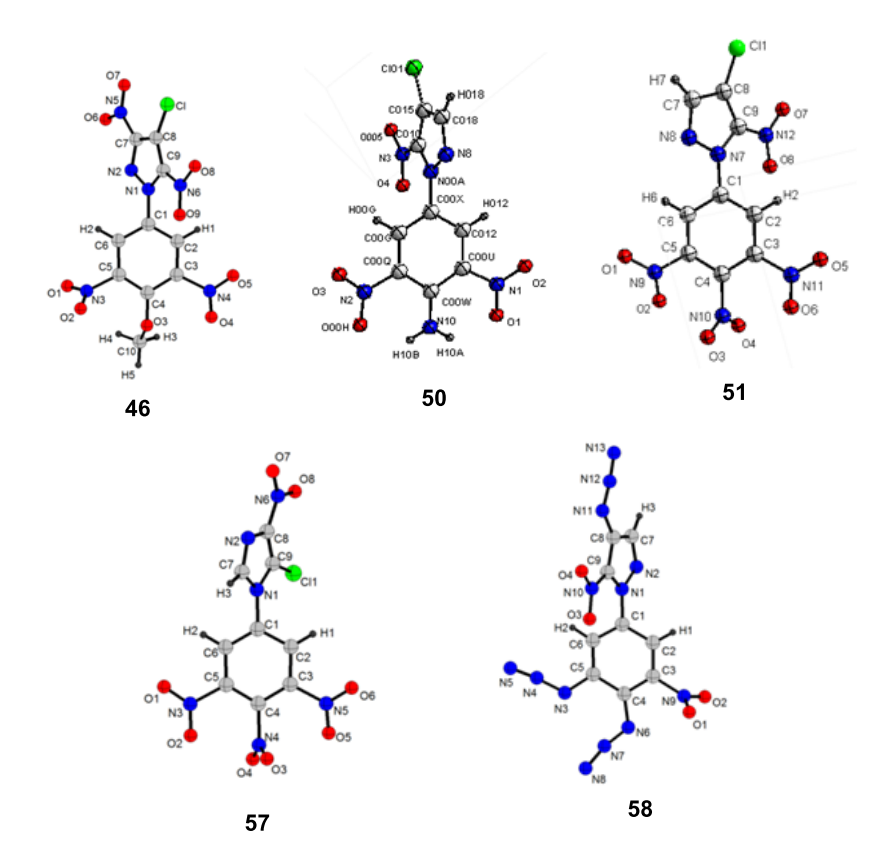


**Figure 3.4.1.** Molecular structure of compounds **46**, **50**, **51**, **57**, and **58**; thermal ellipsoids (30% probability) and for clarity hydrogen atoms are labelled.

Table 3.4.1. Crystallographic data for compounds 46, 50, and 51

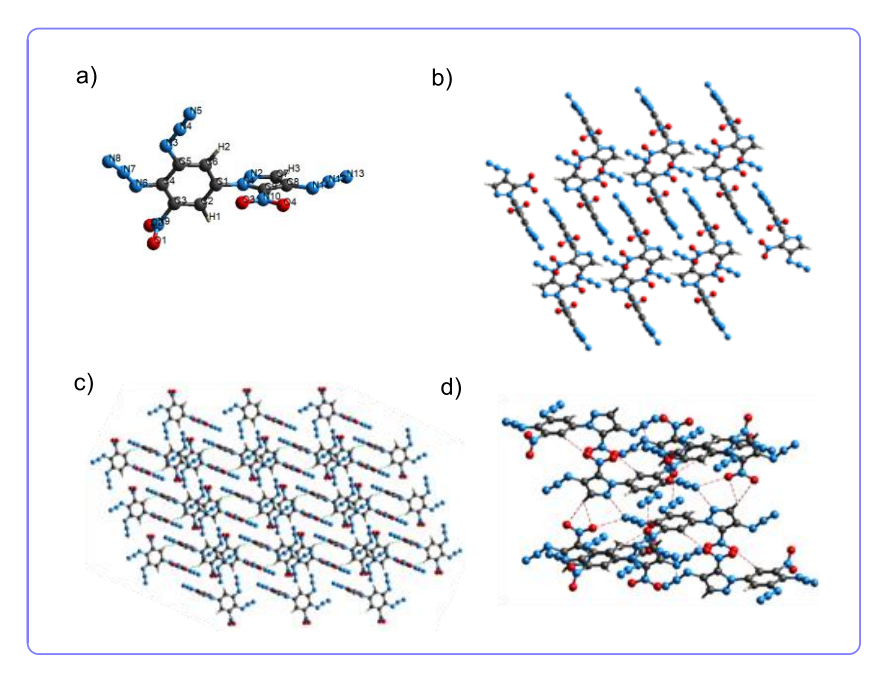
Compound	46	50	51
Formula	$C_{10}H_5N_6O_9Cl$	C <sub>9</sub> H <sub>5</sub> N <sub>6</sub> O <sub>6</sub> Cl	C <sub>9</sub> H <sub>3</sub> N <sub>6</sub> O <sub>8</sub> Cl
$ m M_w$	388.65	328.64	358.62
Crystal system	orthorhombic	monoclinic	monoclinic
Space group	Pbca	$P2_1$	P 21/n
T[K]	293 K	296 K	297 K
<i>a</i> [Å]	15.6979(11)	8.4307(6)	10.1383(9)
$b~[ ext{Å}]$	8.0447(7)	6.0369(4)	11.4586(13)
c [Å]	23.8362(19)	24.8725(13)	11.6570(14)
α[°]	90	90	90
eta [°]	90	90.112(2)	105.941(3)
γ [°]	90	90	90
Z	8	4	4
V [Å]	3010.2(4)	339.20	1302.1(2)
$D_{calc}$ [g/cm <sup>3</sup> ]	1.715	1.724	1.829
$\mu \ [\mathrm{mm}^{-1}]$	0.321	0.347	0.357
Total reflns	3371	2507	2799
Unique reflns	3217	2361	2592
Observed reflns	1200	2297	1721
$R_1[I > 2\sigma(I)]$	0.0852	0.0334	0.0603
$wR_2$ [all]	0.2943	0.0728	0.1882
GOF	0.989	1.912	0.985
Diffractometer	Bruker D8 Quest CCD	Bruker D8 VENTURE Photon III detector	Bruker D8 VENTURE Photon III detector

Table 3.4.2. Crystallographic data for compounds 57 and 58

Compound	57	58		
Formula	$C_9H_3N_6O_8Cl$	C <sub>9</sub> H <sub>3</sub> N <sub>13</sub> O <sub>4</sub>		
$M_{ m w}$	339.20	357.24		
Crystal system	orthorhombic	Triclinic		
Space group	$P2_{1}/c$	P -1		
T[K]	298 K	294 K		
a [Å]	15.5810(16)	7.5738(3)		
$b  [ ext{Å}]$	25.545(3)	8.1558(3)		
c [Å]	13.7141(10)	12.3306(4)		
$\alpha [^\circ]$	90	108.028(1)		
eta [°]	90	103.904(1)		
γ [°]	90	94.444(1)		
Z	16	2		
V [Å]	5458.4(9)	693.47(4)		
D <sub>calc</sub> [g/cm <sup>3</sup> ]	1.746	1.711		
$\mu \ [mm^{-1}]$	0.340	0.141		
Total reflns	13558	3427		
Unique reflns	13297	3302		
Observed reflns	4022	1454		
$R_1[I > 2\sigma(I)]$	0.1013	0.1034		
$wR_2$ [all]	0.3791	0.3693		
GOF	0.957	1.116		
Diffractometer	Bruker D8 VENTURE Photon III detector	Bruker D8 VENTURE Photon III detector		

Compound **58** crystallized with triclinic symmetry with density 1.71 g/cm<sup>3</sup> at 294 K. Interestingly, functional groups of azole ring are perfectly perpendicular to the benzene ring as shown in **Figure 3.4.2a**. The bond length N2–N4 and N4–C9 is in the range of 1.33–1.42 Å, while N–N bond lengths in aryl ring is in the range 1.09–1.24 Å. As shown in **Figure 3.4.2c**, the azido groups lies outside the plane of aryl-azole ring. The bond length of three nitrogen atoms N–N–N of azido group in azole ring is 1.13–1.24 Å, while N–N–N bond length of azido group in aryl ring is

1.15–1.22 Å. The two intermolecular hydrogen bonds formed in packing diagram between  $O(4)\cdots H(1)-C(2)$  and  $C(2)-H(1)\cdots O(4)$  are 2.36 Å and 2.36 Å, respectively (**Figure 3.4.2d**) and the bond lengths between N–O is in the range of 1.05–1.21 Å.



**Figure 3.4.2.** (a) The molecular structure of **58**, (b) The stacking crystal structure of **58**, (c) Ball and stick packing diagram and dashed lines represent hydrogen bonds, (d) Supramolecular interaction between the molecules of **58**.

# 3.5. Energetic Properties

Tri/tetra/penta-nitro substituted aryl-pyrazoles (44, 45, 46, 50, 51, 52, and 53) and di/tri/tetra-nitro substituted aryl-imidazoles (47, 48, 49, 54, 56, 55, and 57) are synthesized as shown in **Scheme 3.3.2** to **Scheme 3.3.5**. The energetic parameters of tri/tetra/penta-nitro substituted aryl-pyrazoles (i.e. 47, 48, 49, 50, 51, 52 and 53) and tri/tetra-nitro substituted aryl-imidazoles (i.e. 56, 57, 58, 59, 60, and 61) are given in **Table 3.5.1**. The structures geometry optimization and frequency analyses are performed using B3LYP functional with 6-31G (+d,p) basis set. <sup>19</sup> Isodesmic reactions are beneficial to the determination of compounds HOFs.

Triazido-dinitro substituted aryl-pyrazole/imidazoles **58** and **60** showed density 1.71 g/cm<sup>3</sup> (crystal density measured at 294K) and 1.76 g/cm<sup>3</sup> (theoretical density by Material studio), respectively. These compounds exhibited positive heats of formation. The heats of formation for **58** (+1309.88 kJ/mol) and **60** (+1230.31 kJ/mol) are calculated and revealed. By using HOFs and crystal density, detonation properties of **58** and **60** are calculated from Explo5 version 6.03 software.<sup>20</sup> Most of the representative compounds show better detonation properties than TNT (**Table 3.5.2**).

**Table 3.5.1.** Physical properties of compounds **50**, **51**, **52**, **53**, **56**, and **57** compared with **TNT**  $^{21,22}$  and **RDX**  $^{21,22}$ .

Cmpnd	$\Delta H_{\rm f}^{[a]}$	$T_{d}^{[b]}$	OB[c]	$ ho^{[d]}$	$\mathbf{P}^{[\mathbf{f}]}$	$\mathbf{D}_{\mathrm{v}}^{[\mathrm{g}]}$	IS <sup>[h]</sup>	h] FS <sup>[i]</sup>	
	(kJ mol <sup>-1</sup> )	(° C)	(%)	(g cm <sup>-3</sup> )	(GPa)	$(m s^{-1})$	$(\mathbf{J})$	( <b>N</b> )	
50	263.1	210	-68.2	1.72 <sup>[e]</sup>	18.3	6730	_	_	
51	275.2	275	-49.1	1.83 <sup>[e]</sup>	25.8	7676	_	_	
52	293.1	215	-49.2	1.79	23.6	7460	-	_	
53	410.5	203	-33.7	1.87	30.7	8248	-	_	
56	483.6	245	-68.2	1.72	20.1	6995	_	_	
57	601.9	266	-49.1	1.75	25.6	7676	_	_	
TNT	-67.0	295	-24.7	1.65	19.5	6881	15	353	
RDX	80.0	204	0	1.80	35.0	8762	7.4	120	

<sup>&</sup>lt;sup>a</sup> Heat of formation using MOPAC software; <sup>b</sup> Temperature of decomposition (onset) under nitrogen gas (DSC−TGA, 10 °C min<sup>-1</sup>); <sup>c</sup> OB = oxygen balance (%); for C<sub>a</sub>H<sub>b</sub>O<sub>c</sub>N<sub>d</sub>: 1600(c-2a-b/2)/MW; MW = molecular weight of the compound; <sup>d</sup> Theoretical density; <sup>e</sup> Crystal density (294K); <sup>f</sup> Calculated detonation pressure (EXPLO5 v6.03); <sup>g</sup> Calculated detonation velocity (EXPLO5 v6.03); <sup>h</sup> Impact sensitivity (BAM drophammer, method 1 of 6); <sup>i</sup> Friction sensitivity (BAM friction tester, method 1 of 6).

**Table 3.5.2.** Physical properties of triazido-functionalized energetic compounds and compared with **TNT**, <sup>21, 22</sup> **PETN**, <sup>23</sup> and **DDNP**<sup>24</sup>.

Cmpnd	$\Delta H_{f}^{[a]}(kJ$	$T_d^{[b]}$	N <sup>[c]</sup>	OB <sup>[d]</sup>	ρ <sup>[e]</sup>	$\mathbf{P}^{[g]}$	$\mathbf{D}_{\mathrm{v}}^{[\mathrm{h}]}$	IS <sup>[i]</sup>	FS <sup>[j]</sup>
	mol <sup>-1</sup> )	(° <b>C</b> )	(%)	(%)	(g cm <sup>-3</sup> )	(GPa)	$(m s^{-1})$	$(\mathbf{J})$	(N)
58	+1309.88	-	50.98	-69.42	$1.71^{[f]}$	23	7672	-	_
60	+1230.31	_	50.98	-69.42	1.76	24	7787	_	_
TNT	-67.0	295	18.5	-24.67	1.65	19.5	6881	15	353
PETN	-502.8	160	22.22	15.18	1.78	31.4	8564	3	60
DDNP	60.0	158	26.67	-15.23	1.63	20.0	7205	1	5

<sup>&</sup>lt;sup>a</sup> Heat of formation using isodesmic reaction; <sup>b</sup> Temperature of decomposition (onset) under nitrogen gas (DSC–TGA, 10 °C min<sup>-1</sup>); <sup>c</sup> Nitrogen content; <sup>d</sup> OB = oxygen balance (%); for  $C_aH_bO_cN_d$ : 1600(c-2a-b/2)/MW; MW = molecular weight of the compound; <sup>e</sup> Theoretical density by Material studio; <sup>f</sup> Crystal density (294K); <sup>g</sup> Calculated detonation pressure (EXPLO5 v6.03);

<sup>h</sup> Calculated detonation velocity (EXPLO5 v6.03); <sup>i</sup> Impact sensitivity (BAM drophammer, method 1 of 6); <sup>j</sup> Friction sensitivity (BAM friction tester, method 1 of 6).

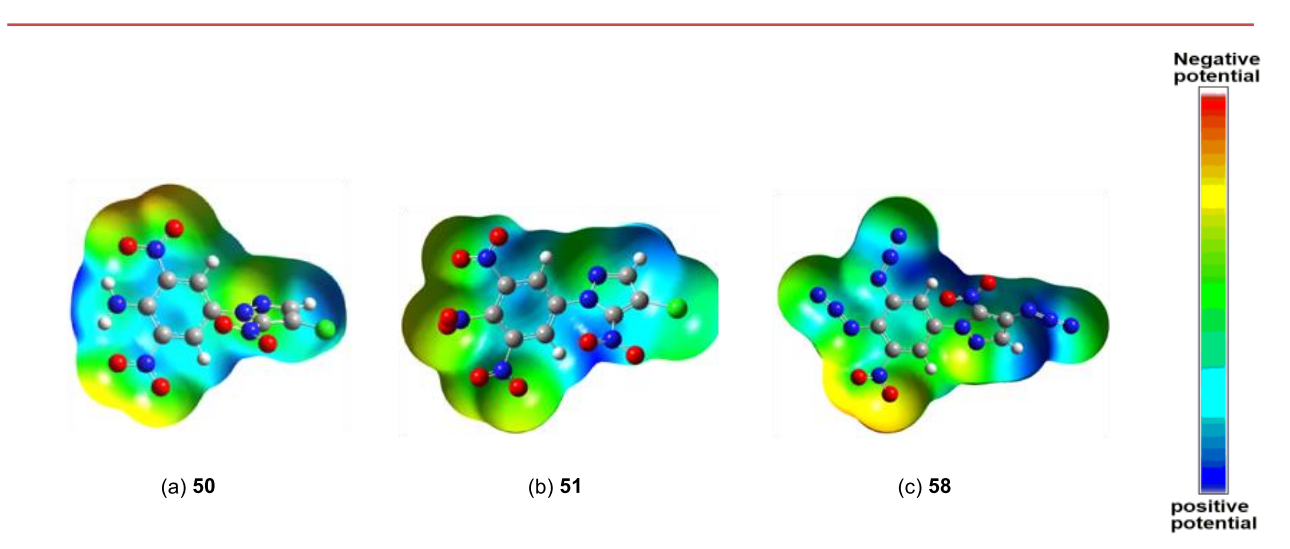


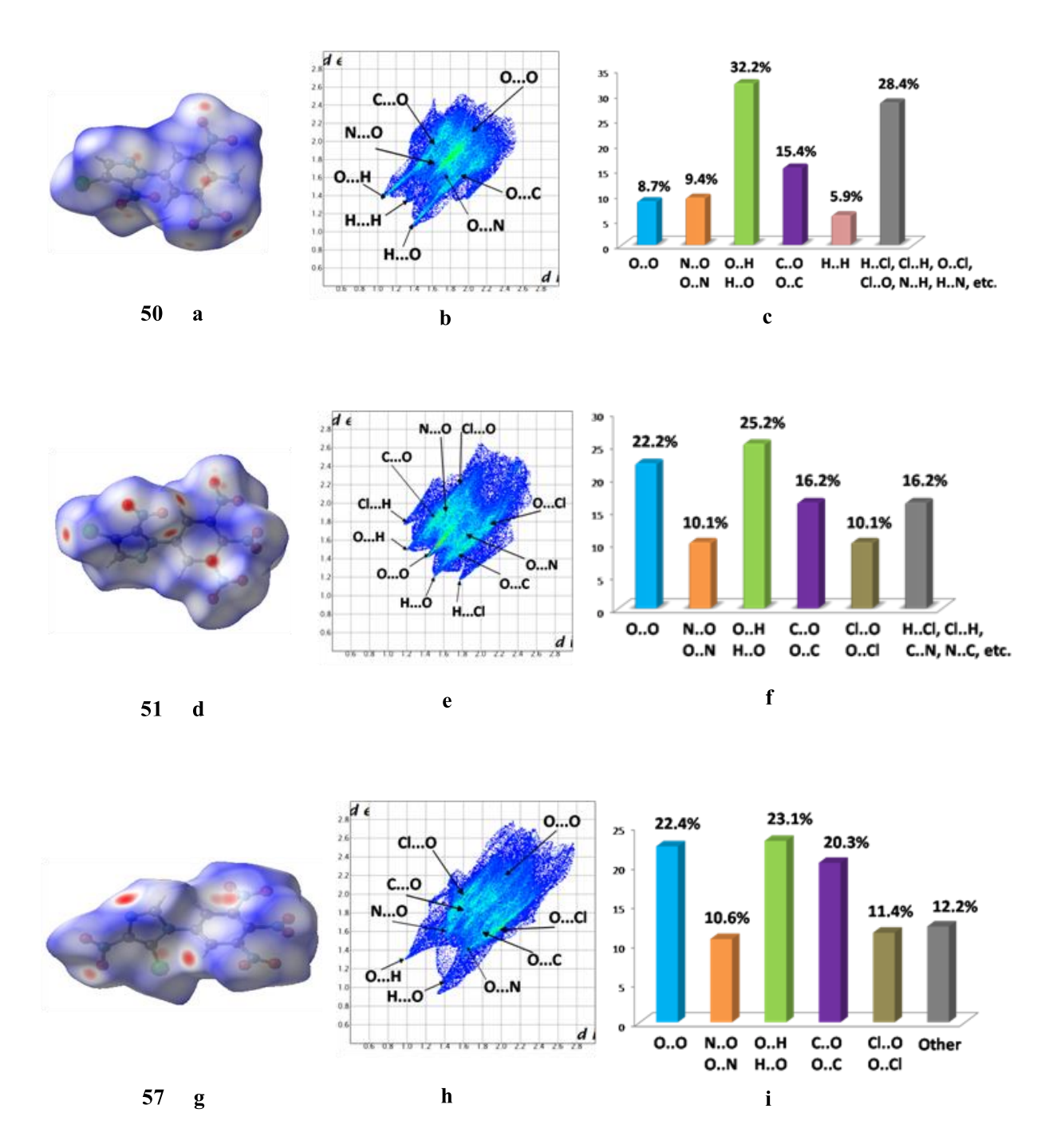
Figure 3.5.1. Electrostatic potential (ESP) of (a) 50, (b) 51, (c) 58

The electrophilic and nucleophilic reactivity of molecule solely depends on electron density potential site of the molecular entity.<sup>25</sup> As shown in **Figure 3.5.1a**, positive regions (blue) are localized on nitrogen in **50**; the compounds are therefore nucleophilic. Introduction of oxygen on figure **50** (a) makes the nitrogen and oxygen atoms more negative (red region) on **51** (**Figure b**). It is mainly focused on nitro groups of six-membered ring in **50** (**Figure a**) and **51** (**Figure b**). By substitution of azido group in **51** (**Figure b**) makes the more blue region (positive) on nitrogen atoms of three azido groups in six-membered ring and azole ring of **58** (**Figure c**), suggesting that **58** (**Figure c**) could be more sensitive than **51** (**Figure b**). Thus, compounds **50** (**Figure 3.5.1a**), **51** (**Figure 3.5.1b**), and **58** (**Figure 3.5.1c**) have positive regions than negative regions; consequently, these compounds could be probably reactive and sensitive to harsh conditions.<sup>26</sup>

## 3.6. Hirshfeld surface analysis

To understand structure and property relationship, the Hirshfeld surfaces and two-dimensional finger print plots of compounds **50**, **51**, **57**, and **58** by using Crystal explorer 17.5<sup>27</sup> are calculated (**Figure 3.6.1**). The N···N, H···N/N···H, H···O/O···H, O···O, C···O/O···C and N···O/O···N are major interactions in the compound (**Figure 3.6.1**). While compounds **50**, **51**, and **57** show higher H···O/O···H interactions than **58**. The compound **58** showed N···N (23.5%) as well H···N/N···H interactions (12.6%) (**Figure 3.6.1**, **58**; **1**). The compounds **50**, **51**, and **57** showed O···O interaction percentages 8.7%, 22.2%, and 22.4%, respectively. For compound **58**, percentage 23.5%, 25.7%, 11%, and 5.8% corresponds to N···N, N···O, N···C, and C···O interaction,

respectively. The total contact percentage for **58** is 66.1%; this value indicates lack of sufficient hydrogen bonds in the molecule **58**. Thus, theoretically **58** is sensitive to impact (**Figure 3.6.1**).<sup>28</sup>



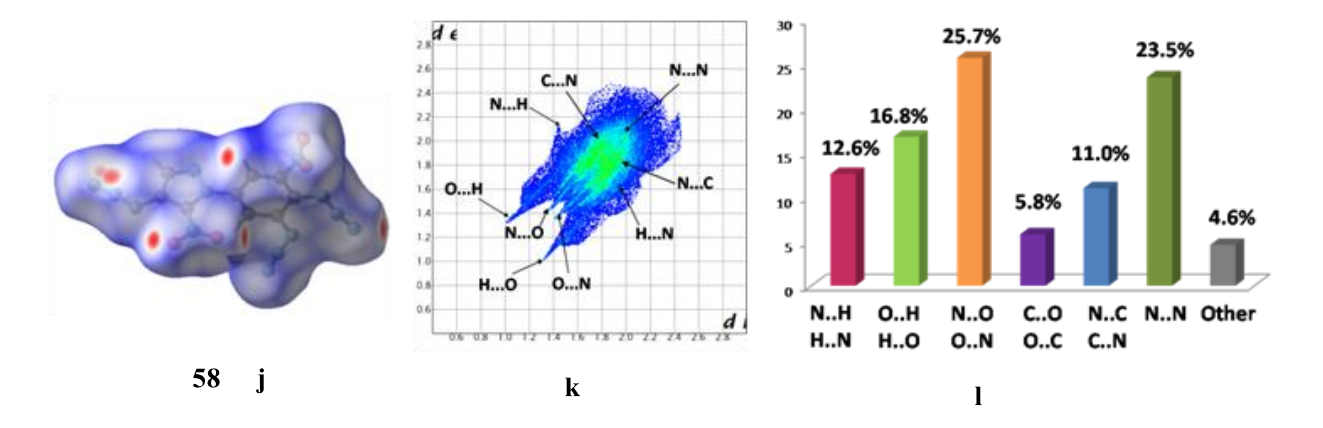


**Figure 3.6.1.** Hirshfeld surface calculations of **50**, **51**, **57**, and **58** as well as two-dimensional fingerprint plots in the crystal structures. Images (a), (d), (g), and (j) are the Hirshfeld surface graphs with proximity of close contacts around **50**, **51**, **57**, and **58** molecules (white, d = van der Waals (vdW) distance; blue, d >vdW distance; red, d <vdW distance). The fingerprint plots in crystal stacking found in **50** (b), **51** (e), **57** (h) and **58** (k). The 3D graphs (c), (f), (i), and (l) for **50**, **51**, **57**, and **58** show the percentage contributions of the individual atomic contacts to the Hirshfeld surface.

#### 3.7. Conclusions

In conclusion, polynitro/azido-*N*-aryl-C-nitro pyrazole/imidazole derivatives are synthesized from readily accessible chlorine substituted *p*-methoxy-aryl-pyrazole/imidazole precursors **42** and **43**. The molecular structures of the representative compounds are characterized by <sup>1</sup>H, <sup>13</sup>C NMR, IR, HRMS and some of the compounds are further confirmed by single crystal X-ray diffraction analysis. The Hirshfeld surface graphs and fingerprint plot analysis of compounds **50**, **51**, and **57** affirm that the crystal lattices are stabilized due to C···O/O···C, N···O/O···N, O···H/H···O and O···O intermolecular interactions. While compound **58** showed major N···N and N···O/O···N interactions. The experimental energetic parameters suggest that most of the compounds are thermally stable energetic materials (except azido compounds). Triazido-trinitroaryl-pyrazole/imidazole derivatives **58** and **60** exhibit density 1.71 g/cm<sup>3</sup> and 1.76 g/cm<sup>3</sup>, respectively, high positive heats of formation (+1309.88 kJ/mol and +1230.31 kJ/mol).

# 3.8. Experimental

#### 3.8.1. General Experimental

All the reactions were performed in an oven-dried round bottomed flask. Commercial grade solvents were distilled prior to use. Column chromatography was performed using silica gel (100-200 Mesh) with hexanes and ethyl acetate mixture. Thin layer chromatography (TLC) was performed on silica gel GF254 plates. Visualization of spots on TLC plate was accomplished with UV light (254 nm) and staining over I<sub>2</sub> chamber.

Proton and carbon nuclear magnetic resonance spectra (<sup>1</sup>H NMR, <sup>13</sup>C NMR) were recorded on a 400 MHz (<sup>1</sup>H NMR, 400 MHz) spectrometer, 500 MHz (<sup>1</sup>H NMR, 500 MHz; <sup>13</sup>C NMR, 126 MHz) spectrometer and 600 MHz (<sup>1</sup>H NMR, 600 MHz; <sup>13</sup>C NMR, 151 MHz; <sup>15</sup>N NMR, 61 MHz; spectra were recorded with a JEOL JNM-ECZ-600R/M1) spectrometer, respectively. The chemical shift values (ppm) are expressed relative to the chemical shift of [D] solvent or to the external standard Liq. NH<sub>3</sub> without correction (<sup>15</sup>N NMR). Data for <sup>1</sup>H NMR are reported as follows: chemical shift (ppm), multiplicity (s = singlet; brs = broad singlet; d = doublet; bd = broad doublet; dd = doublet of doublet; dt = doublet of triplet; tt = triplet of triplet; t = triplet; bt = broad triplet; q = quartet; pent = pentet, m = multiplet), coupling constants *J* in (Hz), and integration. <sup>13</sup>C NMR was reported in terms of chemical shift (ppm). Melting points and decomposition temperatures (DTA) were determined by DSC–TGA measurements. IR spectra were recorded on FT/IR spectrometer and are reported in cm<sup>-1</sup>. High resolution mass spectra (HRMS) were obtained in ESI mode. X-ray data was collected at 296 K, 298 K, 294 K and 293 K on a 'Bruker D8 VENTURE Photon III detector' and 'Bruker D8 Quest CCD' diffractometer using Mo-Kα radiation (0.71073Å).

- **3.8.2. Caution!** All the nitro substituted aryl-azole (pyrazole/imidazole) derivatives are energetic materials and they tend to explode under certain conditions unpredictably. However, none of the compounds described herein has exploded or detonated in the course of performing research described in this chapter. Caution should be exercised at all times during the synthesis, characterization, and handling of any of these materials, and mechanical actions involving scratching or scraping must be avoided. Ignoring safety precautions can lead to serious injuries.
- **3.8.3. Materials:** Unless otherwise noted, all the reagents were obtained commercially and used without purification. 4-Iodoanisole, pyrazole, imidazole, *N*-chlorosuccinimide, 30% aqueous H<sub>2</sub>O<sub>2</sub>, sodium bicarbonate (NaHCO<sub>3</sub>), aqueous ammonia, acetonitrile (CH<sub>3</sub>CN), tetrahydrofuran (THF), sodium azide, dimethyl sulfoxide (DMSO) were commercially available and used as received. Concentrated H<sub>2</sub>SO<sub>4</sub> and fuming HNO<sub>3</sub> were commercial available as used for nitration.

## 3.8.4. X-ray Crystallography<sup>18</sup>

Single crystal X-ray data for the compounds **46** was collected using the 'Bruker D8 Quest CMOS detector' system [ $\lambda$ (Mo-K $\alpha$ ) = 0.71073Å] at 293 K graphite monochromator with a  $\omega$  scan width of 0.30, crystal-detector distance 60 mm, collimator 0.5 mm. The SMART software was used for the intensity data acquisition and the SAINTPLUS Software was used for the data extraction. In each case, absorption correction was performed with the help of SADABS program, an empirical absorption correction using equivalent reflections was performed with the program. The structure was solved using SHELXS-97, and full-matrix least-squares refinement against F2 was carried out using SHELXL-97. All non-hydrogen atoms were refined anisotropically. Aromatic and methyl hydrogens were introduced on calculated positions and included in the refinement riding on their respective parent atoms.

Single crystal X-ray data for the compounds **50**, **51**, **57**, and **58** were collected using 'Bruker D8 VENTURE Photon III detector' system [Mo-K $\alpha$  fine focus sealed tube  $\lambda$ = 0.71073 Å] at 296 K, 297 K, 298 K, and 294 K graphite monochromator with a  $\omega$  scan. Data reduction was performed using Bruker SAINT<sup>2</sup> software. Intensities for absorption were corrected using SADABS 2014/5. Structure solution and refinement were carried out using Bruker SHELX-TL.

## 3.8.5. Hirshfeld Surface Analysis<sup>27</sup>

From Hirshfeld surface image shown in **Figure 3.6.1**, the red spots signify high contact populations, while blue and white spots are for low contact populations. This suggests that the negative (red) or positive value (blue and white) of  $d_{norm}$  depends on the intermolecular contacts being shorter (red) or longer (blue and white) than the van der Waals separations. For each point on the Hirshfeld surface, the normalized contact distance ( $d_{norm}$ ) was determined by the equation as shown below.

$$[d_{norm} = (\ d_i - {d_i}^{vdW})/{r_i}^{vdW} + (d_e - {d_e}^{vdW}/{r_e}^{vdW}]$$

In which  $d_i$  is measured from the surface to the nearest atom interior to the surface interior, while  $d_e$  is measured from the surface to the nearest atom exterior to the surface interior, where  $r_i^{vdW}$  and  $r_e^{vdW}$  are the van der Waals radii of the atoms. Hirshfeld surface graphs and two-dimensional fingerprint plots of **50**, **51**, **57**, and **58** were analyzed using Crystal explorer17.5 software.

#### 3.8.6. Isodesmic reactions for the prediction of heat of formation:

## 3.8.7. General procedure

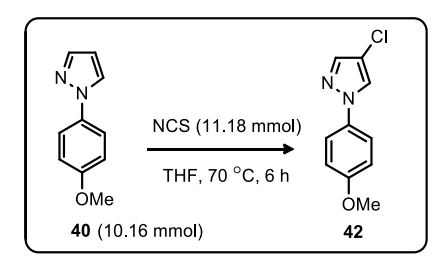
#### 3.8.7.1. General procedure for the preparation of 42 and 43 (GP-1):

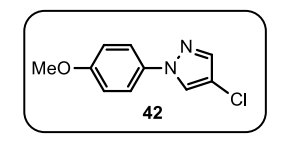
A solution of aryl-azole derivative (1.00 mmol) and *N*-chlorosuccinimide (1.1 mmol) in THF was taken in a round bottom flask. The resulting reaction mixture was stirred at room temperature or 70 °C and then diluted with EtOAc, and washed with brine. The organic layer was dried over Na<sub>2</sub>SO<sub>4</sub>, concentrated in vacuo and purified by flash chromatography on silica gel.

Physical characterization data is exactly matching with the reported values for the respective compound 42.

#### 4-Chloro-1-(4-methoxyphenyl)-1*H*-pyrazole (42):

Following the general procedure (GP-1), solution of aryl-azole derivative **40** (1.77 g, 10.16 mmol) and *N*-chlorosuccinimide (1.50 g, 11.18 mmol) in THF (40.0 mL) was taken in a RB flask. The resulting reaction mixture was refluxed at 70 °C for 6 h and cooled to room temperature, diluted with EtOAc, and washed with brine. The organic layer was dried over Na<sub>2</sub>SO<sub>4</sub>, concentrated in vacuo and purified by flash chromatography on silica gel.





1.81 g, yield: 85%. White solid. <sup>1</sup>H NMR (600 MHz, DMSO– $d_6$ ):  $\delta = 8.67$  (s, 1H), 7.80 (s, 1H), 7.71 (dq, J = 4.8 Hz, 1.8 Hz, 2H), 7.05 (dq, J = 4.8 Hz, 2.4 Hz, 2H), 3.78 (s, 3H); <sup>13</sup>C NMR (101 MHz, DMSO– $d_6$ ):  $\delta = 4.8$  Hz, 2.4 Hz, 2H), 3.78 (s, 3H); <sup>13</sup>C NMR (101 MHz, DMSO– $d_6$ ):  $\delta = 4.8$  Hz, 2.4 Hz, 2H), 3.78 (s, 3H); <sup>13</sup>C NMR (101 MHz, DMSO– $d_6$ ):  $\delta = 4.8$  Hz, 2.4 Hz, 2H), 3.78 (s, 3H); <sup>13</sup>C NMR (101 MHz, DMSO– $d_6$ ):  $\delta = 4.8$  Hz, 2.4 Hz, 2H), 3.78 (s, 3H); <sup>13</sup>C NMR (101 MHz, DMSO– $d_6$ ):  $\delta = 4.8$  Hz, 2.4 Hz, 2H), 3.78 (s, 3H); <sup>13</sup>C NMR (101 MHz, DMSO– $d_6$ ):  $\delta = 4.8$  Hz, 2.4 Hz, 2H), 3.78 (s, 3H); <sup>13</sup>C NMR (101 MHz, DMSO– $d_6$ ):  $\delta = 4.8$  Hz,  $\delta = 4.8$ 

158.0, 138.5, 132.9, 125.9, 119.9, 114.6, 110.5, 55.4 ppm. IR(Neat)  $\nu_{\text{max}}$  3102, 2934, 2839, 1608, 1512, 1460, 1302, 1246, 1173, 1026, 989, 823, 719 cm<sup>-1</sup>. HRMS (ESI) for  $C_{10}H_{10}ClN_2O^+$  (M+H)<sup>+</sup>: calcd 209.0482, found 209.0482.

# 5-Chloro-1-(4-methoxyphenyl)-1*H*-imidazole (43):

Following the general procedure (GP-1), solution of aryl-azole derivative **41** (1.0 g, 5.74 mmol) and *N*-chlorosuccinimide (843 mg, 6.31 mmol) in THF (15.0 mL) was taken in a RB flask. The resulting reaction mixture was stirred at room temperature for 3 h. After 3 h, the crude mixture was diluted with EtOAc, and washed with brine. The organic layer was dried over Na<sub>2</sub>SO<sub>4</sub>, concentrated in vacuo, and purified by flash chromatography on silica gel.

274 mg, yield: 23%. White solid. <sup>1</sup>H NMR (600 MHz, DMSO– $d_6$ ):  $\delta = 7.92$  (s, 1H), 7.39 (d, J = 8.4 Hz, 2H), 7.10 (t, J = 8.4 Hz, 3H), 3.81 (s, 3H); <sup>13</sup>C NMR (151 MHz, DMSO– $d_6$ ):  $\delta = 159.5$ , 138.2, 127.4, 127.0, 125.9, 117.0,

114.6, 55.5 ppm. IR(Neat)  $\nu_{\text{max}}$  3102, 2934, 2839, 1608, 1512, 1460, 1302, 1246, 1173, 1026, 989, 823, 719 cm<sup>-1</sup>. HRMS (ESI) for  $C_{10}H_{10}ClN_2O^+$  (M+H)<sup>+</sup>: calcd 209.0482, found 209.0466.

#### Procedure for the preparation of 44 and 45 (GP-2):

A mixture of 98% sulphuric acid (10.0 mL) and 95% nitric acid (5.0 mL) were added to 42 (1.0g, 4.79 mmol) at 0 °C. The reaction was conducted at 0 °C for 2 h. The reaction mixture was cooled by the addition of ice and neutralized with saturated aqueous solution of NaHCO<sub>3</sub>. The organic layer was separated and the aqueous layer was extracted with ethyl acetate (4×50 mL). The combined organic extracts were washed with water (3×30 mL), brine (30 mL) and dried over Na<sub>2</sub>SO<sub>4</sub>. Solvent was filtered and evaporated under vacuum. The crude residue was purified using column chromatography on silica gel to afford the desired tri-nitration products (44) and (45) in 18% (298 mg) and 31% (510 mg) yields, respectively as colorless solid.

#### 4-Chloro-1-(4-methoxy-3, 5-dinitrophenyl)-3-nitro-1*H*-pyrazole (44):

$$\begin{array}{c|c}
O_2N & NO_2\\
MeO & NO_2
\end{array}$$

$$O_2N & 44$$

Following the general procedure (GP-2): DSC–TGA (10 °C min<sup>-1</sup>, °C): 120 °C (T<sub>m</sub>) & 194 °C (T<sub>d</sub>). <sup>1</sup>H NMR (500 MHz, DMSO– $d_6$ ):  $\delta = 8.68$  (s, 2H), 8.21 (s, 1H), 4.03 (s, 3H); <sup>13</sup>C NMR (151 MHz, DMSO– $d_6$ ):  $\delta$ 

= 146.2, 144.5, 140.3, 132.5, 125.8, 125.5, 110.1, 64.6 ppm. IR(Neat)  $\nu_{\text{max}}$  3458, 3339, 3091, 1644, 1624, 1573, 1530, 1487, 1403, 1339, 1246, 1180, 976, 893, 805, 722, 644 cm<sup>-1</sup>. HRMS (ESI) for  $C_{10}H_5ClN_5O_7^-$  (M-H)<sup>-</sup>: calcd 341.9878, found 341.9873.

#### 4-Chloro-1-(4-methoxy-3, 5-dinitrophenyl)-5-nitro-1*H*-pyrazole (45):

Following the general procedure (GP-2), DSC-TGA (10 °C min<sup>-1</sup>, °C): 150 °C ( $T_m$ ) & 221 °C ( $T_d$ ). <sup>1</sup>H NMR (600 MHz, DMSO- $d_6$ ):  $\delta$  = 8.76 (s, 2H), 8.35 (s, 1H), 4.04 (s, 3H); <sup>13</sup>C NMR (151 MHz, DMSO- $d_6$ ):  $\delta$ 

=147.2, 144.0, 141.9, 140.8, 133.8, 127.8, 111.8, 64.7 ppm. IR(Neat)  $\nu_{\text{max}}$  3461, 3344, 3082, 2919, 1641, 1587, 1567, 1533, 1513, 1454, 1331, 1233, 1180, 996, 899, 773 cm<sup>-1</sup>. HRMS (ESI) for C<sub>10</sub>H<sub>7</sub>ClN<sub>5</sub>O<sub>7</sub><sup>+</sup> (M+H)<sup>+</sup>: calcd 344.0034, found 344.0013.

# Preparation of 4-chloro-1-(4-methoxy-3, 5-dinitrophenyl)-3, 5-dinitro-1*H*-pyrazole (46):

A mixture of 98% sulphuric acid (30.0 mL) and 95% nitric acid (15.0 mL) were added to **42** (3.2 g, 15.34 mmol) at 0 °C. The reaction temperature was refluxed at 70 °C for 4 h. The reaction mixture was cooled by the addition of ice. The precipitate was filtered and washed with cold water to give tetra-nitration product **46** (3.3 g) in 55% yield as yellow solid.

$$\begin{array}{c|c}
O_2N & NO_2\\
MeO & NO_2N \\
O_2N & O_2N
\end{array}$$

DSC-TGA (10 °C min<sup>-1</sup>, °C): 176 °C (T<sub>m</sub>) & 278 °C (T<sub>d</sub>). <sup>1</sup>H NMR (600 MHz, DMSO- $d_6$ ):  $\delta = 8.85$  (s, 2H), 4.07 (s, 3H); <sup>13</sup>C NMR (151 MHz, DMSO- $d_6$ ):  $\delta = 150.0$ , 148.5, 144.1, 143.1, 132.5, 128.5, 107.2, 64.8

ppm. IR(Neat)  $\nu_{\text{max}}$  3649, 3567, 1749, 1716, 1647, 1558, 1541, 1507, 1457, 1323, 904, 84, 669 cm<sup>-1</sup>. HRMS (ESI) for  $C_{10}H_5ClN_6O_9^+$  (M)<sup>+</sup>: calcd 387.9807, found 387.9803.

#### Preparation of 5-chloro-1-(4-methoxy-3,5-dinitrophenyl)-1*H*-imidazole (47):

A mixture of 98% sulphuric acid (10.0 mL) and 95% nitric acid (5.0 mL) was added to **43** (0.8 g, 3.84 mmol) at 0 °C. The reaction mixture was stirred at 0 °C for 2 h. After 2 h, the crude mixture was cooled by the addition of ice and neutralized with saturated aqueous solution of NaHCO<sub>3</sub>. The organic layer was separated and the aqueous layer was extracted with ethyl acetate (4 ×30 mL). The combined organic extracts were washed with water (3×20 mL), brine (20 mL) and dried over Na<sub>2</sub>SO<sub>4</sub>. Solvent was filtered and evaporated to afford the desired di-nitration product **47** in 81% (942 mg) yield as yellow solid.

123

$$\begin{array}{c|c} O_2N \\ MeO & N \\ O_2N & CI \\ 47 \end{array}$$

DSC-TGA (10 °C min<sup>-1</sup>, °C): 137 °C ( $T_m$ ) & 332 °C ( $T_d$ ). <sup>1</sup>H NMR (600 MHz, DMSO- $d_6$ ):  $\delta = 8.61$  (s, 2H), 8.13 (s, 1H), 7.23 (s, 1H), 4.0 (s, 3H); <sup>13</sup>C NMR (151 MHz, DMSO- $d_6$ ):  $\delta = 146.1$ , 144.5, 138.5, 129.5, 127.0,

126.8, 116.8, 64.6 ppm. IR (Neat)  $\nu_{\text{max}}$  3374, 3118, 2221, 1632, 1553, 1489, 1343, 1205, 1092, 974 cm<sup>-1</sup>. HRMS (ESI) for C<sub>10</sub>H<sub>8</sub>ClN<sub>4</sub>O<sub>5</sub><sup>+</sup> (M+H)<sup>+</sup>: calcd 299.0183, found 299.0183.

### Preparation of 5-chloro-1-(4-methoxy-3,5-dinitrophenyl)-4-nitro-1*H*-imidazole (48):

A mixture of 98% sulphuric acid (6.0 mL) and 95% nitric acid (3.0 mL) were added to **43** (300 mg, 1.44 mmol) at 0 °C. The reaction was refluxed at 70 °C for 3 h. The reaction mixture was cooled by the addition of ice. The precipitate was filtered and washed with cold water to give trinitration product **48** (247 mg) in 50% yield as yellow solid.

$$\begin{array}{c|c}
O_2N & & \\
MeO & & N \\
O_2N & & CI \\
\hline
48
\end{array}$$

DSC-TGA (10 °C min<sup>-1</sup>, °C): 184 °C (T<sub>d</sub>). <sup>1</sup>H NMR (600 MHz, DMSO- $d_6$ ):  $\delta = 8.78$  (s, 2H), 8.31 (s, 1H), 4.04 (s, 3H); <sup>13</sup>C NMR (151 MHz, DMSO- $d_6$ ):  $\delta = 147.7$ , 144.3, 141.9, 136.6, 128.6, 128.0, 120.3,

64.7 ppm. IR (Neat)  $\nu_{max}$  3123, 1623, 1535, 1492, 1396, 1359, 1269, 1171, 1080, 983, 841, 759 cm<sup>-1</sup>. HRMS (ESI) for  $C_{10}H_7ClN_5O_7^+$  (M+H)<sup>+</sup>: calcd 344.0034, found 344.0030.

#### **Preparation of 4-(4-chloro-5-nitro-1***H***-pyrazol-1-yl)-2,6-dinitroaniline (50):**

An aqueous solution of ammonia (0.9 mL) was added to a solution of compound **45** (800 mg, 2.33 mmol) in acetonitrile (30.0 mL). The resulting solution was refluxed at 80 °C for 24 h. The solvent was evaporated under reduced pressure and solid was filtered, washed with DCM and dried in air to afford **50** (590 mg) in 77% yield as red solid.

$$\begin{pmatrix} O_2N & & & \\ H_2N & & & & \\ O_2N & & & O_2N \end{pmatrix} CI$$

DSC-TGA (10 °C min<sup>-1</sup>, °C): 149 °C (T<sub>m</sub>) & 210 °C (T<sub>d</sub>). <sup>1</sup>H NMR (500 MHz, DMSO- $d_6$ ):  $\delta = 8.84$  (s, 2H), 8.66 (s, 2H), 8.26 (s, 1H), <sup>13</sup>C NMR (126 MHz, DMSO- $d_6$ ):  $\delta = 142.4$ , 141.6, 140.4, 134.6, 132.3, 125.0,

124

111.5 ppm. IR(Neat)  $\nu_{\text{max}}$  3459, 3343, 1640, 1534, 1414, 1353, 1232, 1179, 1098, 924, 821, 772 cm<sup>-1</sup>. HRMS (ESI) for C<sub>9</sub>H<sub>4</sub>ClN<sub>6</sub>O<sub>6</sub><sup>-</sup> (M–H)<sup>-</sup>: calcd 326.9881, found 326.9887.

#### Preparation of 4-(4-chloro-3, 5-dinitro-1*H*-pyrazol-1-yl)2,6-dinitroaniline (52):

An aqueous solution of ammonia (0.5 mL) was added to a solution of compound **46** (500 mg, 1.29 mmol) in acetonitrile (20.0 mL). This mixture was stirred at room temperature for 1 h. The solvent was evaporated under reduced pressure and solid was filtered, washed with DCM and dried in air to afford **52** (468 mg) in 98% yield as red solid.

DSC-TGA (10 °C min<sup>-1</sup>, °C): 215 °C (T<sub>d</sub>). <sup>1</sup>H NMR (600 MHz, DMSO- $d_6$ ):  $\delta = 8.90$  (s, 2H), 8.74 (s, 2H); <sup>13</sup>C NMR (151 MHz, DMSO- $d_6$ ):  $\delta = 149.5$ , 143.0, 141.8, 134.3, 131.9, 123.1, 106.6 ppm.

IR(Neat)  $\nu_{\text{max}}$  3459, 3347, 2920, 2851, 1642, 1534, 1414, 1364, 1230, 1095, 915, 845, 734 cm<sup>-1</sup>. HRMS (ESI) for C<sub>9</sub>H<sub>3</sub>ClN<sub>7</sub>O<sub>8</sub><sup>-</sup> (M–H)<sup>-</sup>: calcd 371.9732, found 371.9734.

## **Preparation of 4-(5-chloro-1***H***-imidazol-1-yl)-2,6-dinitroaniline (54):**

An aqueous solution of ammonia (0.8 mL) was added to a solution of compound **47** (700 mg, 2.34 mmol) in acetonitrile (25.0 mL). The resulting solution was stirred at room temperature for 3–5 h. The solvent was evaporated under reduced pressure and solid was filtered, washed with DCM and dried in air to afford **54** (508 mg) in 77% yield as an orange solid.

DSC-TGA (10 °C min<sup>-1</sup>, °C): 241 °C (T<sub>d</sub>). <sup>1</sup>H NMR (600 MHz, DMSO- $d_6$ ):  $\delta = 8.61$  (s, 2H), 8.51 (s, 2H), 8.10 (s, 1H), 7.16 (s, 1H); <sup>13</sup>C NMR (151 MHz, DMSO- $d_6$ ):  $\delta = 140.5$ , 138.4, 134.7, 131.2, 126.2, 119.6,

117.0 ppm. IR(Neat)  $\nu_{\text{max}}$  3436, 3271, 3112, 1645, 1537, 1414, 1354, 1288, 1158, 1022, 826 cm<sup>-1</sup>. HRMS (ESI) for C<sub>9</sub>H<sub>7</sub>ClN<sub>5</sub>O<sub>4</sub><sup>+</sup> (M+H)<sup>+</sup>: calcd 284.0187, found 284.0186.

#### Preparation of 4-(5-chloro-4-nitro-1*H*-imidazol-1-yl)-2,6-dinitroaniline (56):

An aqueous solution of ammonia (0.3 mL) was added to a solution of compound **48** (200 mg, 0.58 mmol) in acetonitrile (10.0 mL). The resulting solution was stirred at room temperature for 3 h. The solvent was evaporated under reduced pressure and solid was filtered, washed with DCM and dried in air to afford **56** (227 mg) in 100% yield as red solid.

$$\begin{array}{c|c}
O_2N & & \\
H_2N & & & \\
O_2N & & & \\
\hline
 & & &$$

DSC–TGA (10 °C min<sup>-1</sup>, °C): 245 °C (T<sub>d</sub>). <sup>1</sup>H NMR (600 MHz, DMSO– $d_6$ ):  $\delta = 8.84$  (s, 2H), 8.64 (s, 2H), 8.24 (s, 1H); <sup>13</sup>C NMR (151 MHz, DMSO– $d_6$ ):  $\delta = 141.7$ , 141.3, 136.7, 134.6, 132.4, 120.9, 118.3

ppm. IR(Neat)  $\nu_{\text{max}}$  3413, 3278, 1640, 1537, 1494, 1453, 1417, 1358, 1260, 1162, 1055, 916, 828, 772 cm<sup>-1</sup>. HRMS (ESI) for C<sub>9</sub>H<sub>4</sub>ClN<sub>6</sub>O<sub>6</sub><sup>-</sup> (M–H)<sup>-</sup>: calcd 326.9881, found 326.9888.

## Preparation of 4-chloro-5-nitro-1-(3, 4, 5-trinitrophenyl)-1*H*-pyrazole (51):

Compound **50** (300 mg, 0.91 mmol) was dissolved in sulphuric acid (20.0 mL) at 0 °C. Hydrogen peroxide (30%, 10.0 mL) was then added drop-wise to the reaction mixture and stirred at room temperature for 24 h and then poured into ice cold water. The precipitate was filtered and washed with cold water to afford **51** (202 mg) in 62% yield as pale-yellow solid.

$$\begin{array}{c|c}
\hline
O_2N \\
O_2N \\
O_2N \\
O_2N
\end{array}$$
CI

DSC-TGA (10 °C min<sup>-1</sup>, °C): 139 °C ( $T_m$ ) & 275 °C (Onset) ( $T_d$ ). <sup>1</sup>H NMR (500 MHz, DMSO- $d_6$ ):  $\delta = 8.58$  (s, 2H), 8.26 (s, 1H); <sup>13</sup>C NMR (126 MHz, DMSO- $d_6$ ):  $\delta = 148.0$ , 142.3, 140.7, 140.3, 128.5, 128.4, 111.9 ppm.

IR(Neat)  $\nu_{\text{max}}$  3446, 3337, 3091, 2919, 1645, 1538, 1415, 1397, 1330, 1256, 1235, 1099, 900, 822 cm<sup>-1</sup>. HRMS (ESI) for C<sub>9</sub>H<sub>2</sub>ClN<sub>6</sub>O<sub>8</sub><sup>-</sup> (M–H)<sup>-</sup>: calcd 356.9623, found 356.9609.

## Preparation of 4-chloro-3, 5-dinitro-1-(3, 4, 5-trinitrophenyl)-1*H*-pyrazole (53):

Compound **52** (300 mg, 0.80 mmol) was dissolved in sulphuric acid (15.0 mL) at 0 °C. Hydrogen peroxide (30%, 8.0 mL) was then added drop-wise to the reaction mixture and stirred

at room temperature for 12 h and then poured into ice cold water. The precipitate was filtered and washed with cold water to provide **53** (232 mg) in 72% yield as pale-yellow solid.

$$\begin{pmatrix}
O_2N & N & NO_2 \\
O_2N & O_2N & CI \\
S3 & S3
\end{pmatrix}$$

DSC-TGA (10 °C min<sup>-1</sup>, °C): 203 °C (T<sub>d</sub>). <sup>1</sup>H NMR (600 MHz, Acetone– $d_6$ ):  $\delta = 7.35$  (d, J = 3.6 Hz, 2H); <sup>13</sup>C NMR (600 MHz, Acetone– $d_6$  + two drops of CD<sub>3</sub>CN):  $\delta = 147.5$ , 143.7, 131.7, 130.2,

128.3, 127.2, 106.5 ppm. IR(Neat)  $\nu_{\text{max}}$  3648, 2970, 1559, 1520, 1435, 1365, 1216, 910, 838, 731, 527 cm<sup>-1</sup>. HRMS (ESI) for C<sub>9</sub>HClN<sub>7</sub>O<sub>10</sub><sup>-</sup> (M–H)<sup>-</sup>: calcd 401.9474, found 401.9481.

#### Preparation of 5-chloro-1-(3,4,5-trinitrophenyl)-1*H*-imidazole (55):

Compound **54** (300 mg, 1.06 mmol) was dissolved in sulphuric acid (20.0 mL) at 0 °C. Hydrogen peroxide (30%, 10.0 mL) was then added drop-wise to the reaction mixture and stirred at room temperature for 24 h and then poured into ice cold water. The precipitate was filtered and washed with cold water to afford **55** (116 mg) in 35% yield as pale-yellow solid.

$$\begin{array}{c|c}
O_2N & & \\
O_2N & & & \\
O_2N & & & CI
\end{array}$$

DSC-TGA (10 °C min<sup>-1</sup>, °C): ND. <sup>1</sup>H NMR (600 MHz, CD<sub>3</sub>CN):  $\delta$  = 8.93 (s, 2H), 8.52 (s, 2H); <sup>13</sup>CNMR (151 MHz, DMSO- $d_6$ ):  $\delta$  = 155.8, 145.2, 143.3, 136.9, 130.5, 118.6, 98.8 ppm. IR(Neat)  $\upsilon_{\text{max}}$  3282, 3099, 2194, 1675,

1544, 1335, 1272, 1174, 925, 843 cm $^{-1}$ . HRMS (ESI) for  $C_9H_5ClN_5O_6^+$  (M+H) $^+$ : calcd 313.9928, found 313.9924.

## Preparation of 5-chloro-4-nitro-1-(3, 4, 5-trinitrophenyl)-1*H*-imidazole (57):

Compound **56** (300 mg, 0.91 mmol) was dissolved in sulphuric acid (20.0 mL) at 0 °C. Hydrogen peroxide (30%, 10.0 mL) was then added drop-wise to the reaction mixture and stirred at room temperature for 24 h and then poured into ice cold water. The precipitate was filtered and washed with cold water gave **57** (148 mg) in 45% yield as pale-yellow solid.

$$\begin{pmatrix}
O_2N & & & \\
O_2N & & & & \\
O_2N & & & & \\
O_2N & & & & \\
\hline
S7 & & & & \\
\hline
S7 & & & & \\
\hline
S7 & & & & \\
\hline
S8 & & & & \\
\hline
S9 & & & & \\
S9 & & & & \\
\hline
S9 & & & \\
\hline
S9 & & & \\
\hline
S9 & & & \\
S9 & & & & \\
\hline
S9 & &$$

DSC-TGA (10 °C min<sup>-1</sup>, °C): 266 °C (Onset) (T<sub>d</sub>). <sup>1</sup>H NMR (600 MHz, DMSO- $d_6$ ):  $\delta = 9.27$  (s, 2H), 8.35 (s, 1H); <sup>13</sup>C NMR (151 MHz, DMSO- $d_6$ ):  $\delta = 154.8$ , 142.6, 142.1, 137.5, 129.9, 122.0, 117.4 ppm.

IR(Neat)  $\nu_{\text{max}}$  3088, 1555, 1539, 1492, 1355, 1339, 1300, 1234, 1074, 1000, 926, 869, 731 cm<sup>-1</sup>. HRMS (ESI) for C<sub>9</sub>H<sub>3</sub>ClN<sub>6</sub>O<sub>8</sub><sup>+</sup> (M)<sup>+</sup>: calcd 357.9701, found 357.9706.

#### Preparation of 4-azido-1-(3, 4-diazido-5-nitrophenyl) 5-nitro-1*H*-pyrazole (58):

Compound **51** (300 mg, 0.83 mmol) and sodium azide (163 mg, 2.5 mmol) was suspended in DMSO (5.0 mL). The reaction mixture was stirred at room temperature for 12 h and then poured into ice cold water. The precipitate was filtered and washed with cold water gave **58** (65 mg) in 22% yield as yellow solid.

$$\begin{array}{c|c}
O_2N \\
N_3 & N_3 \\
N_3 & O_2N
\end{array}$$

<sup>1</sup>H NMR (600 MHz, CD<sub>3</sub>CN):  $\delta$  = 7.87 (s, 1H), 7.73 (s, 1H), 7.62 (s, 1H); <sup>13</sup>C NMR (151 MHz, CD<sub>3</sub>CN):  $\delta$  = 137.1, 135.7, 134.5, 125.2, 124.7, 121.4, 118.6 ppm. IR(Neat)  $\nu_{\text{max}}$  3352, 2924, 2831, 2133, 2035, 2009, 1981, 1738,

 $1447, 1268, 1113, 1024, 736 \text{ cm}^{-1}.$ 

## Preparation of 4-azido-1-(3, 4-diazido-5-nitrophenyl)5-nitro-1*H*-Imidazole (60):

Compound **57** (100 mg, 0.28 mmol) and sodium azide (55 mg, 0.84 mmol) was suspended in DMSO (10.0 mL). The reaction mixture was stirred at room temperature for 12 h and then poured into ice cold water. The precipitate was filtered and washed with cold water to afford **60** (37 mg) in 37% yield as yellow solid.

128

<sup>1</sup>H NMR (600 MHz, CD<sub>3</sub>CN):  $\delta$  = 8.48 (s, 2H), 7.63 (s, 1H); <sup>13</sup>C NMR (151 MHz, CD<sub>3</sub>CN):  $\delta$  = 150.1, 139.0, 133.4, 129.9, 124.6, 122.1, 119.2 ppm. IR (Neat)  $\nu_{\text{max}}$  3397, 2922, 2852, 2210, 2159, 2028, 1999, 1970, 1641, 1547,

1435, 1314, 1014, 950 cm $^{-1}$ . HRMS (ESI) for  $C_9H_4N_{13}O_4^+$  (M+H) $^+$ : calcd 358.0509, found 358.0502.

#### 3.9. References

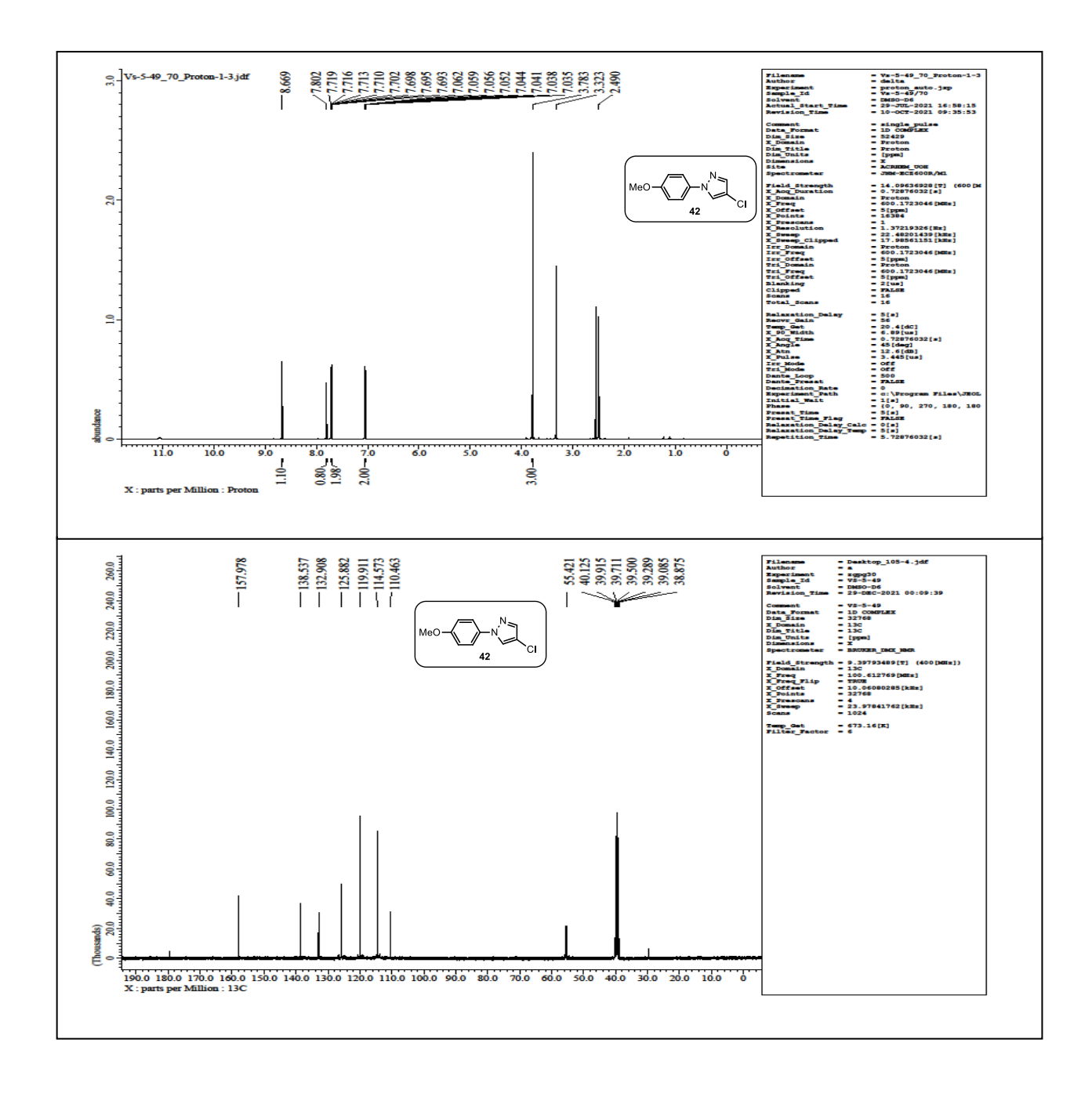
- 1. J. W. A. M. Janssehn, H. J. Koeners, C. G. Kruse, and C. L. Habraken, *J. Org. Chem.*, **1973**, 38, 1777.
- 2. P. Yin, J. Zhang, C. He, D. A. Parrish, and J. M. Shreeve, *J. Mater. Chem.A*, **2014**, 2, 3200–3208.
- 3. K. Hou, C. Ma, and Z. Liu, New J. Chem., 2013, 37, 2837.
- 4. P. Yin, Q. Zhang, J. Zhang, D. A. Parrish, and J. M. Shreeve, J. Mater. Chem.A, 2013, 1, 7500.
- 5. D. Chand, C. He, L. A. Mitchell, D. A. Parrish, and J. M. Shreeve, *Dalton Trans.*, **2016**, *45*, 13827.
- 6. S. G. Il'yasov, E. O. Danilova, Propellants Explos. Pyrotech., 2012, 37, 427–431.
- 7. J. Zhang, C. He, D. A. Parrish, and J. M. Shreeve, *Chem.–Eur. J.*, **2013**, *19*, 8929–8936.
- 8. J. Zhang, D. A. Parrish and J. M. Shreeve, Chem.-Asian J., 2014, 9, 2953.
- 9. J. Zhang, P. Yin, L. A. Mitchell, D. A. Parrish, and J. M. Shreeve, *J. Mater. Chem.A*, **2016**, *4*, 7430.
- 10. Y. Tang, C. He, P. Yin, G. H. Imler, D. A. Parrish, and J. M. Shreeve, *Eur. J. Org. Chem.* **2018**, 2273–2276.
- 11. A. V. Shastin, T. I. Godovikova, B. L. Korsunskii, *Khim. Geterotsikl. Soedin.*, **2003**, 722 [*Chem. Heterocycl. Compd. (Engl. Transl.)*, **2003**].
- 12. A. V. Shastin, T. I. Godovikova, and B. L. Korsunskii, Russ. Chem. Bull., Int. Ed., 2011, 60, 6.
- 13. M. V. Huynh, M. A. Hiskey, E. L. Hartline, D. P. Montoya, and Richard Gilardi, *Angew. Chem. Int. Ed.*, **2004**, *43*, 4924–4928.
- 14. (a) Po Man Liu, C. G. Frost, *Org. Lett.*, **2013**, *15*,5862–5865; (b) M.Taillefer, N. Xia, A. Ouali, *Angew. Chem. Int. Ed.*, **2007**, *46*, 934–936; (c) G. G. Pawar, W. Haibo, D. Subhadip, D. Maa, *Adv. Synth. Catal.*, **2017**, *359*, 1631–1636; (d) X. Wang, M. Wang, and J. Xie, *Syn. Commun.*, **2017**, *47*, 1797–1803; (e) S. Das, P. Natarajan, and B. König, *Chem. Eur. J.*, **2017**, *23*, 18161–18165.
- 15. (a) R. F. W. Bader, M. T. Carroll, J. R. Cheeseman, C. Chang, *J. Am. Chem. Soc.*, **1987**, *109*, 7968–7979; (b) J. S. Murray, P. Politzer, *Croat. Chem. Acta*, **2009**, 82, 267–275; (c) P. Politzer, J.
- S. Murray, F. A. Bulat, *J. Mol. Model.*, **2010**, *16*, 1731–1742; (d) V. D. Ghule, D. Srinivas, K. Muralidharan, *Asian J. Org. Chem.*, **2013**, 2, 662–668; (e) D. Srinivas, V. D. Ghule, K. Muralidharan, *New J. Chem.***2014**, *38*, 3699–3707.
- 16. N. Kommu, M. Balaraju, V. D. Ghule, A. K. Sahoo, J. Mater. Chem. A, 2017, 5, 7366–7371.
- 17. (a) P. Yin, D. A. Parrish, and J. M. Shreeve, *Chem. Eur. J.*, **2014**, 20, 6707–6712; (b) J. Zhang,
- C. He, D. A. Parrish, and J. M. Shreeve, Chem. Eur. J., 2013, 19, 8929-8936; (c) R. Wang, Y.
- Guo, R. Sa, and J. M. Shreeve, *Chem. Eur. J.*, **2010**, *16*, 8522–8529; (d) Y. Zhang, Y. Guo, Y. H.

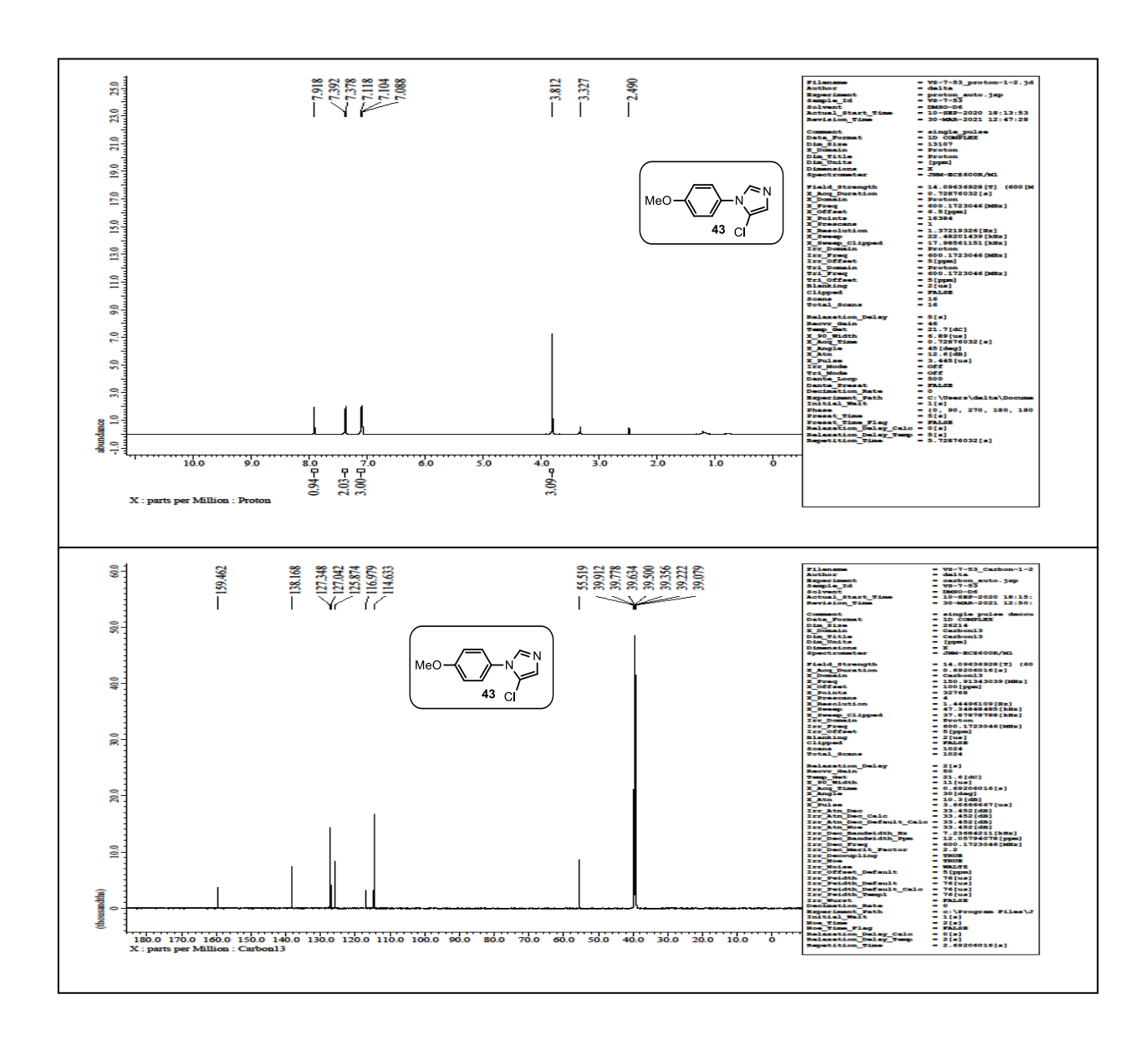
- Joo, D. A. Parrish, and J. M. Shreeve, *Chem. Eur. J.*, **2010**, *16*, 10778–10784; (e) J. Zhang, D. A. Parrish and J. M. Shreeve, *Chem. Commun.*, **2015**, *51*, 7337–7340.
- 18. (a) O. V. Dolomanov, A. J. Blake, N. R. Champness, M. Schroder, *J. Appl. Cryst.*, **2003**, *36*, 1283; (b) SAINT, version 6.45 /8/6/03 and version 8.34A, Bruker Apex-III, **2003**, **2014**; (c) G. M. Sheldrick, *SHELXS-97*, University of Gottingen, Germany, **1997**; (d) Sheldrick, G. M.; SADABS and SADABS 2014/5, *Program for Empirical Absorption Correction of Area Detector Data*, University of Göttingen, Germany, **1997**, **2014**; (e) *SMART*(*version5.625*), *SHELX-TL*(*version6.12*), Bruker AXS Inc. Madison, WI, **2000**.
- 19. Gaussian 09, Revision C.01, M. J. Frisch, G. W. Trucks, H. B. Schlegel, G. E. Scuseria, M. A. Robb, J. R. Cheeseman, G. Scalmani, V. Barone, B. Mennucci, G. A. Petersson, H. Nakatsuji, M. Caricato, X. Li, H. P. Hratchian, A. F. Izmaylov, J. Bloino, G. Zheng, J. L. Sonnenberg, M. Hada, M. Ehara, K. Toyota, R. Fukuda, J. Hasegawa, M. Ishida, T. Nakajima, Y. Honda, O. Kitao, H. Nakai, T. Vreven, J. A. Montgomery, Jr., J. E. Peralta, F. Ogliaro, M. Bearpark, J. J. Heyd, E. Brothers, K. N. Kudin, V. N. Staroverov, R. Kobayashi, J. Normand, K. Raghavachari, A. Rendell, J. C. Burant, S. S. Iyengar, J. Tomasi, M. Cossi, N. Rega, J. M. Millam, M. Klene, J. E. Knox, J. B. Cross, V. Bakken, C. Adamo, J. Jaramillo, R. Gomperts, R. E. Stratmann, O. Yazyev, A. J. Austin, R. Cammi, C. Pomelli, J. W. Ochterski, R. L. Martin, K. Morokuma, V. G. Zakrzewski, G. A. Voth, P. Salvador, J. J. Dannenberg, S. Dapprich, A. D. Daniels, O. Farkas, J. B. Foresman, J. V. Ortiz, J. Cioslowski, D. J. Fox, Gaussian, Inc., Wallingford CT, 2009.
- 20. M. Suceska, *EXPLO5 version6.03*, **2014**.
- 21. V. Thottempudi, H. Gao, J. M. Shreeve, J. Am. Chem. Soc., 2011, 133, 6464–6471.
- 22. V. D. Ghule, J. Phys. Chem. A, 2012, 116, 9391–9397.
- 23. (a)V. Thottempudi, P. Yin, J. Zhang, D. A. Parrish and J. M. Shreeve, *Chem.–Eur. J.*, **2014**, 20, 542; (b) R. Meyer, J. Kçhler, A. Homburg, *Explosives*, 5th ed., Wiley-VCH, Weinheim, **2002**, p.235.
- 24. (a) C. K. Lowe-Ma, R. A. Nissan, W. S. Wilson, *Navel weapons center*, **1987**, AD-A197439; (b) Z. Yang, Y. Liu, D. Liu, L. Yan, J. Chen, *J. Hazard. Mater.*, **2010**, *177*, 938–943.
- 25. (a) P. Politzer, J. S. Murray, J. M. Seminario, P. Lane, M. E. Grice and M. C. Concha, *J. Mol. Struct.*, **2001**, *573*, 1–10; (b) B. M. Rice and J. J. Hare, *J. Phys. Chem.*, **2002**, *106*, 1770–1783; (c) B. M. Rice, *Adv. Ser. Phys. Chem.*, **2005**, *16*, 335–367.
- 26. J. Zhang and J. M. Shreeve, J. Am. Chem. Soc., **2014**, 136, 4437–4445.
- 27. (a) Spackman, M. A.; McKinnon, J. J. Fingerprinting intermolecular interactions in molecular crystals. *CrystEngComm.*, **2002**, *4*, 378-392; (b) Spackman, M. A.; Jayatilake, D. Hirshfeld surface analysis. *CrystEngComm.*, **2009**, *11*, 19-32; (c) Zhang, C.; Xue, X.; Cao, Y.; Zhou, Y.; Li, H.; Zhou, J.; Gao, T. Intermolecular friction symbol derived from crystal

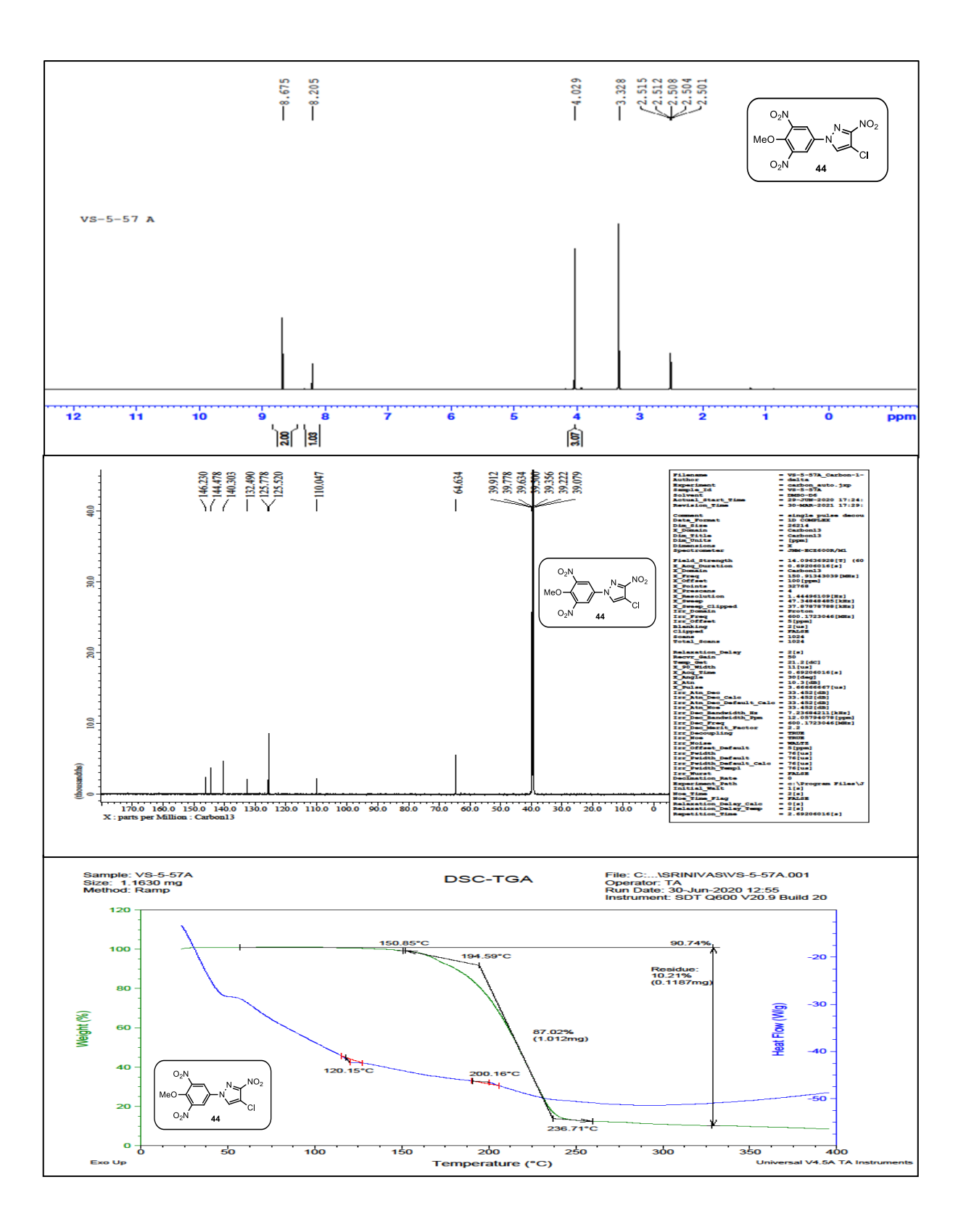
information. *CrystEngComm.*, **2013**, *15*, 6837–6844; (d) Turner, M.J.; McKinnon, J.J.; Wolff, S.K.; Grimwood, D.J.; Spackman, P.R.; Jayatilaka, D.; Spackman, M.A. Crystal Explorer 17; University of Western Australia: Pert, Australia, **2017**.

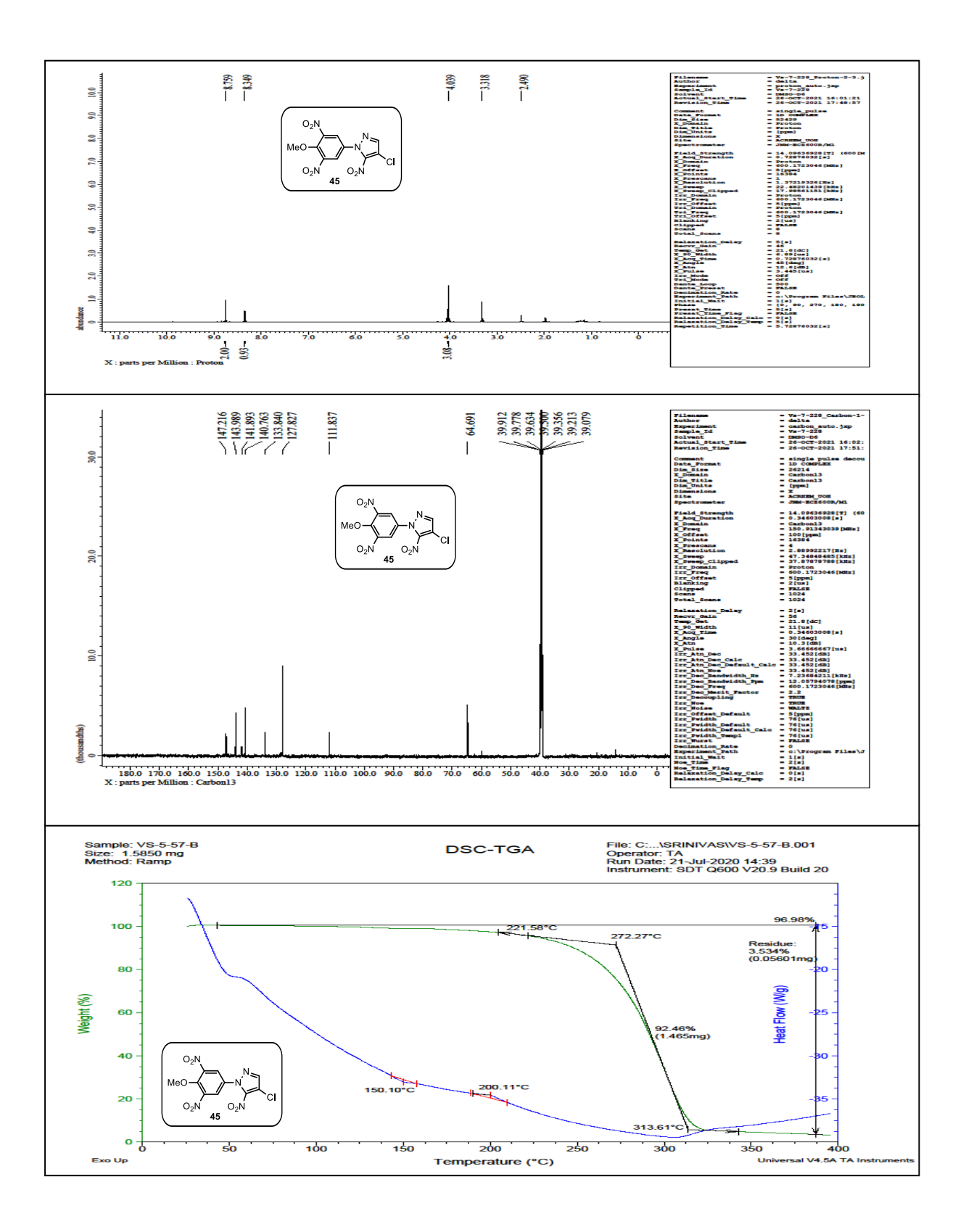
28. J. S. Murray, M. C. Concha and P. Politzer, Mol. Phys., 2009, 107, 89.

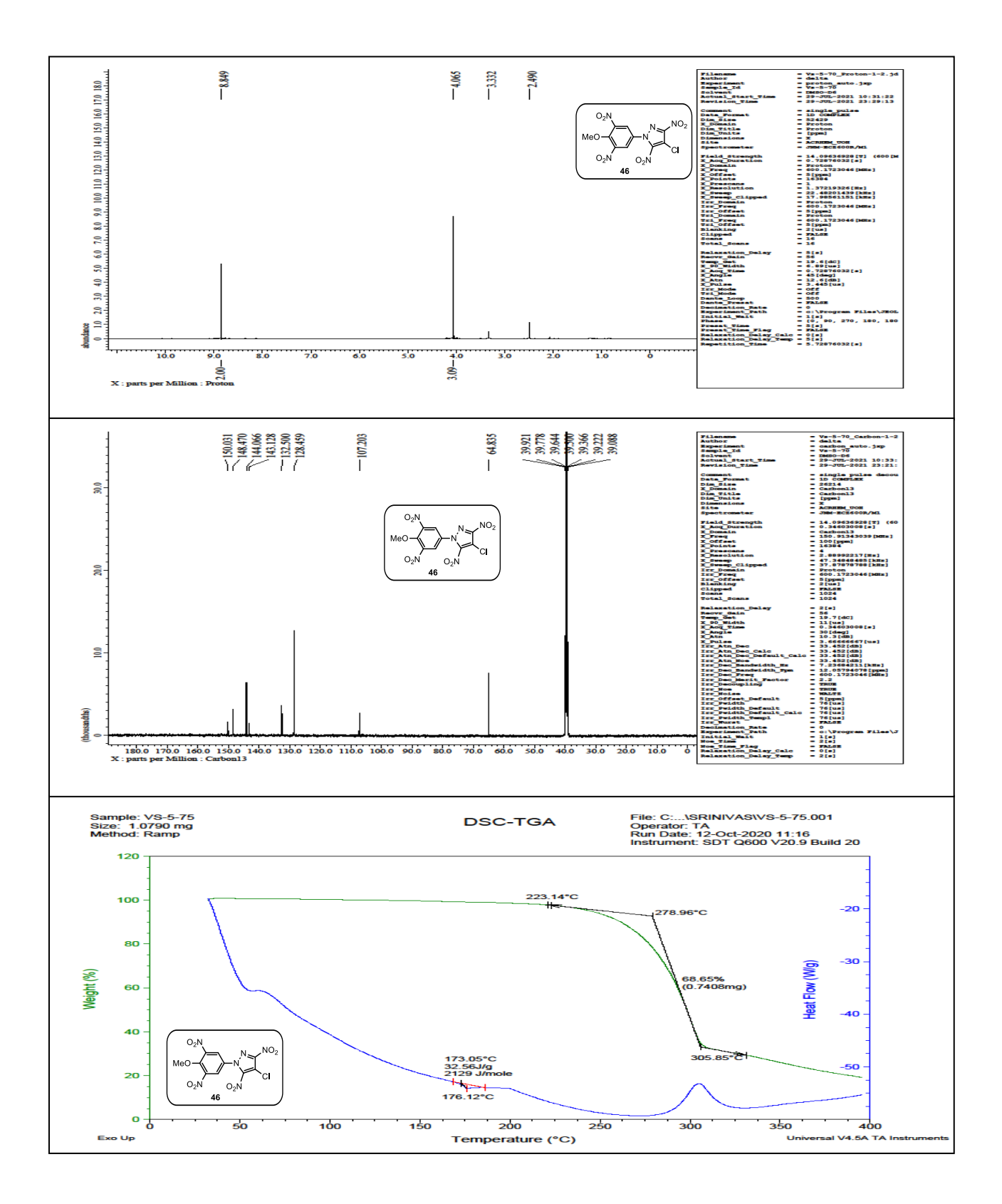
# 3.10. Spectral data

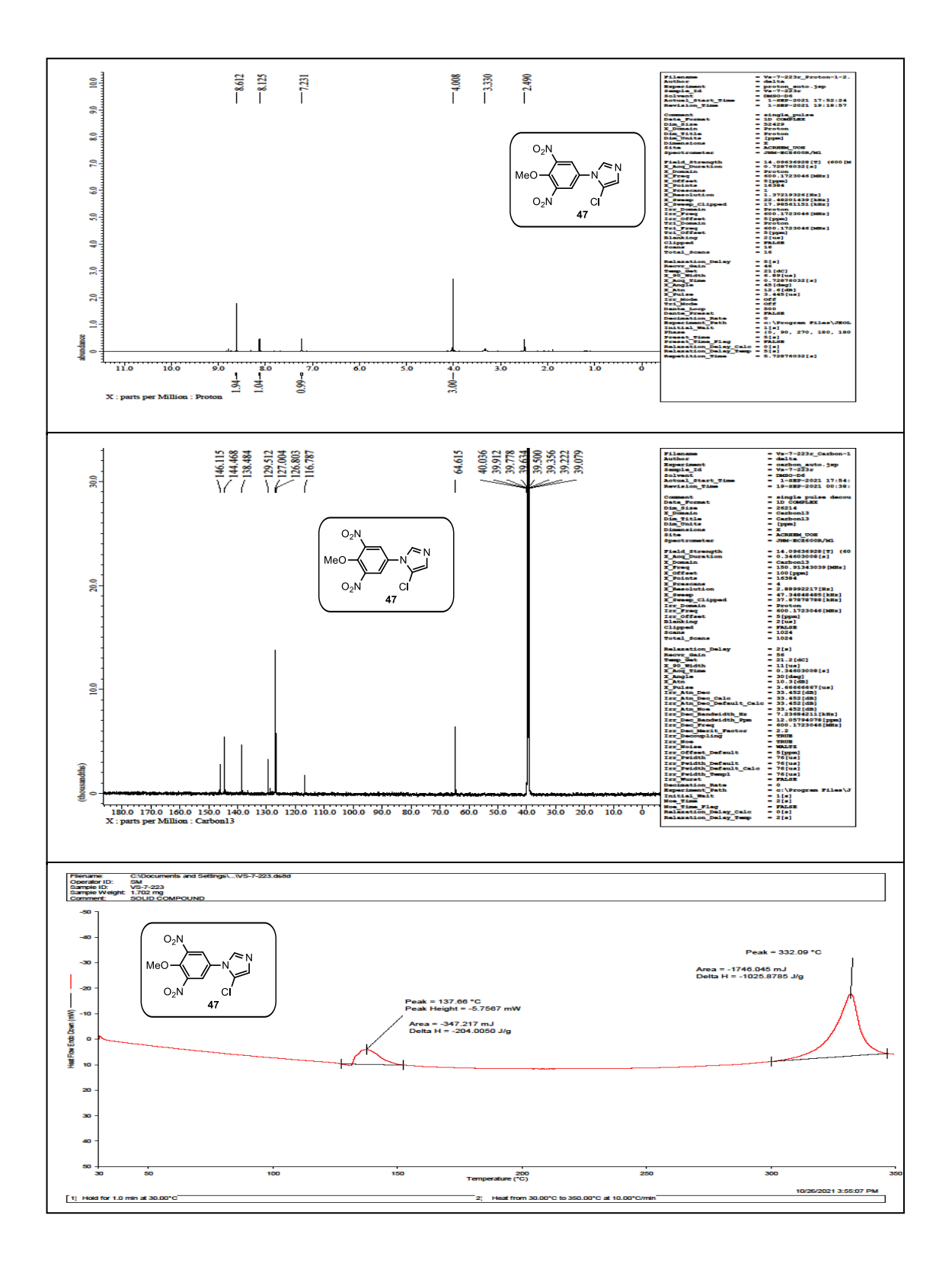


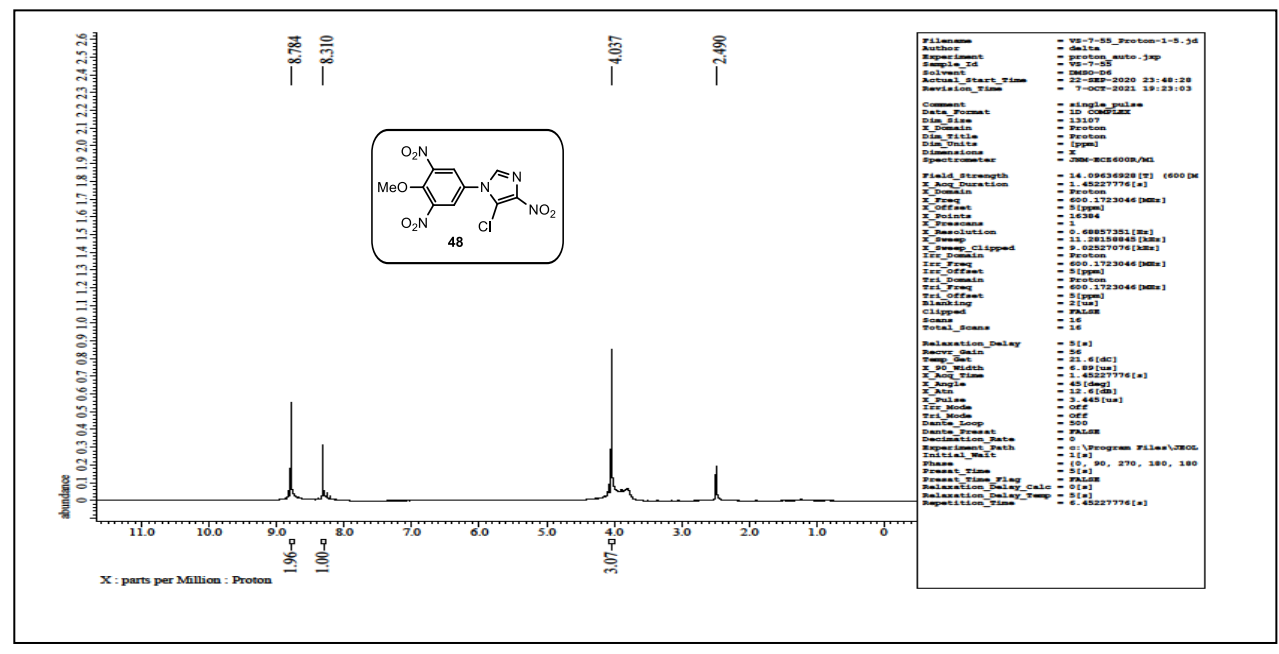


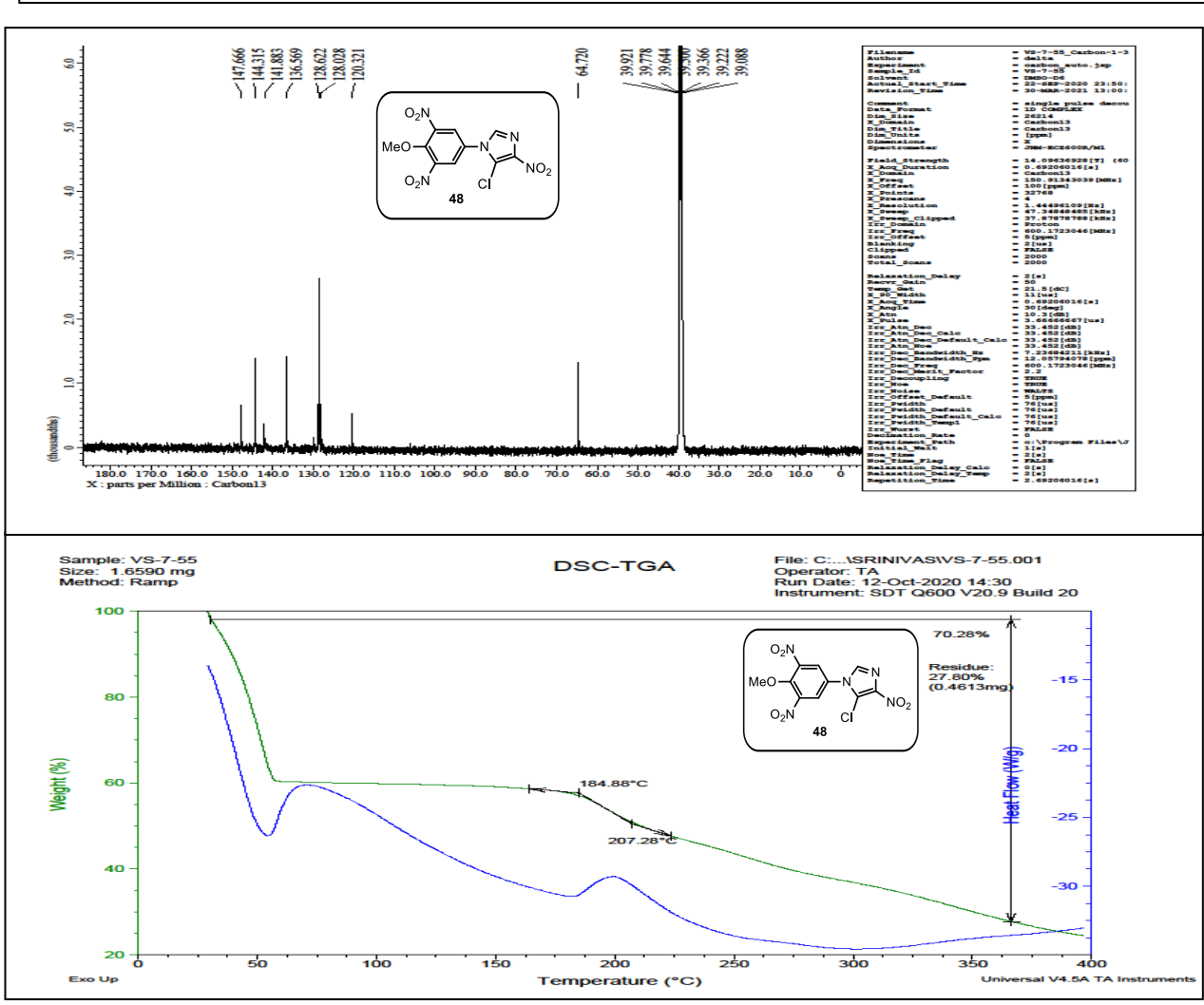


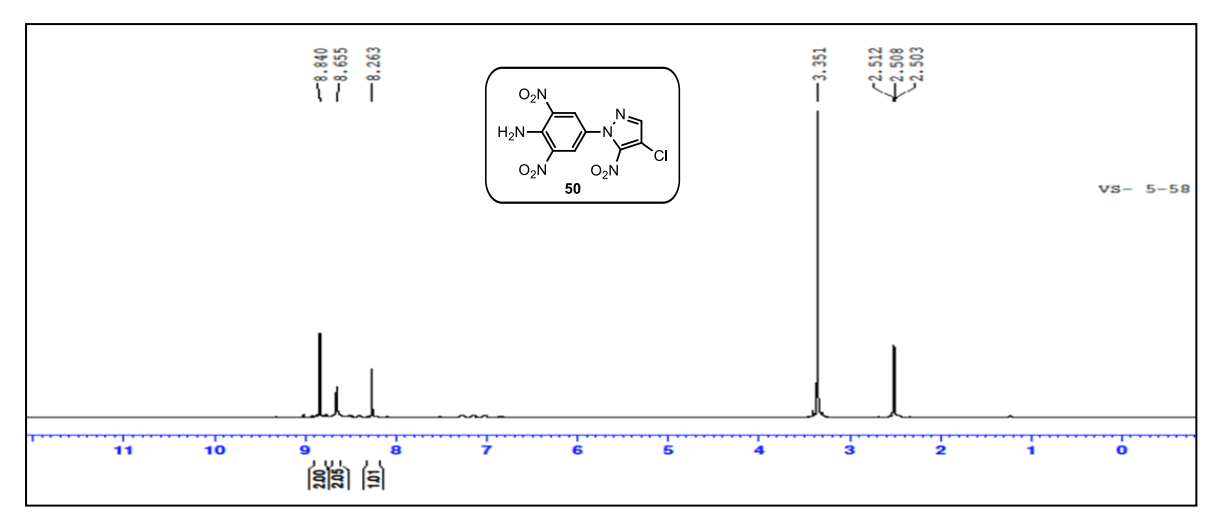


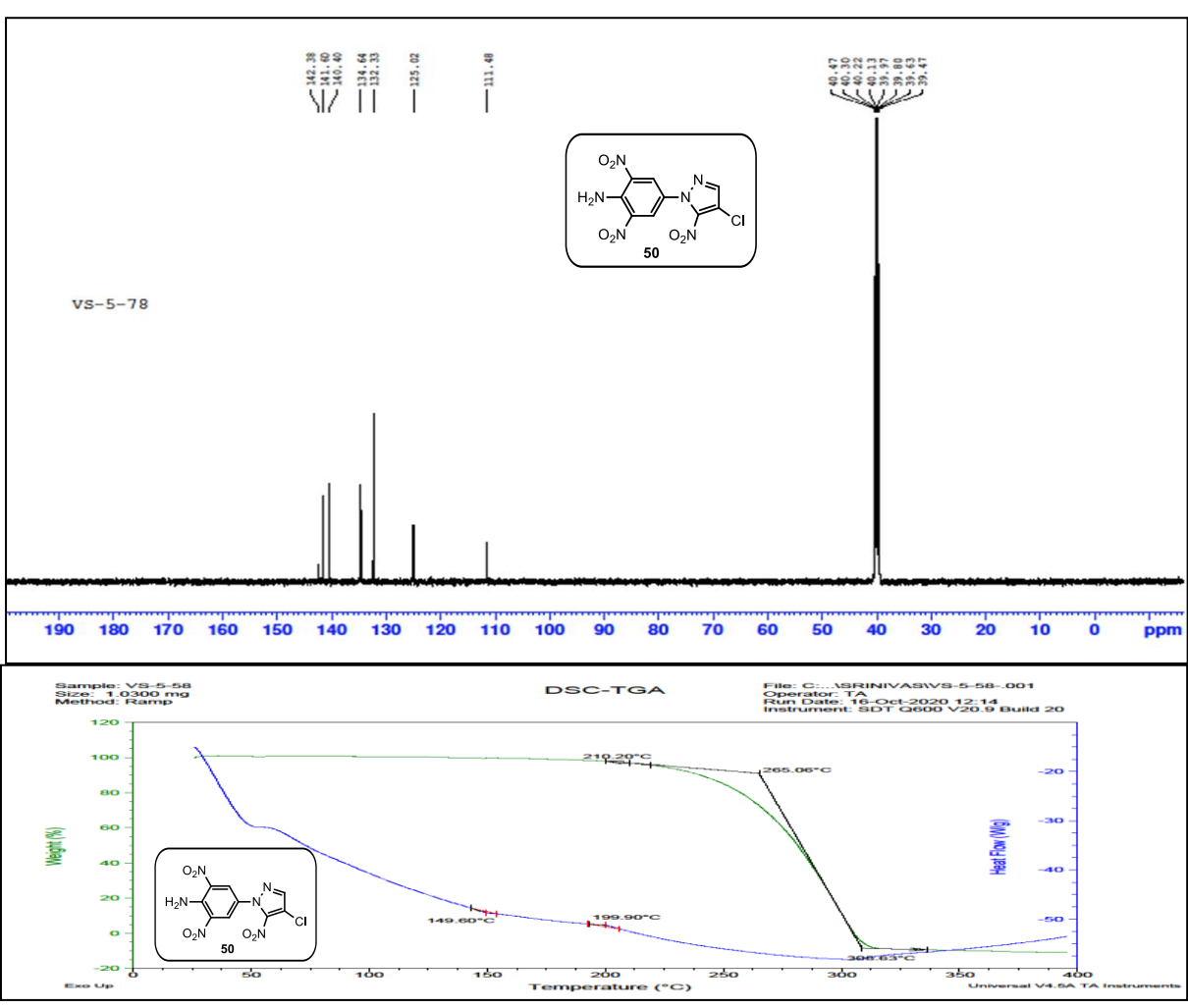


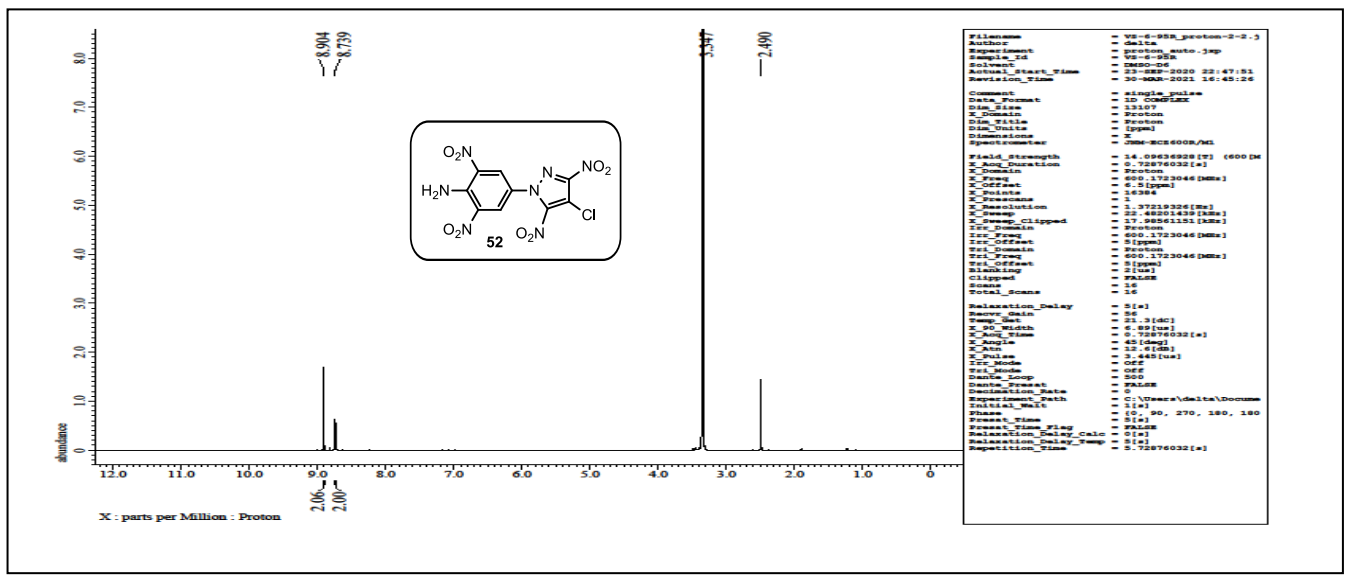


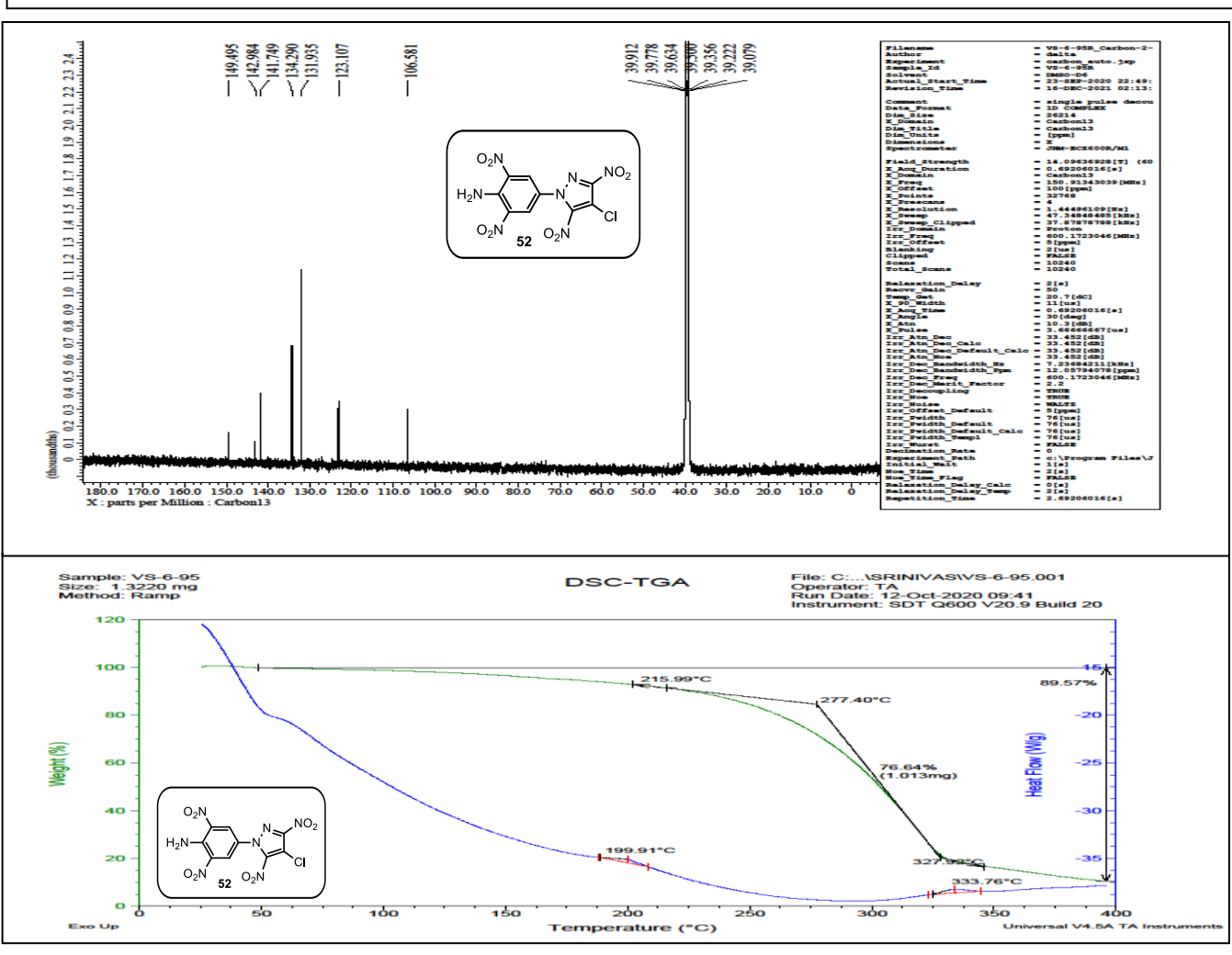


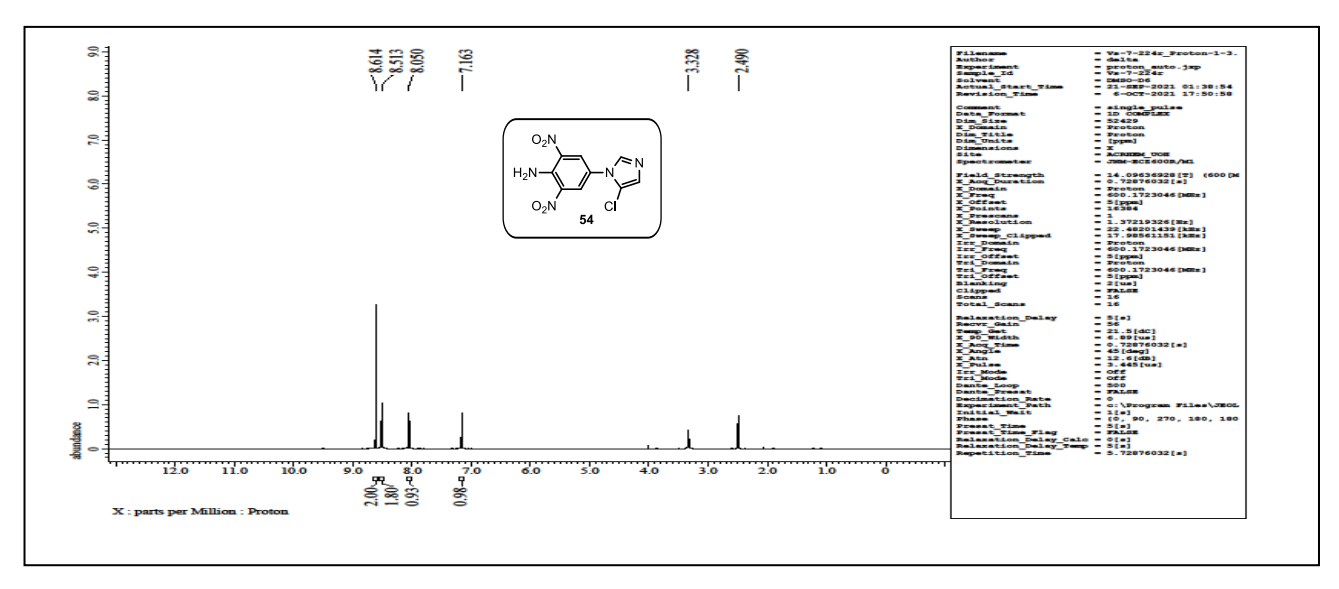


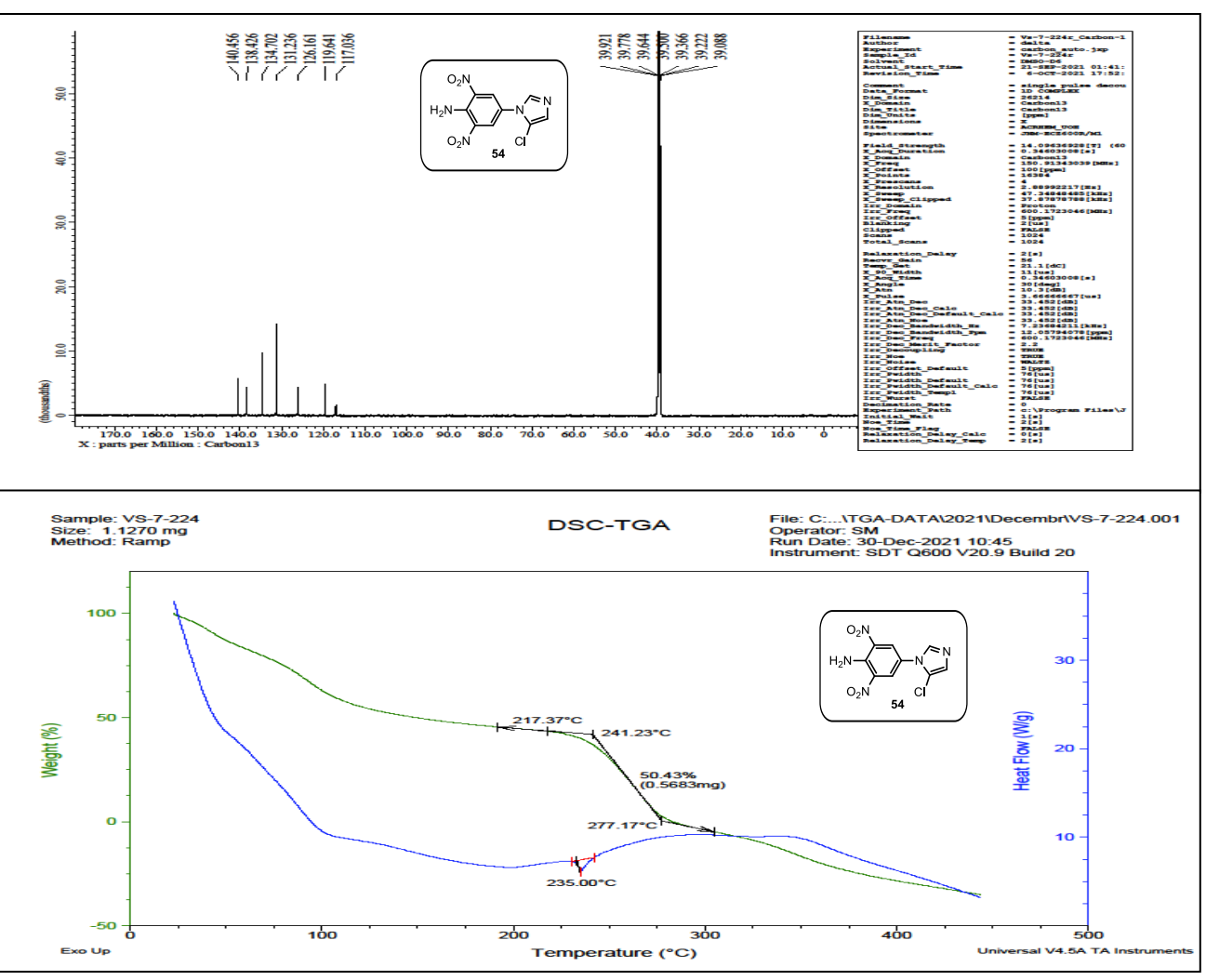


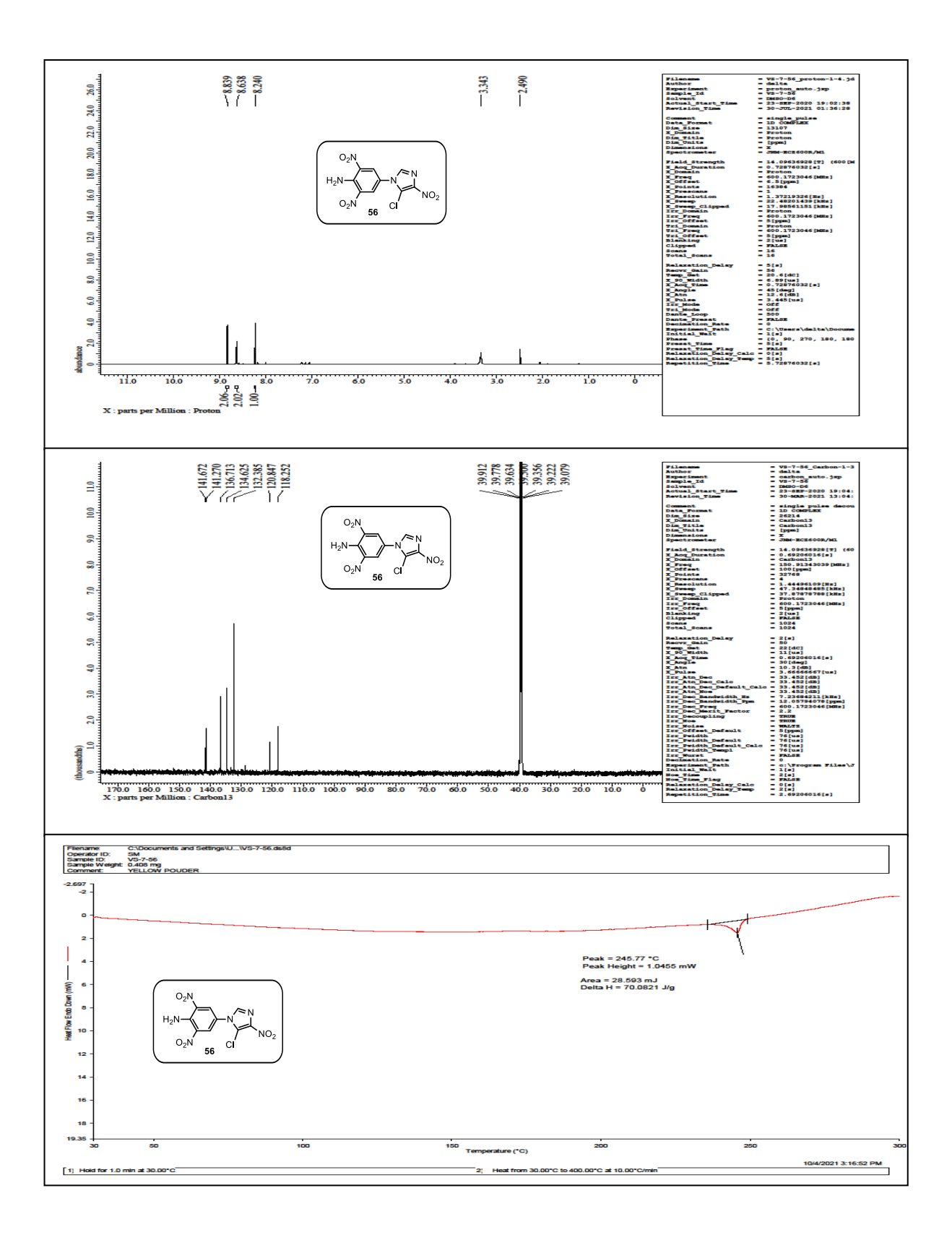


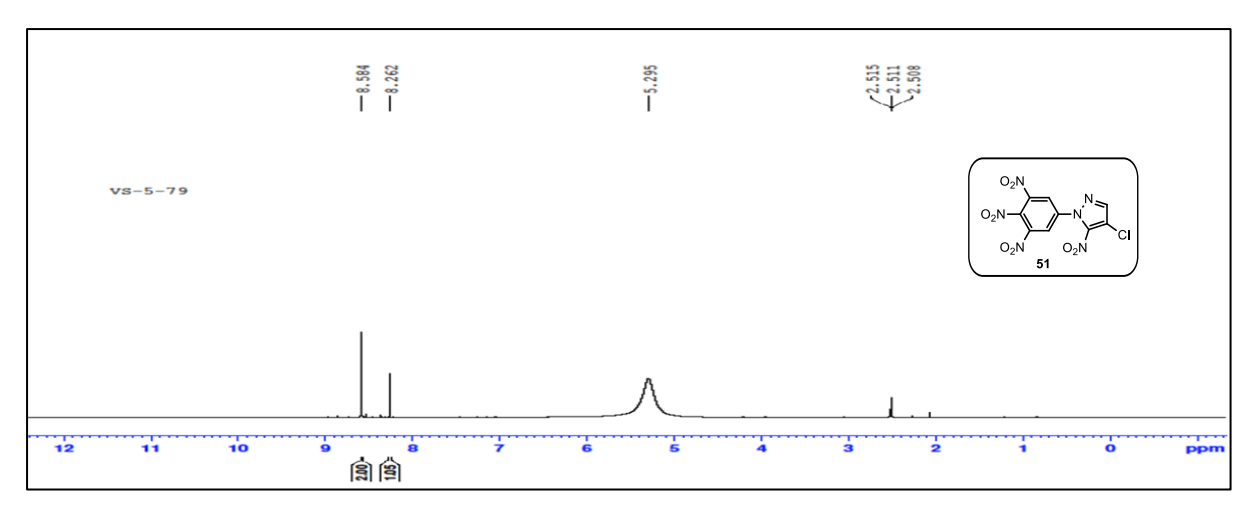


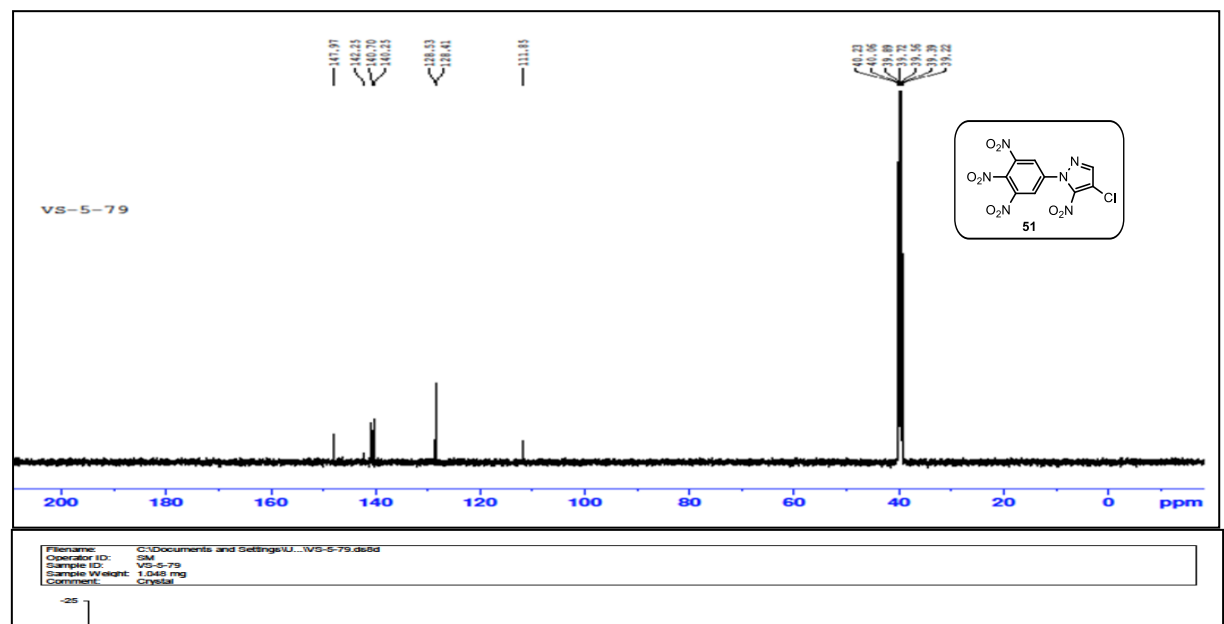


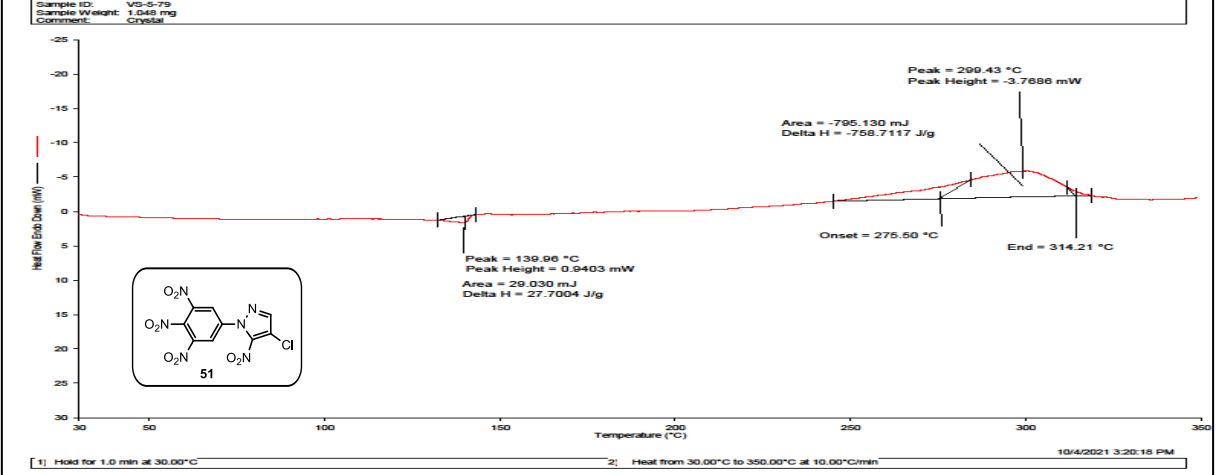


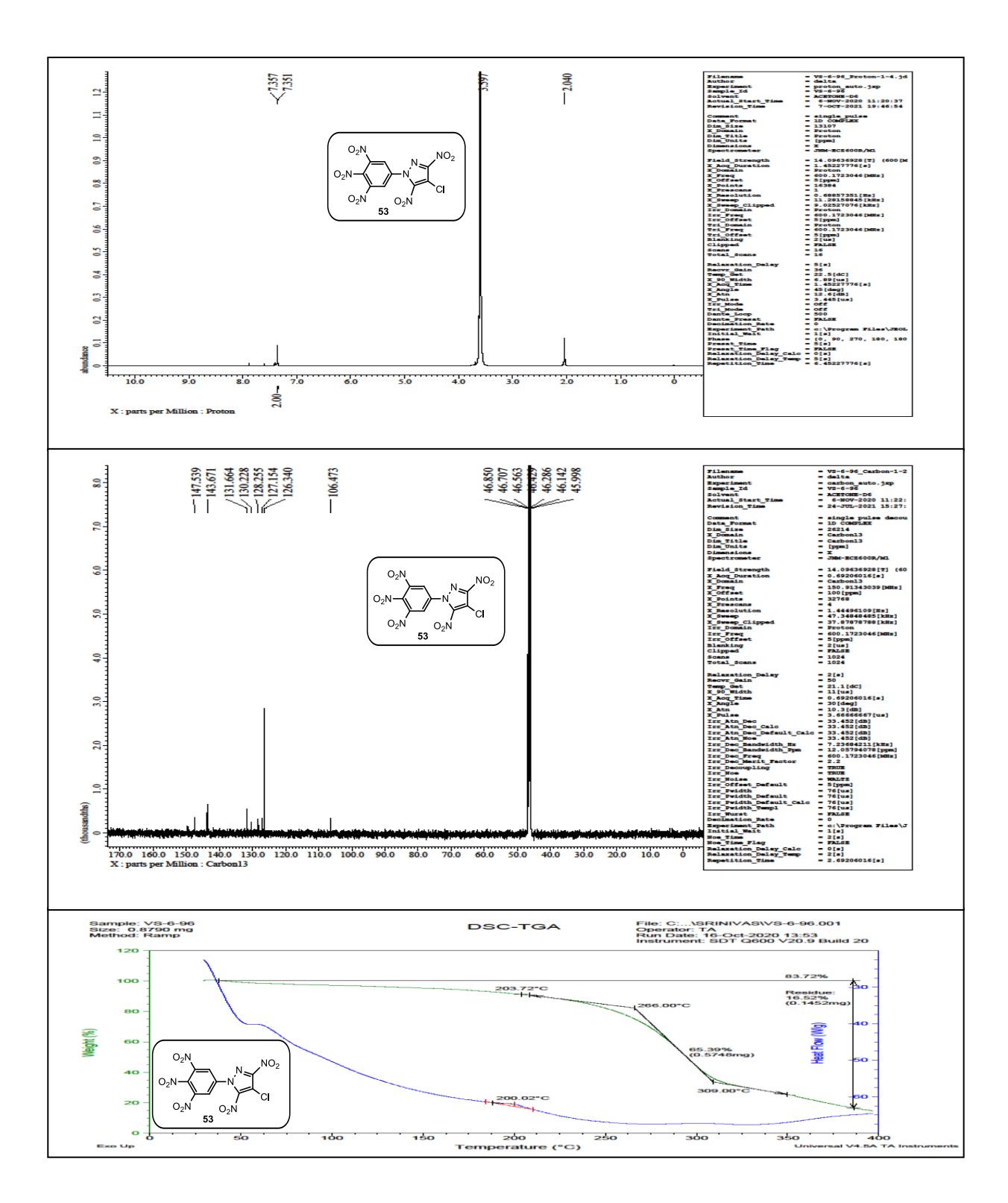


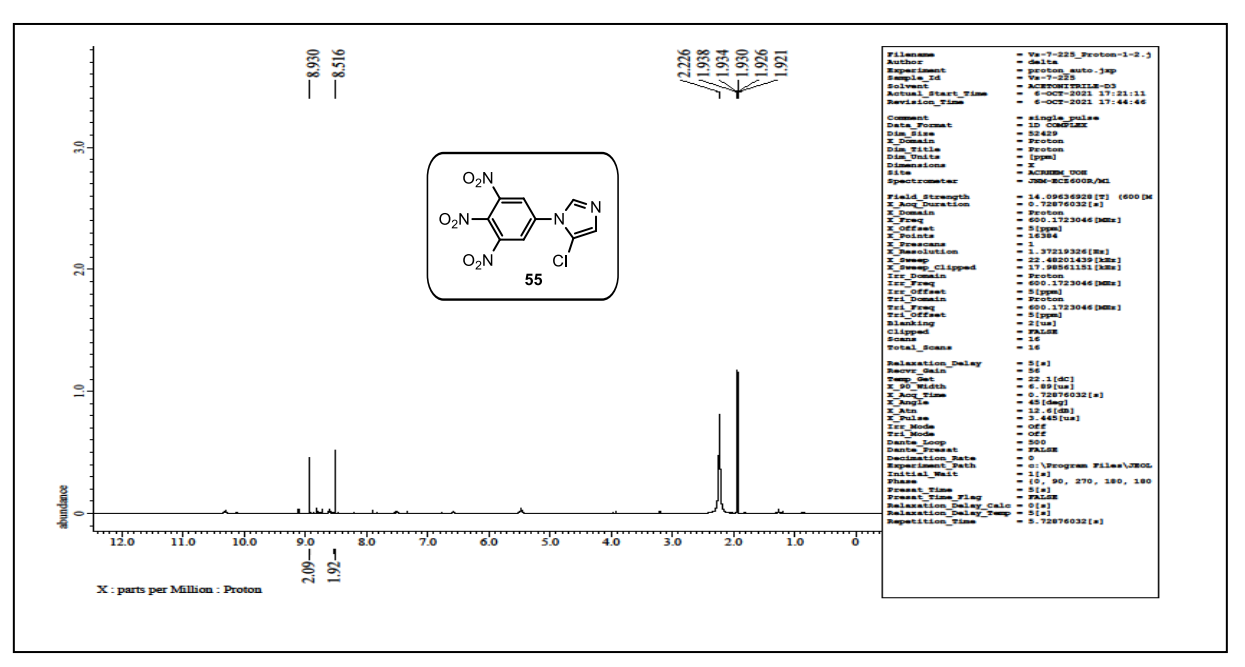


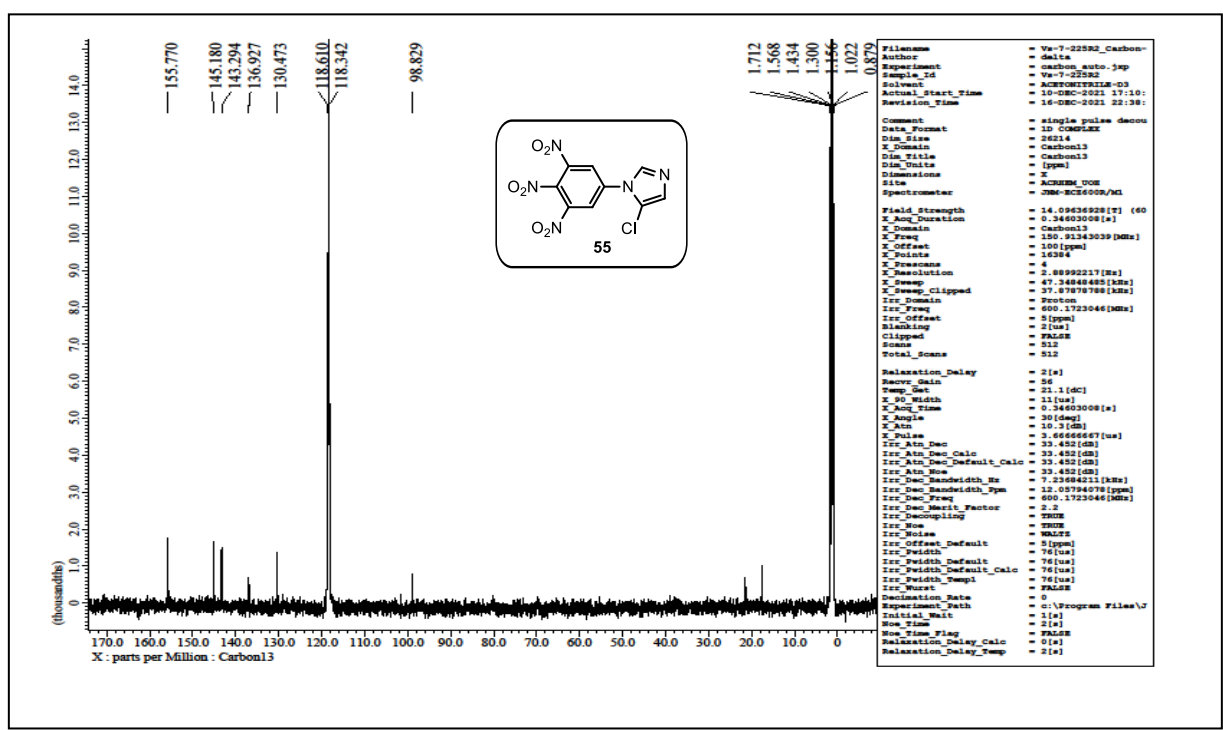


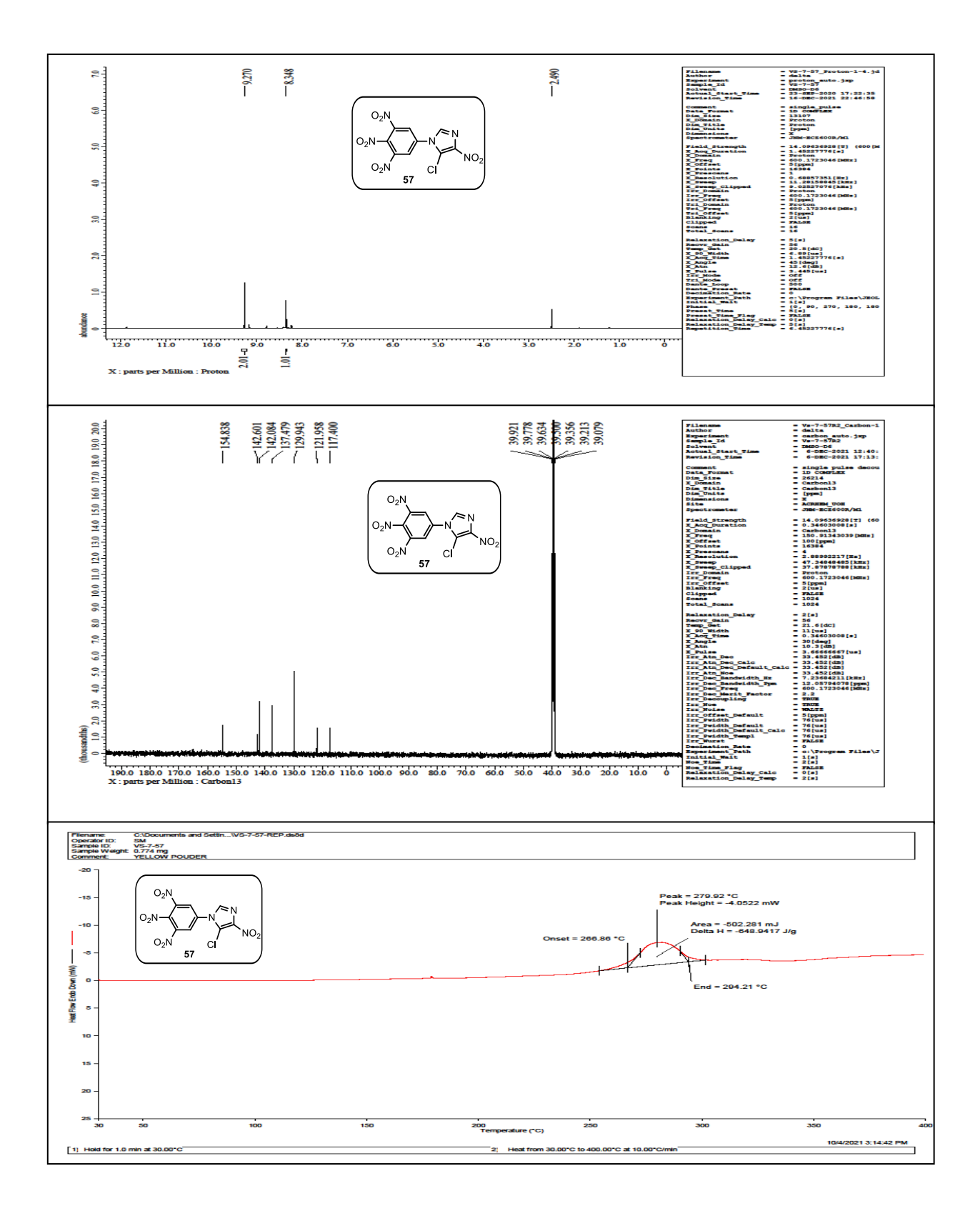


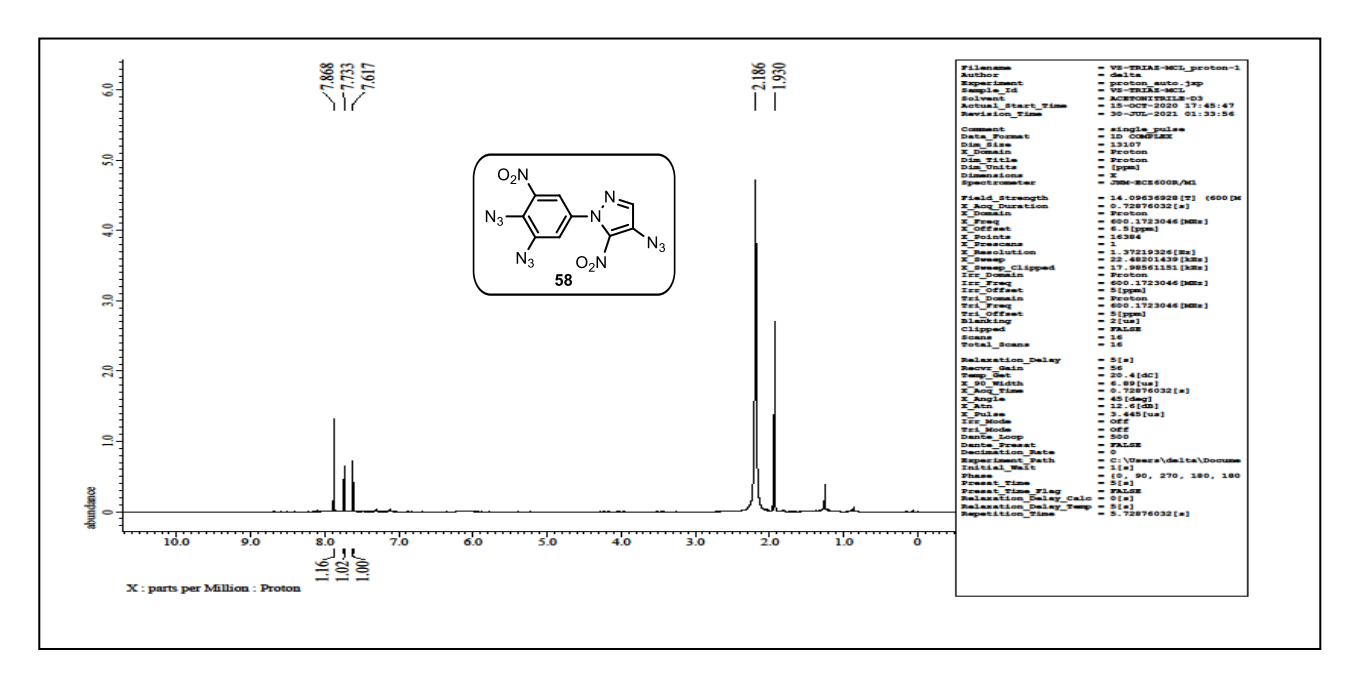


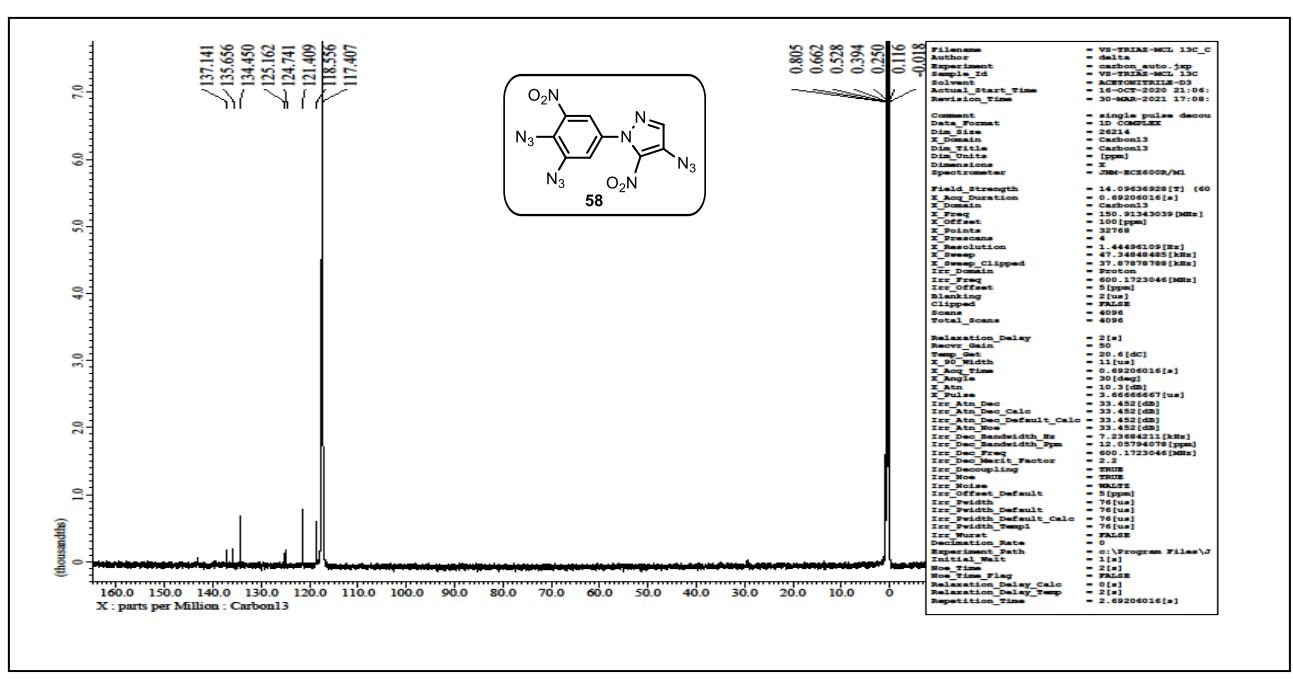


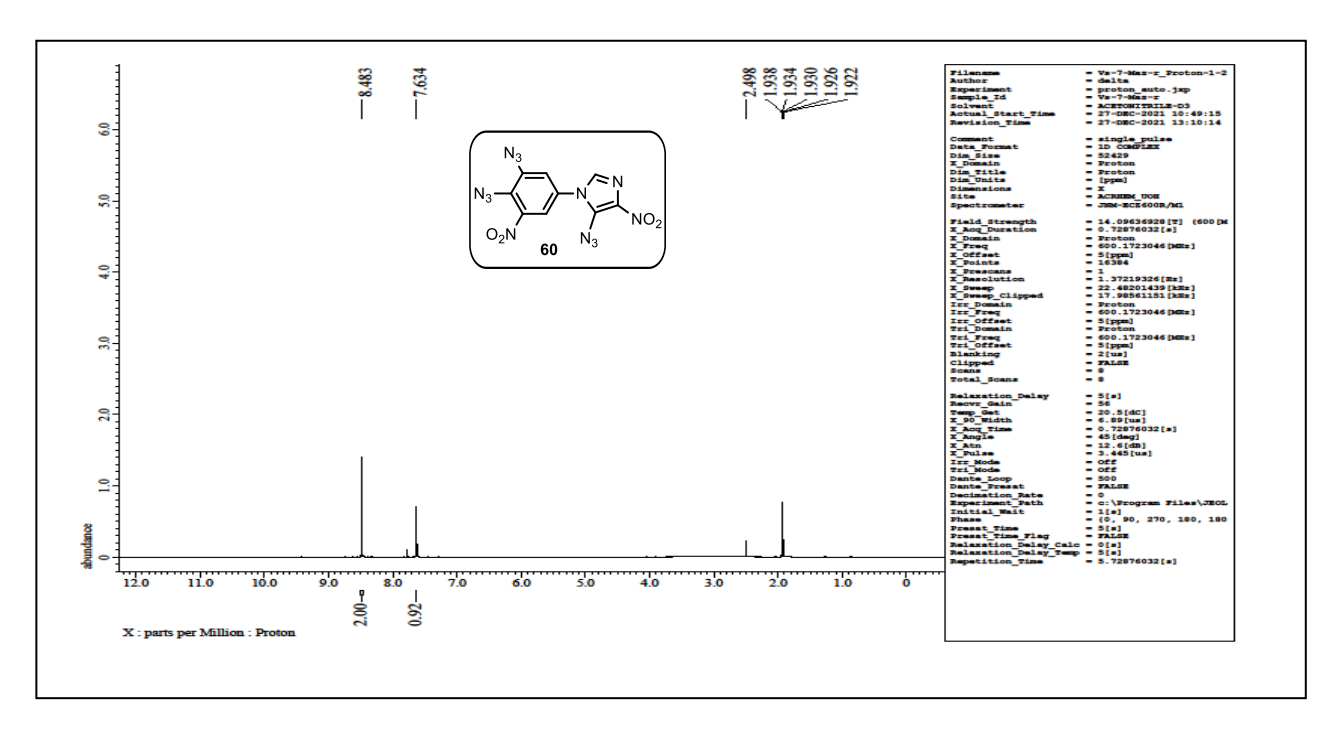


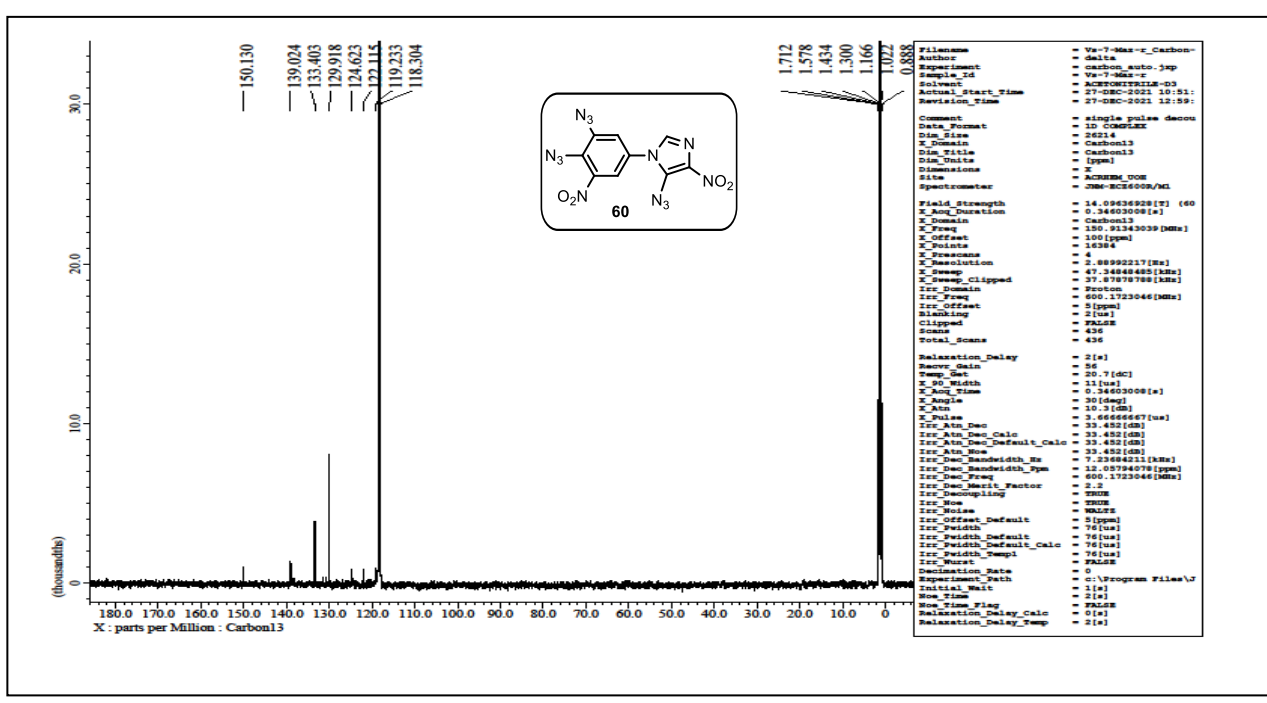












**Chapter-4** 

# Combination of 1,2,4-Oxadiazole and Nitro/Nitroamino Substituted Azoles as Energetic Derivatives

**Chapter 4** 

#### **Abstract**

Ring formation
$$\begin{array}{c}
(NH_2)_n & NH_2\\
N & NH_2
\end{array}$$

$$\begin{array}{c}
N & N \\
N & N
\end{array}$$

$$\begin{array}{c}
N & N \\
N & N
\end{array}$$

$$\begin{array}{c}
N & N \\
N & N
\end{array}$$

$$\begin{array}{c}
N & N \\
N & N
\end{array}$$

$$\begin{array}{c}
N & N \\
N & N
\end{array}$$

$$\begin{array}{c}
N & N \\
N & N
\end{array}$$

$$\begin{array}{c}
N & N \\
N & N
\end{array}$$

$$\begin{array}{c}
N & N \\
N & N
\end{array}$$

$$\begin{array}{c}
N & N \\
N & N
\end{array}$$

$$\begin{array}{c}
N & N \\
N & N
\end{array}$$

$$\begin{array}{c}
N & N \\
N & N
\end{array}$$

$$\begin{array}{c}
N & N \\
N & N
\end{array}$$

$$\begin{array}{c}
N & N \\
N & N
\end{array}$$

$$\begin{array}{c}
N & N \\
N & N
\end{array}$$

$$\begin{array}{c}
N & N \\
N & N
\end{array}$$

$$\begin{array}{c}
N & N \\
N & N
\end{array}$$

$$\begin{array}{c}
N & N \\
N & N
\end{array}$$

$$\begin{array}{c}
N & N \\
N & N
\end{array}$$

$$\begin{array}{c}
N & N \\
N & N
\end{array}$$

$$\begin{array}{c}
N & N \\
N & N
\end{array}$$

$$\begin{array}{c}
N & N \\
N & N
\end{array}$$

$$\begin{array}{c}
N & N \\
N & N
\end{array}$$

$$\begin{array}{c}
N & N \\
N & N
\end{array}$$

$$\begin{array}{c}
N & N \\
N & N
\end{array}$$

$$\begin{array}{c}
N & N \\
N & N
\end{array}$$

$$\begin{array}{c}
N & N \\
N & N
\end{array}$$

$$\begin{array}{c}
N & N \\
N & N
\end{array}$$

$$\begin{array}{c}
N & N \\
N & N
\end{array}$$

$$\begin{array}{c}
N & N \\
N & N
\end{array}$$

$$\begin{array}{c}
N & N \\
N & N
\end{array}$$

$$\begin{array}{c}
N & N \\
N & N
\end{array}$$

$$\begin{array}{c}
N & N \\
N & N
\end{array}$$

$$\begin{array}{c}
N & N \\
N & N
\end{array}$$

$$\begin{array}{c}
N & N \\
N & N
\end{array}$$

$$\begin{array}{c}
N & N \\
N & N
\end{array}$$

$$\begin{array}{c}
N & N \\
N & N
\end{array}$$

$$\begin{array}{c}
N & N \\
N & N
\end{array}$$

$$\begin{array}{c}
N & N \\
N & N
\end{array}$$

$$\begin{array}{c}
N & N \\
N & N
\end{array}$$

$$\begin{array}{c}
N & N \\
N & N
\end{array}$$

$$\begin{array}{c}
N & N \\
N & N
\end{array}$$

$$\begin{array}{c}
N & N \\
N & N
\end{array}$$

$$\begin{array}{c}
N & N \\
N & N
\end{array}$$

$$\begin{array}{c}
N & N \\
N & N
\end{array}$$

$$\begin{array}{c}
N & N \\
N & N
\end{array}$$

$$\begin{array}{c}
N & N \\
N & N
\end{array}$$

$$\begin{array}{c}
N & N \\
N & N
\end{array}$$

$$\begin{array}{c}
N & N \\
N & N
\end{array}$$

$$\begin{array}{c}
N & N \\
N & N
\end{array}$$

$$\begin{array}{c}
N & N \\
N & N
\end{array}$$

$$\begin{array}{c}
N & N \\
N & N
\end{array}$$

$$\begin{array}{c}
N & N \\
N & N
\end{array}$$

$$\begin{array}{c}
N & N \\
N & N
\end{array}$$

$$\begin{array}{c}
N & N \\
N & N
\end{array}$$

$$\begin{array}{c}
N & N \\
N & N
\end{array}$$

$$\begin{array}{c}
N & N \\
N & N
\end{array}$$

$$\begin{array}{c}
N & N \\
N & N
\end{array}$$

$$\begin{array}{c}
N & N \\
N & N
\end{array}$$

$$\begin{array}{c}
N & N \\
N & N
\end{array}$$

$$\begin{array}{c}
N & N \\
N & N
\end{array}$$

$$\begin{array}{c}
N & N \\
N & N
\end{array}$$

$$\begin{array}{c}
N & N \\
N & N
\end{array}$$

$$\begin{array}{c}
N & N \\
N & N
\end{array}$$

$$\begin{array}{c}
N & N \\
N & N
\end{array}$$

$$\begin{array}{c}
N & N \\
N & N
\end{array}$$

$$\begin{array}{c}
N & N \\
N & N
\end{array}$$

$$\begin{array}{c}
N & N \\
N & N
\end{array}$$

$$\begin{array}{c}
N & N \\
N & N
\end{array}$$

$$\begin{array}{c}
N & N \\
N & N
\end{array}$$

$$\begin{array}{c}
N & N \\
N & N
\end{array}$$

$$\begin{array}{c}
N & N \\
N & N
\end{array}$$

$$\begin{array}{c}
N & N \\
N & N
\end{array}$$

$$\begin{array}{c}
N & N \\
N & N
\end{array}$$

$$\begin{array}{c}
N & N \\
N & N
\end{array}$$

$$\begin{array}{c}
N & N \\
N & N$$

$$\begin{array}{c}
N & N \\
N & N
\end{array}$$

$$\begin{array}{c}
N & N \\
N & N
\end{array}$$

$$\begin{array}{c}
N & N \\
N & N$$

$$\begin{array}{c}
N & N \\
N & N$$

$$\begin{array}{c}
N & N \\
N & N$$

Nitrogen and oxygen rich azole-based compounds with mono-1,2,4-oxadiazole and bis-1,2,4-oxadiazole motifs are synthesized. The Sc(OTf)<sub>3</sub> mediated reaction of amidoximes with trimethyl orthoformate has led to oxadiazoles. The five-membered azole backbone with –NO<sub>2</sub> and –CH(NO<sub>2</sub>)<sub>2</sub> and –C(NO<sub>2</sub>)<sub>3</sub> groups makes the molecule energetic. The compounds have been fully characterized by NMR, IR, HRMS, and TGA–DSC measurements. Molecular topology of some compounds has been established by X-ray diffraction analysis. In most cases, synthesized compounds displayed good oxygen balance, high positive heats of formation, good performance with detonation pressure or velocity and good thermal stability. The Hirshfeld surface analysis shed insights of molecules sensitivity.

#### 4.1. Introduction

Oxadiazoles are five-membered unsaturated aromatic heterocyclic compounds consisting two carbon atoms, two nitrogen atoms, and one oxygen atom. In broad view, 1,2,5-oxadiazole, 1,2,3-oxadiazole, 1,2,4-oxadiazole, and 1,3,4-oxadiazole are four isomers of oxadiazole scaffolds (**Figure 4.1.1**).

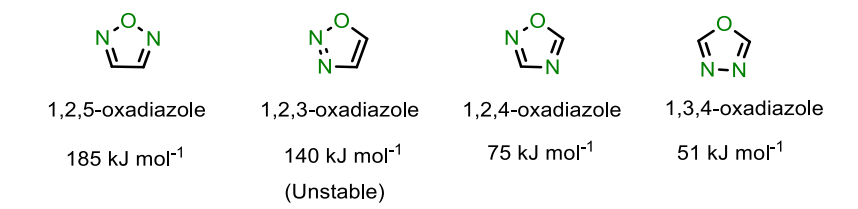


Figure 4.1.1. Four types of oxadiazole isomers

Efforts to synthesize new energetic materials are of considerable interest in both civilian and military fields. In recent years, attempts to develop oxadiazoles as a new class of energetic materials have been received considerable attention.<sup>1</sup> 1,2,5-Oxadiazole (furazan) has been well exploited and has potential application in both propellant and explosive formulations.<sup>2</sup> Among them, 1,2,4-oxadiazole isomer show special interest in the design of biologically active compounds as well as material community.<sup>3</sup>

Recent decades have seen a growing interest in nitrogen-rich energetic compounds, due to their high nitrogen content, high heats of formation and good oxygen balance a result of large number of N-N, C-N, and N-O bonds present in the backbones. Prior to this, Klapötke et. al revealed that the combination of C–C bond bridged 1,2,4-oxadiazoles with energetic moieties like gem-dinitro, trinitromethyl, and fluoro dinitromethyl groups exhibit high detonation performance, good oxygen balance, and low sensitivity to impact.<sup>4</sup> In 2018, Johnson et. al synthesized bis-(1,2,4-oxadiazole)bis(methylene)dinitrate high density molecule that show detonation pressure 50% higher than that of TNT, high decomposition temperature, and decreased sensitivity to impact and friction compared with RDX.<sup>5</sup> A combination of 1,2,4oxadiazole and 1,2,5-oxadiazole backbones with energetic groups like -ONO2 and -NHNO2 has led to a molecule with good detonation performance and high insensitivity (Zhang et. al made this in 2020).6 Taking this background into account, we report a series of new combination of nitrogen-rich azole-based five-membered heterocycles and 1,2,4-oxadiazole as nitrogen rich energetic compounds, which are synthesized from readily available cyanoazoles precursors. Herein, synthesis and characterization of these compounds have been extensively discussed.

# 4.1.1. Background of the applications of 1,2,4-Oxadiazole derivatives as energetic materials

**Figure 4.1.2.** Known molecules of 1,2,4-oxadiazole derivatives

In 2016, Shreeve and coworkers reported 3-amino-5-nitramino-1,2,4-oxadiazole (1) that contain both amino (-NH<sub>2</sub>) and nitramino (-NHNO<sub>2</sub>) group in the same molecular backone (**Scheme 4.1.1**). Initially, 3,5-diamino-1,2,4-oxadiazole (8) was synthesized utilizing known synthetic procedure. Subsequently, exposing compound 8 with ethyl chloroformate in presence of BF<sub>3</sub>.OEt<sub>2</sub> in dioxane delivered 9 (**Scheme 4.1.1**). The *N*-nitration of 9 happened when exposed to an acidic mixture of 100% HNO<sub>3</sub> and acetic anhydride to produce 10. Later, treating 10 with hydrazine hydrate in acetonitrile delivered 11, which upon acidification with hydrochloric acid afforded 1 in 81% yield. Interestingly, compound 11 showed high detonation velocity (8897 m/s) which is superior to RDX, acceptable impact sensitivity (20 J) and friction sensitivity (240 N). Moreover, compound 1 exhibited moderate detonation performance (P = 25.6 GPa, vD = 8033 m/s) and has negative heat of formation due to the presence of water molecule but is insensitive to impact (40 J) and friction (360 N).

$$\begin{array}{c} NH_2 \\ NH$$

**Scheme 4.1.1:** Synthesis of 3-amino-5-nitramino-1,2,4-oxadiazole (1)

Diaminoglyoxime **14** was synthesized from glyoxal (**12**) and glyoxime (**13**). <sup>9,10</sup> Next, cyclization of **14** with trimethyl orthoformate gave 1,2,4-oxadiazole-3-carboxy amidoxime (**15**). Chlorination of **15** with sodium nitrite in diluted hydrochloric acid formed 1,2,4-

oxadiazole-3-chloroxime (**16**). Later, nitration of **16** using mixture of 100% HNO<sub>3</sub>/TFAA in CHCl<sub>3</sub>, subsequently treating with KI in methanol provided potassium salt of 3-dinitromethyl-1,2,4-oxadiazole (**18**). Finally, acidification of **18** with diluted hydrochloric acid delivered gem-dinitromethyl 1,2,4-oxadiazole **2** (**Scheme 4.1.2**). The compound **2** exhibits moderate decomposition temperature 165 °C and is highly sensitive to impact (4 J) and friction (84 N). The compound **2** exhibits density 1.85 g/cm<sup>3</sup> and also showed good detonation performance (P = 32.3 GPa, vD = 8527 m/s) comparable to RDX.

**Scheme 4.1.2:** Synthesis of 3-(dinitromethyl)-1,2,4-oxadizole (2)

The synthesis of bis-hydroxylammonium 5.5'-dinitro-3.3' bis(1.2.4-oxadiazole) **3** as an ionic CHNO explosive was reported by Klapötke *et. al* in 2014 (**Scheme 4.1.3**). The 3.3'-bis(1.2.4-oxadiazole)-5.5'-diacetic acid diethyl ester (**19**) was at first synthesized from diaminoglyoxime (**14**) with malonic acid diethyl ester. Later, treating the compound **19** with conc. sulfuric acid and excess amount of fuming nitric acid delivered bis-gem dinitro-(1.2.4-oxadiaole) **20**. Further decarboxylation of **20** by using aqueous ammonia in methanol provided ammonium salt **21** (97% yield) with density  $1.90 \text{ g/cm}^3$ , good detonation velocity (8618 m/s), decomposition temperature ( $1.90 \text{ g/cm}^3$ ). Finally, metathesis reaction of **21** with silver nitrate forms the silver salt **22**, which underwent another metathesis with hydroxylammonium hydrochloride to obtain bis-hydroxylammonium 1.5.5'-dinitro-1.5.

**Scheme 4.1.3:** Synthesis of bis-hydroxylammonium 5,5'-dinitromethyl-3,3'-bis(1,2,4-oxadiazolate) (3)

Following the known procedure, 3-amino-4-amidoximinofurazan (AAOF) **23** was at first synthesized.<sup>13</sup> The reaction of AAOF **23** with cyanogen bromide in ethanol delivered diamino product **24**. Later, nitration of **24** using fuming nitric acid at -5 °C gave dinitramino compound, which was extracted from diethyl ether. Gaseous ammonia was bubbled into the organic layer to yield the yellow ammonium salt **25** as precipitate. The corresponding silver salt **26** was obtained by treating **25** with silver nitrate, which then undergoes metathesis reaction with aqueous hydroxyl ammonium hydrochloride to obtain **4** (**Scheme 4.1.4**).<sup>14</sup> Compound **4** has a high density (1.85 g/cm<sup>3</sup>), great detonation pressure (37.3 GPa), and high velocity of detonation (9046.2 m/s), which is far superior to standard explosives such as TNT and RDX. Moreover, the compound **4** showcased perfect oxygen balance, good thermal stability (T<sub>d</sub> = 218 °C), and acceptable sensitivity (IS = 16 J, FS = 160 N).

**Scheme 4.1.4:** Synthesis of dihydroxylammonium 3-nitroamino-4-(5-nitroamino-1,2,4-oxadiazol-3-yl)furazan (4)

Huang *et al.* revealed the synthesis of 1,2,4-oxadizole rings **28** from the reaction of dihydroxyimino-malonic acid **27** with trichloroacetic anhydride. Subsequently, ammonolysis of **28** with excess quantity of ammonia bubbled in methanol gave diamino product **29**.

Further nitration of **29** by the widely used N<sub>2</sub>O<sub>5</sub>/CHCl<sub>3</sub> system delivered **5** (71% yield) in high purity (**Scheme 4.1.5**). The compound **5** has acceptable thermal stability ( $T_d = 152$  °C) and is sensitive to impact (5 J) and friction (160 N). The detonation values of **5** (D = 1.74 g/cm<sup>3</sup>, P = 26.4 GPa, vD = 7787 m/s) were higher than that of TNT (D = 1.65 g/cm<sup>3</sup>, P = 21.3 GPa, vD = 7303 m/s).

**Scheme 4.1.5:** Synthesis of N,N'-(methylenebis(1,2,4-oxadiazole-3,5-diyl)dinitramide (5) In 2014, Shreeve *et al.* demonstrated the synthesis of diamino-1,2,4-oxadiazole **8** from sodium dicyanamide with hydroxylamine in ethanol solution. Next, reaction of **8** with potassium permanganate in hydrochloric acid led to diazo compound **30**. Nitration of **30** with nitric acid in acetic anhydride produced **6** (**Scheme 4.1.6**). The decomposition temperature of **30** and **6** are  $T_d = 350$  °C and 153 °C, respectively. These compounds are also insensitive to impact (>40 J), making them less sensitive than TNT and RDX. In 2016, the same group attempted nitration of **30** when exposed to 100% HNO<sub>3</sub> to obtain **7** (**Scheme 4.1.6**). Compound **7** showed excellent detonation properties (D = 1.90 g/cm<sup>3</sup>, P = 37.5 GPa, vD = 9190 m/s) which are higher than RDX. Unfortunately, compound **7** has moderate decomposition temperature  $T_d = 140$  °C and is highly sensitive to impact sensitivity of 2 J

and friction sensitivity of 10 N.

**Scheme 4.1.6:** Synthesis of 3,3'-azo-1,2,4-oxadiazol-5,5'-dione (**6**) and 5,5'-dinitramino-3,3'-azo-1,2,4-oxadiazole (**7**).

#### 4.2. Motivation and Design Plan

Generally, 1,2,4-oxadiazoles are useful intermediates for dye-stuffs, ionic liquids, biomedical, and polymer applications.<sup>18</sup> Recently, 1,2,4-oxadiazole heterocycles have attracted a lot of attention as potential materials for the development of safe, high-performing, and safe energy sources. An abundance of energetic N–N, C–N, and N–O bonds in the 1,2,4-oxadiazole ring contributes to good heats of formation and oxygen balance. The N- and O-rich 1,2,4-oxadiazole ring-fused energetic compounds show better detonation performance. Despite the advantages, synthesis of energetic functional groups bearing 1,2,4-oxadiazoles remains poorly explored. In this chapter, a new series of azole-based nitrogen rich heterocyclic compounds (isoxazole, pyrazole, imidazole, and triazoles) and 1,2,4-oxadiazoles with energetic functional group (*N*-nitro, gem-nitro and trinitromethyl) have been designed and synthesized. The molecules show good oxygen balance, high nitrogen content with better detonation properties, and low sensitivity. The energetic properties are higher than traditional explosives TNT and PETN. The 1,2,4-oxadiazole skeletons are accessed through cyclization of amidoxime, obtained from cyanoazoles, followed by salt formation and nitration sequence. The reaction pathways are delineated in **Scheme 4.2.1**.

**Scheme 4.2.1.** Brief sketch for the synthesis of N, O-rich oxadiazoles

#### 4.3. Results and Discussion

To begin with, the mono-azole-amidoximes 37–39 and bis-azole-amidoximes 40–42 was prepared from corresponding cyano (–CN) group substituted azoles 31–36 by reacting with hydroxylamine hydrochloride in the presence of base (50% NH<sub>2</sub>OH solution) as shown in scheme 4.3.1.<sup>19</sup> Among compounds 37–42, 37, 38, and 41 were synthesised for the first time in good yields.

Figure 4.3.1. Carbonitrile functionalized azoles 31-36

Scheme 4.3.1: Synthesis of mono-amidoximes (37–39) and bis-amidoximes (40–42)

The research work was focused in the preparation of mono/bis-1,2,4-oxadiazole scaffolds coupled with various azole motifs. Thus, scandium triflate mediated cyclization of azole-amidoximes in presence of excess trimethyl orthoformate led to respective azole-1,2,4-oxadiazoles.<sup>20</sup>

Scheme 4.3.2: Synthesis of 1,2,4-oxadiazoles (43–48) from amidoximes

At first, individually treating **37–39** with 10 mol% Sc(OTf)<sub>3</sub> delivered **43–45** in 51%, 82%, 90% yields, respectively (**Scheme 4.3.2**). To our surprise, the reactions provide access to **43–45** and **48** were highlight efficient (the respective reaction completed in 3 h), whereas 12 h was adequate to get **46** and **47**. Likewise, cyclization of bis-amidoximes **40–42** with 20 mol% Sc(OTf)<sub>3</sub> in presence of trimethyl orthoformate provided the respective bis-1,2,4-oxadiazoles **46**, **47**, and **48** in good yields (**Scheme 4.3.2**).

The successful syntheses of azole-1,2,4-oxadiazole derivatives inspired us to make new energetic molecules by incorporating nitro groups in the molecular scaffolds. In 2019, Chavez and co-workers synthesized bis-(1,2,4-oxadiazolyl) furoxan; its calculated detonation pressure was 20% higher than TNT and most importantly, the compound is insensitive to impact and friction.<sup>21</sup> We thus intend to functionalize the free *N*–H moiety of bis-(1,2,4-oxadiazolyl) triazole **48**; the synthetic viability is shown in **Scheme 4.3.3**.

At first, exposing **48** with hydrazine hydrate in methanol delivered hydrazinium salt of bis-(1,2,4-oxadiazolyl) triazolate (**49**) in 45% yield. While *N*-nitration of **48** with acetic anhydride and conc. HNO<sub>3</sub> produced **51** in 84% yield.<sup>22</sup> Later, *N*-alkylation of compound **48** with methylvinylketone (MVK) in the presence of triethylamine gave **52** in 98% yield. In general, nitration of *N*-heteroaryl substituted propanones/butanones produces energetic gemdintromethyl/trinitromethyl derivatives.<sup>23</sup> By employing this synthetic method, nitration of **52** in a acidic mixture of conc. sulfuric acid and 100% nitric acid delivered trinitro-substituted bis-(1,2,4-oxadiazolyl) triazole (**53**) in 57% yield. The molecular structure of **53** was confirmed by single crystal X-ray diffraction analysis (**Figure 4.5.1**). Interestingly, treating **53** with hydrazine hydrate formed hydrazinium salt of dinitromethanide-bis-(1,2,4-oxadiazolyl)-triazole (**54**) in 49% yield. Further acidification of compound **54** with dilute

hydrochloric acid produces gemdinitro-substituted bis-(1,2,4-oxadiazolyl) triazole (**55**) in 77% yield (**Scheme 4.3.3**).<sup>24</sup>

**Scheme 4.3.3:** Synthesis of energetic functionalized 1,2,4-oxadiazoles

## 4.4. <sup>15</sup>N NMR Spectroscopy

Compound **53** was characterized by <sup>15</sup>N NMR (**Figure 4.4.1**) and recorded in CD<sub>3</sub>CN (with respect to the chemical shift of CH<sub>3</sub>NO<sub>2</sub> as an external standard). The peaks were assigned based on GIAO NMR calculations using Gaussian 09 suite program.<sup>25</sup>

The three C–NO<sub>2</sub> functional groups (N2) bonded to triazole ring are resonated downfield appearing at  $\delta = -43$  ppm. While <sup>15</sup>N signals of 1,2,4-oxadiazole ring were detected at  $\delta = -17$  (N1) and -139 (N4). The signals (N3 and N5) of the triazole ring were observed at  $\delta = -43$ , -151 ppm, respectively (**Figure 4.4.1**).

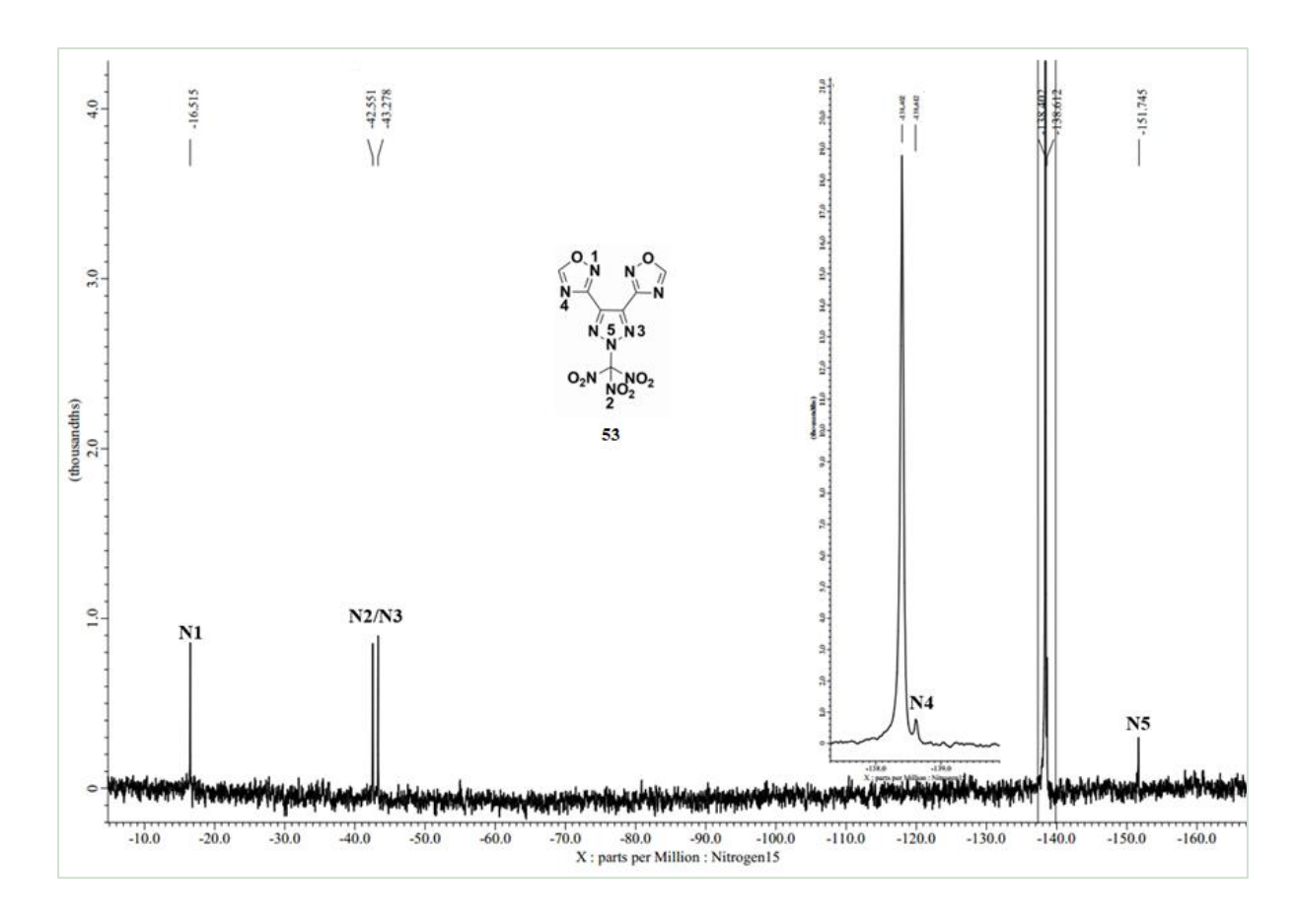
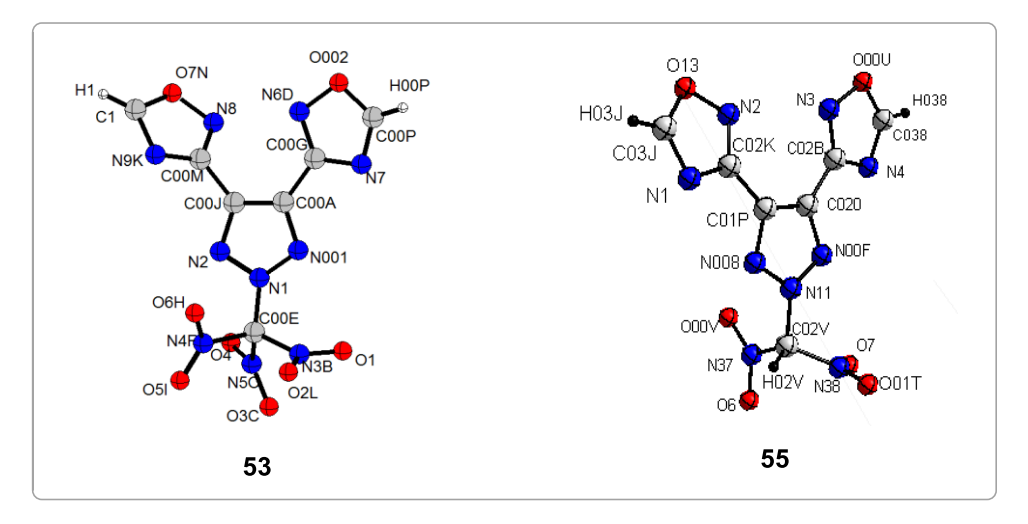


Figure 4.4.1: <sup>15</sup>N spectrum of compound 53

### 4.5. X-ray crystallography

Slow evaporation of **53** and **55** in ethyl acetate solution at room temperature gave suitable crystals for X-ray diffraction analysis (**Figure 4.5.1**). Molecular structure of **53** and **55** 



**Figure 4.5.1.** Molecular structures compounds of **53** and **55**; thermal ellipsoids (30% probability) and for clarity hydrogen atoms are labelled.

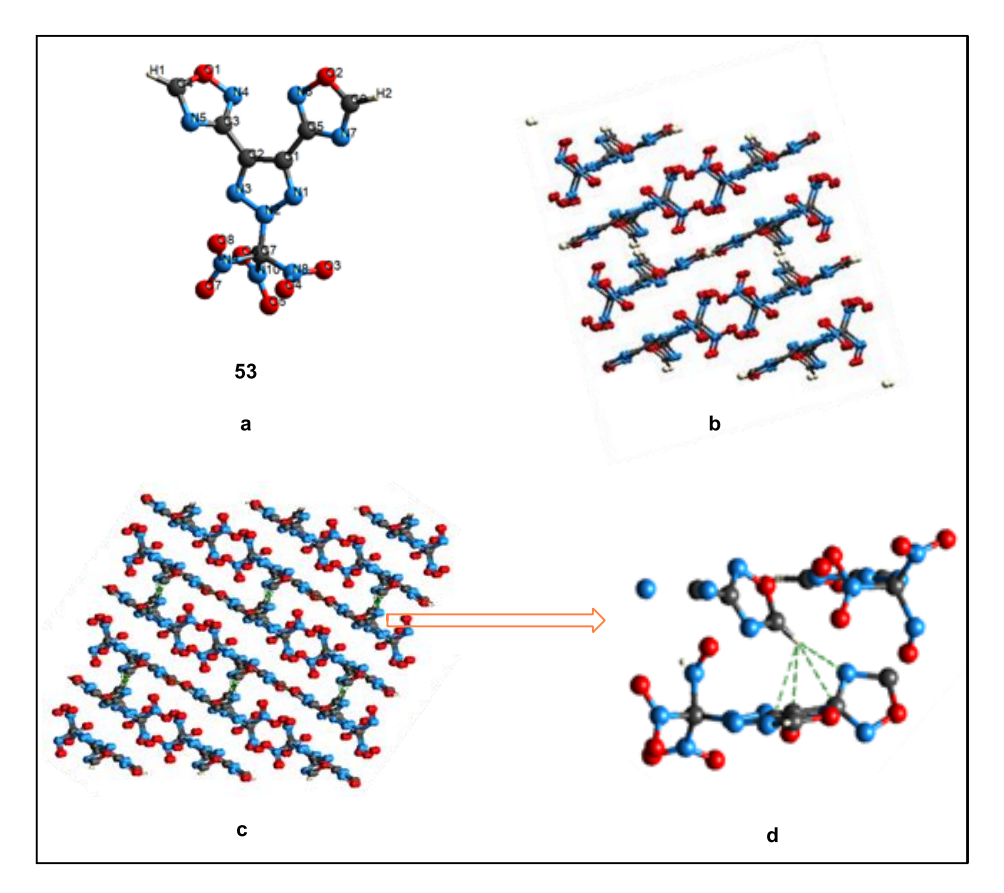
-reveals key intermolecular interactions in the crystal packing of X-ray diffraction analysis.<sup>26</sup> Especially intermolecular interactions of **53** and **55** play key role in crystal packing that increases stability of the molecule.

Table 4.5.1. Crystallographic data for compounds 53 and 55.

Compound	53	55
Formula	C <sub>7</sub> H <sub>2</sub> N <sub>10</sub> O <sub>8</sub>	C <sub>7</sub> H <sub>3</sub> N <sub>9</sub> O <sub>6</sub>
$ m M_w$	354.19	309.18
Crystal system	monoclinic	Triclinic
Space group	P <sub>21</sub>	P -1
T [K]	293 K	293 K
a [Å]	8.5672(4)	9.0233(16)
$b  [ ext{Å}]$	8.6047(3)	19.023(4)
c [Å]	9.6790(4)	22.733(4)
α [°]	90	110.687(5)
β [°]	108.030(1)	100.874(5)
γ [°]	90	92.850(5)
Z	2	12
V [Å]	678.48(5)	3556.1(12)
D <sub>calc</sub> [g/cm <sup>3</sup> ]	1.734	1.732
μ [mm <sup>-1</sup> ]	0.159	0.153
Total reflns	3394	17645
Unique reflns	2993	17585
Observed reflns	2388	5382
$R_1[I > 2\sigma(I)]$	0.0751	0.0989
$wR_2$ [all]	0.2313	0.2158
GOF	1.056	1.091
Diffractometer	Bruker D8 VENTURE Photon III detector	Bruker D8 VENTURE Photon III detector

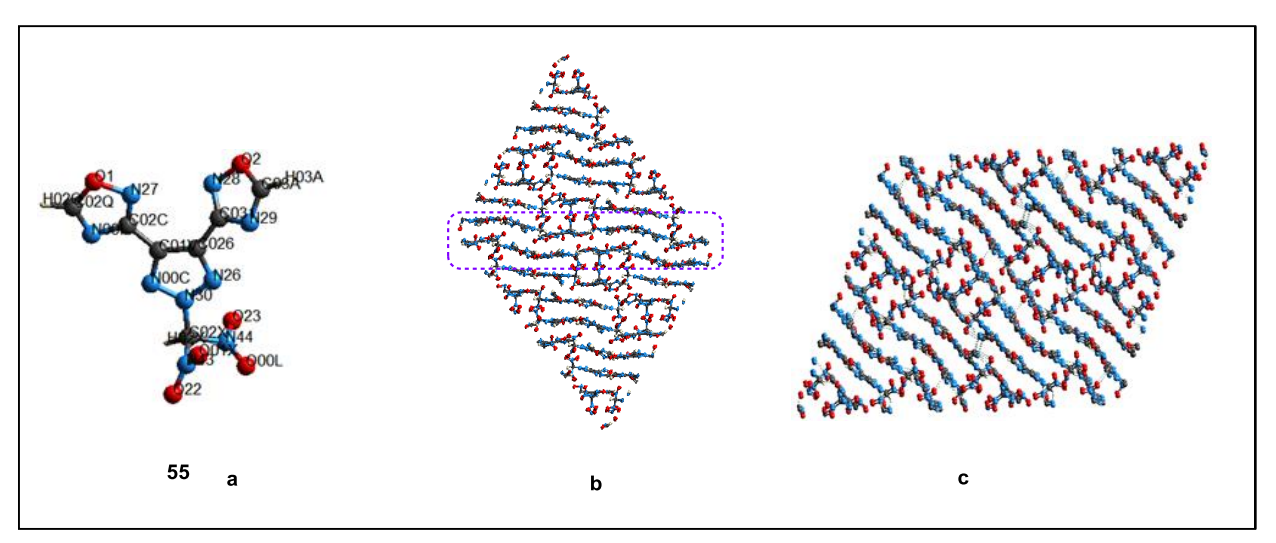
Compound **53** crystallized in monoclinic *P21* space group at 293 K (**Table 4.5.1**). The packing structure of **53** is setup with four pairs of intermolecular hydrogen bonding interactions (**Figure 4.5.2c**). In each molecule two oxadiazole rings connected with two

adjacent molecules *via* hydrogen bonds C(4)– $H\cdots C(1)$ , C(4)– $H\cdots C(2)$ , C(4)– $H\cdots C(3)$  and C(4)– $H\cdots N(5)$  that has observed in 3D supramolecular structure in **Figure 4.5.2c**. The N···O bond is found at a distance between 1.19–1.40 Å.



**Figure 4.5.2.** (a) The molecular structure of **53**, (b) Thermal ellipsoids are set at 20% stacking crystal structure of **53**, (c) Ball and stick packing diagram and green colour dashed lines indicate intermolecular hydrogen bonds.

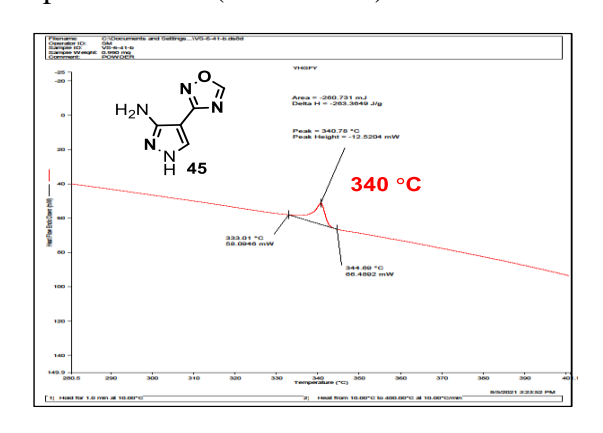
Compound **55** crystallized in triclinic P-1 space groups by single crystal X-ray diffraction analysis at 293 K (**Table 4.5.1**). The packing structure of **55** is setup of seven intermolecular interactions (see: **Figure 4.5.3c**). In each molecule, two oxadiazole rings are connected with two adjacent molecules *via* four pairs hydrogen bonds  $N\cdots H-C$  and  $C-H\cdots N$  (distance in the range of 2.63–2.65 Å) that has been observed in 3D supramolecular structure shown in **Figure 4.5.3c**. The distance of  $N\cdots O$  is found in the range of 1.18–1.40 Å.

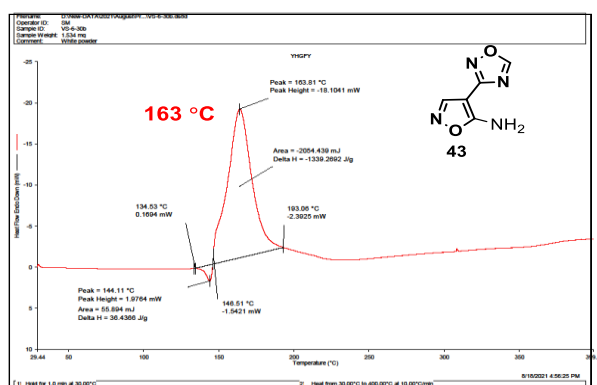


**Figure 4.5.3.** (a) The molecular structure of **55**, (b) The wave-like layer thermal ellipsoids are set at 20% stacking crystal structure of **55**, (c) Ball and stick packing diagram and green color dashed lines represent intermolecular hydrogen bonds.

#### 4.6. Energetic Properties

Thermal stabilities of all compounds are tested in DSC measurements scanning at 10 °C min<sup>-1</sup>. Compound **48** exhibit decomposition temperature 189 °C. Interestingly, compounds **44** and **45** show highest decomposition temperatures 329 °C and 340 °C, respectively. Compounds **43** and **47** have acceptable decomposition temperature 163 °C and 151 °C. Surprisingly, compounds **49**, **51**, **53**, and **55** show better decomposition temperatures 147 °C, 192 °C, 154 °C, and 214 °C, respectively (**Figure 4.6.1**). From single crystal X-ray diffraction analysis, compounds **53** and **55** show density 1.734 and 1.732 g/cm<sup>3</sup>, respectively; the density is better that TNT (1.65 g/cm<sup>3</sup>). Detonation parameters are calculated by Explo5 version 6.03 software taking density and heats of formation of compounds **46**, **47**, **48**, **51**, **53**, and **55**.<sup>27</sup> To our delight, these compounds display better performance over traditional explosive TNT (**Table 4.6.1**).





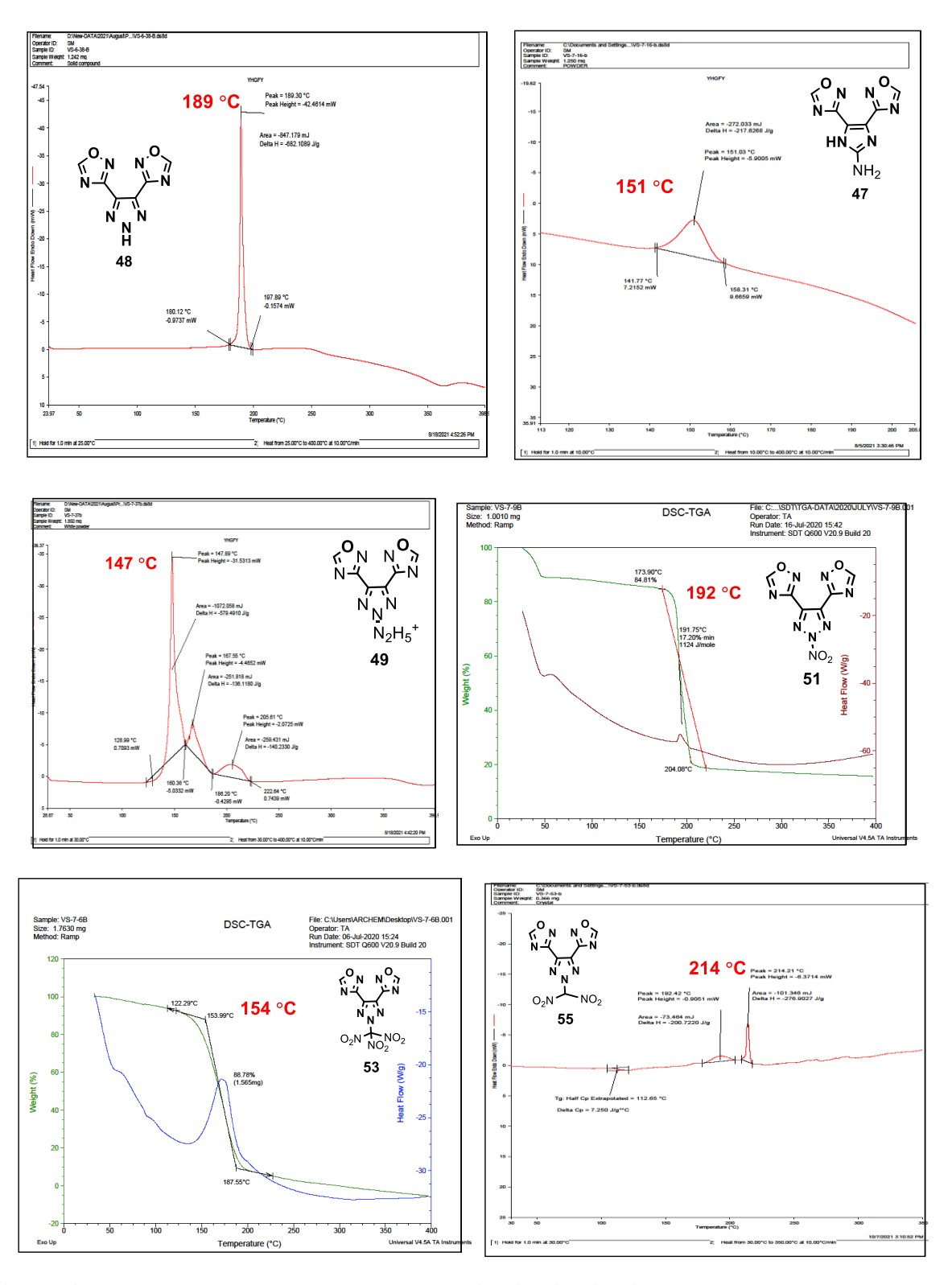


Figure 4.6.1. DSC-TGA curve of compounds 43, 45, 47, 48, 49, 51, 53, and 55

**Table 4.6.1.** Physical energetic properties of synthesized compounds (46, 47, 48, 51, 53, and 55) with respect to TNT<sup>28,30</sup>, PETN<sup>29</sup>, and RDX<sup>28,30</sup>.

C	$ ho^{[a]}$	$T_{d}^{[c]}$	OB <sup>[d]</sup>	$\Delta H_{f}^{[e]}$	$\mathbf{P}^{[\mathbf{f}]}$	$\mathbf{D}_{\mathrm{v}}^{[\mathrm{g}]}$	IS <sup>[h]</sup>	FS <sup>[i]</sup>
Cmpnd	(g cm <sup>-3</sup> )	(° <b>C</b> )	(%)	(kJ mol <sup>-1</sup> )	(GPa)	$(m s^{-1})$	$(\mathbf{J})$	( <b>N</b> )
46	1.62	191	-109.7	429.26	15.9	6512	_	_
47	1.61	151	-105.9	442.10	15.4	6667	_	_
48	1.69	189	30.4	581.49	30.4	8583	_	_
51	1.79	192	-57.6	695.44	26.9	8089	_	_
53	1.86 (1.73) <sup>[b]</sup>	154	-31.6	751.90	34.8	8865	_	_
55	1.80 (1.73) <sup>[b]</sup>	214	-49.2	665.36	28.7	8230	_	_
TNT	1.65	295	-24.7	-67.0	19.5	6881	15	353
PETN	1.78	160	15.18	-502.8	31.4	8564	3	60
RDX	1.80	204	0	80.0	35.0	8762	7.4	120

<sup>a</sup> Theoretical density; <sup>b</sup> Crystal density (294K); <sup>c</sup> Temperature of decomposition (onset) under nitrogen gas (DSC–TGA, 10 °C min<sup>-1</sup>); <sup>d</sup> OB = oxygen balance (%); for C<sub>a</sub>H<sub>b</sub>O<sub>c</sub>N<sub>d</sub>: 1600(c-2a-b/2)/MW; MW = molecular weight of the compound; <sup>e</sup> Heat of formation using MOPAC software; <sup>f</sup> Calculated detonation pressure (EXPLO5 v6.03); <sup>g</sup> Calculated detonation velocity (EXPLO5 v6.03); <sup>h</sup> Impact sensitivity (BAM drop-hammer, method 1 of 6); <sup>i</sup> Friction sensitivity (BAM friction tester, method 1 of 6).

# 4.7. The Hirshfeld surface and fingerprint plot analysis

The Hirshfeld surface analysis was used for the hydrogen bonding effect of the compounds. This is a key factor for structure and property relationship that has been constructed by using Crystal explorer 17.5<sup>31</sup> (**Figure 4.7.1**). For compounds **53** and **55**, interactions of O···O, N···O, O···H, C···O, and N···H are observed in pie diagram (**Figure 4.7.1**, **c** & **f**). The sum of interaction percentages of O···O, N···O, C···O accounts for 63.7% (**53**) and 59% (**55**). Possibly, **53** is relatively less sensitive than **55** due to more intermolecular hydrogen bonds.<sup>6</sup>

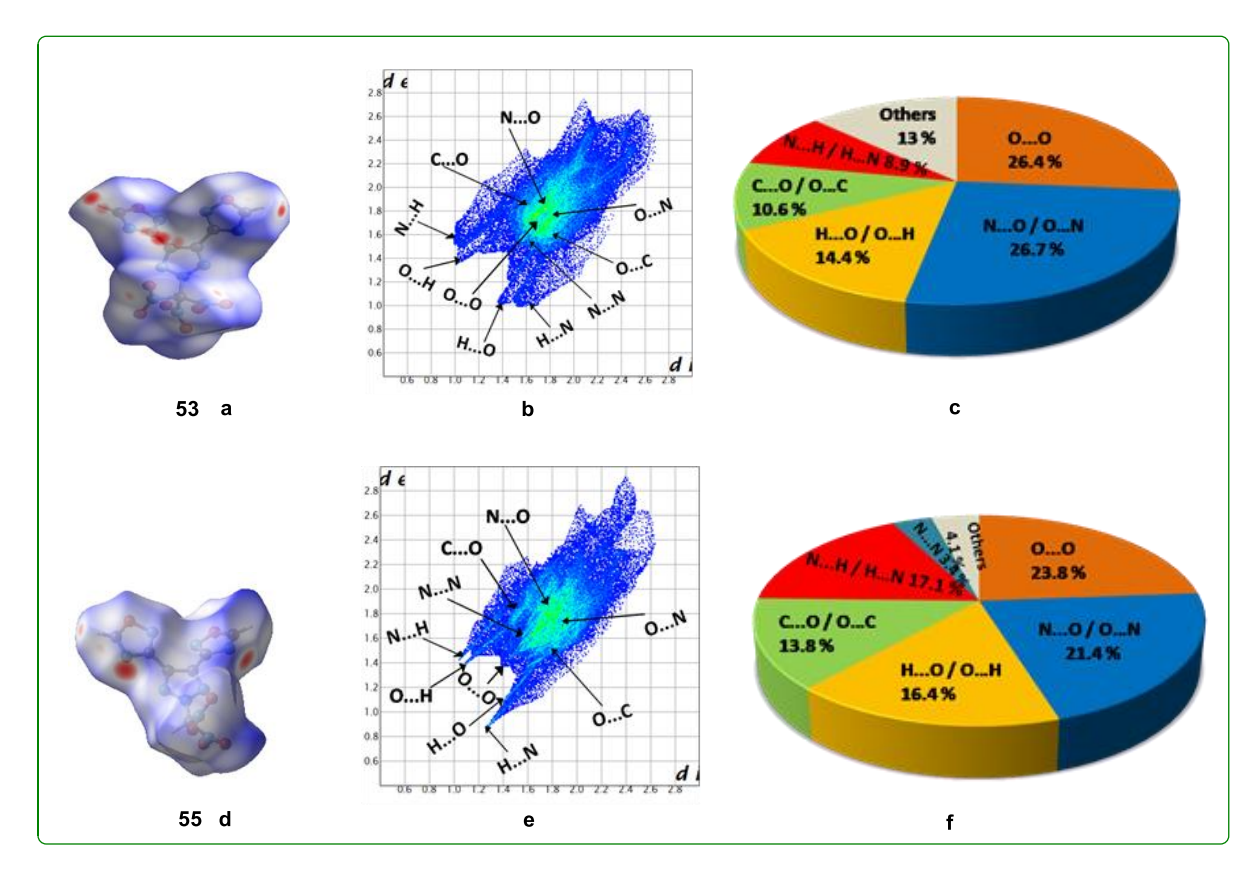


**Figure 4.7.1.** Hirshfeld surface calculations of **53** and **55** as well as two-dimensional fingerprint plots in the crystal structures. Images (a) and (d) are the Hirshfeld surface graphs with proximity of close contacts around **53** and **55** molecules. The 2D fingerprint plots in crystal stacking found in **53** (b) and **55** (e). The 3D bar graphs for **53** (c) and **55** (f) show percentage contributions of the individual atomic contacts to the Hirshfeld surface.

#### 4.8. Conclusions

New molecular scaffolds by combining mono/bis-1,2,4-oxadiazole with various azole (isoxazole/pyrazole/imidazole/triazole) substituted derivatives were synthesized in moderate to good yields. The compounds are characterized by NMR, IR, HRMS, and TGA-DSC measurements. X-ray diffraction analysis confirms the structure of gem-dinitro methyl and trinitromethyl substituted bis-oxadiazoles. Most of the compounds exhibit high positive heats of formation. Particularly, *N*-nitro/gem-dintromethyl/trinitromethyl substituted 1,2,4-oxadiazole derivatives **51**, **53**, and **55** show good oxygen balance, high thermal stability, better calculated density [1.79 g/cm³, 1.86 g/cm³ (crystal density is 1.73 g/cm³ at 293 K), and 1.80 g/cm³ (crystal density is 1.73 g/cm³ at 293 K)], high detonation performance (P = 26.9 GPa, vD = 8089 m/s for **51**; P = 34.8 GPa, vD = 8865 m/s for **53**; P = 28.7 GPa, vD = 8230 m/s for **55**). Hirshfeld surface analysis ofcompounds **53** and **55** attributes to major interaction percentages of O···O, N···O, C···O accounting 63.7% (**53**) and 59% (**55**).

# 4.9. Experimental

#### 4.9.1. General Experimental

All the reactions were performed in an oven-dried round bottomed flask. Commercial grade solvents were distilled prior to use. Column chromatography was performed using silica gel (100–200 Mesh) with hexanes and ethyl acetate mixture. Thin layer chromatography (TLC) was performed on silica gel GF254 plates. Visualization of spots on TLC plate was accomplished with UV light (254 nm) and staining over I<sub>2</sub> chamber.

Proton and carbon nuclear magnetic resonance spectra (<sup>1</sup>H NMR, <sup>13</sup>C NMR) were recorded on a 400 MHz (<sup>1</sup>H NMR, 400 MHz; <sup>13</sup>C NMR, 101 MHz) spectrometer, 500 MHz (<sup>1</sup>H NMR, 500 MHz; <sup>13</sup>C NMR, 126 MHz) spectrometer and 600 MHz (<sup>1</sup>H NMR,600 MHz; <sup>13</sup>C NMR, 151 MHz; <sup>15</sup>N NMR, 61 MHz; spectra were recorded with a JEOL JNM-ECZ-600R/M1) spectrometer, respectively. The chemical shift values (ppm) are expressed relative to the chemical shift of deuterated-solvent or to the external standard Liq. NH<sub>3</sub> without correction (<sup>15</sup>N NMR). Data for <sup>1</sup>H NMR are reported as follows: chemical shift (ppm), multiplicity (s = singlet; bs = broad singlet; d = doublet; bd = broad doublet; dd = doublet of doublet; dt = doublet of triplet; tt = triplet of triplet; t = triplet; bt= broad triplet; q = quartet; pent = pentet, m = multiplet), coupling constants *J* in (Hz), and integration. <sup>13</sup>C NMR was reported in terms of chemical shift (ppm). Melting points and decomposition temperatures (DTA) were determined by DSC-TGA measurements. IR spectra were recorded on FT/IR spectrometer and are reported in cm<sup>-1</sup>. High resolution mass spectra (HRMS) were obtained in ESI mode. X-ray data was collected at 293 K on a 'Bruker D8 VENTURE Photon III detector' diffractometer using Mo-Kα radiation (0.71073 Å).

- **4.9.2. Caution!** The functionalized 1,2,4-oxadiazole derivatives are energetic materials and they tend to exploded or detonated under certain conditions such as impact, friction in the course of the research. Safety precautions including gloves, safety goggles, and face shields should be used all the time.
- **4.9.3. Materials:** Unless otherwise noted, all the reagents were obtained commercially and used without purification. Sc(OTf)<sub>3</sub>, trimethylorthoformate, hydroxylamine hydrochloride, 50% hydroxylamine, hydrazine hydrate, hydrochloric acid, acetic anhydride, acetonitrile (CH<sub>3</sub>CN) were commercially available and used as received. Concentrated H<sub>2</sub>SO<sub>4</sub> and fuming HNO<sub>3</sub> were commercial available and used for nitration.

# 4.9.4. X-ray Crystallography<sup>26</sup>

Single crystal X-ray data for the compounds **53** and **55** were collected using the 'Bruker D8 VENTURE Photon III detector' system [Mo-K $\alpha$  fine focus sealed tube  $\lambda = 0.71073$  Å] at 293 K graphite monochromator with a  $\omega$  scan. Data reduction was performed using Bruker SAINT<sup>2</sup> software. Intensities for absorption were corrected using SADABS 2014/5, Structure solution and refinement were carried out using Bruker SHELX-TL.

# 4.9.5. Hirshfeld Surface Analysis<sup>31</sup>

The Hirshfeld surface image (**Figure 4.7.1**) in which, the red spots signify the high contact populations, while blue and white spots are for low contact populations. This suggests that the negative (red) or positive value (blue and white) of  $d_{norm}$  depends on the intermolecular contacts being shorter (red) or longer (blue and white) than the van der Waals separations. For each point on the Hirshfeld surface, the normalized contact distance ( $d_{norm}$ ) was determined by the equation as shown below.

$$[d_{norm} = (d_i - d_i^{vdW})/r_i^{vdW} + (d_e - d_e^{vdW}/r_e^{vdW}]$$

In which  $d_i$  is measured from the surface of nearest atom interior to the surface interior, while  $d_e$  is measured from the surface of nearest atom exterior to the surface interior, where  $r_i^{vdW}$  and  $r_e^{vdW}$  are the van der Waals radii of the atoms. Hirshfeld surface graphs and two-dimensional fingerprint plots of **53** and **55** were analyzed using Crystal explorer17.5 software.

## 4.9.6. Isodesmic reactions for the prediction of heat of formation<sup>25a</sup>

#### 4.9.7. General Procedure

#### 4.9.7.1. General procedure for preparation of amidoximes (37–42) (GP-1):

Oxime derivatives (37, 39, 40, 41, and 42) were obtained from correpsonding cyanoazoles (31, 33, 34, 35, and 36) when treated independently with hydroxylamine (1.2 equiv.), while 2.4 equiv. hydroxylamine was adequate for the synthesis of bis-oxime derivative; the reaction was carried out in methanol or ethanol at room temperature or 70 °C. The solid was filtered and dried in air to afford amidoximes 37, 39, 40, 41, and 42.

Physical characterization data is exactly matching with the reported values for the respective compound 39, 40, and 42.

#### (Z)-5-Amino-N'-hydroxyisoxazole-4-carboximidamide (37):

Following the general procedure (GP-1): 355 mg, Yield: 55%. White solid.

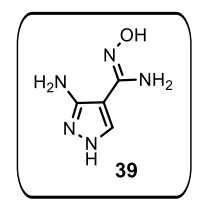
<sup>1</sup>H NMR (400 MHz, DMSO– $d_6$ ):  $\delta = 9.07$  (s, 1H), 8.49 (s, 1H), 7.11 (s, 2H),

5.79 (s, 2H); <sup>13</sup>C NMR (101 MHz, DMSO– $d_6$ ):  $\delta = 167.1$ , 149.3, 147.3, 85.8

ppm. IR(Neat)  $v_{\text{max}}$  3467, 3350, 2523, 2149, 1679, 1582, 1464, 1215, 1029,

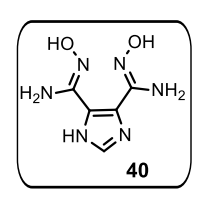
911, 828 cm<sup>-1</sup>. HRMS (ESI) for C<sub>4</sub>H<sub>7</sub>N<sub>4</sub>O<sub>2</sub><sup>+</sup> (M+H)<sup>+</sup>: calcd 143.0569, found 143.0564.

#### (Z)-3-Amino-N'-hydroxy-1H-pyrazole-4-carboximidamide (39):



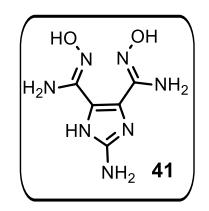
Following the general procedure (GP-1):  $^{1}$ H NMR (600 MHz, DMSO– $d_6$ ):  $\delta$  = 11.59 (s, 1H), 8.98 (s, 1H), 7.66 (s, 1H), 5.54 (s, 2H), 5.21 (bs, 2H); IR(Neat)  $\upsilon_{\text{max}}$  3412, 3164, 1638, 1597, 1506, 1364, 1045, 932, 856, 777 cm<sup>-1</sup>. HRMS (ESI) for C<sub>4</sub>H<sub>8</sub>N<sub>5</sub>O<sup>+</sup> (M+H)<sup>+</sup>: calcd 142.0729, found 142.0724.

#### (4Z,5Z)-N',N'-Dihydroxy-1H-imidazole-4,5-bis(carboximidamide) (40):



Following the general procedure (GP-1):  $^{1}$ H NMR (600 MHz, DMSO– $d_6$ ):  $\delta$  = 7.91 (s, 1H), 7.59 (s, 2H), 5.83 (bs, 4H); IR(Neat)  $\upsilon_{\text{max}}$  3371, 3114, 2914, 2847, 2229, 1962, 1739, 1650, 1589, 1409, 1302, 1156, 940, 864, 790 cm<sup>-1</sup>. HRMS (ESI) for C<sub>5</sub>H<sub>9</sub>N<sub>6</sub>O<sub>2</sub><sup>+</sup> (M+H)<sup>+</sup>: calcd 185.0787, found 185.0779.

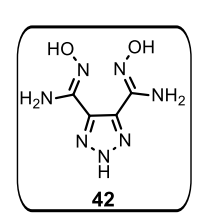
#### $(4\mathbb{Z},5\mathbb{Z})$ -2-Amino-N',N'-dihydroxy-1H-imidazole-4,5-bis(carboximidamide) (41):



Following the general procedure (GP-1): 222 mg, Yield: 62%. White solid. <sup>1</sup>H NMR (600 MHz, DMSO– $d_6$ ):  $\delta$  = 10.30 (bs, 1H), 9.50 (bs, 1H), 9.14 (bs, 1H), 5.60 (s, 2H), 5.40 (s, 4H); <sup>13</sup>C NMR (151 MHz, DMSO– $d_6$ ):  $\delta$  = 149.2, 148.9, 145.7, 127.2, 115.9 ppm. IR(Neat)  $\nu_{\text{max}}$  3360, 2742, 1966, 1618, 1565,

1503, 1450, 1357, 122, 1122, 1122, 930 cm $^{-1}$ . HRMS (ESI) for  $C_5H_{10}N_7O_2^+$  (M+H) $^+$ : calcd 200.0896, found 200.0896.

#### (4Z,5Z)-N',N'-Dihydroxy-2H-1,2,3-triazole-4,5-bis(carboximidamide) (42):



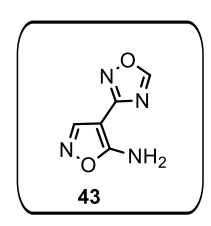
Following the general procedure (GP-1):  $^{1}$ H NMR (600 MHz, DMSO– $d_6$ ):  $\delta$  = 9.94 (bs, 2H), 6.70 (bs, 4H); IR(Neat)  $\upsilon_{max}$  3469, 3350, 2147, 1678, 1630, 1581, 1468, 1346, 1214, 1105, 1003, 913, 826 cm<sup>-1</sup>. HRMS (ESI) for  $C_4H_8N_7O_2^+$  (M+H)<sup>+</sup>: calcd 186.0739, found 186.0731.

#### 4.9.7.2. General procedure for preparation of mono and bis-1,2,4-oxadiazoles (GP-2):

To suspension of amidoximes (37, 38, 39, 40, 41, and 42), Sc(OTf)<sub>3</sub> was added in trimethyl orthoformate at room temperature under inert atmosphere. Then water was added, solid was filtered, washed with water and dried in air to afford mono and bis-1,2,4-oxadiazole derivative (43, 44, 45, 46, 47, and 48) as white solids.

# **4-(1,2,4-Oxadiazol-3-yl)isoxazol-5-amine (43):**

Following the general procedure (GP-2), to suspension of **37** (0.2 g, 1.42 mmol), Sc(OTf)<sub>3</sub> (0.06 g, 0.14 mmol) was added in trimethyl orthoformate (0.5 mL) at room temperature under inert atmosphere. The resulting mixture was stirred for 3 h. Then water was added, solid was filtered, washed with water and dried in air to afford **43** (110 mg) in 51% yield as a white solid.

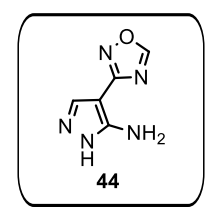


DSC-TGA (10 °C min<sup>-1</sup>, °C): 163 °C (T<sub>d</sub>). <sup>1</sup>H NMR (600 MHz, DMSO- $d_6$ ):  $\delta = 9.58$  (s, 1H), 8.62 (s, 1H), 7.63 (s, 2H); <sup>13</sup>C NMR (151 MHz, DMSO- $d_6$ ):  $\delta = 170.1$ , 166.8, 162.3, 150.6, 81.9 ppm. IR(Neat)  $\upsilon_{\text{max}}$  3300, 3200, 3138, 2922, 2177, 1992, 1814, 1731, 1528, 1278, 910 cm<sup>-1</sup>.

HRMS (ESI) for  $C_5H_5N_4O_2^+$  (M+H)<sup>+</sup>: calcd 153.0413, found 153.0410.

#### 4-(1,2,4-Oxadiazol-3-yl)-1*H*-pyrazol-5-amine (44):

Following the general procedure (GP-2), to suspension of **38** (0.075 g, 0.71 mmol) in trimethyl orthoformate (0.6 mL) and then Sc(OTf)<sub>3</sub> (0.034 g, 0.071 mmol) was added at room temperature under inert atmosphere. The resulting mixture was stirred for 3 h. Then water was added, solid was filtered, washed with water and dried in air to afford **44** (88 mg) in 82% yield as a white solid.

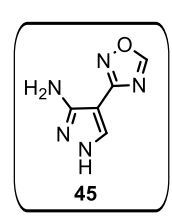


DSC-TGA (10 °C min<sup>-1</sup>, °C): 329 °C (T<sub>d</sub>). <sup>1</sup>H NMR (600 MHz, DMSO- $d_6$ ):  $\delta = 13.78$  (bs, 1H), 8.98 (bs, 2H), 8.55 (s, 1H), 8.14 (s, 1H) ppm; IR(Neat)  $\nu_{\text{max}}$  3342, 3048, 2163, 2030, 1656, 1592, 1542, 1480, 1398, 1272, 1121, 907, 804, 702 cm<sup>-1</sup>. HRMS (ESI) for C<sub>5</sub>H<sub>6</sub>N<sub>5</sub>O<sup>+</sup> (M+H)<sup>+</sup>: calcd

152.0572, found 152.0570.

#### 4-(1,2,4-Oxadiazol-3-yl)-1*H*-pyrazol-3-amine (45):

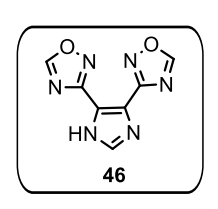
Following the general procedure (GP-2), to suspension of **39** (0.2 g, 1.41 mmol) in trimethyl orthoformate (0.6 mL) and then Sc(OTf)<sub>3</sub> (0.069 g, 0.14 mmol) was added at room temperature under inert atmosphere. The resulting mixture was stirred for 3 h. Then water was added, obtained solid was filtered and washed with water and dried in air to form **45** (192 mg) in 90% yield as a white solid.



DSC-TGA (10 °C min<sup>-1</sup>, °C): 340 °C (T<sub>d</sub>). <sup>1</sup>H NMR (600 MHz, DMSO- $d_6$ ):  $\delta$  = 13.78 (bs, 1H), 8.97 (bs, 2H), 8.55 (s, 1H), 8.14 (s, 1H) ppm; IR(Neat)  $\nu_{\text{max}}$  3339, 3048, 2504, 1914, 1656, 1589, 1480, 1328, 1214, 1121, 907, 804, 702 cm<sup>-1</sup>. HRMS (ESI) for C<sub>5</sub>H<sub>6</sub>N<sub>5</sub>O<sup>+</sup> (M+H)<sup>+</sup>: calcd 152.0572, found 152.0568.

## **3,3'-(1***H***-Imidazole-4,5-diyl)bis(1,2,4-oxadiazole) (46):**

Following the general procedure (GP-2), to suspension of **40** (0.5 g, 2.71 mmol) in trimethyl orthoformate (5.0 mL) and then Sc(OTf)<sub>3</sub> (267 mg, 0.54 mmol) was added at room temperature under inert atmosphere. The resulting mixture was stirred for 12 h. Then DCM was added, solid was precipitated, washed with DCM and dried in air to obtain **46** (490 mg) in 88% yield as a white solid.

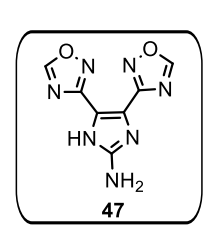


DSC-TGA (10 °C min<sup>-1</sup>, °C): 191 °C (T<sub>d</sub>). <sup>1</sup>H NMR (600 MHz, DMSO- $d_6$ ):  $\delta = 9.68$  (s, 2H), 8.10 (s, 1H); <sup>13</sup>C NMR (151 MHz, DMSO- $d_6$ ):  $\delta = 168.7$ , 160.1, 142.0, 114.8 ppm. IR(Neat)  $\upsilon_{\text{max}}$  3455, 3391, 3131, 1914, 2846, 2234, 1635, 1535, 1475, 1391, 1265, 1164, 1074, 969,

894, 753 cm $^{-1}$ . HRMS (ESI) for  $C_7H_3N_6O_2^-$  (M-H) $^+$ : calcd 203.0318, found 203.0323.

#### **4,5-Di(1,2,4-oxadiazol-3-yl)-1***H***-imidazole-2-amine (47):**

Following the general procedure (GP-2), to suspension of **41** (0.3 g, 1.50 mmol) in trimethyl orthoformate (2.0 mL) and then Sc(OTf)<sub>3</sub> (0.15 g, 0.30 mmol) was added at room temperature under inert atmosphere. The resulting mixture was stirred for 12 h. Then DCM was added, solid was precipitated, washed with DCM and dried in air to obtain **47** (150 mg) in 45% yield as a white solid.

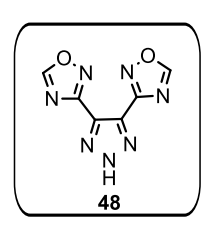


DSC-TGA (10 °C min<sup>-1</sup>, °C): 151 °C (T<sub>d</sub>). <sup>1</sup>H NMR (600 MHz, DMSO- $d_6$ ): 9.70 (s, 2H), 5.70 (bs, 2H); <sup>13</sup>C NMR (151 MHz, DMSO- $d_6$ ):  $\delta$  = 166.9, 166.4, 152.7, 121.8, 119.6 ppm. IR(Neat)  $\upsilon_{\text{max}}$  3204, 1649, 1536, 1364, 1241, 1024, 957, 885, 749 cm<sup>-1</sup>. HRMS (ESI) for C<sub>7</sub>H<sub>6</sub>N<sub>7</sub>O<sub>2</sub><sup>+</sup>

(M+H)<sup>+</sup>: calcd 220.0583, found 220.0580.

#### 4,5-Di(1,2,4-oxadiazol-3-yl)-2*H*-1,2,3-triazole (48):

Following the general procedure (GP-2), to suspension of **42** (0.2 g, 1.08 mmol) in trimethyl orthoformate (0.8 mL) and then Sc(OTf)<sub>3</sub> (0.2 g, 0.22 mmol) was added at room temperature under inert atmosphere. The resulting mixture was stirred for 3 h. Then water was added, solid was filtered, washed with water and dried in air gave **48** (188 mg) in 85% yield as a white solid.

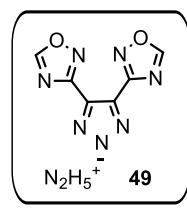


DSC-TGA (10 °C min<sup>-1</sup>, °C): 189 °C (T<sub>d</sub>). <sup>1</sup>H NMR (600 MHz, DMSO- $d_6$ ):  $\delta = 16.58$  (bs, 1H), 9.83 (s, 2H); <sup>13</sup>C NMR (151 MHz, DMSO- $d_6$ ):  $\delta = 167.8$ , 160.2, 133.3 ppm. IR(Neat)  $v_{max}$  3188, 3108, 2163, 2030, 1577, 1461, 1340, 1222, 1111, 922, 819, 746 cm<sup>-1</sup>. HRMS (ESI) for

 $C_6H_4N_7O_2^+$  (M+H)+: calcd 206.0426, found 206.0422.

#### **Hydrazinium 4,5-di(1,2,4-oxadiazol-3-yl)-2***H***-1,2,3-triazolate (49):**

A suspension of **48** (0.36 g, 1.75 mmol) in MeOH was treated with hydrazine hydrate (3.51 mmol) at room temperature. The resulting reaction mixture was heated at 50 °C for 1 h. The solvent was removed by blowing air to produce **49** (188 mg) in 45% yield as a white solid.

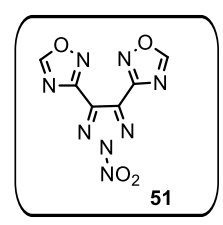


DSC-TGA (10 °C min<sup>-1</sup>, °C): 147 °C (T<sub>d</sub>). <sup>1</sup>H NMR (600 MHz, DMSO- $d_6$ ):  $\delta = 9.51$  (s, 2H), 7.20 (bs, 5H); <sup>13</sup>C NMR (151 MHz, DMSO- $d_6$ ):  $\delta = 166.0$ , 163.4, 131.4 ppm. IR(Neat)  $\upsilon_{max}$  3360, 3087, 2765, 2164, 1969, 1595, 1513, 1408, 1319, 1285, 1104, 967, 873 cm<sup>-1</sup>. HRMS (ESI) for C<sub>6</sub>H<sub>2</sub>N<sub>7</sub>O<sub>2</sub><sup>-1</sup>

 $(M-N_2H_5)^-$ : calcd 204.0270, found 204.0266.

#### 3,3'-(2-nitro-2*H*-1,2,3-triazole-4,5-diyl)bis(1,2,4-oxadiazole) (51):

Compound **48** (0.5 g, 2.43 mmol) was added in portions to the acidic mixture [mixture of acetic anhydride (5.0 mL) and fuming HNO<sub>3</sub> (1.2 mL)] at 0 °C. The resulting reaction mixture was stirred at ambient temperature for 12 h. The mixture was then poured into ice water, precipitate was filtered and washed with cold water to deliver **51** (510 mg) in 84% yield as a white solid.



DSC-TGA (10 °C min<sup>-1</sup>, °C): 192 °C (T<sub>d</sub>). <sup>1</sup>H NMR (600 MHz, Acetone– $d_6$ ):  $\delta = 9.66$  (d, J = 3.0 Hz, 2H); <sup>13</sup>C NMR (151 MHz, Acetone– $d_6$ ):  $\delta = 168.6$ , 160.1, 136.7 ppm. IR(Neat)  $\upsilon_{\text{max}}$  3180, 3105, 2074, 1657, 1591, 1541, 1392, 1263, 1110, 992, 830, 748 cm<sup>-1</sup>.

#### 4-(4,5-Di(1,2,4-oxadiazol-3-yl)-2*H*-1,2,3-triazol-2-yl)butan-2-one (52):

Compound **48** (150 mg, 0.73 mmol) was dissolved in CH<sub>3</sub>CN (4.0 mL) and then triethylamine (220 mg, 2.19 mmol) was added. To this solution methylvinylketone (102 mg, 1.46 mmol) was added and the mixture was stirred for 5 h. Then precipitate was filtered, washed with CH<sub>3</sub>CN to obtain **52** (196 mg) in 98% yield as a white solid.

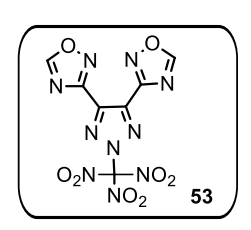
O. N N.O N N N N N N N N N N N C CH<sub>2</sub>)<sub>2</sub>COCH<sub>3</sub>

DSC-TGA (10 °C min<sup>-1</sup>, °C): 167 °C; <sup>1</sup>H NMR (600 MHz, CD<sub>3</sub>CN):  $\delta$  = 9.12 (s, 2H), 4.81 (t, J = 6.6 Hz, 2H), 3.27 (t, J = 6.6 Hz, 2H), 2.20 (s, 3H); <sup>13</sup>C NMR (151 MHz, CD<sub>3</sub>CN):  $\delta$  = 206.2, 167.6, 161.5, 135.7, 51.7, 42.1, 30.1 ppm. IR(Neat)  $\nu_{\text{max}}$  3099, 3015, 2025, 1867, 1718, 1598, 1410,

1328, 1185, 1018, 903, 890, 774 cm $^{-1}$ . HRMS (ESI) for  $C_{10}H_{10}N_7O_3^+$  (M+H) $^+$ : calcd 276.0845, found 276.0841.

#### 3,3'-(2-(Trinitromethyl)-2*H*-1,2,3-triazole-4,5-diyl)bis(1,2,4-oxadiazole) (53):

Compound **52** (0.84 g, 3.05 mmol) was dissolved in portions to a mixture of concentrated sulphuric acid (7.0 mL) and 100% nitric acid (6.0 mL) at 0 °C. The mixture was slowly warmed to rt and stirred for 12 h. Crushed ice was then poured, precipitate was filtered, washed with cold water, and dried in air to give **53** (620 mg) in 57% yield as yellow solid.

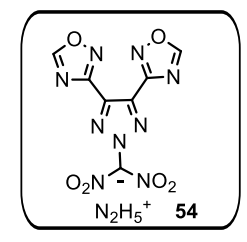


DSC-TGA (10 °C min<sup>-1</sup>, °C): 154 °C (T<sub>d</sub>). <sup>1</sup>H NMR (600 MHz, Acetone– $d_6$ ):  $\delta = 9.70$  (s, 2H); <sup>13</sup>C NMR (151 MHz, Acetone– $d_6$ ):  $\delta = 168.8$ , 159.6, 143.1 ppm. <sup>15</sup>N NMR (61 MHz, DMSO– $d_6$ ): 361.8, 335.8, 335.0, 239.7, 226.6 ppm. IR(Neat)  $\upsilon_{\text{max}}$  3149, 3093, 1628, 1606, 1528,

1387, 1276, 1100, 951, 889, 777 cm $^{-1}$ . HRMS (ESI) for  $C_7H_2N_9O_6^-$  (M $-HNO_2$ ) $^-$ : calcd 308.0128, found 308.0117.

#### Hydrazinium (4,5-di(1,2,4-oxadiazol-3-yl)-2H-1,2,3-triazol-2-yl)dinitromethanide (54):

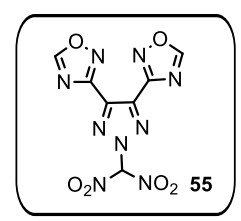
A suspension of **53** (0.2 g, 0.56 mmol) in MeOH was treated with hydrazine hydrate at rt. The resulting mixture was heated at 50 °C for 1 h. The solvent was removed by blowing air to obtain red colour solid. The solid was filtered and washed with water to give **54** (95 mg) in 49% yield as a red solid.



DSC–TGA (10 °C min<sup>-1</sup>, °C): ND. <sup>1</sup>H NMR (600 MHz, DMSO– $d_6$ ):  $\delta$  = 9.90 (s, 2H), 7.12 (bs, 5H); IR(Neat)  $\upsilon_{\text{max}}$  3120, 2235, 2176, 1578, 1489, 1365, 1222, 1143, 1096, 950, 882, 734 cm<sup>-1</sup>. HRMS (ESI) for  $C_7H_2N_9O_6^-$  (M– $N_2H_5$ )<sup>-</sup>: calcd 308.0133, found 308.0125.

#### 3,3'-(2-(Dinitromethyl)-2*H*-1,2,3-triazole-4,5-diyl)bis(1,2,4-oxadiazole) (55):

A suspension of hydrazinium salt **54** (80 mg, 0.23 mmol) to a hydrochloric acid (2%, 4.0 mL), while maintaining the reaction temperature at 0 °C. It was stirred for 2 h and then poured into ice-cold water, the precipitate was filtered off and washed with cold water to give **55** (56 mg) in 77% yield as a white solid.



DSC-TGA (10 °C min<sup>-1</sup>, °C): 214 °C. <sup>1</sup>H NMR (600 MHz, DMSO- $d_6$ ):  $\delta = 4.10$  (s, 1H), 9.90 (s, 2H); IR(Neat)  $\upsilon_{\text{max}}$  3525, 2918, 2851, 2161, 2029, 1737, 1364, 1215, 840, 670 cm<sup>-1</sup>. HRMS (ESI) for C<sub>7</sub>H<sub>6</sub>N<sub>10</sub>O<sub>6</sub><sup>+</sup> (M+NH<sub>3</sub>)<sup>+</sup>: calcd 326.0472, found 326.0454.

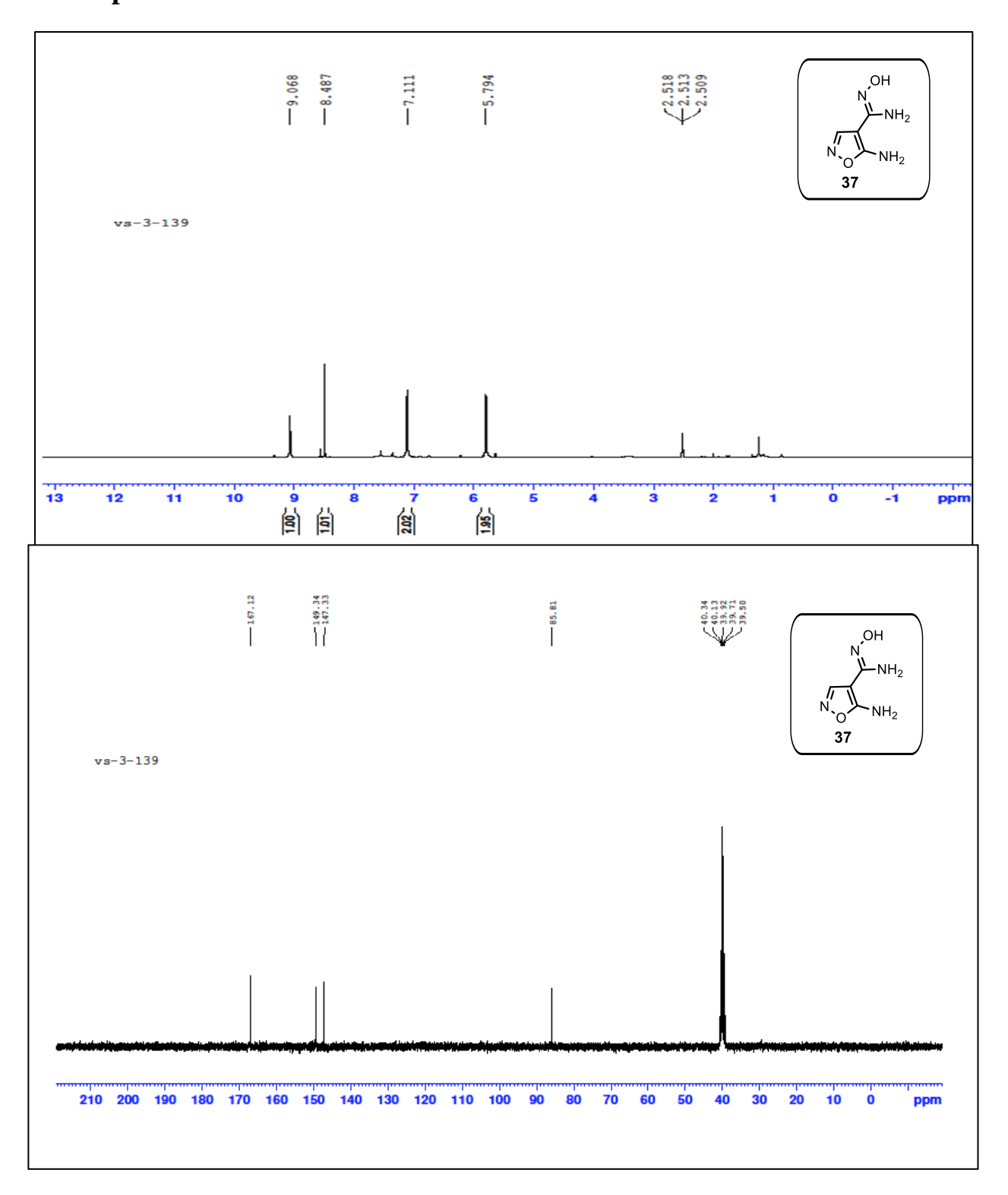
#### 4.10. References

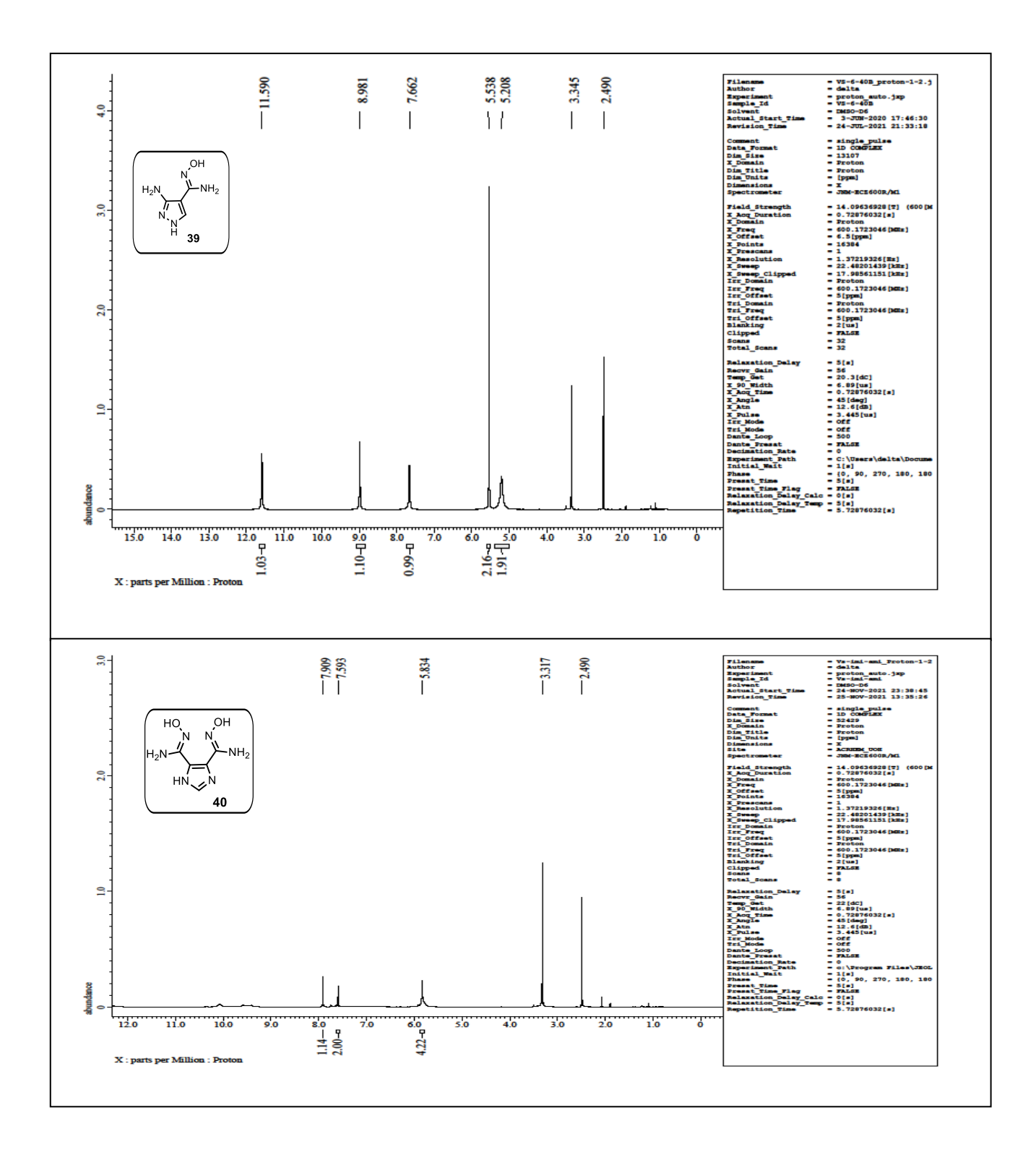
- 1. (a) A. K. Zelenin, M. L. Trudell, R. D. Gilardi, J. Heterocycl. Chem., 1998, 35, 151–155; (b) A. B. Sheremetev, V. O. Kulagina, N. S. Aleksandrova, D. E. Dmitriev, Y. A. Strelenko, V. P. Lebedev, Y. N. Matyushin, Propellants Explos. Pyrotech., 1998, 23, 142–149; (c) J. M. Veauthier, D. E. Chavez, B. C. Tappan, D. A. Parrish, J. Energ. Mater., 2010, 28, 229–249; (d) J. Zhang, J. M. Shreeve, J. Am. Chem. Soc., 2014, 136, 4437–4445; (e) T. I. Godovikova, S. P. Golova, Y. A. Strelenko, M. Y. Antipin, Y. T. Struchkov, L. I. Khmel linitskii, Mendeleev Commun., 1994, 4, 7-9; (f) Z. Fu, R. Su, Y. Wang, Y.-F. Wang, W. Zeng, N, Xiao, Y. Wu, Z. Zhou, J. Chen, F. Chen, Chem. Eur. J., 2012, 18, 1886–1889; (g) Z. X. Li, S.-Q. Tang, J. T. Liu, Chin. J. Org. Chem., 2002, 22, 902–904 (in Chinese); (h) A. R. Katritzky, G. L. Sommen, A. V. Gromova, R. M. Witek, P. J. Steel, R. Damavarapu, Chem. Heterocycl. Compd., 2005, 41, 111-118; (i) I. V. Ovchinnikov, K. A. Lyssenko, N. N. Makhova, Mendeleev Commun., 2009, 19, 144–146; (j) V. Thottempudi, J. Zhang, C. He, J. M. Shreeve, RSCAdv., 2014, 4, 50361-50364; (k) M. A. Kettner, T. M. Klapötke, T. G. Witkowski, F. Hundling, Chem. Eur. J., 2015, 21, 4236–4241; (1) M. A. Kettner, K. Karaghiosoff, T. M. Klapötke, M.Suc´eska, S. Wunder, Chem. Eur. J., 2014, 20, 7622–7631; (m) Z.Fu, Y. Wang, Li. Yang, R. Su, J. Chen, F. Nie, J. Huang, F.-X.Chen, RSC Adv., 2014, 4, 11859–11861; (n) G.-X. Wang, X.-D. Gong, Y. Liu, H.-C. Du, X.-J. Xu, H.-M. Xiao, Chin. J. Chem., 2010, 28, 1345–1354; (o) E. O. John, R. L. Kirchmeier, J. M.Shreeve, J. Fluorine Chem., 1990, 47, 333-343; (p) D. J. Whelan, M. R. Fitzgerald, J. Energ. Mater., 1994, 12, 181-195; (q) M. E. Sitzmann, J. Energ. Mater., 1988, 6, 129–144.
- (a) B. Wang, G. Zhang, H. Huo, Y. Fan, X. Fan, *Chin. J. Chem.*, **2011**, 29, 919–924; (b) P.
   W. Leonard, D. E. Chavez, P. F. Pagoria, D. L. Parrish, *Propellants Explos. Pyrotech.*, **2011**, 36, 233–239.
- 3. (a) L. A. Kayukova, *Pharm. Chem. J.*, **2005**, *39*, 539; (b) L. Fershtat, I. Ananyev and N. Makhova, *RSC Adv.*, **2015**, *5*, 47248.
- 4. (a) T. M. Klapötke, N. Mayr, J. Stierstorfer and M. Weyrauther, *Chem. Eur. J.*, **2014**, *20*, 1410; (b) M. A. Kettner, K. Karaghiosoff, T. M. Klapötke, M. Sućeskaand S. Wunder, *Chem. Eur. J.*, **2014**, *20*, 7622.
- 5. E. C. Johnson, J. J. Sabatini, D. E. Chavez, R. C. Sausa, E. F. C. Byrd, L. A. Wingard, and P. E. Guzman, *Organic Process Res. Dev.*, **2018**, 22, 736–740.
- 6. Q. Xue, F-q. Bi, J-l Zhang, Z-j Wang, L-j Zhai, H. Huo, B-z Wang and S-y Zhang, *Front. Chem.*, **2020**, *7*, 942.

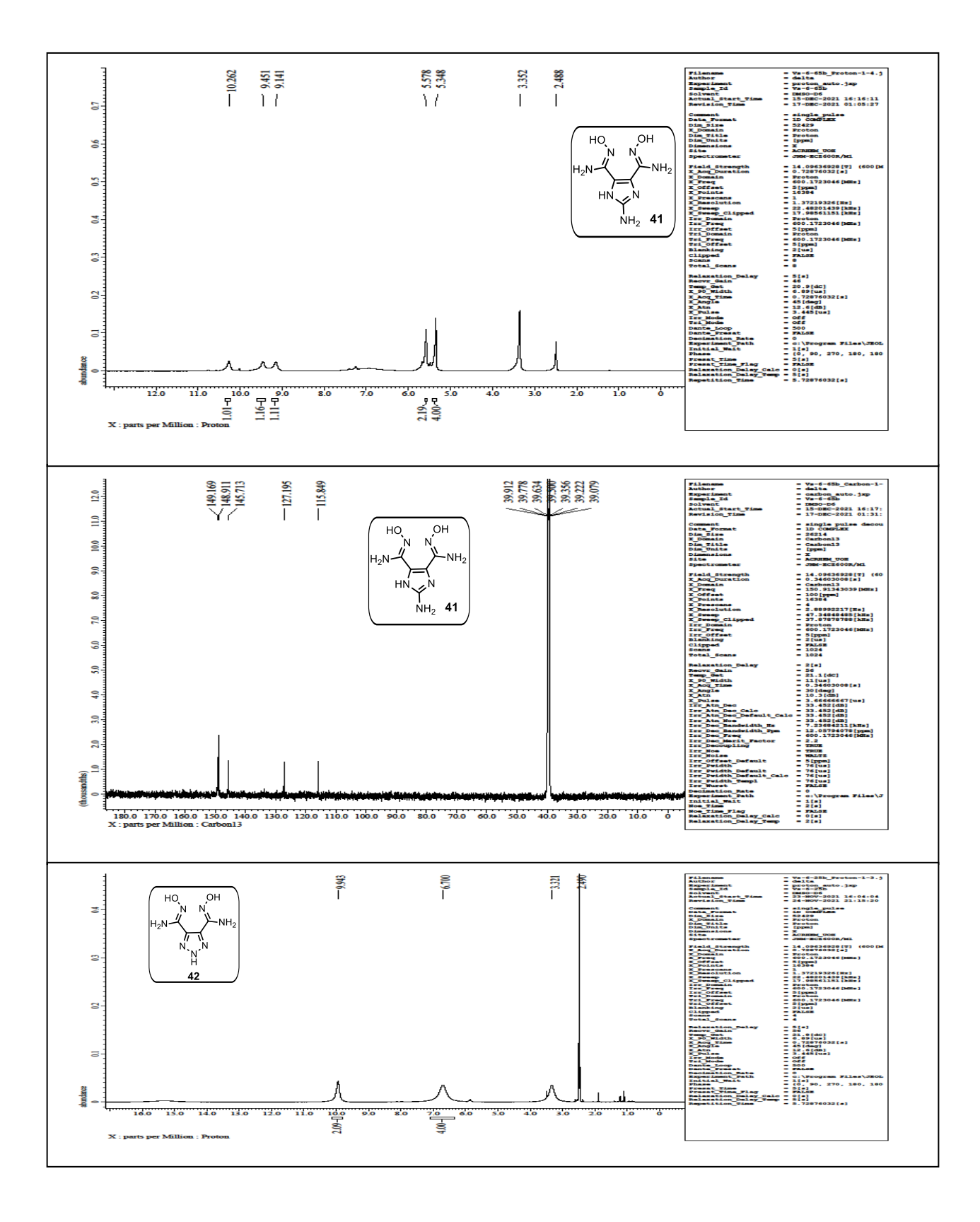
- 7. Y. Tang, H. Gao, L. A. Mitchell, D. A. Parrish, and J. M. Shreeve, *Angew. Chem. Int. Ed.*, **2016**, *55*, 1147–1150.
- 8. V. Thottempudi, J. Zhang, C. He, J. M. Shreeve, *RSC Adv.*, **2014**, *4*, 50361–50364.
- 9. P. L. van der Peet, T. U. Connell, C. Gunawan, J. M. White, P. S. Donnelly and S. J. Williams, *J. Org. Chem.*, **2013**, 78, 7298.
- 10. A. Gunasekaran, T. Jayachandran, J. H. Boyer and M. L. Trudell, *J. Heterocycl. Chem.*, **1995**, *32*, 1405.
- 11. C. Yan, K. Wang, T. Liu, H. Yang, G. Cheng and Q. Zhang, *Dalton Trans.*, **2017**, *46*, 14210–14218.
- 12. T. M. Klapötke, N. Mayr, J.Stierstorfer, and M.Weyrauther, *Chem. Eur. J.*, **2014**, *20*, 1410–1417.
- 13. R. Wang, Y. Guo, Z. Zeng, B. Twamley, J. M. Shreeve, *Chem. Eur. J.*, **2009**, *15*, 2625–2634.
- 14. H. Wei, C. He, J. Zhang, and J. M. Shreeve, *Angew. Chem. Int. Ed.*, **2015**, *54*, 9367–9371.
- 15. Y. Cao, X. Lin, J. Yang, X. Gong, G. Fan and H. Huang, New J. Chem., **2019**, 43, 5441–5447.
- 16. V. Thottempudi, J. Zhang, C. He and J. M. Shreeve, *RSC Adv.*, **2014**, *4*, 50361–50364.
- 17. Y. Tang, H. Gao, L. A. Mitchell, D. A. Parrish, and J. M. Shreeve, *Angew. Chem. Int. Ed.*, **2016**, *55*, 3200–3203.
- 18. (a) D. A. Brooks, *United States Patent*, **1969**, *3*, 615, 633; (b) O. Trauth, Badische Anilinund Soda-Fabrik, *Deutsches Patentamt*, **1957**, 1049025; (c) C. Zhao, H. Wang, X. Ran, B. Bai, Y. Zhang, M. Li, *Chin. J. Chem.*, **2012**, *30*,785–790; (d) C. K. C. Nagaraj, M. S. Niranjan, S. Kiran, *Int. J. Pharm. Pharm. Sci.*, **2011**, *3*, 9–16.
- 19. (a) Y. Liu, X. Qi, W. Zhang, P. Yin, Z. Cai, and Q. Zhang, *Org. Lett.*, **2021**, *23*, 734–738; (b) S. P. Kelley, P. S. Barber, P. H. K. Mullins and R. D. Rogers, *Chem. Commun.*, **2014**, *50*, 12504–12507; (c) A. A. Dippold, D. Izsák, T. M. Klapötke, C. Pflüger, *Chem. Eur. J.*, **2016**, 22, 1768–1778.
- 20. L. L. Fershtat, I. V. Ananyev and N. N. Makhova, RSC Adv., 2015, 5, 47248–47260.
- 21. E. C. Johnson, E. J. Bukowski, J. J. Sabatini, R. C. Sausa, E. F. C. Byrd, Melissa A. Garner, and D. E. Chavez, *ChemPlusChem*, **2019**, *84*, 1–5.
- 22. V. Thottempudi, F. Forohor, D. A. Parrish, and J. M. Shreeve, *Angew. Chem. Int. Ed.*, **2012**, *51*, 9881–9885.

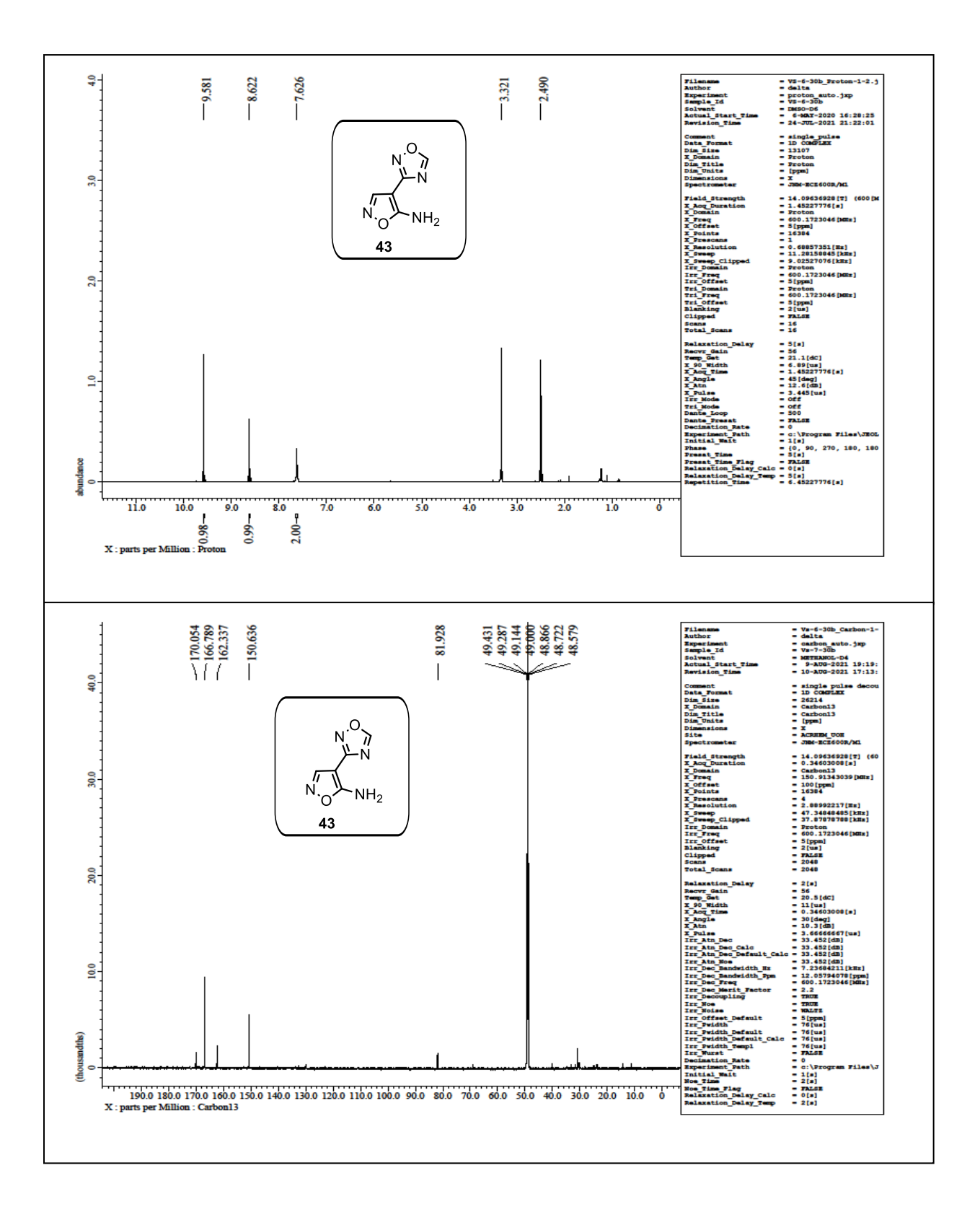
- 23. (a) S. Huang, J. Tian, X. Qi, K. Wang, and Q. Zhang, *Chem. Eur. J.*, **2017**, *23*, 1–9; (b) X. X. Zhao, S. H. Li, Y. Wang, Y. C. Li, F. Q. Zhao and S. P. Pang, *J. Mater. Chem. A*, **2016**, *4*, 5495–5504; (c) Y. Tang, C. He, G. H. Imler, D. A. Parrish and J. M. Shreeve, *J. Mater. Chem. A*, **2018**, *6*, 5136–5142; (d) V. V. Semenov, S. A. Shevelev, A. B. Bruskin, A. Kh. Shakhnes, V. S. Kuz'min, *Chemistry of Heterocyclic Compounds*, **2017**, *53*(6/7), 728–732; (e) K. Mohammad, V. Thaltiri, N. Kommu and A. A. Vargeese, *Chem. Commun.*, **2020**, *56*, 12945–12948.
- 24. Y. Tang, H. Gao, G. H. Imler, D. A. Parrish and J. M. Shreeve, *RSC Adv.*, **2016**, *6*, 91477–91482.
- 25. (a) M. J. Frisch, *et al.*, *Gaussian 09*, *Revision C.01*, Gaussian, Inc., Wallingford CT, **2010**; (b) R. Marek and A. Lycka, *Curr. Org. Chem.*, **2002**, *6*, 35–66.
- 26. (a) O. V. Dolomanov, A. J. Blake, N. R. Champness, M. Schroder, *J. Appl. Cryst.*, **2003**, 36, 1283; (b) SAINT, version 6.45 /8/6/03 and version 8.34A, Bruker Apex-III, **200**3, **2014**; (c) G. M. Sheldrick, *SHELXS-97*, University of Gottingen, Germany, **1997** (d) Sheldrick, G. M.; SADABS and SADABS 2014/5, *Program for Empirical Absorption Correction of Area Detector Data*, University of Göttingen, Germany, **1997**, **2014**; (e) *SMART*(*version5.625*), *SHELXTL*(*version6.12*), Bruker AXS Inc. Madison, WI, **2000**.
- 27. M. Suceska, EXPLO5 version 6.03, 2014.
- 28. V. Thottempudi, H. Gao, J. M. Shreeve, J. Am. Chem. Soc., **2011**, 133, 6464–6471.
- 29. (a) V. Thottempudi, P. Yin, J. Zhang, D. A. Parrish and J. M. Shreeve, *Chem.–Eur. J.*, **2014**, 20, 542; (b) R. Meyer, J. Kçhler, A. Homburg, *Explosives*, 5th ed., Wiley-VCH, Weinheim, **2002**, p.235.
- 30. V. D. Ghule, J. Phys. Chem. A, 2012, 116, 9391–9397.
- 31. (a) Spackman, M. A.; McKinnon, J. J. Fingerprinting intermolecular interactions in molecular crystals. *CrystEngComm.*, **2002**, *4*, 378–392; (b) Spackman, M. A.; Jayatilake, D. Hirshfeld surface analysis. *CrystEngComm.*, **2009**, *11*, 19–32; (c) Zhang, C.; Xue, X.; Cao, Y.; Zhou, Y.; Li, H.; Zhou, J.; Gao, T. Intermolecular friction symbol derived from crystal information. *CrystEngComm.*, **2013**, *15*, 6837–6844; (d) Turner, M.J.; McKinnon, J.J.; Wolff, S.K.; Grimwood, D.J.; Spackman, P.R.; Jayatilaka, D.; Spackman, M.A. Crystal Explorer 17; University of Western Australia: Pert, Australia, **2017**.

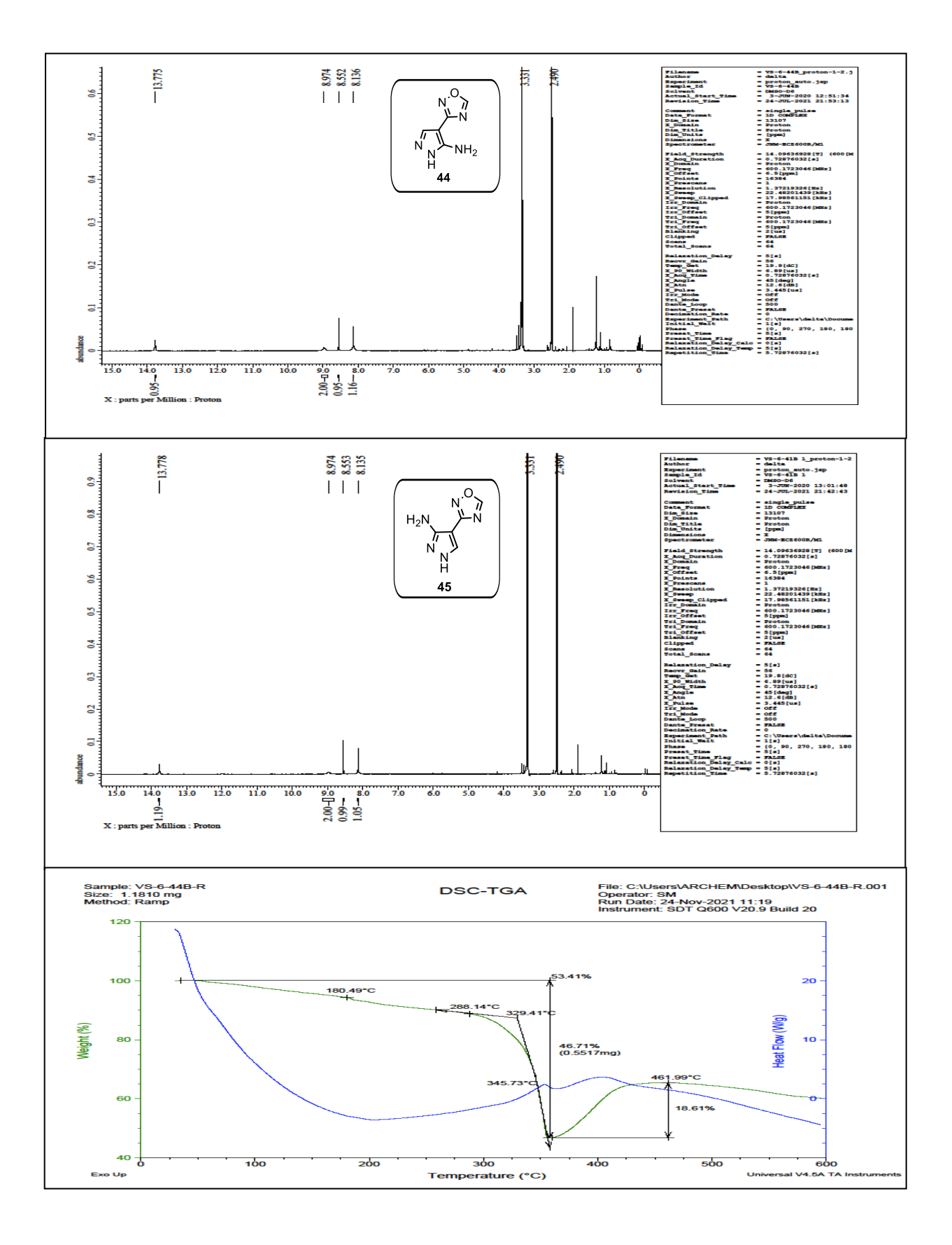
# 4.11. Spectral data

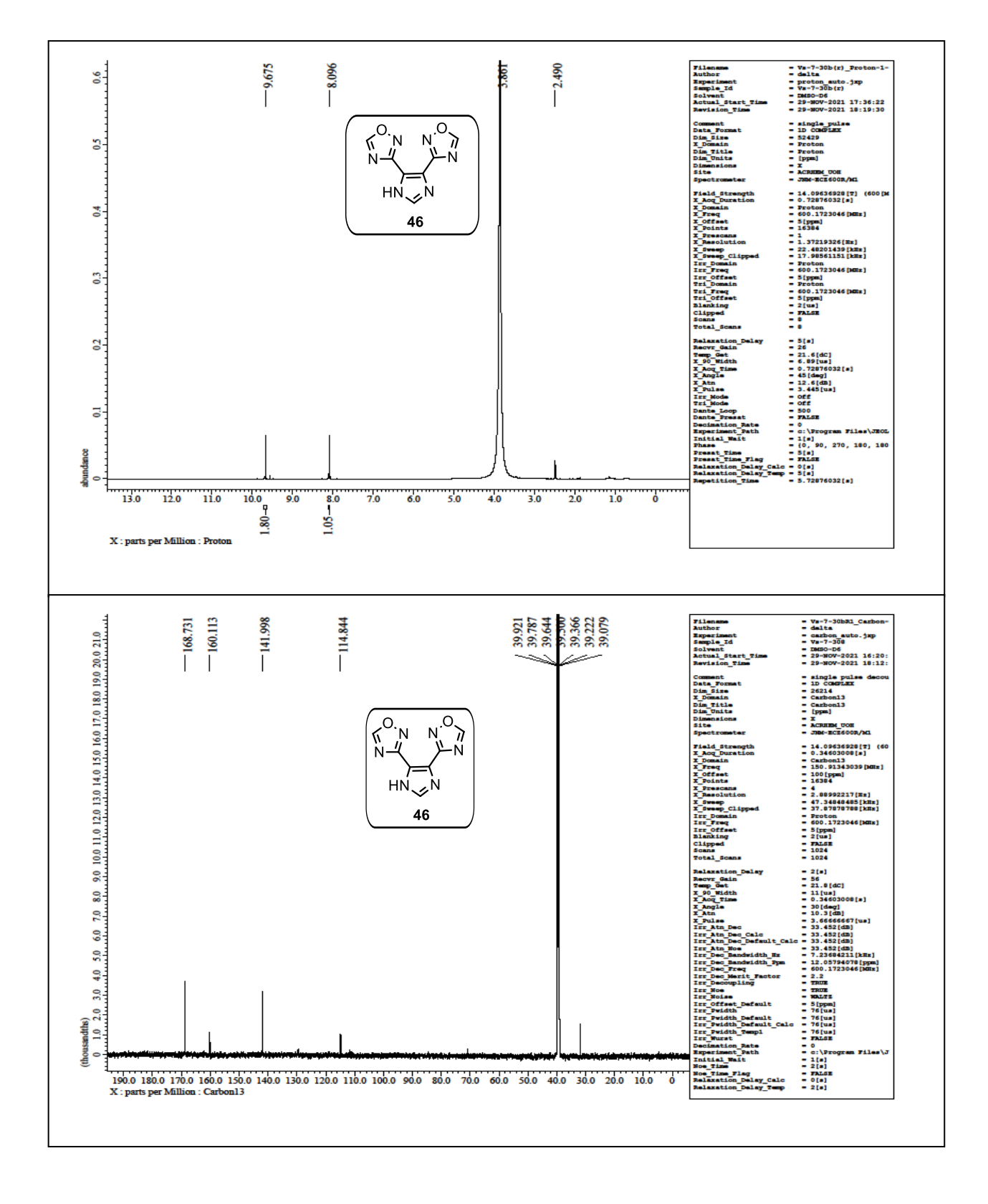


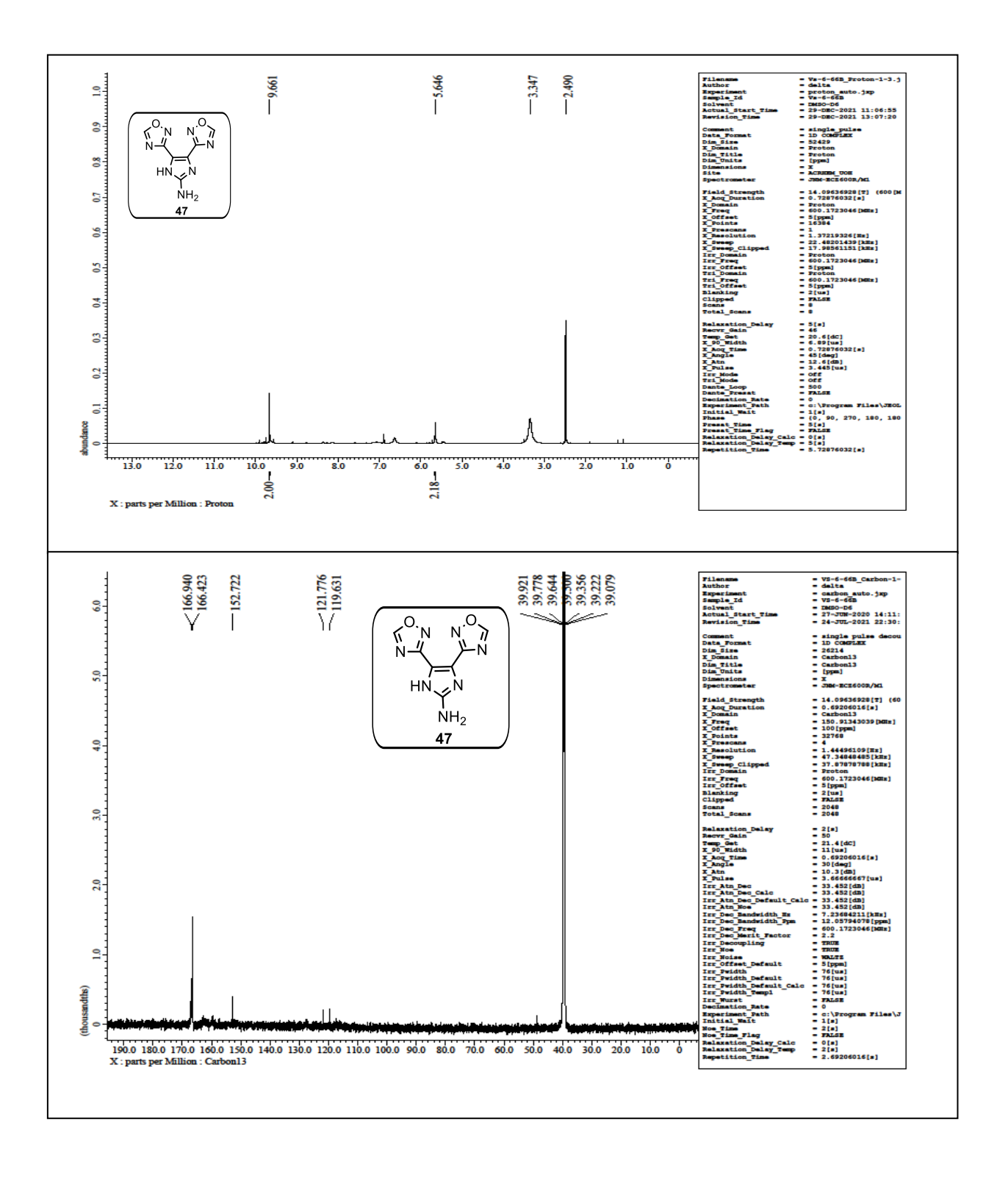


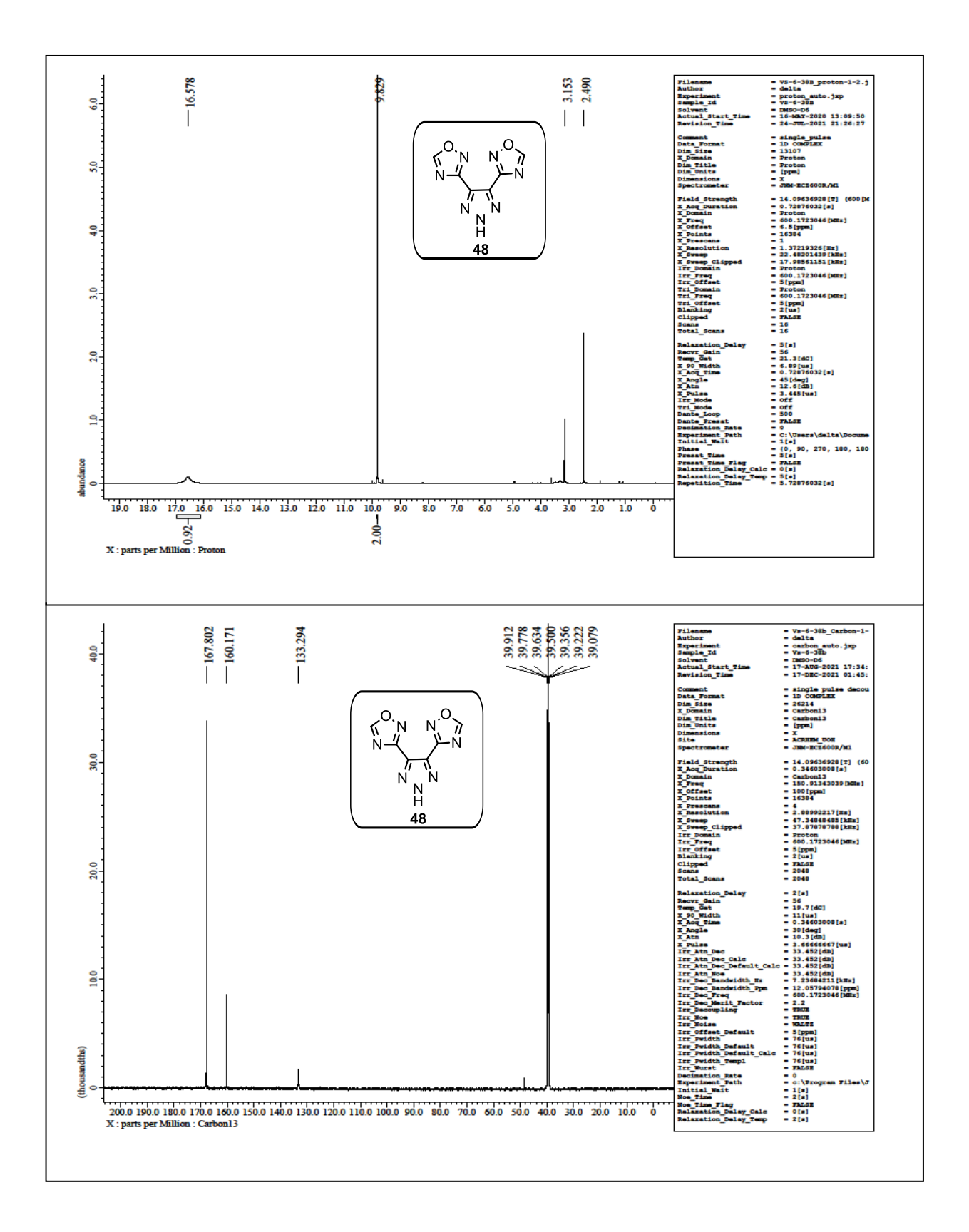


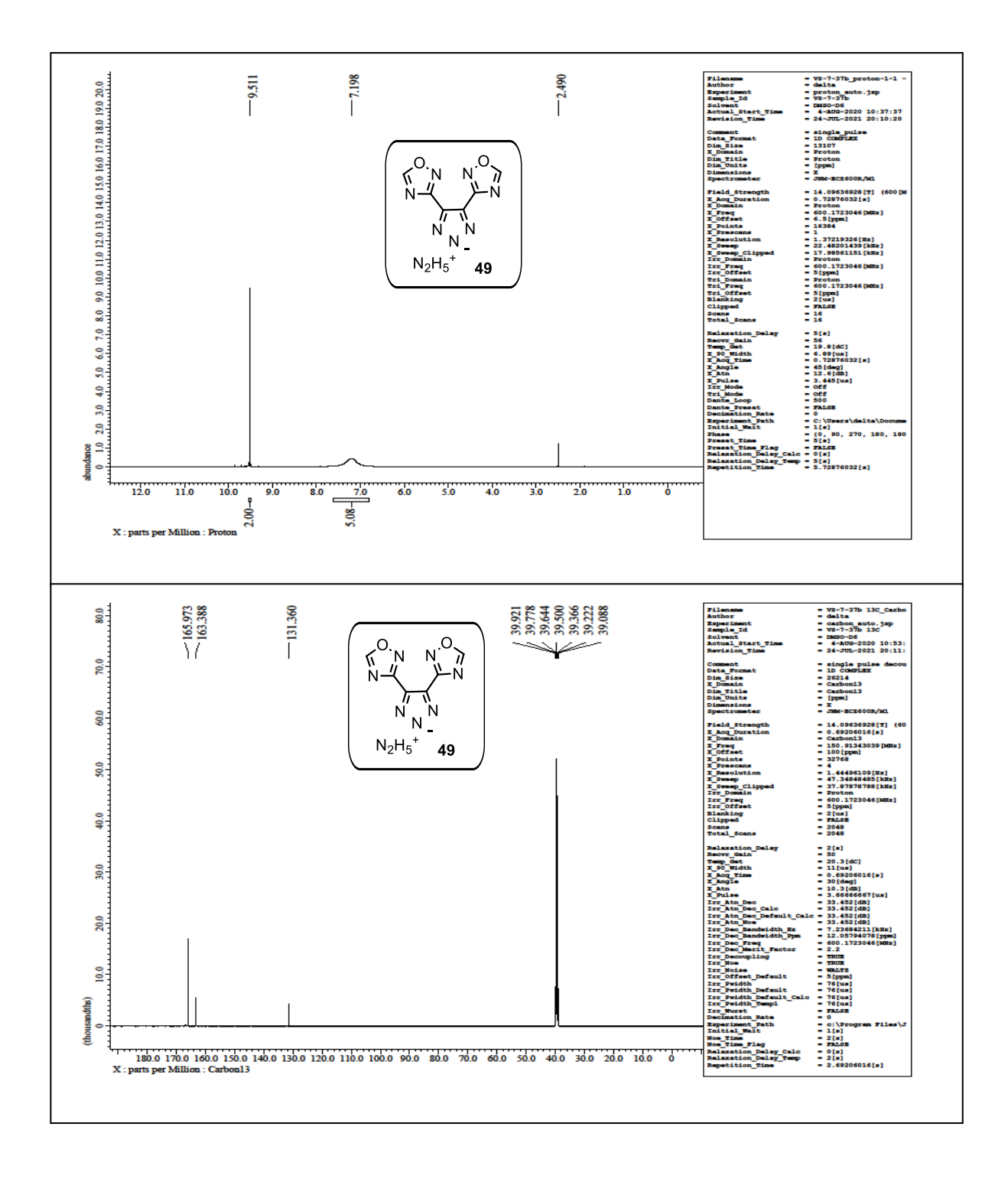


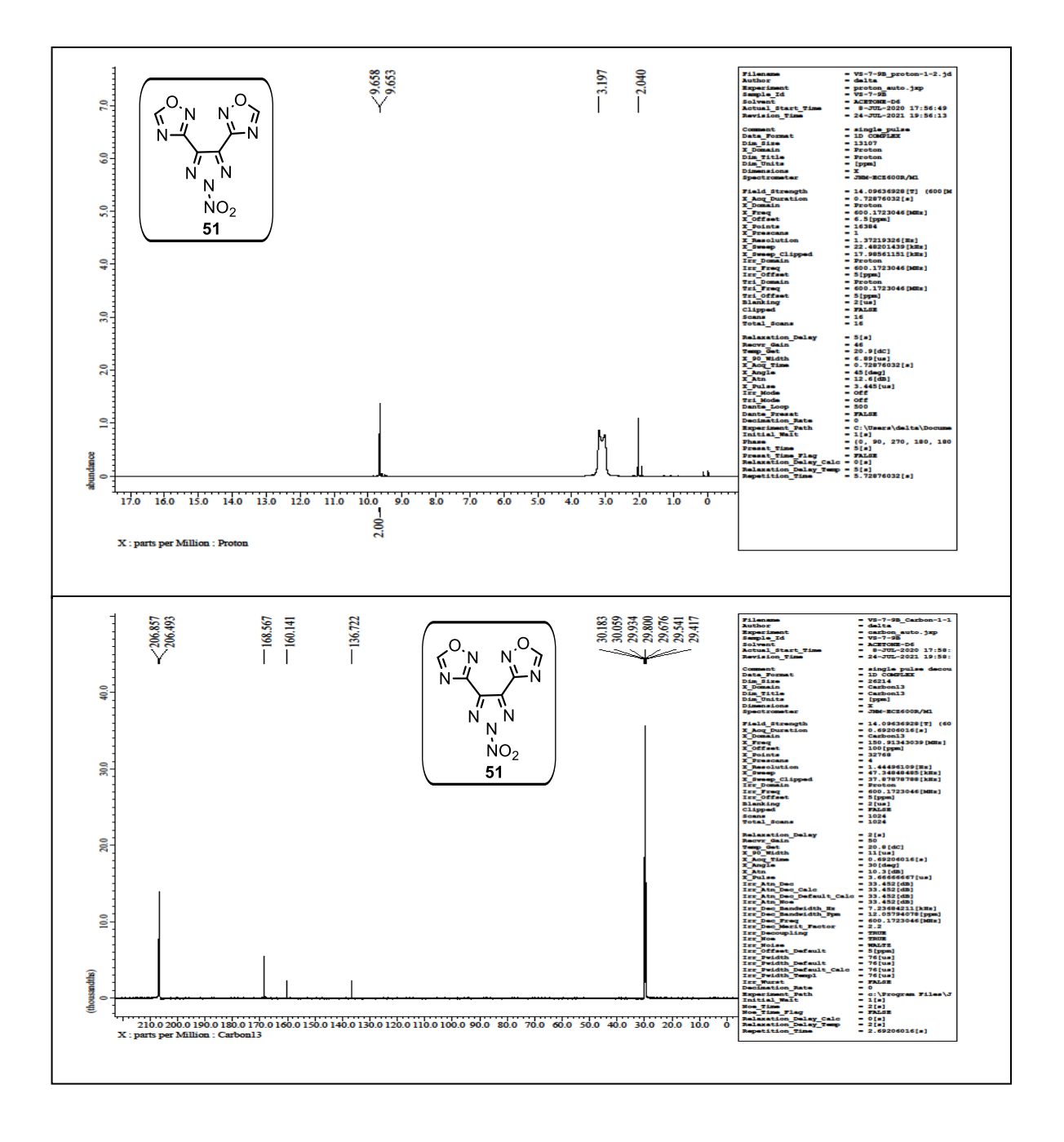


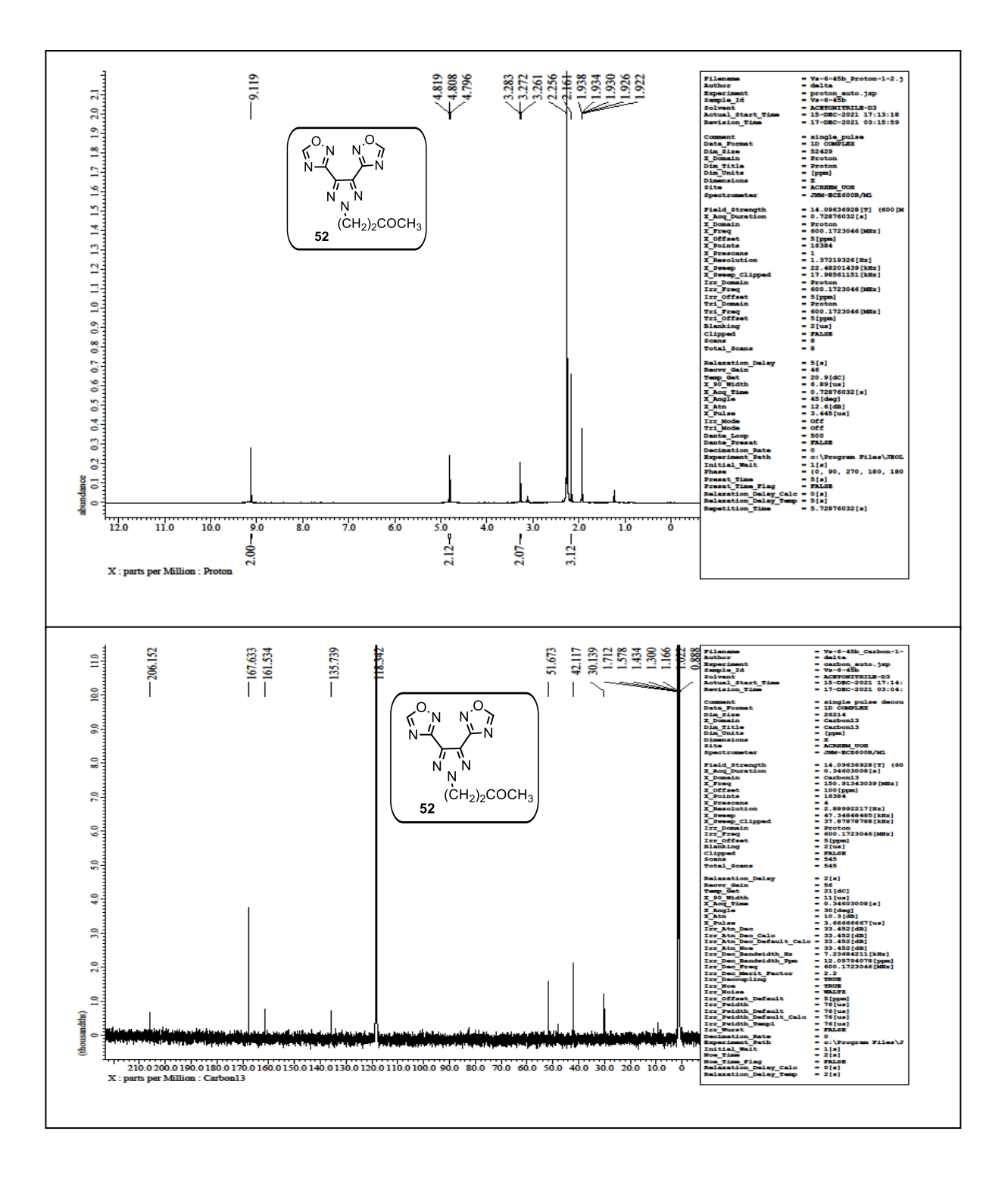


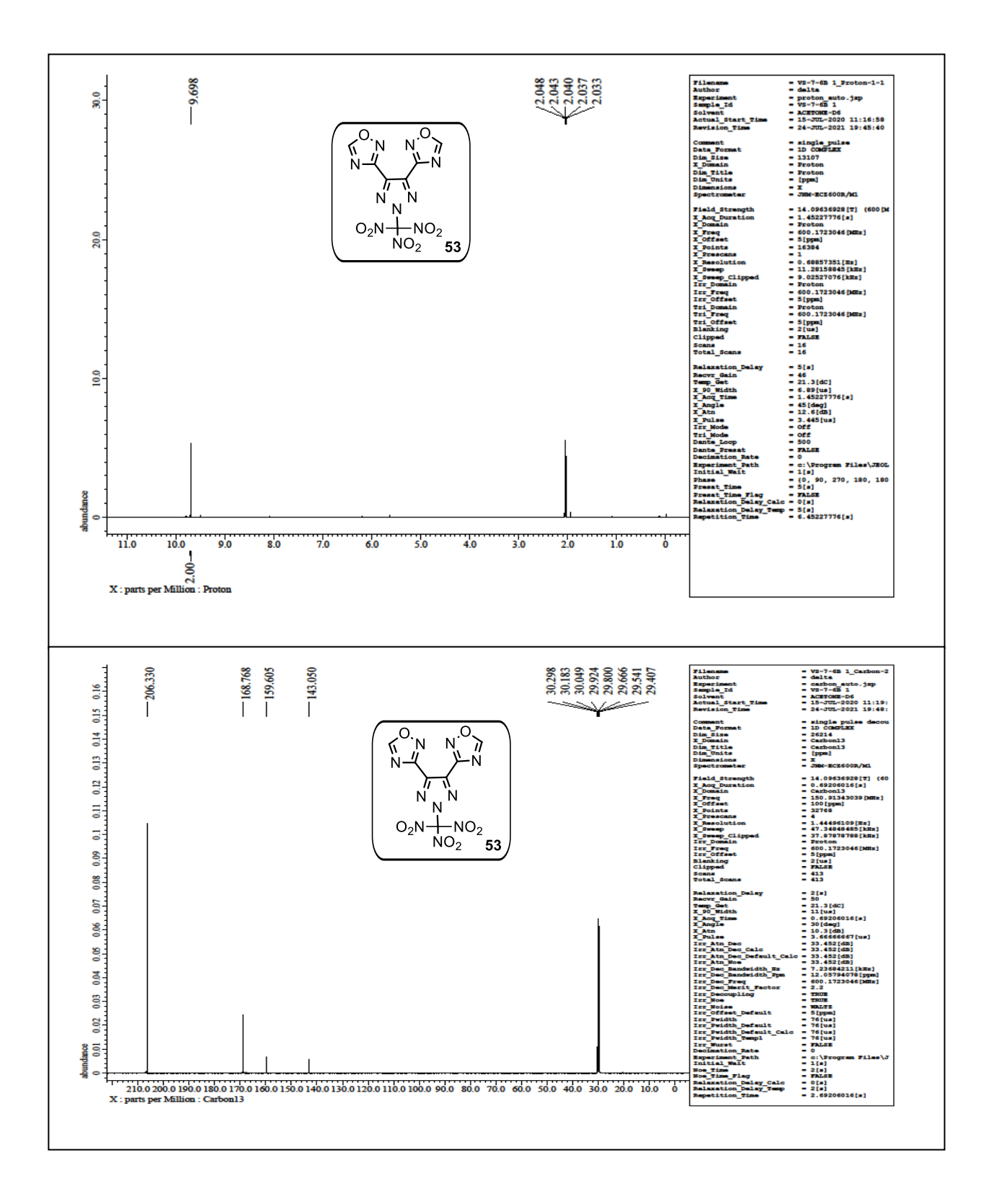


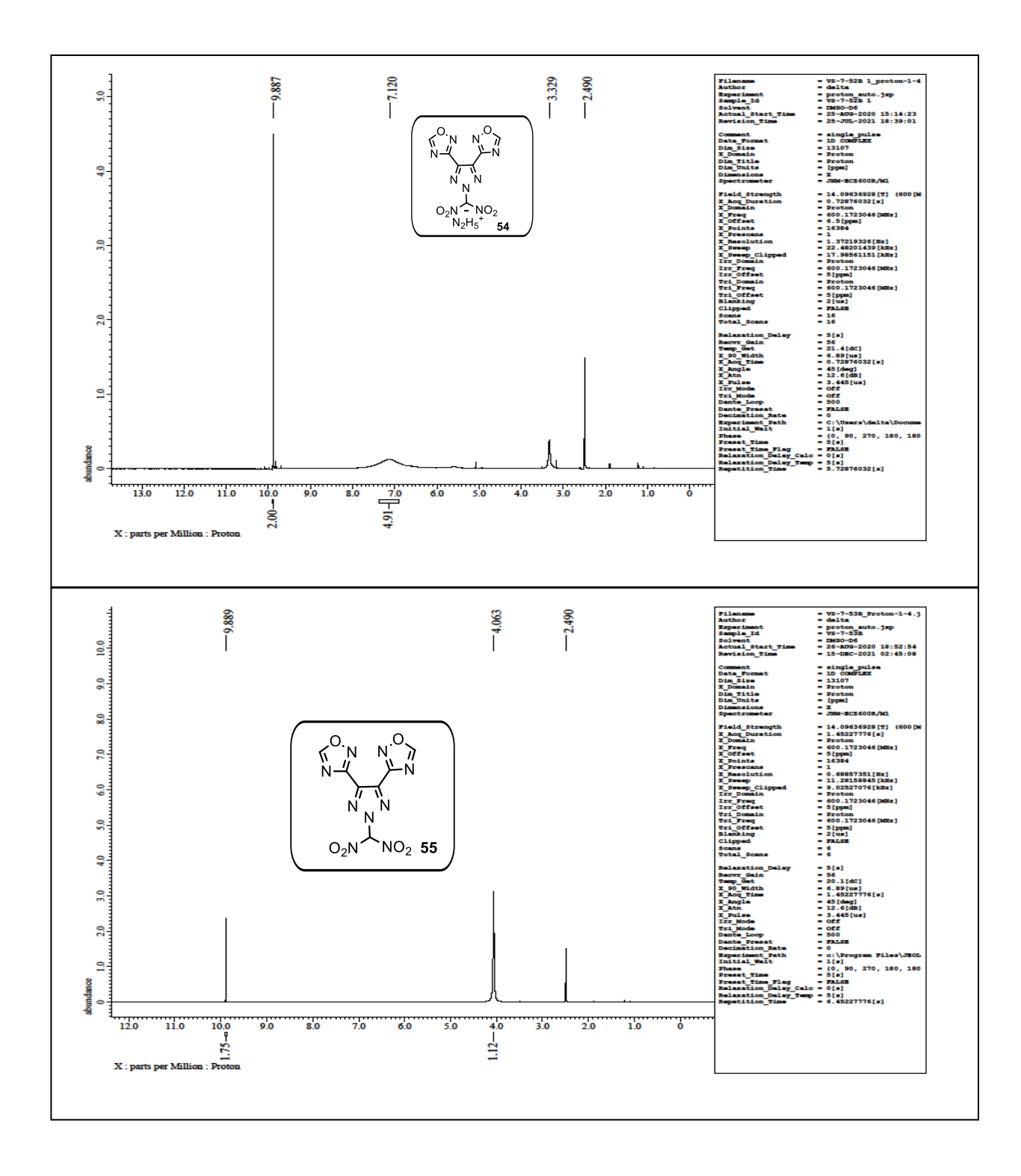












# **List of Publications**

- 9. C–N Linked Biheterocyclic Compounds towards Explosive Applications (*Communicated*) M. Balaraju, Nagarjuna Kommu, **Srinivas Vangara**, and Akhila K. Sahoo\*
- 8. Metal-Free Stereoselective Addition of Propiolic acids to Ynamides: A Concise Synthetic Route to Highly Substituted Ene-Diyne-/Dienyne-(E)-N,O-Acetals (*Communicated*)

Rangu Prasad, Suresh Kanikarapu, Shubham Dutta, Srinivas Vangara, and Akhila K. Sahoo\*

7. Combination of 1,2,4-Oxadiazole and Nitro/Nitroamino Substituted Azoles as Energetic Derivatives (*Communicated*)

Srinivas Vangara, Nagarjuna Kommu, and Akhila K. Sahoo\*

6. Polynitro-azido Functionalized-N-aryl-C-nitro Pyrazole/Imidazole Derivatives as Energetic Materials (*Communicated*)

Srinivas Vangara, Nagarjuna Kommu, Vikranth Thaltiri, and Akhila K. Sahoo\*

5. Polynitro-N-aryl-C-nitro-pyrazole/imidazole Derivatives: Thermally Stable-Insensitive Energetic Materials (*Communicated*)

Srinivas Vangara, Nagarjuna Kommu, Vikranth Thaltiri, M. Balaraju, and Akhila K. Sahoo\*

4. Design, Synthesis, and Antiviral activity of 1,2,3,4-Tetrahydropyrimidine Derivatives Acting as Novel entry Inhibitors to Target at "Phe43 cavity" of HIV-1 gp120

Jagadeesh Senapathi, Bommakanti Akhila, Veena Kusuma, **Srinivas Vangara**, and Anand K. Kondapi\* *Bioorg. Med. Chem.*, **2021**, *52*, 116526.

3. Design, Synthesis, and Evaluation of HIV-1 entry Inhibitors Based on Broadly Neutralizing Antibody 447-52D and gp120 V3loop Interactions

Jagadeesh Senapathi, Bommakanti Akhila, **Srinivas Vangara**, and Anand K. Kondapi\* *Bioorg. Chem.*, **2021**, *116*, 105313.

2. Lewis Acid-Driven Meyer-Schuster-Type Rearrangement of Yne-Dienone

Rajendra K. Mallick, **Srinivas Vangara**, Nagarjuna Kommu, Tirumaleswararao Guntreddi, and Akhila K. Sahoo\* *J. Org. Chem.*, **2021**, *86*, 7059–7068.

1. Synthesis and Energetic Properties of Polynitroaryl-azole Derivatives **Srinivas Vangara**, Nagarjuna Kommu, M. Balaraju, and Akhila K. Sahoo\* *J. Phys.: Conf. Ser.*, **2021**, *1721*, 012007.

# **Conference Attended**

1. Polynitro Aryl-Azole (Pyrazole/Imidazole) Derivatives: Synthesis, Characterization and Energetic Properties

**Srinivas Vangara** and Akhila K. Sahoo\*

Oral Presentation at "Chem Fest-2021" held at School of Chemistry, University of Hyderabad, Hyderabad, India on March, 2021.

- 2. Participated in "RSC Desktop Seminar Lectureship Series with Journals of Materials Chemistry A, B, & C" which was held on 25-Mar-2021, RSC Publishing Webinars.
- 3. Synthesis and Energetic Properties of Polynitro Aryl-Azole Derivatives
  Srinivas Vangara, Nagarjuna Kommu, Muntha Balaraju, and Akhila K. Sahoo\*

**"2020 International Conference on Defence Technology (ICDT-2020)"** which was held on **26-Oct-2020** to **29-Oct-2020**, Beijing, China. (*Paper accepted in conference proceedings*)

4. Polynitro Aryl Based Pyrazole/Imidazole Derivatives: Synthesis, Characterization and Energetic Properties

Srinivas Vangara, Nagarjuna Kommu, Muntha Balaraju, and Akhila K. Sahoo\*

Oral Presentation at "12th International High Energy Materials Conference & Exhibits (HEMCE-2019)" which was held on 16-Dec-2019 to 18-Dec-2019, in IIT Madras, Chennai, India.

- 5. Participated in "11th International High Energy Materials Conference & Exhibits (HEMCE-2017)" which was held on 23-Nov-2017 to 25- Nov-2017, HEMRL, Pune, India.
- 6. Participated in "10<sup>th</sup> International High Energy Materials Conference & Exhibits (HEMCE-2016)" which was held on 11-Feb-2016 to 13-Feb-2016, Hyderabad, India.

# Synthetic Manifestation of Polynitro Functionalized Azoles (Pyrazole/Imidazole/1,2,4-Oxadiazole) as Potential Energetic Materials

by Srinivas Vangara

**Submission date:** 31-Dec-2021 12:03PM (UTC+0530)

**Submission ID:** 1736597513

File name: Srinivas\_Vangara-15CHPH10\_1.pdf (8.31M)

Word count: 15848 Character count: 83985 Synthetic Manifestation of Polynitro Functionalized Azoles (Pyrazole/Imidazole/1,2,4-Oxadiazole) as Potential Energetic Materials

Mat	terials				0
ORIGINA	ALITY REPORT				
	5% ARITY INDEX	9% INTERNET SOURCES	13% PUBLICATIONS	3% STUDENT PA	PERS
PRIMAR	RY SOURCES		•		
1	pubs.rso				1 %
2	Submitte Hyderak Student Paper		of Hyderabac	Ι,	1 %
3	edoc.ub		1 %		
4	baadals		1 %		
5	www.mc				<1%
6		g Gao, Jean'ne M nergetic Salts",	Chemical Revi	ews,	<1%
The high is entha	lun-Oing	Tao, Qamar-un-lao, Yang, Jian-Guo s on the nitroge index is due to the enal research; makin pressure landy index is	Nisa Tariq, Zhi	School of Chemistry of Hydere	1 %

Exclude quotes On Exclude matches < 14 words

Exclude bibliography On